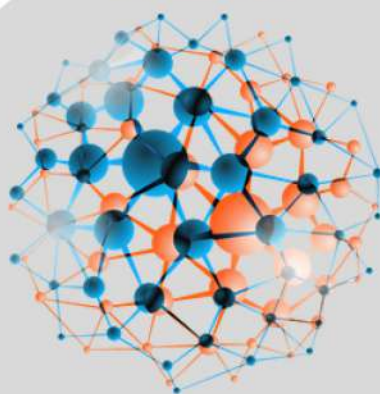


ANNIC 2021

APPLIED NANOTECHNOLOGY AND NANOSCIENCE
INTERNATIONAL CONFERENCE

BOOK OF ABSTRACTS



24, 25, 26 MARCH 2021

ONLINE

Table of Contents

TBD	1
<u>Prof. Rose Amal</u>	
What is flexoelectricity, and why is it so important at the nanoscale	2
<u>Prof. Gustau Catalan</u>	
Solar-driven Photocatalytic Activity of Metal Halide Perovskite	3
<u>Dr. Lorenzo Malavasi</u>	
TPU Nanocomposite Coated Multifunctional Textiles Based on Graphene oxide and Clay Nanoplatelets: Influence on Gas Barrier, Weather Resistance, Thermal and Flame Retardant Properties	4
<u>Dr. Neeraj Kumar Mandlekar</u> , Mr. Rishabh Tiwari, Mr. Mohammad Abuzar, Prof. Mangala Joshi	
fabrication and characterization of poly(aniline-co-2-bromoaniline)/Clay nanocomposite	6
<u>Ms. nour el houda bouabida</u> , Prof. aicha hachemaoui, Prof. ahmed yahiaoui	
Development of a new generation of reusable PPE with anti-bacteriological properties by functionalization with zinc nanoparticles	8
<u>Ms. Inês Boticas</u> , Mr. Pedro Silva, Mr. João Bessa, Mr. Fernando Cunha, Mrs. Clementina Freitas, Dr. Raul Figueiro	
Synthesis and characterization of polyynes by pulsed laser ablation in organic solvents	10
<u>Dr. Pietro Marabotti</u> , <u>Dr. Sonia Peggiani</u> , Dr. Anna Facibeni, Dr. Patrick Serafini, Prof. Alberto Milani, Prof. Valeria Russo, Prof. Andrea Li Bassi, Prof. Carlo Casari	
TBD	11
<u>Dr. Yu Kui</u>	
Light-enhanced H₂O₂ sensing by supported AgAu bimetallic nanoshells as plasmonic nanozymes	12
<u>Mr. Rafael Trivella P. da Silva</u> , Ms. Maria Paula de Souza Rodrigues, Mr. Adriano Marchini Rodrigues Puerta da Silva, Ms. Gabriela DAVilla, Prof. Susana Inés Cordoba de Torresi	
Examining the Efficacy of Freezing-thawing Cycles for Size Reduction of Beta-cyclodextrin Dextran Vesicles	14
Mrs. Rukan Genç Altürk, Ms. Pınar Karacabey, <u>Ms. Gamze Doğan</u>	
Transparent Multi-Color Emitting Carbon Dot/Polymer Films and Applications Thereof	15
<u>Dr. Rûkan GENÇ ALTÜRK</u> , Ms. Melis Özge ALAŞ, Mr. Sadin Özdemir, Mr. Mustafa Serkan Yalçın	
Spatial defects nanoengineering for bipolar conductivity in MoS₂	16
<u>Dr. Annalisa Calò</u>	
Use of magnetic field for structuring supercapacitor electrodes	17
<u>Dr. Nicolas Goubard</u> , Dr. Frédéric Favier, Prof. Thierry Brousse	

Surface Functionalized Nickel Sulfide Nanostructures for pH Responsive Selective Adsorption of Pollutants	18
<u>Ms. SUNITA KUMARI</u>	
Electrocatalytic properties of synthesized Co-Fe nanocones obtained using crystal growth modifier with applied, superimposed magnetic field	20
<u>Ms. Katarzyna Skibińska, Dr. Karolina Kolczyk-Siedlecka, Dr. Dawid Kutyla, Mrs. Anna Jedraczka, Prof. Piotr Zabinski</u>	
Hydrogen production using Au@ZnO-Graphene by Water Splitting	22
<u>Mr. Bryan Bentz</u>	
Sub-nano Gold-Cobalt Particles as Effective Catalysts in the Synthesis of Propargylamines	24
<u>Dr. BERRICHI AMINA, Prof. Bachir Redoaune, Prof. Bedrane Sumeya, Ms. Bensaad meriem, Prof. Choukchou-Braham Nouredine</u>	
Effect of surfactant on TiO₂ electrophoretic deposition for the formation of photocatalytically active layers	25
<u>Ms. larisa sorokina, Dr. Egor Lebedev, Mr. Sergey Dubkov, Mr. Roman Ryazanov, Prof. Tomasz Maniecki, Prof. Dmitry Gromov</u>	
Sub-10 nm resolution patterning of pockets for enzyme immobilization via tc-SPL	26
<u>Dr. Annalisa Calò</u>	
A two-dimensional photonic crystal resonator for high pressure sensing	27
<u>Dr. Amel Bounouioua, Ms. Ahlem BENMERKHI, Prof. Bouchemat mohamed</u>	
Hybrid Soret Nano-Assemblies for Mobile Phone-based Ultrasensitive Copper Ion Sensing	28
<u>Mr. Seemesh Bhaskar, Dr. Sai Sathish Ramamurthy</u>	
Nanofabrication of controlled design plasmonic gold substrates by direct laser writing	30
<u>Dr. Nicoleta Tosa, Dr. Lucian Barbu-Tudoran, Dr. Cosmin Farcau</u>	
Characterization of transport properties and field emission in MoS₂ Field-Effect Transistors	31
<u>Dr. Filippo Giubileo, Mr. Aniello Pelella, Mr. Enver Faella, Mr. Alessandro Grillo, Dr. Francesca Urban, Prof. Antonio Di Bartolomeo</u>	
Grafted Zinc Phthalocyanine to Organic Copolymers as Effective Photosensitizer for Photodynamic Processes	32
<u>Dr. Tamara Potlog, Mr. Pavel Tiuleanu, Mr. Ion Lungu, Dr. Stefan Robu</u>	
Electron emission by slow He ions impact on free-electron metal surfaces	34
<u>Dr. pierfrancesco riccardi</u>	
Influence of cationic substitution on antibacterial activity of nanosized calcium phosphate	35
<u>Dr. Agnese Brangule, Dr. Ingus Skadiņš, Prof. Dace Bandere</u>	
Hybrid Concept to Develop Next-Generation Energy-Storage Technologies	36
<u>Ms. anukriti pokhriyal, Prof. Pedro Gómez-Romero</u>	
Enhancing the Perovskite Solar Cells Efficiency by Carbon Dots Integration into the PCBM Electron Transport Layer	38
<u>Ms. Melis Özge ALAŞ, Mr. Adem Mutlu, Prof. Emre Gür, Prof. Ceylan Zafer, Dr. Rükan GENÇ ALTÜRK</u>	

Local heat sources based on Al-CuOx multilayer structures: formation features and thermal properties	39
<u>Dr. Egor Lebedev, Ms. Larisa Sorokina, Mr. Roman Ryazanov, Mr. Artem Sysa</u>	
Optimization of eco-friendly synthesis of silver nanoparticles from leaves extract of <i>Alstonia angustiloba</i>.	40
<u>Mrs. NURHIDAYAH AB. RAHIM, Prof. MD AZMAN SEENI MOHAMED</u>	
Atomically dispersed Fe in C₂N framework as sulfur host materials for Efficient Lithium-Sulfur Batteries	41
<u>Mr. Zhifu Liang, Mr. Dawei Yang, Dr. Pengyi Tang, Dr. Jordi Llorca, Dr. Marc Heggen, Dr. Rafal E Dunin-Borkowski, Dr. Yingtang Zhou, Dr. Joan Ramon Morante, Dr. Andreu Cabot, Dr. Jordi Arbiol</u>	
Grewia tenax leaves extract mediated silver nanoparticles applications for antibacterial, antibiofilm and antifungal activity	43
<u>Mrs. Priyanka Yadav, Ms. Monisha Singhal, Dr. Surendra Nimesh, Dr. Sreemoyee Chatterjee, Dr. Nidhi Gupta</u>	
1D sp-carbon chains-based nanocomposites by laser ablation in polymeric solutions	44
<u>Dr. Sonia Peggiani, Dr. Pietro Marabotti, Dr. Anna Facibeni, Prof. Alberto Milani, Prof. Valeria Russo, Prof. Andrea Li Bassi, Prof. Carlo Casari</u>	
Development of chitosan/gelatin/ silver nanoparticles based bionanocomposite films for wound healing applications	46
<u>Ms. Isha Gupta, Dr. Sonia Gandhi, Prof. Sameer Sapra</u>	
Secondary Electron emission in the interaction of low Energy ions and electrons from graphene based materials	48
<u>Dr. pierfrancesco riccardi</u>	
In-situ fabrication of ZnO-rGO nanomaterials and their photocatalytic performance	49
<u>Mrs. Aura Merlano, Dr. Ángel Salazar</u>	
Regularities of the catalyst nanoparticles formation and the synthesis of CNTs in PECVD process	50
<u>Dr. Evgeniy Kitsyuk, Ms. Yulia Fedorova, Dr. Alexander Dudin</u>	
Electron beam-plasma vacuum deposition of very thin carbon films on quartz and sapphire substrate for transmissive photocathode applications	51
<u>Dr. Jozef Huran, Dr. Nikolay Balalykin, Dr. Mikhail Nozdrin, Dr. Vlasta Sasinková, Mrs. Eva Kováčová, Mr. Alexander Skrypnik, Dr. Alexander Kobzev, Dr. Grigory Shirkov</u>	
Pseudocapacitive electrodes: a journey from nano to micro	52
<u>Prof. Thierry Brousse</u>	
Electrodeposition of metal-organic frameworks for energy and environment applications	53
<u>Dr. Xuan Zhang, Mr. Wei Guo, Mr. Sijie Xie, Prof. Jan Fransaer</u>	
Eco-friendly synthesis of noble metallic nanoparticles: from theory to practice	54
<u>Ms. Ana-Alexandra Sorescu, Dr. Alexandrina Nuta, Dr. Suica-Bunghez Ioana-Raluca, Dr. Mariana Calin</u>	
Preparation of TiO₂ thin films covered by plasmonic Ag nanoparticles by laser ablation technique for visible-light water splitting	55
<u>Dr. Martin Kostejn, Dr. Radek Fajgar, Dr. Vladislav Drinek, Dr. Vera Jandova, Dr. Jaroslav Kupcik, Dr. Snejana Bakardijeva</u>	
Green Energy hybrid graphene device	57
<u>Dr. javier martinez</u>	

PCE-based additives enable the formulation of highly-loaded, high-performance ceramic inks for extrusion printing	59
Mr. Omid Akhlaghi, Mr. Amin Hodaei, Mr. Can Akaoglu, Mr. navid Khani, Ms. Ferdows Afghah, Mr. Bahattin Koc, Ms. Ozge Akbulut	
Tumor-Targeted Indocyanine Green-Loaded Ferritin Nanotracers for Intraoperative Detection of Cancer Tissue on an Orthotopic Murine Model of Breast Cancer	60
Dr. Serena Mazzucchelli, <u>Dr. Marta Sevieri</u> , Dr. Leopoldo Sitia, Dr. Arianna Bonizzi, Dr. Raffaele Allevi, Dr. marta truffi, Dr. Carlo Morasso, Prof. Fabio Corsi	
A Nanotoxicology Study: The Impact of Size of Silver & Gold Nanoparticles on Lung Cells	62
Ms. Hanouf Bafhaid, Dr. Zubair Ahmed, Dr. Youcef Mehellou, Dr. Hanene Ali-Boucetta	
Tunable hydrogel nanostructures by microfluidics to control Hydrodenticity effect for multimodal imaging applications	63
Mr. Alessio Smeraldo, Prof. Enza Torino	
Fighting Helicobacter pylori with drug-free nanostructured lipid carriers (NLC)	64
Ms. Rute Chitas, Dr. Catarina L. Seabra, Dr. Cláudia Nunes, Dr. Paula Parreira, Prof. M. Cristina L. Martins	
TBD	65
<u>Dr. Steven George</u>	
Plasmonic metal oxide nanocrystals	66
<u>Prof. Delia Milliron</u>	
TBD	67
<u>Prof. Manish Chhowalla</u>	
Nanocrystals as chemical building blocks	68
<u>Prof. Helmut Cölfen</u>	
TBD	69
<u>Ms. Lianzhou Wang</u>	
Hydroxyapatite Growth on the Carbon Dot entegrated TiO₂Nanoneedles in Simulated-Body-Fluids(SBF)	70
<u>Mr. aziz rahman aylak</u> , Dr. Rükan GENÇ ALTÜRK	
Characterization and in-vitro hemolysis evaluation of carboxy methyl cellulose capped silver nano particles .	71
Ms. Archi Ghosh, Dr. Mahua Ghosh Chaudhuri, Dr. Prasanta Kumar Maiti, Prof. Kumkum Bhattacharyya	
GREEN BIOSYNTHESIS OF MULTIFUNCTIONAL NANOMATERIALS	73
<u>Prof. Malik Maaza</u>	
Optical Properties of Layered Hybrid Perovskites: Nano @ Bulk	74
<u>Prof. Angshuman Nag</u>	
Hybrid luminescent systems on the base of PbS nanocrystals and freestanding porous silicon microcavities in the near-infrared range	75
Ms. Irina Kriukova, Dr. Pavel Samokhvalov, Prof. Igor Nabiev	
Morphologically controlled synthesis of Ag@S where S= CZTS,PbS based hybrid nanostructures	76
<u>Ms. Anchal Yadav</u> , Prof. Bart Follink, Dr. Alison Funston	

Implementation of disordered hyperuniform micro and nano architectures via nano-imprint lithography of metal oxides	77
<u>Dr. Zeinab CHEHADI</u> , Dr. Mohammed Bouabdellaoui, Mrs. Mehrnaz Modaresialam, Prof. David Grosso, Dr. Marco Abbarchi	
Quantum Dots dimers: fabrication and insight on interaction mechanisms	78
<u>Mr. Carlo Nazareno Dibenedetto</u> , Prof. Elisabetta Fanizza, Dr. Liberato De Caro, Dr. Rosaria Brescia, Dr. Annamaria Panniello, Prof. Raffaele Tommasi, Dr. Chiara Ingrosso, Dr. Cinzia Giannini, Prof. Angela Agostiano, Prof. Maria Lucia Curri, Dr. Marinella Striccoli	
Detailed calorimetric analysis of micelle formation from aqueous binary surfactant mixtures for design of nanoscale drug carriers	80
<u>Dr. Ádám Juhász</u> , Mr. László Seres, Dr. Edit Csapó	
Local Administration of Nanoparticles for Chronic Lung Fibrotic Disorders	81
<u>Dr. laura pandolfi</u> , Ms. Vanessa Frangipane, Ms. Roberta Fusco, Mr. Marco Giustra, Dr. Rosanna Di Paola, Prof. Jorge Distler, Dr. Veronica Codullo, Prof. Miriam Colombo, Dr. Sara Bozzini, Dr. Monica Morosini, Prof. Davide Prosperi, Prof. Salvatore Cuzzocrea, Prof. Federica Meloni	
Complexation of glycogen with magnetic nanoparticles towards the formulation of biocompatible nanocarriers	82
<u>Dr. Maria Karayianni</u> , Dr. Stergios Pispas, Dr. Evangelia D. Chrysina	
The bittersweet symphony of Pexiganan-A grafted chitosan microparticles & Helicobacter pylori	84
<u>Ms. Diana R. Fonseca</u> , Ms. Ana Moura, Dr. Cátia Teixeira, Dr. Catarina Leal Seabra, Dr. Victoria Leiro, Dr. Berta Estevinho, Prof. Paula Gomes, Dr. Paula Parreira, Prof. M. Cristina L. Martins	
Brain-targeted nanoparticles for enzyme replacement therapy in neuropathic lysosomal storage disorders: application to Krabbe disease.	85
<u>Dr. Ambra Del Grosso</u> , Dr. Marianna Galliani, Ms. Lucia Angella, Dr. Melissa Santi, Dr. Ilaria Tonazzini, Mr. Gabriele Parlanti, Dr. Giovanni Signore, Dr. Marco Cecchini	
Isobaric labeling proteomics allows an easy and high-throughput investigation of protein corona orientation	86
<u>Dr. Nara Liessi</u> , Dr. Luca Maragliano, Dr. Valentina Castagnola, Dr. Mattia Bramini, Prof. Fabio Benfenati, Dr. Andrea Armirotti	
Quantum mechanics and Molecular dynamics investigations on carbon-based nanofluidic device	88
<u>Dr. Alia Mejri</u> , Dr. Guillaume Herlem, Dr. Fabien Picaud	
Supercapacitor electrodes based on carbon nanostructures	89
<u>Dr. Roger Amade Rovira</u> , Mr. Joan Martí Gonzalez, Mr. Islam Alshaikh, Prof. Esther Pascual, Dr. Jose Luis Andújar, Prof. Enric Bertran Serra	
Multicomponent suspensions for electrophoretic deposition of composites with carbon nanotubes	91
<u>Mr. Aleksey Alekseyev</u> , Dr. Egor Lebedev, Prof. Dmitry Gromov, Mrs. Svetlana Pereverzeva, Mr. Roman Ryazanov, Dr. Alexander Dudin	
Bioinspired Polymer Nanocomposites Providing Scalable Solution for Thermal Management	93
<u>Dr. George Stiubianu</u> , Dr. Maria Cazacu, Dr. Carmen Racles, Dr. Mihaela Dascalu, Dr. Alexandra Bargin, Dr. Adrian Bele, Dr. Codrin Tugui, Dr. Cristian Ursu	

Microstructural properties and electrochemical performance of electrospun Ge-doped Fe₂O₃ nanofibers as anode material in sodium-ion batteries	95
Dr. Beatrix Petrovicova, Dr. Chiara Ferrara, Dr. Gabriele Brugnetti, Dr. Clemens Ritter, Dr. Martina Fracchia, Dr. Paolo Ghigna, Dr. Pollastri Simone, <u>Dr. Claudia Triolo</u> , Dr. Lorenzo Spadaro, Prof. Riccardo Ruffo, Prof. Saveria Santangelo	
Microfluidic synthesis of PLGA nanocarriers for the controlled delivery of bioactive compounds in plants of agronomic interest	96
Dr. Laura Chronopoulou, Ms. Francesca Portoghesi, Dr. Elisa Brasili, Dr. Giulia De Angelis, Dr. Anastasia Orekhova, Dr. Giovanna Simonetti, Prof. Gabriella Pasqua, Prof. Cleofe Palocci	
Understanding the pathological versus physiological effects of Sr²⁺ on bone by substitution in biomimetic apatite	98
Dr. Camila Tovani, Dr. Alexandre Gloter, Dr. Thierry Azais, Mr. Mohamed Selmane, Dr. Ana P Ramos, Dr. Nadine Nassif	
Designing functionalized polyelectrolyte microcapsules for cancer-cell-targeting and cancer treatment	99
<u>Mrs. Daria Kalenichenko</u> , Dr. Galina Nifontova, Dr. Alyona Sukhanova, Prof. Igor Nabiev	
Hybrid Nanoparticle-Doped Polyelectrolyte Microcapsules with Controlled Photoluminescence for Bioimaging Applications	101
<u>Dr. Galina Nifontova</u> , Dr. Victor Krivenkov, Ms. Mariya Zvaigzne, Dr. Anton Efimov, Mr. Evgeny Korostylev, Mr. Sergei Zarubin, Prof. Alexander Karaulov, Prof. Igor Nabiev, Dr. Alyona Sukhanova	
Theranostic Hyaluronic Acid Nanoparticles (Thera-ANG-cHANPs) for Dual Targeting and Boosted Imaging of Glioma Cells	103
<u>Mrs. ANGELA COSTAGLIOLA DI POLIDORO</u> , Dr. Laura Mezzanotte, Prof. Enza Torino	
Bioresponsive nanocaplets prepared via “templated-polymerization” for gene and protein delivery	104
<u>Dr. Hashim P.K</u>	
Bottom-up Synthesis of Layered Metal Chalcogenides: Chemical Routes to New 2D Materials	105
<u>Prof. David Lewis</u>	
Synthesis and Optimization of Magnetic Polymer Nanocomposites for Biomedical Applications	106
<u>Mr. Eoin McKiernan</u>	
Indium-Filled Porous Silicon Formed by Electrochemical Deposition	108
<u>Mr. Nikita Grevtsov</u> , Dr. Eugene Chubenko, Dr. Vitaly Bondarenko, Dr. Ilya Gavrilin, Dr. Alexey Dronov, Dr. Sergey Gavrilov	
ZnO nano tetrapods based coatings and their application	110
Dr. Rasa Mardosaite, Dr. Agne Sulciute, Mr. Mindaugas Ilickas, Mr. Paulius Laurikenas, <u>Dr. Simas Račkauskas</u>	
Spatially Controlled Atomic Layer Deposition within Polymer Templates for Multi-Material Nanorods Fabrication	111
<u>Ms. Rotem Azoulay</u> , Dr. Neta Shomrat, Ms. Inbal Weisbord, Dr. Galit Atiya, Dr. Tamar Segal Peretz	
Metal halide perovskites: a journey through structure, properties and stability	113
<u>Dr. Ana Flavia Nogueira</u>	

Supported metallic heterogeneous catalysts in light of density functional theory calculations: from single atoms to subnanometric clusters	114
<u>Dr. Céline Chizallet</u>	
TBD	116
<u>Prof. Kimberly Dick Thelander</u>	
TBD	117
<u>Prof. Rainer Haag</u>	
Anisotropic Plasmonic Nanoparticles with Wide Range Resonance Tunability	118
<u>Dr. Supriya Atta, Dr. Ted Tsoulos, Ms. Kaleigh Ryan, Prof. Laura Fabris</u>	
Plasmonic mesoporous silica coated copper sulfide nanoparticles as near infrared absorbing photothermal agents	119
<u>Prof. Elisabetta Fanizza, Ms. Orietta Pugliese, Ms. Rita Mastrogiacomo, Dr. Luciano De Sio, Dr. Alexa Guglielmelli, Dr. Federica Rizzi, Mr. Pierluigi Lasala, Dr. Maria Principia Scavo, Dr. Gennaro Gentile, Dr. Rachele Castaldo, Prof. Angela Agostiano, Dr. Marinella Striccoli, Dr. Nicoletta Depalo, Prof. Maria Lucia Curri</u>	
Size, shape and phase modulation of colloidal plasmonic copper sulphide nanocrystals	121
<u>Ms. Mariangela Giancaspro, Dr. Teresa Sibillano, Ms. Francesca Panzarea, Dr. Cinzia Giannini, Ms. Silvia Schmitzer, Mr. Fabio Vischio, Dr. Nicoletta Depalo, Prof. Angela Agostiano, Prof. Maria Lucia Curri, Dr. Marinella Striccoli, Prof. Elisabetta Fanizza</u>	
Plasmonic biocatalysis: using light for the regulation of enzyme activity on plasmonic nanoparticles	123
<u>Dr. Heloise Ribeiro de Barros, Prof. Pedro Camargo, Prof. Susana Inés Cordoba de Torresi, Prof. Fernando López-Gallego, Prof. Luis Liz-Marzán</u>	
From whole blood to isolated extracellular vesicles: SERS for efficient cancer diagnostics	125
<u>Dr. Tatu Rojalin, Ms. Hanna Koster, Prof. Randy Carney</u>	
Functionalized drug loaded H-Ferritin nanocages target Cancer Associated Fibroblasts in vitro and in vivo	126
<u>Dr. Leopoldo Sitia, Dr. Arianna Bonizzi, Dr. Serena Mazzucchelli, Dr. Sara Negri, Dr. Cristina Sottani, Dr. Elena Grignani, Dr. Maria Antonietta Rizzuto, Prof. Davide Prosperi, Dr. Luca Sorrentino, Dr. Carlo Morasso, Dr. Raffaele Allevi, Dr. Marta Sevieri, Dr. Filippo Silva, Dr. marta truffi, Prof. Fabio Corsi</u>	
Dissecting how cells internalize and process nano-sized drug carriers for nanomedicine applications	128
<u>Ms. Anna Salvati</u>	
Hybrid diatomite-based nanocarriers for release and intracellular monitoring of Galunisertib to colorectal cancer cells.	129
<u>Ms. Chiara Tramontano, Ms. Giovanna Chianese, Dr. Luca De Stefano, Dr. Anna Chiara De Luca, Dr. Stefano Managò, Dr. Enza Lonardo, Dr. Donatella Delle Cave, Dr. Ilaria Rea</u>	
Towards low-cost metal-enhanced fluorescence biosensor based on 3D bio-responsive hydrogels	131
<u>Mr. Bruno Miranda, Dr. Rosalba Moretta, Dr. Selene De Martino, Dr. Ilaria Rea, Dr. Principia Dardano, Dr. Carlo Forestiere, Dr. Luca De Stefano</u>	
Inexpensive and Scalable Production of High Performance Thermoelectric Materials through Solution Methods	133
<u>Prof. Maria Ibáñez</u>	

Variable angle spectroscopic ellipsometry characterization of turbostratic CVD-grown bilayer and tri-layer graphene	134
<u>Mrs. Grazia Giuseppina Politano, Dr. Carlo Vena, Dr. Giovanni Desiderio, Prof. Carlo Versace</u>	
Perspectives for Human Angiotensin I-Converting Enzyme registration by the Surface Enhanced Raman Spectroscopy	135
<u>Dr. Irina Boginskaya, Dr. Olga Kost, Mrs. Natalia Nechaeva, Dr. Victoria Tikhomirova, Dr. Olga Kryukova, Dr. Naida Bulaeva, Dr. Elena Golukhova, Dr. Ilya Ryzhikov, Dr. Ilya Kurochkin, Mr. Konstantin Afanasev, Dr. Valery Evdokimov</u>	
Excitable cells activity detection through graphite-patterned diamond biosensors	136
<u>Ms. Veronica Varzi, Mr. Pietro Aprà, Mrs. Giulia Tomagra, Prof. Andrea Marcantoni, Prof. Alberto Pasquarelli, Prof. Paolo Olivero, Prof. Valentina Carabelli, Dr. Federico Picollo</u>	
Nanomaterial-based Dual Luminescence Aptasensor for Pathogen Detection	137
<u>Dr. Milad Torabfam, Dr. Hasan Kurt, Dr. Mustafa Kemal Bayazıt, Prof. Meral Yüce</u>	
Variable Angle Spectroscopic Ellipsometry Characterization of Reduced Graphene Oxide Stabilized with Poly(Sodium 4-Styrenesulfonate)	138
<u>Mrs. Grazia Giuseppina Politano, Dr. Carlo Vena, Dr. Giovanni Desiderio, Prof. Carlo Versace</u>	
Synthesis of 2D nanomaterials (h-BN, Bi₂Te₃, MoS₂) by top-down techniques	139
<u>Mr. Jesús Javier Castellanos González, Dr. Antonio Esau Del Río Castillo, Dr. Ana Laura Martínez Hernández, Dr. Carlos Velasco Santos</u>	
Surface layer thickness determination in case of “island” structure by X-ray Photoelectron Spectroscopy	141
<u>Dr. Viktor Afanas’ev, Mr. Daniil Selyakov</u>	
Nanocomposites of PMMA and rose-like BiOCl nanostructure: Synthesis and characterization	143
<u>Ms. Sakshi Sharma, Dr. Aman Deep Acharya</u>	
Wearable Graphene-Kapton Sensor for Blood Toxicity Monitoring	145
<u>Mr. Mohamed Bouherour, Dr. Nabila Aouabdia, Prof. Azzedine Bellel</u>	
Electrical Properties of Epoxy Composites Containing Carbon Black and Carbon Nanotube	147
<u>Dr. Raja Nor Raja Othman, Mr. Afham Zaim</u>	
A comparison Study in Synthesis of Aluminum and Copper Nanoparticles using Pulsed Laser Ablation in Liquid	149
<u>Dr. Ridha Hamdi, Dr. Tahani Felemban, Mr. Hassan Al-khabbaz, Dr. Alheshibri Alheshibri, Dr. SULTAN AKHTAR, Prof. Khaled A Elsayed</u>	
Cedar essential oil - β-cyclodextrin nanocomplex formation for the effective inhibition of acetylcholinesterase	150
<u>Ms. Annita Katopodi, Ms. Ioanna Pitterou, Ms. Georgia Petridou, Ms. Rafaella Spanou, Dr. Eleni Kavetsou, Prof. Anastasia Detsi</u>	
Development of solid lipid nanoparticles (SLNs) and nanostructured lipid carriers (NLCs) for the encapsulation and sustained release of the flavonoid naringin	151
<u>Ms. Ioanna Pitterou, Ms. Annita Katopodi, Dr. Eleni Kavetsou, Prof. Anastasia Detsi</u>	

Topical Formulation with AS1411-Gold Nanoparticles as Cervical Cancer Drug Delivery System	152
<u>Ms. Jéssica Nunes, Ms. Ana S. Agonia, Mr. Tiago Rosado, Dr. Eugénia Gallardo, Dr. Rita Palmeira-de-Oliveira, Dr. Ana Palmeira-de-Oliveira, Prof. José Martinez-de-Oliveira, Dr. José Fonseca-Moutinho, Dr. Maria Paula Cabral Campello, Dr. António Paulo, Prof. Andrew D. Ellington, Dr. Carla Cruz</u>	
Biodegradable lipid-polymer nanoparticles with predictable in vivo miRNA delivery activity	154
<u>Ms. Felicia Roffo, Prof. Enza Torino</u>	
Chitosan covered calcium phosphate particles as a vehicle for ocular drugs	155
<u>Mrs. Ekaterina Popova, Dr. Victoria Tikhomirova, Mrs. Olga Beznos, Mrs. Natalia Chesnokova, Dr. Olga Kost</u>	
Double polymer shell liposomes for oral delivery of curcumin	156
<u>Ms. Anna Maria Maurelli, Dr. Vincenzo De Leo, Dr. Fulvio Ciriaco, Dr. Roberto Comparelli, Prof. Angela Agostiano, Prof. Lucia Catucci</u>	
Redox-responsive mesoporous silica nanoparticles for cancer therapy	157
<u>Dr. Rosemeyre Cordeiro, Ms. Ana Maria Carvalho, Prof. Luísa Durães, Dr. Henrique Faneca</u>	
Photophysical Probing of Squaraine Nanoenvironment, Diffusion Dynamics and Energy Transfer in Conjugated Polymer Nanoparticles	159
<u>Ms. Clara Zehe, Prof. Gareth Redmond</u>	
Hydrogen Production and Degradation of Antibiotics Using Silver-Based TiO₂ and ZnO Catalysts	161
<u>Mr. Carlos A. Valentin, Dr. Loraine Soto-Vázquez, Dr. Abniel Machin, Mr. Kenneth Fontáñez, Dr. Francisco Márquez, Ms. Carla Colón-Cruz, Mr. Gerardo Claudio, Dr. Edgard Resto, Dr. Carmen Morant, Dr. Florian I. Petrescu</u>	
Amine assisted synthesis of dual metal shells on semiconductor nanostructures	163
<u>Ms. Anchal Yadav, Prof. Bart Follink, Dr. Alison Funston</u>	
Fluorescence enhancement and cetuximab-conjugation of nanodiamonds for drug delivery	164
<u>Mr. Pietro Aprà, Mr. Mirko Sacco, Ms. Veronica Varzi, Dr. Valentina Boscaro, Prof. Margherita Gallicchio, Prof. Alessandro Barge, Dr. Federico Picollo</u>	
A sustainable bottom-up synthetic approach for carbon dots	165
<u>Mr. Gianluca Minervini, Dr. Marinella Striccoli, Prof. Elisabetta Fanizza, Prof. Angela Agostiano, Prof. Maria Lucia Curri, Dr. Annamaria Panniello</u>	
NOTEWORTHY THERMAL CONDUCTIVITY ENHANCEMENT IN Ag-GRAPHENE/ ETHYLENE GLYCOL BASED NANOFLUID	167
<u>Prof. Malik Maaza</u>	
Quantum oscillations in topological insulator microwires contacted with superconducting leads	168
<u>Dr. Leonid Konopko, Prof. Albina Nikolaeva, Prof. Tito Huber</u>	
One-step microwave synthesis of functionalized magnetic nanoparticles	169
<u>Mr. Thomas Girardet, Ms. Amel Cherraj, Dr. Franck Cleymand, Dr. Solenne Fleutot</u>	
2D-Composites for the Development of Miniaturized Lithium Ion Batteries	170
<u>Ms. Carla Colon-Cruz, Dr. Abniel Machin, Dr. Maria Cotto, Dr. Carmen Morant, Dr. Francisco Marquez</u>	
Quantum size effect and surface state of “topological insulator” in Bi_{1-x}Sb_x wires near the gapless state	171
<u>Prof. Albina Nikolaeva, Dr. Leonid Konopko, Prof. Tito Huber, Mr. Ivan Popov, Ms. Oxana Botnari</u>	

Kinetics of the electrochemical precipitation of lead on FTO substrate at different temperatures	173
<u>Dr. Ridha Hamdi, Dr. Amani Rached, Dr. Amor BEN Ali</u>	
On quantum dynamics of magnetic dipoles in diamagnetic crystals	174
<u>Dr. Mikhail Kuchеров</u>	
optimisation of the coupling length of magneto photonic slab waveguide based on a square lattice	175
<u>Dr. Salim ghalem, Dr. lebbal mohamedredha, Prof. Bouchemat mohamed, Prof. Boumaza-Bouchemat Touraya</u>	
Enhancing the antioxidant activity of the natural coumarin daphnetin and its substituted analogues by their encapsulation in Solid Lipid Nanoparticles	176
<u>Ms. Annita Katopodi, Ms. Kyriaki Safari, Ms. Aikaterini Spanou, Dr. Eleni Kavetsou, Prof. Anastasia Detsi</u>	
A targeted delivery nanosystem to mediate a combined antitumor strategy to HCC	178
<u>Ms. Dina Farinha, Dr. Michael Migawa, Dr. Anabela Sarmento, Dr. Henrique Faneca</u>	
Title: Development of flexible nanovesicles for transdermal drug delivery of Azilsartan medoxomil	179
<u>Ms. aparanjitha r</u>	
Bacteriophage T7 single-stranded DNA-binding protein displays template-catalyzed recycling	181
<u>Dr. Jordi Cabanas-Danes, Mr. Longfu Xu, <u>Mr. Matthew Halma</u>, Dr. Sarah Stratmann, Prof. Antoine van Oijen, Prof. Erwin Peterman, Prof. Gijs Wuite</u>	
Encapsulation of Dopamine and L-DOPA in various biodegradable nanosystems	182
<u>Ms. Ioanna Pitterou, Mr. Isidoros Stamatiou, Dr. Eleni Kavetsou, Dr. Eleni Alexandratou, Prof. Anastasia Detsi</u>	
pre-miR-149 G-quadruplex as a molecular recognition agent of Nucleolin	183
<u>Mr. Tiago Santos, Mr. André Miranda, Mr. Lionel Imbert, Dr. Gilmar Salgado, Prof. Eurico Cabrita, Dr. Carla Cruz</u>	
Effectiveness of azelaic acid inclusion complex and its derivative selection in nanovesicles on cell lines	184
<u>Dr. Atchara Panyosak</u>	
Optical Properties Analysis of Local Structural Change Induced by Gamma Irradiation in Al_{1.9}Eu_{0.1}Sr₆Cs₂(PO₄)₆(OH)₂	186
<u>Mr. Ayumu Masuda, Dr. Shinta Watanabe, Dr. Masahiko Nakase, Prof. Kenji Takeshita</u>	
Nano-domain patterning by focused ion beam in nonpolar-cut MgOLN and PMN-PT single crystals covered by artificial dielectric layer	188
<u>Ms. Elena Pashnina, Mr. Dmitry Chezganov, Ms. Alla Nuraeva, Prof. Vladimir Shur</u>	
Local and non-local charge transfer of slow alkali ions at surfaces	190
<u>Dr. pierfrancesco riccardi</u>	
UV photodetector based on Zn_{1-x}Mg_xO thin films	191
<u>Mr. Vadim Morari, Dr. Rusu Emil, Dr. Ursachi Veaceslav, Prof. Tighineanu Ion</u>	
Performance and electrochemical studies of lithium ion hybrid supercapacitor	193
<u>Ms. Sarah Alshehri, Prof. Gregory G.Wildgoose, Dr. John Fielden</u>	
Spectroscopic investigation of water soluble QDs with Proteinase K: FRET Approach	194
<u>Mr. Mallikarjun Patil, Dr. Sanjeev R. Inamdar, Dr. Kotresh M.G, Mr. Tilakraj T.S, Mr. Vighneshwar S Bhat, Mr. Vikram S Pujari</u>	

Methylated Silica Surfaces Having Tapered Nipple-Dimple Nanopillar Morphologies as Robust Broad-Angle and Broadband Antireflection Coatings	196
<u>Mrs. Mehrnaz Modaresialam, Dr. Marco Abbarchi, Prof. David Grosso, Dr. Jena -Benoit Claude</u>	
Nanostructured ceria-titania photocatalysts for environmental and energy-related applications	197
<u>Prof. Elisa Moretti</u>	
Investigations on Spatial Self-Phase Modulation of Fullerenes in Solution	198
<u>Ms. Stefanie Dengler, Dr. Bernd Eberle</u>	
Sensitized photoluminescence of rare earth-based semiconducting nanocrystals	200
<u>Dr. Guillaume Gouget, Dr. Morgane Pellerin, Dr. Rabih Al Rahal Al Orabi, Dr. Lauriane Pautrot-D'Alençon, Dr. Thierry Le Mercier, Prof. Christopher B. Murray</u>	
TOWARDS MULTIFUNCTIONAL VO₂ MEMRISTORS FOR ULTRAFAST TUNABLE NANO-OPTOELECTRONICS	201
<u>Prof. Malik Maaza</u>	
Heterogeneous catalysts at atomic scale: from growth mechanisms to properties	202
<u>Dr. Maria Chiara Spadaro</u>	
Zeolitic-Imidazolate Framework-8 Nanoparticles as mediators to control the selectivity in the oxidative ring-opening reaction of dimethylfuran	203
<u>Dr. Carolina Carrillo Carrion</u>	
Silver and molybdenum disulfide photocatalysts for the production of hydrogen and degradation of ciprofloxacin	205
<u>Mr. Gerardo Claudio, Dr. Abniel Machin, Dr. Loraine Soto-Vázquez, Ms. Carla Colón-Cruz, Mr. Carlos A. Valentin, Mr. Kenneth Fontánez, Dr. Florian I. Petrescu, Dr. Edgard Resto, Dr. Carmen Morant, Dr. Francisco Márquez</u>	
The surface chemistry of colloidal nanocrystals; empowered by NMR	206
<u>Prof. Jonathan De Roo</u>	
Estimating the effect of semiconductor quantum dot surface charge on their interaction with proteins	207
<u>Mrs. Tatiana Tsoy, Prof. Alexander Karaulov, Prof. Igor Nabiev, Dr. Alyona Sukhanova</u>	
Full ground states of dipolar particles controlled from external fields	208
<u>Mr. Ebenezer KEMGANG</u>	
Coated superparamagnetic iron oxide nanoparticles: synthesis and characterization	209
<u>Dr. Solenne Fleutot, Dr. Pierre Venturini, Mr. Thomas Girardet, Dr. Franck Cleymand</u>	
TBD	210
<u>Ms. Aleksandra Radenovic</u>	
Scanning transmission electron microscopy at high spatial and energy resolution	211
<u>Prof. Quentin Ramasse</u>	

TBD

Wednesday, 24th March - 09:00: Plenary Session 1 (Room 1) - Abstract ID: 305

Prof. Rose Amal ¹

1. UNSW Sydney

TBD

What is flexoelectricity, and why is it so important at the nanoscale

Wednesday, 24th March - 09:45: Plenary Session 1 (Room 1) - Abstract ID: 275

Prof. Gustau Catalan¹

1. ICREA and ICN2-Institut Catala de Nanociencia i Nanotecnologia

What is flexoelectricity, and why is it so important at the nanoscale

Gustau Catalan, ICREA and ICN2-Institut Catala de Nanociencia i Nanotecnologia, Barcelona, Catalonia.

Flexoelectricity is the ability of all non-metallic materials to generate an electrical polarization in response to an inhomogeneous deformation (a strain gradient). Although this property is universal, its magnitude is often negligible at the macroscale, so it has classically received little attention. At the nanoscale, however, strain gradients can be many orders of magnitude larger than at the macroscale, and as a consequence flexoelectricity also becomes large.

In this talk, I will cover basic aspects and relevant results of this emerging property. These include the discovery of flexoelectric effects on materials as wide-ranging as halide semiconductors, ferroelectrics and even biological materials such as bones [1-5]. I will also show how flexoelectricity can affect other physical properties of materials such as their mechanical toughness or their photovoltaic response.

1. Longlong Shu, Shanming Ke, Linfeng Fei, Wenbin Huang, Zhiguo Wang, Jinhui Gong, Xiaoning Jiang, Li Wang, Fei Li, Shuijin Lei, Zhenggang Rao, Yangbo Zhou, Ren-Kui Zheng, Xi Yao, Yu Wang, Massimiliano Stengel & **Gustau Catalan**, Photoflexoelectric effect in halide perovskites, *Nature Materials* 19, 605–609 (2020).
2. K. Cordero-Edwards, H. Kianirad, C. Canalias, J. Sort, **G. Catalan**, Flexoelectric Fracture-ratchet effect in ferroelectrics, *Physical Review Letters* **13**, 135502 (2019).
3. A. Abdollahi, N. Domingo, I. Arias, **G. Catalan**, Converse Flexoelectricity yields large piezoresponse force microscopy signals in non-piezoelectrics Materials, *Nature Communications* **10**, 1266 (2019)
4. F. Vazquez-Sancho, A. Abdollahi, D. Damjanovic, **G. Catalan**. Flexoelectricity in bones. *Advanced Materials*. 1705316 (2018)
5. J. Narvaez, F. Vazquez, **G. Catalan**, Enhanced flexoelectric-like response in oxide semiconductors, *Nature* **538**, 219 (2016)

Solar-driven Photocatalytic Activity of Metal Halide Perovskite

Wednesday, 24th March - 10:50: Oral Session 1-1 (Room 1) - Abstract ID: 306

Dr. Lorenzo Malavasi¹

1. University of Pavia

TBD

TPU Nanocomposite Coated Multifunctional Textiles Based on Graphene oxide and Clay Nanoplatelets: Influence on Gas Barrier, Weather Resistance, Thermal and Flame Retardant Properties

Wednesday, 24th March - 11:20: Oral Session 1-1 (Room 1) - Abstract ID: 156

Dr. Neeraj Kumar Mandlekar¹, Mr. Rishabh Tiwari¹, Mr. Mohammad Abuzar¹, Prof. Mangala Joshi¹

1. Department of Textile and Fibre Engineering, Indian Institute of Technology Delhi, Hauz Khas, New Delhi 110016, India

Introduction:

In the last two decades, thermoplastic polyurethane (TPU) based coatings are in great demand in various applications due to its versatile properties such as excellent flexibility, low-temperature performance, chemical resistance, transparency, good oil and grease resistance, abrasion resistance, etc. In particular, TPU based textile coating have been exploited for lightweight and high-performance inflatable structures such as lifeboat, flexible gas storage tanks, gas holding balloons and inflatable hull structures for advanced lighter than air (LTA) systems, etc. In such applications, excellent gas barrier and weather-resistant properties are required. Inferior helium gas barrier and UV resistant properties of TPU limits its potential application in developing inflatable hull structure for advanced LTA systems like aerostat and airship [1]. Researchers have exploited 2D nanometric particles such as nano-clay, graphene, or graphene oxide to improve gas barrier and weather resistance of TPU coated textile [2,3]. These nanoplatelets have great potential to enhance the gas barrier property when dispersed and oriented properly in the polymer matrix [4]. Moreover, presence of these layered nanoparticles also improves weather resistance and flame retardant properties.

Methodology:

In this study, an approach has been employed to improve the performance of an aliphatic grade TPU. In a systematic study, the effect of nano-clay and graphene oxide (GO) nanoplatelets on the helium and nitrogen gas barrier of TPU nanocomposite coated textile have been studied. Formulations are shown in Table 1. In order to improve the weather resistance property organic UV additives were also added in combination with GO and clay. Nylon fabric (135 gsm) was used as substrate and nanocomposites were prepared by solution mixing in N-N-Dimethyl formamide (DMF). A multi-layered coating of nanocomposite TPU was applied on fabric by direct solution coating on continuous coating machine to achieve 100 gsm coating. opposite side was also coated by 50 gsm and a 12 micron PET film was applied for better gas barrier properties. Emphasis is given to analyze the helium and nitrogen gas barrier and artificial weathering test. In addition to this thermal and flame retardant properties were also evaluated.

Results and Discussion:

In order to evaluate the gas barrier performance of prepared coated fabric the helium and nitrogen gas permeability was studied, results are shown in Figure 1. It is observed that introduction of clay or GO certainly decrease the permeability of testing gas. However, combination of clay and GO has less positive effect than using them individual with TPU matrix.

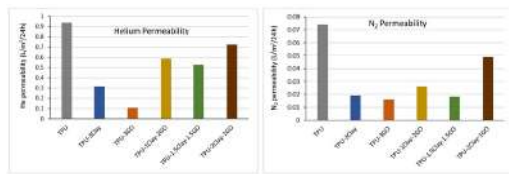


Image-1.jpg

Sample name	Clay (%)	GO (%)
TPU	-	-
TPU-1Clay-2GO	1	2
TPU-1.5Clay-1.5GO	1.5	1.5
TPU-2Clay-1GO	2	1
TPU-3Clay	3	0
TPU-3GO	0	3

TPU – Thermoplastic Polyurethane, CA – Claytone APA, GO – Graphene Oxide, subscript represents its concentration in %.

Table 1.jpg

References

1. Chatterjee, U.; Butola, B.S.; Joshi, M. Optimal designing of polyurethane-based nanocomposite system for aerostat envelope. *Journal of Applied Polymer Science* **2016**, *133*, 1–9, doi:10.1002/app.43529.
2. Adak, B.; Joshi, M.; Butola, B.S. Polyurethane/functionalized-graphene nanocomposite films with enhanced weather resistance and gas barrier properties. *Composites Part B: Engineering* **2019**, *176*, 107303, doi:10.1016/j.compositesb.2019.107303.
3. Adak, B.; Butola, B.S.; Joshi, M. Effect of organoclay-type and clay-polyurethane interaction chemistry for tuning the morphology, gas barrier and mechanical properties of clay/polyurethane nanocomposites. *Applied Clay Science* **2018**, *161*, 343–353, doi:10.1016/j.clay.2018.04.030.
4. Joshi, M.; Adak, B.; Butola, B.S. Polyurethane nanocomposite based gas barrier films, membranes and coatings: A review on synthesis, characterization and potential applications. *Progress in Materials Science* **2018**, *97*, 230–282.

References.jpg

fabrication and characterization of poly(aniline-co-2-bromoaniline)/Clay nanocomposite

Wednesday, 24th March - 11:35: Oral Session 1-1 (Room 1) - Abstract ID: 51

Ms. nour el houda bouabida ¹, Prof. aicha hachemaoui ¹, Prof. ahmed yahiaoui ¹

1. universite of Mascara

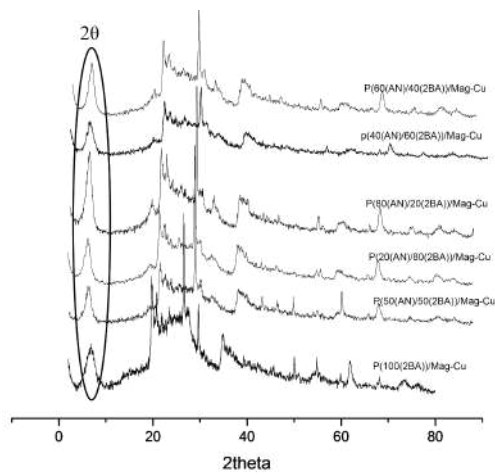
Abstract:

The vast majority of conventional polymers are insulating, but a new class of polymers revealed by the work of Mac Diarmid, Heeger and Shirikaw has expanded their application fields. These polymers are conjugated polymer, such as polyaniline made conductive by doping. Their electrical properties make them good candidates for the realization of chemical sensors in particular their use as a sensitive layer based on the modulation of their doping level during chemical reactions, which is carried out by oxidation –reduction reactions or by acid base treatment. Polyaniline have attracted great interest in view of scientific because of its high stability in the presence of air and humidity , electrical conductivity ,easy preparation and the low cost of the aniline monomer . it's have been the subject of great interest to chemists because these potential applications including electronic devices ,light emitting diodes ,electrostatic discharge protection ,secondary batteries and corrosion protecting paint. In the present paper , a detailed study about synthesis and characterization of copolymerization between ,Aniline and 2-Bromoaniline , in the presence of Cu^{++} /montmorillonite (MMT-Cu^{++})by in situ oxidative polymerization . for achieving this purpose ,we started in the first stage with the organophilization of the clay to (MMT-Cu^{++}) and secondly we prepared the nanocomposites by in situ oxidative polymerization of Aniline and 2-Bromoaniline ,in acidic medium using ammonium peroxydisulfate (APS) as an initiator ,it's were prepared by intercalating for the two monomers (copolymerization),with different molar ratio.

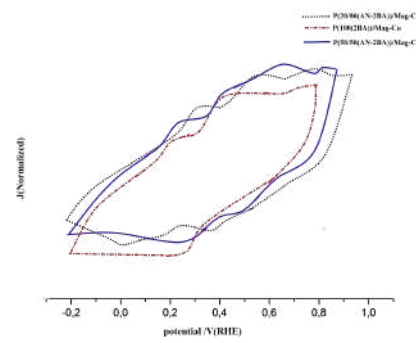
The nanocomposites were characterized by X-Ray diffraction (XRD), UV-vis, FTIR and cyclic voltammogram. The XRD and FTIR also confirms the intercalation or exfoliation of P (ANI-co-2BA) nanocomposite with the different molar ratio into the MMT-Cu^{++} layers.

The UV –vis spectra observed that there is a strong interaction between polymer and clay .for study the electrical property of copolymers we use the cyclic voltammogram , we showed that there is an enhancement in the conductivity values of the prepared nanocomposite.

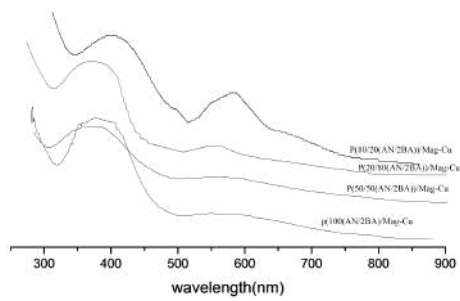
The result of XRD, FTIR and UV confirmed the formation and intercalation of polymer chains in to the cuprous clay .also Nano composite exhibit will-intercalated structure in to the interlayer spacing of the cuprous Montmorillonite.



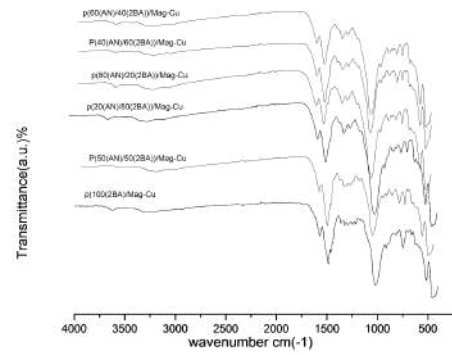
1.png



2.png



3.png



4.png

Development of a new generation of reusable PPE with anti-bacteriological properties by functionalization with zinc nanoparticles

Wednesday, 24th March - 11:50: Oral Session 1-1 (Room 1) - Abstract ID: 181

Ms. Inês Boticas¹, Mr. Pedro Silva¹, Mr. João Bessa¹, Mr. Fernando Cunha¹, Mrs. Clementina Freitas², Dr. Raul Figueiro¹

1. University of Minho, 2. Latino Group

Introduction

In the past 20 years, the prevalence of some infectious diseases has been increasing, and this growth may be intensified in the future. Human activities and fast globalization, increase the transmission across continents of infectious diseases and viruses, resulting in the spread of possible catastrophic pandemics, in specific viral pandemics [1], [2]. The present-day worldwide calamity, caused by severe acute respiratory syndrome coronavirus-2 (SARS-CoV-2), that presents itself as a potentially fatal disease, is responsible for the most recent pandemic health catastrophe, with substantial mortality across the globe [3].

In this work, our main goal was to develop a new generation of reusable PPE with antibacterial and anti-viral properties, for use in a professional context and that present active capability to protect the users against infectious diseases and viruses, by applying a polymeric coating functionalized with zinc oxide nanoparticles, by *knife on roll*.

Materials and Methods

Synthetic polyester fabric was used as the substrate for the polymeric coating functionalized with zinc oxide nanoparticles application. The polymeric coating deposition was made by knife on roll technique, with the application of two different layers: one basecoat and a topcoat polyurethane-based, where the topcoat was doped with zinc oxide nanoparticles. For the application of each layer, there was a drying step at 120 °C for 3 min, and to the topcoat layer, a polymerization step at 160 °C for 3 min. To evaluate the functional behaviour of the prepared samples were performed antibacterial assays against gram-positive and gram-negative bacteria, and anti-viral assays – using bacterial-virus models that mimic the current pandemic virus, after 50 wash cycles – at 60 °C by 20 min.

Results and Discussion

The percentage of bacterial reduction was used to evaluate the antibacterial properties of the developed samples, and the results against gram-positive (*S. epidermis*) bacteria are shown in **Figure1**.

Through the analysis of the results presented it is possible to verify that even after 50 washes the zinc nanoparticles have a more positive influence on bacterial death effect, than before washes. This can be explained by the fact of the before washes nanoparticles are masked by the polymer. In this way, the washes are more on the surface of the substrate, due to the wear of the coating, and its activity is increased. Besides that, the sample identifies as 1%50L show the better behaviour in terms of bacteria reduction, with almost 100 % after 6h.

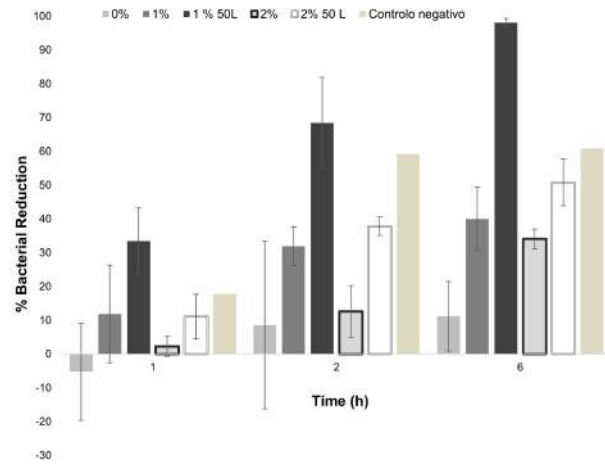


Imagem1.jpg

Synthesis and characterization of polyynes by pulsed laser ablation in organic solvents

Wednesday, 24th March - 12:05: Oral Session 1-1 (Room 1) - Abstract ID: 85

Dr. Pietro Marabotti¹, Dr. Sonia Peggiani¹, Dr. Anna Facibeni¹, Dr. Patrick Serafini¹, Prof. Alberto Milani¹, Prof. Valeria Russo¹, Prof. Andrea Li Bassi¹, Prof. Carlo Casari¹

1. Politecnico di Milano - Department of Energy

During the last decades, carbon atomic wires attracted the general interest of the scientific community thanks to their predicted appealing properties [1]. In particular, polyynes, one of the two possible structures of carbon atomic wires, are characterized by linear chains of alternated single and triple sp-hybridized carbon bonds. Polyynes can be efficiently synthesized by pulsed laser ablation in liquid (PLAL) that grants the possibility to obtain various chain lengths and terminating groups [2].

In this framework, we have analyzed ns-PLAL synthesis of a graphite target in different organic solvents and water. Ablation parameters have been investigated to maximize the synthesis yield and the degree of purity of the solutions was evaluated through UV-Vis absorption spectroscopy. We detected the presence of H-capped long polyynes up to HC₂₂H by high-performance liquid chromatography (HPLC), as reported in Fig. 1a. We also found polyynes with other terminations such as methyl- and cyano-groups (Fig. 1b and 1c), till HC₁₈CH₃ and HC₁₂CN, respectively.

Polyynes were separated through HPLC by their size and terminations to be probed by surface-enhanced Raman spectroscopy (SERS), which exploits the enhancement given by the interaction of carbon chains with metal nanoparticles. We identified the peculiar signal of sp-carbon chains that allowed us to distinguish between polyynes with different sizes and endgroups, as predicted by DFT calculations.

We achieved the synthesis of long polyynes through PLAL in organic solvents and we were able to control their terminating molecules through the choice of the ablation environment. The optimization of the synthesis process will allow us to produce molecules properly functionalized for future optical and electronic applications.

[1] C. S. Casari et al., *Nanoscale*, 2016, 8, 4414–4435.

[2] S. Peggiani et al., *Phys. Chem. Chem. Phys.*, 2020, 22, 26312–26321.

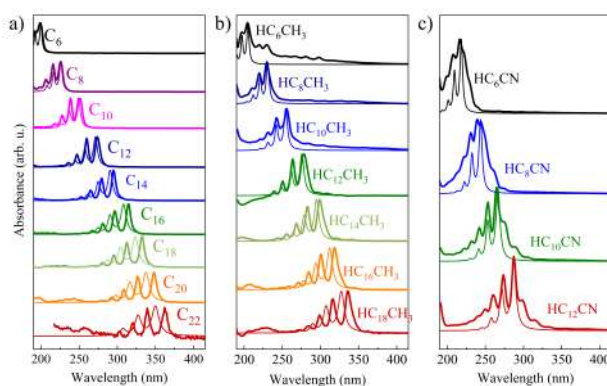


Fig1 annic.png

TBD

Wednesday, 24th March - 10:50: Oral Session 1-2 (Room 2) - Abstract ID: 307

Dr. Yu Kui¹

1. Sichuan University

TBD

Light-enhanced H₂O₂ sensing by supported AgAu bimetallic nanoshells as plasmonic nanozymes

Wednesday, 24th March - 11:20: Oral Session 1-2 (Room 2) - Abstract ID: 153

Mr. Rafael Trivella P. da Silva¹, Ms. Maria Paula de Souza Rodrigues¹, Mr. Adriano Marchini Rodrigues Puerta da Silva¹, Ms. Gabriela DAvilla¹, Prof. Susana Inés Cordoba de Torresi¹

1. University of São Paulo

The electrochemical detection of hydrogen peroxide (H₂O₂) is usually catalyzed by noble metals and, recently, by noble metals nanoparticles. Inorganic nanomaterials that perform enzyme-like reactions are called nanozymes. Nanomaterials show several advantages compared to their bulk counterparts, such as higher surface area and outstanding optical properties, as the localized surface plasmon resonance (LSPR). The LSPR is a phenomenon that has been studied on metallic nanoparticles for several applications, but few works focus on the use of LSPR for electrochemical sensors. In this work, we aim the use of LSPR stimulus to enhance H₂O₂ sensing catalyzed by a nanozyme, which is developed with an *in situ* synthesis of bimetallic nanoshells (AgAu nanoshells) onto two supports, graphene oxide (GOx) and silica (SiO₂).

The synthesis brings an innovative *in situ* approach, in which the previously supported silver nanoparticles (AgNP) are submitted to a galvanic replacement reaction to form the bimetallic AgAu nanoshells, as represented by TEM in Figure 1. ICP-OES analysis demonstrate that the mass ratio (Au:Ag) is approximately 1:1 for both materials. In Figure 2 the change in optical properties is observed by the shift and broadening of the LSPR band after the formation of AgAu nanoshells with the same mass ratio.

The application as H₂O₂ sensors proceeded by its reduction with a fixed potential of -0.3V vs Ag/AgCl KCl sat.. As demonstrated by the calibration curves in Figure 3, in dark conditions the GOx and SiO₂ showed better performance after the modification with the nanoshells. This demonstrates the important catalytic role that metallic NPs play in this reaction. For the plasmon-enhanced studies, laser sources with different wavelengths were used. Both AgAu/GOx and AgAu/SiO₂ improved their sensitivity with green laser incidence, indicating that LSPR stimulus is able to increase the catalyst activity. This mechanism is supported by AgAuGOx results, in which the stimulus by red laser, which is in resonance with the nanoshells maximum LSPR band range, presented an even better response. Besides, when violet laser was applied, which wavelength is outside the LSPR band range, it showed no difference compared to the dark condition, corroborating that the effects are correlated to the LSPR properties.

So far, we have demonstrated the innovative synthesis of a plasmon-responsive nanozyme with high stability for a wide range of substrate concentration. In the next steps we aim a deeper investigation on the material stability and changes in mechanism in the presence of LSPR stimulus.

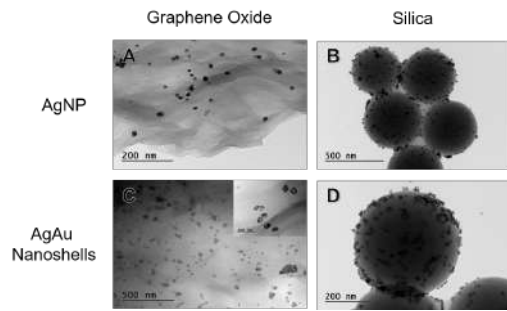


Figure 1.png

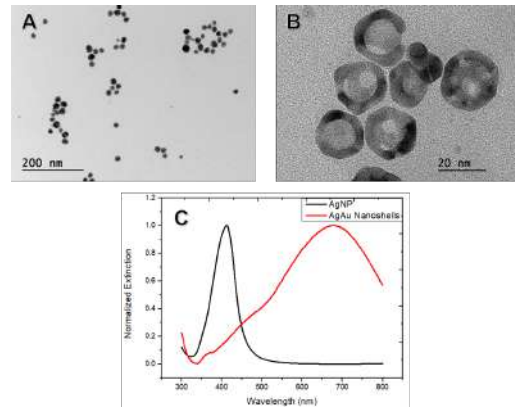


Figure 2.png

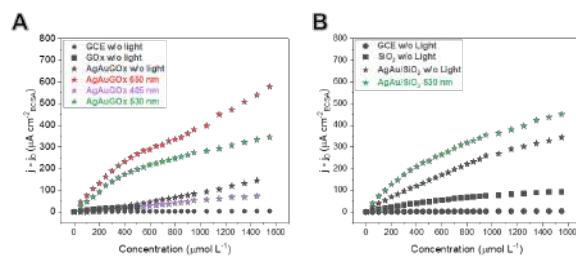


Figure 3.png

Examining the Efficacy of Freezing-thawing Cycles for Size Reduction of Beta-cyclodextrin Dextran Vesicles

Wednesday, 24th March - 11:35: Oral Session 1-2 (Room 2) - Abstract ID: 119

Mrs. Rukan Genç Altürk¹, Ms. Pınar Karacabey¹, Ms. Gamze Doğan²

1. Mersin University, Department of Chemical Engineering, **2.** Izmir Institute of Technology, Department of Bioengineering

In recent years, polymer-based nanomaterials with a focus on cyclodextrin containing ones have become more interesting for researchers since they are highly biocompatible and easy to functionalize (Raju & Werner, 2014; Crini et al., 2018). Besides, these distinguishing properties, homogeneous preparation of cyclodextrin-based nanostructures without use of an additional cross-linking step has been challenging (Kost et al., 2020). In this direction, developing an advanced and simple method to synthesize cyclodextrin nanovesicles has critical importance. In this study, the β -cyclodextrin-dextran polymer was synthesized (Nielsen et al., 2010), and the resulting long-chain polymer was used to form homogenous, perfectly shaped nanovesicles using consequent freeze-thaw cycles as a mild and easy method for the preparation of nanovesicles. After the reaction completed for β -cyclodextrin-dextran polymer, lyophilization was carried out to obtain white solid, then it was dissolved in water and again stored at -80 °C overnight and freeze-dried. The resulting nanovesicles were then characterized using ¹H NMR analysis and SEM images. SEM images of the β -cyclodextrin-dextran polymer dispersed in water, and processed using the freeze-thaw method were shown in Fig. 1. As can be seen from the image, after the first cycle of the lyophilization, particles appear to be a mixture of spherical-elliptic heterogeneous microparticles with a diameter of 1-5 μ m. Whereas, figure 1b shows the SEM images of the sample taken after the second lyophilization. Compared with Figure 1a, it was observed that the particle diameter decreased to an average of 450 nm vesicles successfully transform into highly homogeneous fine shaped nanospheres. Further analysis on drug encapsulation and release capacity of the vesicles showed that cyclodextrin-based nanovesicles obtained with no additional cross-linking step could successfully be implemented into biomedical applications and targeted drug delivery.

Keywords: β -cyclodextrin-dextran, polymeric nanomaterial, nanovesicles, freezing-thawing method

Acknowledgments: This work was supported by the Scientific and Technological Research Council of Turkey (TUBITAK) 1001 Project Grant No: 218M565.

References:

- Crini, G., Fourmentin, S., Fenyvesi, É., Torri, G., Fourmentin, M., & Morin-Crini, N., *Environmental Chemistry Letters*. 2018.16(4).1361–1375.
- Kost, B., Brzezinski, M., Socka, M., Basko, M., & Biela, T., *Molecules*. 2020. 25(15).
- Nielsen, T. T., Wintgens, V., Amiel, C., Wimmer, R., & Larsen, K. L., *Biomacromolecules*. 2010. 11(7). 1710–1715.
- Raju, L. J., & Werner, M. K. R. *Nanomedicine*. 2014. 9(6). 877–894.

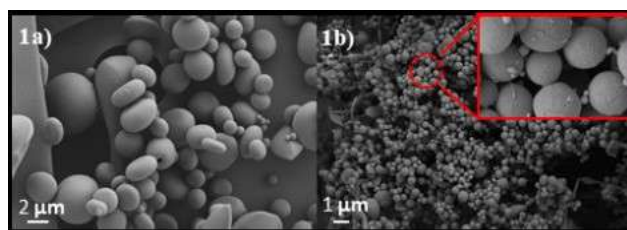


Figure 1. sem images for synthesized the -cyclodextrin-dextran polymers 1a spherical-elliptic shaped -cyclodextrin-dextran microspheres 1b nanovesicles obtained after second round..jpg

Transparent Multi-Color Emitting Carbon Dot/Polymer Films and Applications Thereof

Wednesday, 24th March - 11:50: Oral Session 1-2 (Room 2) - Abstract ID: 128

Dr. Rükan GENÇ ALTÜRK¹, Ms. Melis Özge ALAŞ², Mr. Sadin Özdemir³, Mr. Mustafa Serkan Yalçın⁴

1. Assoc. Prof. Dr. in university of mersin, **2.** Mersin University, Department of Chemical Engineering, **3.** Mersin University, Food Processing Programme, Technical Science Vocational School, **4.** Mersin University, Department of Chemistry and Chemical Processing Technologies

Carbon nanodots (CDs) are new hemispherical carbon-based nanoparticles with particle sizes smaller than 10 nm, which have attracted great attention due to their attractive photophysical properties, easy functionalization, cheap and easy preparation, low toxicity, and biocompatibility¹. CDs with high photoluminescence quantum efficiency have been promising materials for fluorescent materials in applications such as biomedical, sensing, light-emission diode (LED), energy storage and conversion, and optoelectronic devices²⁻⁶. Recently, polymer/quantum dot nanocomposites have received great attention to obtaining solid films of high transparency and high fluorescence for integration in various application areas. The polymer matrix provides mechanical and chemical stability and helps quantum dots to disperse and maintain their fluorescence. In the present study, multi-color emitting CDs were synthesized according to our previously reported method⁷. CDs were synthesized from various carbon sources (molasses, lemon salt, etc.) using a one-step thermal and microwave synthesis method. Fluorescent and transparent CD / Polyvinyl alcohol (PVA) films are prepared using the solvent-casting method by *in situ* embedding CDs into the PVA polymer matrix. Optical (UV-Vis, fluorescence emission), surface morphology (SEM), and chemical (FTIR, TGA) properties and biological activities (anti-microbial, biofilm inhibition) of these films were investigated. Thus, the composite materials obtained could later be used for designing smart polymeric materials for their use in the development of advanced optical devices, skincare materials, and food protection layers.

Acknowledgment

This study was supported by Mersin University Scientific Research Project Unit (Project No: BAP-2019-2-TP3-3599). Furthermore, MOA thanks TUBITAK and the Council of Higher Education of Turkey (YOK) for the doctoral scholarship.

References

- 1 S. D. Çalhan, M. Ö. Alas, M. Aşık, F. N. D. Kaya and R. Genç, *J. Mater. Sci.*, 2018, **53**, 15362–15375.
- 2 R. Genc, M. O. Alas, E. Harputlu, S. Repp, N. Kremer, M. Castellano, S. G. Colak, K. Ocakoglu and E. Erdem, *Sci. Rep.*, 2017, **7**, 11222.
- 3 B. Rezaei, Z. Hassani, M. Shahshahanipour and et al., *Luminescence*, 2018, **33**, 1377–1386.
- 4 Z. Tian, X. Zhang, D. Li, D. Zhou, P. Jing, D. Shen, S. Qu, R. Zboril and A. L. Rogach, *Adv. Opt. Mater.*, 2017, **5**, 1700416.
- 5 R. Bahadur, M. K. Kumawat, M. Thakur and R. Srivastava, *J. Lumin.*, 2019, **208**, 428–436.
- 6 H. Li, W. Shi, W. Huang, E. P. Yao, J. Han, Z. Chen, S. Liu, Y. Shen, M. Wang and Y. Yang, *Nano Lett.*, 2017, **17**, 2328–2335.
- 7 M. O. Alas and R. Genc, *J. Nanoparticle Res.*, 2017, **19**, 185–199.

Spatial defects nanoengineering for bipolar conductivity in MoS₂

Wednesday, 24th March - 12:05: Oral Session 1-2 (Room 2) - Abstract ID: 172

Dr. Annalisa Calò¹

1. IBEC Barcelona

Two-dimensional transition metal dichalcogenides show great potential as a new class of atomically thin semiconductors for electronics and optoelectronics. Understanding the atomistic origin of defects in these materials and their impact on the electronic properties, as well as finding viable ways to dope them is matter of intense scientific and technological interest. In particular, controlling defects could be envisioned as a strategy for the design of ad-hoc electronic and optoelectronic properties. Here, we demonstrate a new integration of thermochemical scanning probe lithography (tc-SPL) with a flow-through reactive gas cell to achieve a nanoscale control of the local thermal activation of defects in monolayer MoS₂. The tc-SPL activated nanopatterns can present either p- or n-type doping on demand, depending on the used gasses, allowing the realization of field effect transistors, and p-n junctions with precise sub-mm spatial control and a rectification ratio over 10⁴. Doping and defects formation mechanisms are elucidated at the molecular level by means of X-Ray photoelectron spectroscopy, scanning transmission electron microscopy, and density functional theory. The p-type doping of locally heated MoS₂ in HCl/H₂O atmosphere is found to be related to the rearrangement of sulfur atoms and the formation of new protruding covalent S-S bonds on the surface, which produce a band structure with p-character. Alternatively, local heating MoS₂ in N₂ produces n-character.

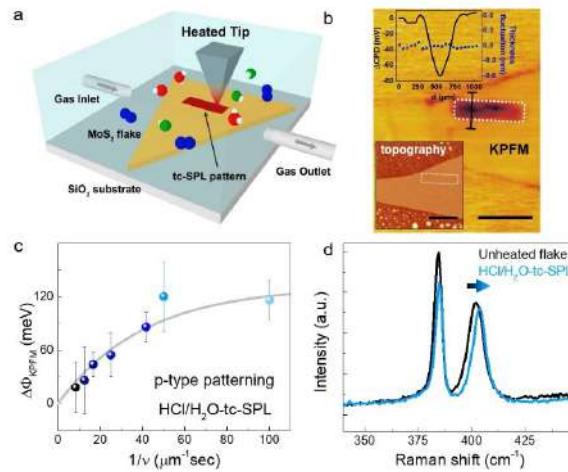


Fig1.jpg

Use of magnetic field for structuring supercapacitor electrodes

Wednesday, 24th March - 13:30: Flash Session 1 (Room 1) - Abstract ID: 127

Dr. Nicolas Goubard¹, Dr. Frédéric Favier², Prof. Thierry Brousse¹

1. Institut des Matériaux Jean Rouxel de Nantes (IMN), Réseau sur le Stockage Electrochimique de l'Énergie (RS2E), **2.** Institut Charles Gerhardt de Montpellier (ICGM), Réseau sur le Stockage Electrochimique de l'Énergie (RS2E)

Supercapacitor and battery electrodes are classically prepared by dispersing an active material, a conductive additive (usually carbon black) and a binder in a solvent, before coating the obtained slurry on a current collector.

An issue of this conventional electrode preparation is the use of an isolating binder, such as polyvinylidene fluoride (PVDF) or polytetrafluoroethylene (PTFE), which has therefore a negative impact on the electronic conductivity of the electrode.

This work deals with another strategy for the manufacturing of binder-free electrodes which relies on the use of ferromagnetic active materials and a magnetic field. Different approaches are studied.

As such, binder-free electrodes are prepared by simply depositing ferromagnetic active materials on a current collector by magnetization. In this case, the use of the magnetic field can allow grain orientation on the current collector, thus reducing tortuosity and providing better access to the active sites for the electrolyte ions.

Among the compounds studied, spinel-structured MnFe_2O_4 offers several advantages. First of all, this ferromagnetic supercapacitor electrode material displays what is commonly known as a pseudocapacitive behavior (see fig. 1). This means that its electrochemical signature is close to that of a capacitive activated carbon, but its origin differs from a simple adsorption of ions at the surface of the electrode. In this case, fast redox reactions occur, potentially leading to higher capacitance values. Moreover, MnFe_2O_4 is fairly easy to synthesize by means of soft chemistry routes as nanoparticles developing a large surface area, which are favorable to pseudocapacitive reactions.

The material was obtained using a solvothermal route and electrodes were prepared by magnetization. Electrochemical measurements were performed in a neutral aqueous electrolyte. The presentation will discuss the different strategies and the results obtained.

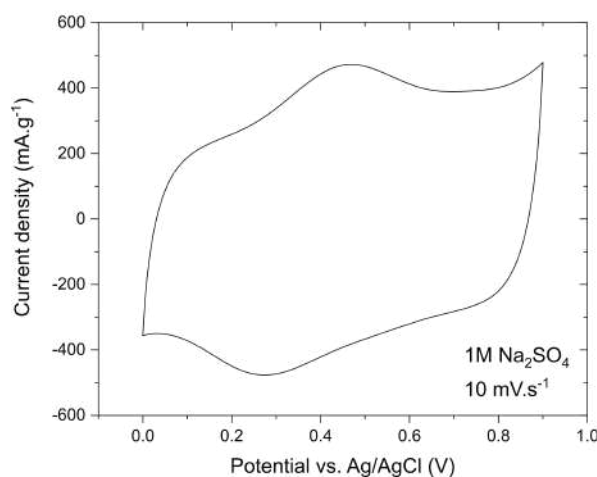


Fig. 1 - electrochemistry mnfe2o4.png

Surface Functionalized Nickel Sulfide Nanostructures for pH Responsive Selective Adsorption of Pollutants

Wednesday, 24th March - 13:33: Flash Session 1 (Room 1) - Abstract ID: 134

***Ms. SUNITA KUMARI*¹**

1. Department of Chemistry, Indian Institute of Technology Patna

Introduction

Organic dyes and antibiotics are some of the foremost contributors to water pollution. In the present scenario, selective adsorption of pollutants by changing only the adsorption conditions is challenging and desirable. Nanostructures with the functionalized surfaces may selectively remove targeted pollutants. Herein, we developed a strategy to functionalize nickel sulfide nanostructures (NS) with cetyltrimethylammonium bromide (CTAB) and sodium dodecyl sulfate (SDS) surfactants containing -NR_3^+ and -OSO_3^- groups for achieving the adsorption selectivity.

Methods

Nickel sulfide (Ni-S) nanostructures were synthesized using a facile precipitation method using nickel acetate tetrahydrate as a metal precursor, thioacetamide as the sulfur source and a mixture of CTAB and SDS in different concentration ratio.

Results

Powder XRD diffraction patterns (Fig 1.) revealed the phase of NS was changed from $\alpha\text{-NiS}$ (NSC-0) to mixed phases after functionalization (NSC-3). The surface area of functionalized NS was significantly enhanced by ~ 5 times of that unfunctionalized NS as $6.6 \text{ m}^2\text{g}^{-1}$ to $30.3 \text{ m}^2\text{g}^{-1}$. This zero point charge value of NS is 10.1 indicating a negative surface charge above pH 10.1 and a positive surface charge below pH 10.1 (Fig. 2). Thus, NS selectively adsorbed MO at pH 4.5 and MB at pH 11.5 (Fig. 3). The adsorption of MO, MB and CIP were well elucidated by the Langmuir isotherm model and the adsorption of TC followed the Temkin isotherm model. The adsorption process followed pseudo-second-order kinetics. The maximum adsorption capacity for MO, MB, TC and CIP are obtained as 1526.3, 1031.2, 1540.8 and 632.4 mg g^{-1} , respectively. The electrostatic interaction is predominantly involved in the adsorption of dyes whereas the adsorption of antibiotics includes hydrogen bonding and metal coordination. Thermodynamics parameters indicated exothermic and spontaneous adsorption of dyes. The adsorbent is easily recyclable up to 4 times.

Fig. 1. Powder XRD patterns of NSC-0 and NSC-3.

Fig. 2. Effect of pH on zeta potential values of NSC-3.

Fig. 3. UV-vis spectra of adsorption of a mixture of MB and MO on NSC-3 at pH 4.5 and pH 11.5.

Discussion

The functionalization of nanostructures was controlled using different concentration ratios of mixed surfactants (CTAB + SDS). The adsorbent revealed impressive pH-responsive surface charge properties and selective adsorption of anionic and cationic dyes. The developed synthetic methodology of nanostructures has the advantages of a simple and cost-effective functionalization process for pH-responsive selective and efficient adsorption of pollutants.

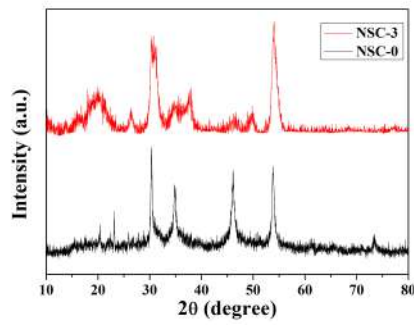


Fig. 1.jpg

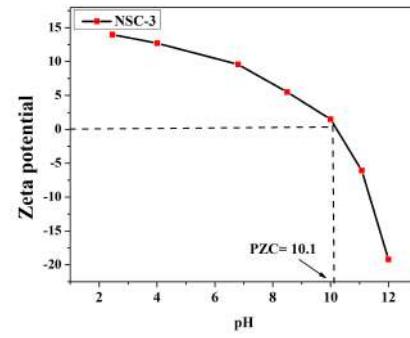


Fig. 2.jpg

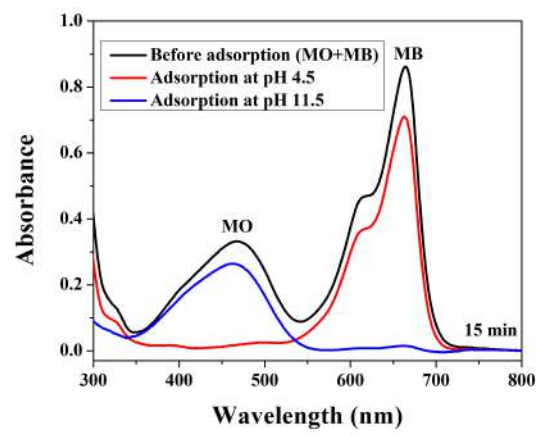


Fig. 3.jpg

Electrocatalytic properties of synthesized Co-Fe nanocones obtained using crystal growth modifier with applied, superimposed magnetic field

Wednesday, 24th March - 13:36: Flash Session 1 (Room 1) - Abstract ID: 1

Ms. Katarzyna Skibińska¹, Dr. Karolina Kolczyk-Siedlecka¹, Dr. Dawid Kutyla¹, Mrs. Anna Jedraczka¹, Prof. Piotr Zabinski¹

1. Faculty of Non-Ferrous Metals, AGH University of Science and Technology, Mickiewicza 30, 30-059, Krakow

Introduction

One-step method allows to obtain materials with various shapes during a single electrodeposition process. It is connected with addition of crystal modifier. The mechanism of synthesis based on screw dislocation driven crystal growth theory. It means that defects are located in specific positions, onto which metal ion is deposited. Crystal modifier promotes the vertical direction of growth and blocks the horizontal one. One-step method is also environment-friendly. It does not require using chromic acid like two-step anodization method. During electrochemical deposition large areas can be covered with differently shaped structures.

Methods

In this work Co-Fe cones were obtained by one-step method. Ammonium chloride was used as a crystal modifier. The influence of electrodeposition parameters was investigated. Electrodeposition conditions, which allow to obtain conical structures characterized by the best quality, were chosen for the application of magnetic field. The quality of obtained structures was investigated using SEM photos. The composition of alloys was analyzed using EDS.

The influence of the applied magnetic field direction and intensity on quality, morphology and composition of alloy was determined.

The electrocatalytic properties of the obtained nanomaterials were measured in 1 M NaOH. These materials can be used as a catalysts in the water splitting reaction. The electrocatalytic activity of these cones were compared with bulk material and cones obtained by two-step anodization method.

Results and discussion

Obtained results confirmed that it is possible to obtain conical Co-Fe structures using crystal modifier. SEM photo of obtained structures is shown in Fig. 1.

Fig. 1 Conical Co-Fe alloy structures obtained from the electrolyte containing crystal modifier.

There is also noticeable influence of magnetic field application on quality of produced deposits. The results are shown in Fig. 2.

Fig. 2 Deposits synthesized in presence of (a) perpendicular and (b) parallel magnetic field.

Acknowledgments

This work was financially supported by Polish National Science Center (NCN) under grant UMO-2016/23/G/ST5/04058.

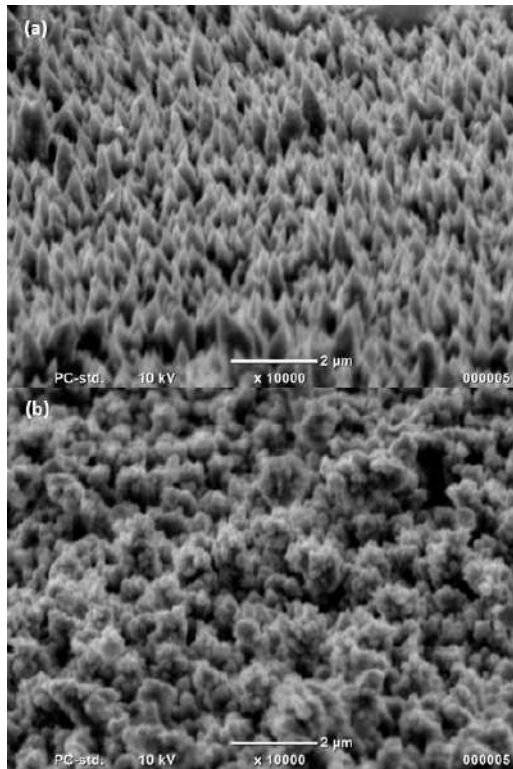


Fig 2.jpg

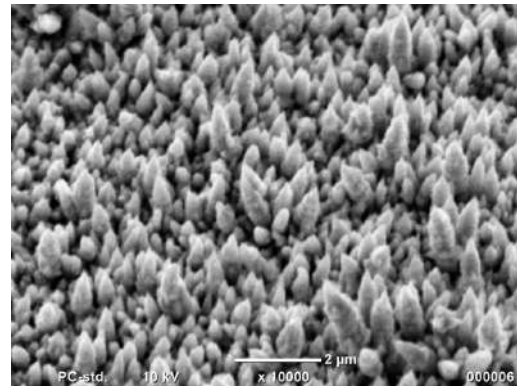


Fig 1.jpg

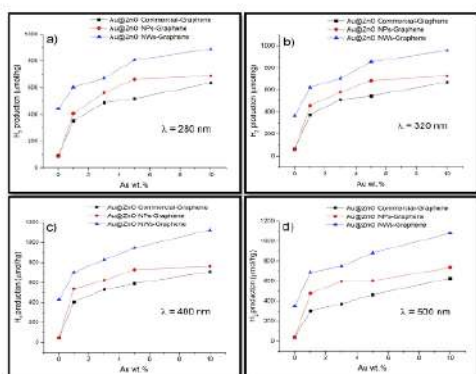
Hydrogen production using Au@ZnO-Graphene by Water Splitting

Wednesday, 24th March - 13:39: Flash Session 1 (Room 1) - Abstract ID: 165

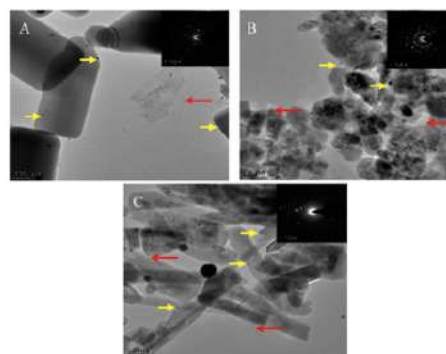
Mr. Bryan Bentz¹

1. Universidad Ana G. Méndez-Gurabo Campus, Gurabo, PR 00778

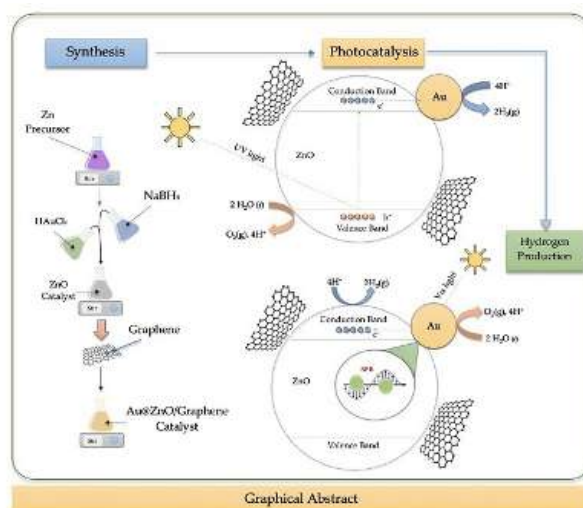
Multiple environmental challenges have been presented in the last century. One of them, is the continuous injection of CO₂ into the atmosphere due to the burning of fossil fuels for energy generation. Is for that reason that one of the focus of the 21st century is to develop clean and renewable sources of energy. One of the candidates that have been proposed as a replacement of fossil fuels is hydrogen. Currently, the production of hydrogen is mainly derived from fossil fuels which release carbon dioxide and other gases to the atmosphere. A potentially viable way forward is to produce hydrogen from water by combining solar energy and heterogeneous photocatalysis. For these reasons, the objectives of these investigations were: 1) Synthesize and characterize different gold-based (1 wt.%, 3 wt.%, 5 wt.%, 10 wt.%) zinc oxide catalysts; 2) produce hydrogen via water splitting using visible and UV light; 3) characterized by FE-SEM, EDS, BET, UV spectroscopy and XRD. The hypothesis of the study was: a) catalyst with higher surface are will produce the largest amount of hydrogen, and b) The gold nanoparticles will enhance the hydrogen production and will allow the use of visible light. The higher hydrogen production obtained using Au@ZnO-Graphene catalysts was 759 $\mu\text{mol/hg}$ at 400 nm and was obtained with 10%Au@ZnO NPs-graphene. The results of this study open the possibility to design green technologies contributing to the development of new and more efficient catalysts, and the development of alternatives for the production of clean and renewable energy.



Screen shot 2021-01-22 at 6.50.53 pm.png



Screen shot 2021-01-22 at 6.50.46 pm.png



Screen shot 2021-01-22 at 6.50.37 pm.png

Sub-nano Gold–Cobalt Particles as Effective Catalysts in the Synthesis of Propargylamines

Wednesday, 24th March - 13:42: Flash Session 1 (Room 1) - Abstract ID: 193

Dr. BERRICHI AMINA ¹, Prof. Bachir Redoaune ¹, Prof. Bedrane Sumeya ¹, Ms. Bensaad meriem ¹, Prof. Choukchou-Braham Nouredine ¹

1. Laboratory of Catalysis and Synthesis in Organic Chemistry, University of Tlemcen, BP 119, Tlemcen, Algeria

Titania supported Au–Co catalysts with nano- and sub-nanoparticles, were prepared with 1% Au and different contents of cobalt by one pot deposition precipitation with urea. Monometallic gold and cobalt catalysts were also prepared

by the same method for a comparative purpose. The characterization of bimetallic catalyst evidenced the presence of subnanoparticles

where 50% of cobalt and 40% of gold particles are smaller than 1 nm and the formation Au–Co particles. The results show a positive effect of cobalt on gold particles size and the catalytic activity. The effectiveness of these catalysts

in the synthesis of several propargylamines via amine, CH_2Cl_2

and alkyne coupling (AHA coupling) was demonstrated.

Different propargylamines were synthesized with very good yields (71%–88%). A comparative study of monometallic gold,

monometallic cobalt and bimetallic gold–cobalt catalysts was investigated. The most efficient catalyst was reused for up to

six reaction cycles without significant activity loss.

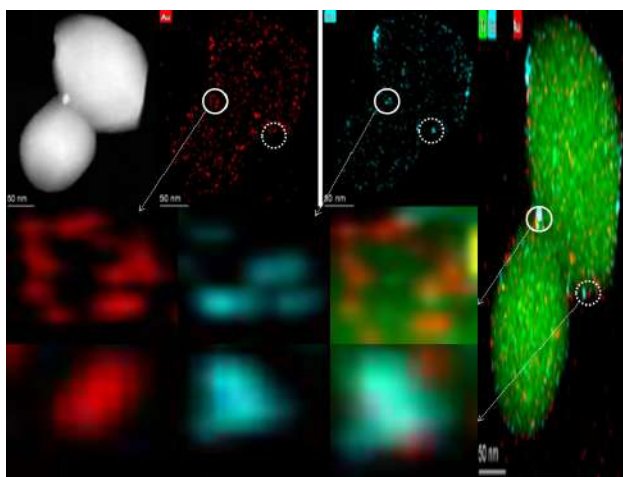


Image met.png

Effect of surfactant on TiO₂ electrophoretic deposition for the formation of photocatalytically active layers

Wednesday, 24th March - 13:45: Flash Session 1 (Room 1) - Abstract ID: 247

***Ms. Larisa Sorokina*¹, *Dr. Egor Lebedev*¹, *Mr. Sergey Dubkov*¹, *Mr. Roman Ryazanov*², *Prof. Tomasz Maniecki*³, *Prof. Dmitry Gromov*¹**

1. National Research University of Electronic Technology - MIET, 2. Scientific-Manufacturing Complex "Technological Centre",

3. Lodz University of Technology

Today, photocatalytic reactions occurring in TiO₂-based materials are actively studied to solve various problems: energy fuel generation, air and water purification, and much more. One of the available methods of forming photocatalytic layers is electrophoretic deposition technology, which is based on the electrokinetic movement of particles from a suspension under the influence of an electric field. The main problem in the development of the electrophoretic deposition technique is the creation of a stable suspension that ensures the process reproducibility. This paper presents the results of the effect of sodium lauryl sulfate (SLS) on the stability of a suspension with TiO₂ particles. The influence of the electrophysical parameters of the deposition process on the layer morphology and the decoration by Au and Ag particles on the photocatalytic activity is also considered.

The electrophoretic deposition was carried out on a stainless-steel mesh substrate from a suspension based on isopropyl alcohol, the TiO₂ nanopowder (particle size 20 nm), and SLS in different weight ratios. Au and Ag particles on the TiO₂ deposited layer were formed by vacuum thermal evaporation. The surface morphology, thickness, and stoichiometry of the obtained samples were studied by scanning electronic microscopy and energy dispersive X-ray analysis. The photocatalytic activity was investigated based on the carbon dioxide photoreduction. The quantitative and qualitative gas analysis was performed on a gas chromatograph with a flame ionization detector.

Based on the results of the experiments, the optimal SLS ratio and the most suitable mode of the process were determined. Figure 1 shows the SEM image of the TiO₂ layer formed by electrophoretic deposition. Figure 2 shows the SEM image of the TiO₂ layer with Au particles. Modification by Au and Ag particles significantly improved photocatalytic activity. The main product of the carbon dioxide photoreduction was methane.

This work was supported by the Russian Science Foundation (project No. 19-19-00595).

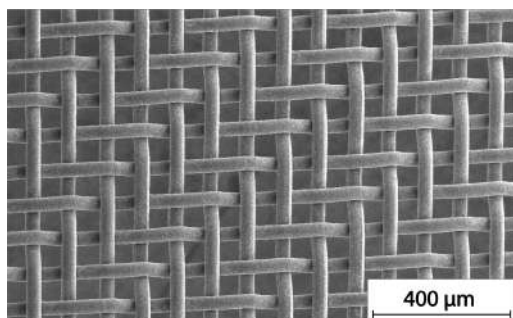


Fig 1 sem image of the tio2 layer on a stainless-steel mesh.png

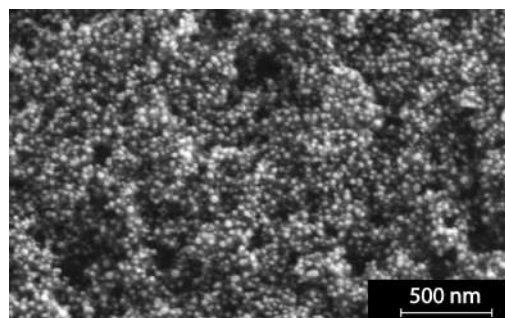


Fig 2 sem image of the tio2 layer with au particles.png

Sub-10 nm resolution patterning of pockets for enzyme immobilization via tc-SPL

Wednesday, 24th March - 13:48: Flash Session 1 (Room 1) - Abstract ID: 173

Dr. Annalisa Calò¹

1. IBEC Barcelona

The ability to precisely control the localization of enzymes on a surface is critical for several applications including biosensing, nano-bioreactors and single molecule studies. Despite recent advances, fabrication of enzyme patterns with resolution at the single enzyme level is limited by the lack of lithography methods that combine high resolution, compatibility with soft, polymeric structures, ease of fabrication and high throughput. Here, a method to generate enzyme nanopatterns on a polymer surface is demonstrated using thermochemical scanning probe lithography (tc-SPL) and the enzyme Thermolysin as a model system. Electrostatic immobilization of negatively charged sulfonated enzymes occurs selectively at positively charged amine nanopatterns produced by thermal deprotection of amines along the side-chain of a methacrylate-based copolymer film via tc-SPL. This process occurs simultaneously with local thermal quasi-3D topographical patterning of the same polymer, offering lateral sub-10 nm resolution and vertical 1 nm resolution, as well as high throughput ($5.2 \times 10^4 \text{ mm}^2/\text{h}$). The obtained patterns with single enzyme resolution are characterized by atomic force microscopy (AFM) and fluorescent microscopy. The enzyme density, the surface passivation and the quasi 3D arbitrary geometry of these patterned pockets are directly controlled in a single step, without the need of markers or masks. Other unique features of this patterning approach include the combined single-enzyme resolution over mm^2 areas and the possibility of fabricating enzymes gradients at the nanoscale.

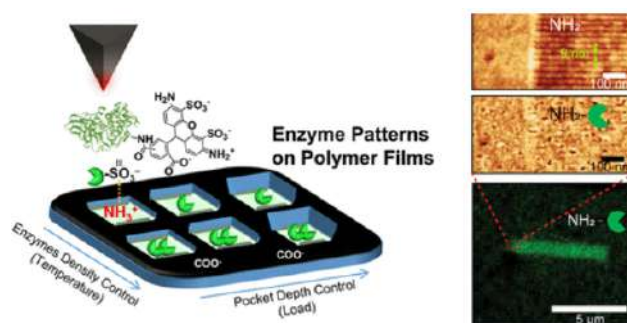


Fig1.png

A two-dimensional photonic crystal resonator for high pressure sensing

Wednesday, 24th March - 13:30: Flash Session 1 (Room 2) - Abstract ID: 286

Dr. Amel Bounouioua¹, Ms. Ahlem BENMERKHI¹, Prof. Bouchemat mohamed²

1. University Constantine, 2. Laboratoire Microsystemes et Instrumentation Département d'Electronique

In this work, a two dimensional photonic crystal pressure sensor with high quality factor, transmission and sensitivity is investigated. The sensor construction is based on an SOI layer of 252 nm high (h) where we have air upper and lower claddings ($n_{air} = 1$) in a silicon slab profile ($n_{Si} = 3.4$). The proposed device structure consists of two waveguides coupled with a middle resonator formed by air pores default. For this optical sensor, the operating mechanism relies on the device optical properties change due to the analyte refractive index (RI) variation. The sensor properties are then optimized by the modification of the number and the position of the resonator neighboring holes. Using the finite difference time domain algorithm, we obtained a linear shift up of the structure resonant wavelength when the applied pressure increases within the range 0-6 GPa. The obtained results are summarized in table 1 and 2. For a certain value of surrounding holes displacement, the device sensitivity becomes very advantageous achieving 19 nm/GPa with relatively high quality factor value of 4812.

Table 1: The corresponding refractive index, resonant mode, and Q factor for different pressures with the four holes positions were adjusted to lie slightly inside the cavity.

Level of pressure	Refractive index	Resonance Wavelength (μm)	Q -factor
0 GPa	2.83000	1.4505	3388.6
1 GPa	2.86967	1.4686	3616.6
2 GPa	2.90935	1.4867	3849.4
3 GPa	2.94902	1.5057	4085.9
4 GPa	2.98870	1.5230	4325.7
5 GPa	3.02838	1.5419	4568
6 GPa	3.06805	1.5595	4812.1

Table 2: The corresponding refractive index, resonant mode, and Q factor for different pressures with the eight holes positions were adjusted to lie slightly inside the cavity.

Level of pressure	Refractive index	Resonance Wavelength (μm)	Q -factor
0 GPa	2.83000	1.4418	2878.8
1 GPa	2.86967	1.4598	3049.5
2 GPa	2.90935	1.4779	3220.6
3 GPa	2.94902	1.4960	3392.6
4 GPa	2.98870	1.5141	3564.6
5 GPa	3.02838	1.5323	3735.8
6 GPa	3.06805	1.5505	3907.5

Tables 1 et 2.png

Hybrid Soret Nano-Assemblies for Mobile Phone-based Ultrasensitive Copper Ion Sensing

Wednesday, 24th March - 13:33: Flash Session 1 (Room 2) - Abstract ID: 115

Mr. Seemesh Bhaskar¹, Dr. Sai Sathish Ramamurthy¹

1. STAR Lab, Central Research Instruments Facility (CRIF), Department of Chemistry, Sri Sathya Sai Institute of Higher Learning, Prashanthi Nilayam, A. P.

Introduction

Utility of functional nanomaterials to augment electromagnetic (EM) field intensity is seldom studied using hybrid nano-assemblies. We demonstrate a thermo-migratively fabricated Soret nano-assembly that enable unique metal-metal, metal-graphene oxide and metal-dielectric resonances. The Soret colloids (SCs) of silver metal with plasmonic NPs: platinum (AgPtSC), 2D material: graphene oxide (AgGOSC) and dielectric NPs: TiC (AgTiCSC), TiN (AgTiNSC) and TiCN (AgTiCNSC) comprehensively have been utilized to achieve >600-fold fluorescence enhancements. The ability to tailor the highly directional and polarized emission enhancements using these well-characterized hybrid soret nano-assemblies has been experimentally demonstrated on surface plasmon-coupled emission (SPCE) platform. The mobile phone-based detection of environmentally relevant Cu²⁺ ions in drinking water using AgPtSC presents low-cost, rapid, simple, sensitive and reliable sensing strategy for Cu²⁺ ion monitoring in resource-limited settings.

Methods

A thermal-gradient driven self-assembly of nanoparticles, under adiabatic conditions, is demonstrated for synthesis of monodisperse nano-assemblies, termed Sorets [1-4]. Briefly, the nanomaterials of interest are admixed along with AgNPs and subjected to defined time interval of adiabatic cooling to obtain hybrid soret colloids. The TEM, HRTEM, SAED images confirming the structural and morphological characteristics of the hybrid sorets synthesized are given in **Figure 1**. These hybrid sorets were interfaced on SPCE substrate (50 nm Ag thin film) and studied in reverse Kretschmann optical configuration using 532 nm laser source in spacer and cavity nanointerfaces (**Figure 2**). Fluorophores used are Rh6G with excitation and emission maximum at 530 nm and 560 nm respectively. The Free space (FS) emission and SPCE were collected and SPCE/FS formula was used to calculate the emission enhancements. The conventional Ocean Optics detector was replaced by user-friendly smartphone (iPhone 4) detector for collection of SPCE.

Results and Discussion

Tunable enhancements were obtained using hybrid multifunctional sorets. Utilization of AgPtSC in spacer nanointerface presented unprecedented >600-fold enhancements, in spacer nanointerface in SPCE with high directionality and p-polarization. In comparison to the standalone plasmonic and dielectric platforms, the Soret colloids possess outstanding nanovoids and nanocavities that display delocalized Bragg and localized Mie plasmon resonances with effective EM field confinement abilities. This high enhancement was utilized for mobile phone-based sensing of Cu²⁺ ions in SPCE (**Figure 3**). The judicious synergy of nanomaterials obtained here, is expected to be of use in diverse applications. This study opens a new window to explore other nanomaterials constituting elements from different parts of periodic table to achieve essential properties for desired applications.

References

1. <https://doi.org/10.1021/acssuschemeng.8b02050>
2. <https://doi.org/10.1021/acssuschemeng.0c00902>
3. <https://doi.org/10.1002/jrs.5587>
4. <https://doi.org/10.1021/acsanm.0c00470>

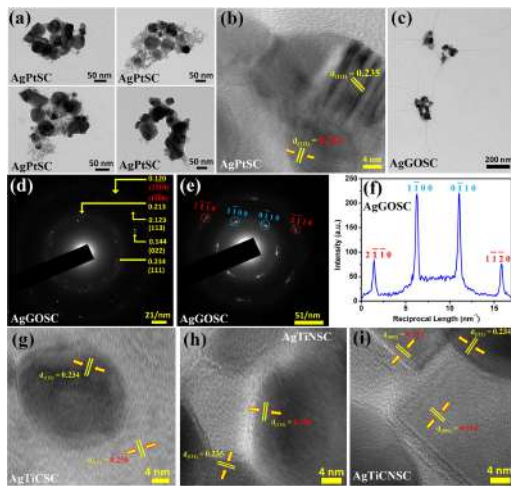


Figure 1 a tem images of agptsc. b hrtem image of agptsc. c tem image of aggosc. d e saed of aggosc. f intensity line-profile for e. hrtem images of g agticsc h agtinsc and i agticnsc..jpg

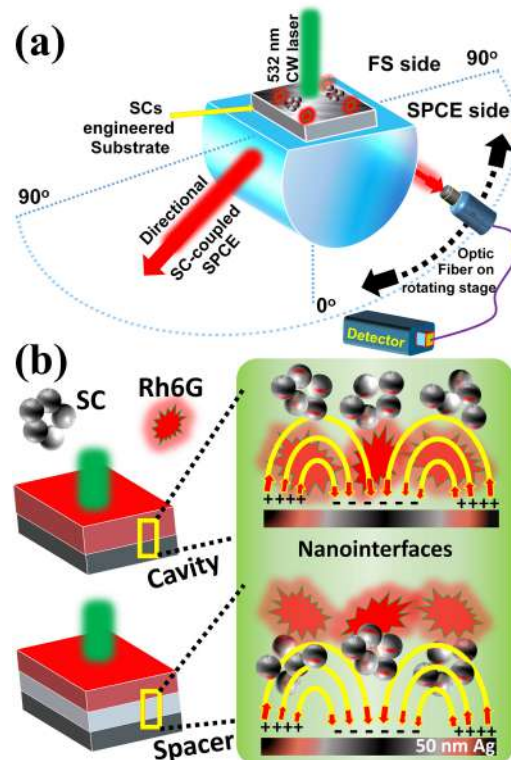


Figure 2. a . conceptual spce optical setup indicating rk excitation of sc engineered spce substrate and directional out-coupled emission. b cavity and spacer nanointerfaces are presented at micro-and nano-resolution..jpg

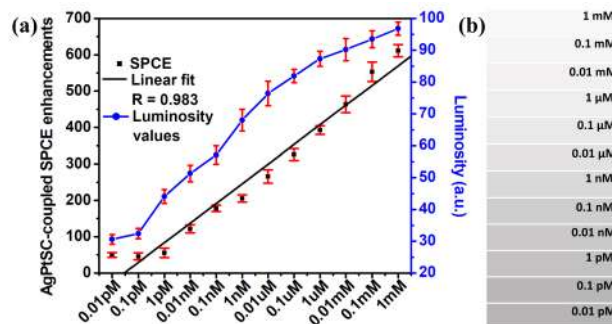


Figure 3. a agptsc-coupled emission enhancements left y-axis and luminosity values right y-axis obtained for different concentrations of cu2 ions. b shade cards corresponding to the luminosity values..jpg

Nanofabrication of controlled design plasmonic gold substrates by direct laser writing

Wednesday, 24th March - 13:36: Flash Session 1 (Room 2) - Abstract ID: 288

Dr. Nicoleta Tosa¹, Dr. Lucian Barbu-Tudoran¹, Dr. Cosmin Farcau¹

1. National Institute for Research and Development of Isotopic and Molecular Technologies

Introduction

The fabrication of metal micro / nanostructures using femtosecond lasers is of great interest, both in terms of the processes that take place and applications. The nature of the material used, the absorption process type as well as the radiation wavelength used represent defining aspects for the fabrication process. The essential aspect consists in the laser-substrate interaction spatial localization at the focal point in a very small volume of the laser spot. Optical lithography by direct laser writing (DLW) thus allows the development of material processing technique for mastering the design of new metallic nanostructured substrates as plasmonic nanomaterials for environmental detection.

Methods

The samples were irradiated at 380 nm using a DLW setup (Olympus IX 71inverted microscope, XYZ piezo nanopositioning system with 1 nm resolution from Physik Instrumente, Yb:KGdW ultrafast femtosecond laser from Light Conversion with 170 fs pulse duration and 80 kHz repetition rate). The samples were spectroscopically investigated (HR2000+ from Ocean Optics) and morphologically characterized by SEM (SU-8230 from Hitachi). All depositions were carried out using tetrachloroauric acid and poly (4-styrenesulfonic acid).

Results

Gold structures with varied geometries were created in thin films by DLW micro/nanopatterning process at varied velocities from 1 $\mu\text{m/s}$ to 25 $\mu\text{m/s}$. The width of the nanopatterned structures is influenced by the laser intensity, ranging from tens to a few microns. Optical images showed regular and reproducible shapes of the nanostructured patterns. UV-Vis spectra were recorded every 5 microns along the pathway and showed a similar plasmonic response, characteristic to the presence of gold nanoparticles. SEM images showed a uniform nanoparticles size distribution within the nanomaterial in agreement with the spectroscopic response.

Discussion

The nanopatterned gold structures were selectively generated in thin film displaying adjustable shapes and dimensions according to the process parameters. The higher the speed, the lower the structure width is due to laser exposure time decrease. Gold written structures are made up of nanoparticles with shape and size evenly distributed along the pattern. Gold nanoparticles are anchored to the activated surface proving that the DLW patterns can serve as plasmonic nanomaterials type support for environmental detection.

The research leading to these results has received funding from the NO Grants 2014-2021, under Project contract no. 32/2020.

Characterization of transport properties and field emission in MoS₂ Field-Effect Transistors

Wednesday, 24th March - 13:39: Flash Session 1 (Room 2) - Abstract ID: 93

Dr. Filippo Giubileo¹, Mr. Aniello Pelella², Mr. Enver Faella², Mr. Alessandro Grillo², Dr. Francesca Urban², Prof. Antonio Di Bartolomeo²

1. CNR-SPIN, 2. University of Salerno

We report a detailed electrical characterization of MoS₂ field-effect transistors (FETs), performed inside a scanning electron microscope (SEM), to study the transport properties and the effects of electron irradiation and of the gas-type and pressure in which the device is placed.

We demonstrate an increase of the carrier mobility and a negative shift of the threshold voltage for successive low-energy irradiations that is explained in terms of positive charge trapped in the SiO₂ gate dielectric, during the irradiation [1]. The transistor channel current is increased up to three orders of magnitudes after the exposure to an irradiation dose of 100 e⁻/nm².

We study the effect of electric stress, gas pressure, and gas type on the hysteresis in the transfer characteristics of monolayer MoS₂ FETs. The presence of defects and point vacancies in the MoS₂ crystal structure facilitates the adsorption of oxygen, nitrogen, hydrogen, or methane, which strongly affects the transistor electrical characteristics. Although the gas adsorption does not modify the conduction type, we demonstrate a correlation between hysteresis width and adsorption energy onto the MoS₂ surface [2].

Moreover, profiting of the measurement setup with nanomanipulated metallic probe-tips inside the SEM chamber, we also perform a complete characterization of the field emission properties of the MoS₂ nanosheets. Indeed, the sharp edges and high aspect ratio of the nanosheets favor the electron emission, making this material suitable to realize field emission cathodes [3,4].

Figure 1: (a) Schematic of the MoS₂ FET under e-beam irradiation. (b) transfer characteristics I_{ds} - V_{gs} measured at $V_{ds} = 1.6$ V for different electron beam irradiation doses. (c) Field emission characterization of MoS₂ flake. I-V curve measured at cathode-anode separation $d = 300$ nm. Left inset: FN-plot of the experimental data. Red line is the linear fit.

REFERENCES

- [1] F. Giubileo, L. Iemmo, M. Passacantando, F. Urban, G. Luongo, ... A. Di Bartolomeo, J. Phys. Chem. C 123 (2019) 1454–1461.
- [2] F. Urban, F. Giubileo, A. Grillo, L. Iemmo, G. Luongo, M. Passacantando, ..., A. Di Bartolomeo, 2D Materials 6 (2019) 045049
- [3] F. Urban, M. Passacantando, F. Giubileo, L. Iemmo, A. Di Bartolomeo, Nanomaterials 8 (2018) 151.
- [4] F. Giubileo, A. Grillo, M. Passacantando, ... A. Di Bartolomeo, Nanomaterials 9 (2019) 717.

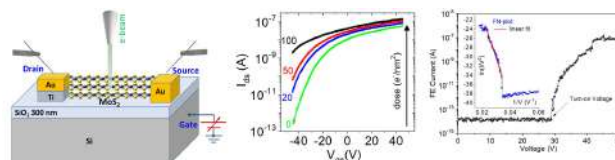


Figura annic.jpg

Grafted Zinc Phthalocyanine to Organic Copolymers as Effective Photosensitizer for Photodynamic Processes

Wednesday, 24th March - 13:42: Flash Session 1 (Room 2) - Abstract ID: 265

Dr. Tamara Potlog¹, Mr. Pavel Tiuleanu¹, Mr. Ion Lungu¹, Dr. Stefan Robu¹

1. Moldova State University

1. Introduction

Zinc phthalocyanine (ZnPc) is currently intensive investigated as effective photosensitizer against malignant tumor cells in photodynamic therapy (PDT) because absorbs strongly in the red and near infrared (NIR) regions [1, 2]. However, the intermolecular forces of π - π conjugation of free-ZnPc leads to low solubility and makes it unable to be applied in PDT.

Herein, to overcome this problem a water-soluble form of ZnPc with a copolymer of acrylic chloride (Cl-Ac) and N-vinylpyrrolidone (N-VP) was synthesized.

2. Methods

The synthesis of binary copolymers N-VP with Cl-Ac was performed by the radical polymerization in the presence of the azo-bis-isobutyronitrile (AIBN) initiator and was grafted to ZnPc by the Friedel-Crafts method. We report the synthesis, structure and photophysical properties of ZnPc:N-VP:Cl-Ac with a content of 10.0; 15.0; 20.0; 30 mol% of ZnPc.

3. Results

The structure of the ZnPc:N-VP:Cl-Ac was confirmed by FTIR spectra. The UV-Vis spectra of solutions (Figure 1) were measured from 200 nm to 1200 nm. The fluorescence spectra of the ZnPc:N-VP:Cl-Ac were excited with $\lambda_{ex} = 750$ nm. (Figure 2). The time resolved fluorescence spectra presented in Figure 3 were collected on an Edinburgh FLS980 spectrometer by using time-correlating single photon counting method.

Figure 1 Absorption spectra of ZnPc:N-VP:Cl-Ac solutions.

Figure 2 Fluorescence emissions of ZnPc:N-VP:Cl-Ac solutions.

Figure 3 Time correlated single photon counting decay curve of ZnPc:N-VP:Cl-Ac solution with 20.0 mol% of ZnPc.

3. Discussions

The FTIR spectra of ZnPc:Cl-Ac revealed bands at $\nu = 890-950$ cm^{-1} and $\nu = 3000-3100$ cm^{-1}

characteristic for the vinyl group $\text{CH}_2 = \text{CH}-$ and at $\nu = 1670-1680$ cm^{-1}

to group $\text{CH}_2 = \text{CH}-\text{CO}-$. The appearance in FTIR spectra of ZnPc:N-VP:Cl-Ac solution of new bands at $\nu = 1580-1605$ cm^{-1} indicate the presence of N-VP nuclei and of the ZnPc. The UV-Vis spectra (Figure 1), ZnPc:N-VP:Cl-Ac show a Q absorption broad band and a band with a maximum situated at 970 nm. The fluorescence spectra of the ZnPc:N-VP:Cl-Ac show remarkable fluorescent properties at $\lambda_{em} = 825$ nm for the compound with 20 mol% of ZnPc. The time evolution of excited state signals for ZnPc:N-VP: Cl-Ac solution revealed relatively longer-lived excited states relaxation 1,2 μs , 4,6 μs and 37 μs , respectively. The results of time-resolved fluorescence spectra studies clearly justify testing them in photodynamic processes.

References

1. Velazquez, F.N., Miretti, et. al. *Sci Rep* **9**,3010 (2019). <https://doi.org/10.1038/s41598-019-39390-0>.
2. L. M. O. Lourenço, P. M. R. Pereira, et al. ,*Chem. un.*, 50, 8363, (2014), <https://doi.org/10.1039/C4CC02226B>

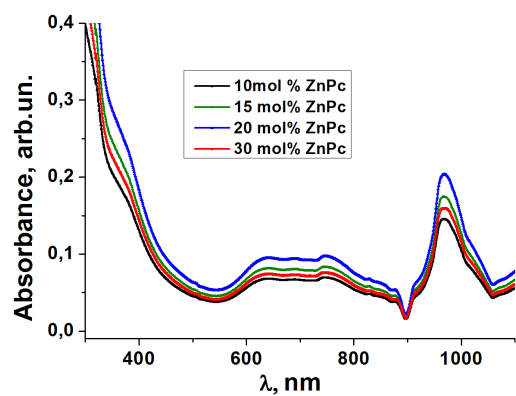


Figure 1 n.png

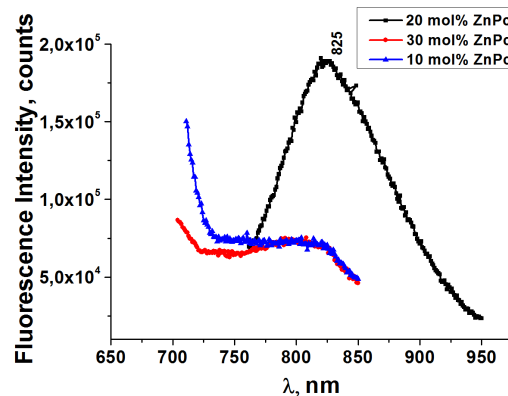


Figure 2 n.png

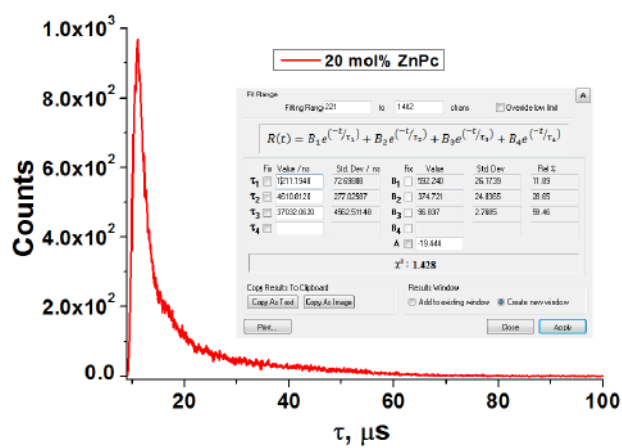


Figure 3.png

Electron emission by slow He ions impact on free-electron metal surfaces

Wednesday, 24th March - 13:45: Flash Session 1 (Room 2) - Abstract ID: 110

Dr. pierfrancesco riccardi¹

1. Dipartimento di Fisica - Università della Calabria and INFN gruppo collegato di Cosenza

Despite of decades of investigation, the electronic stopping of slow He ions interacting with free electron metals surfaces has been recently the matter of an interesting debate [1-3]. Electron emission is an outcome of the inelastic processes that can be studied in detail. Moreover, the small electron mean free path at low energy makes secondary electron emission particularly suited to study surface like nano-objects. Currently there is a renewed interest in electron emission under electron and ion impact, as this represents the most widely used imaging mode in the scanning electron microscope (SEM) and in scanning helium ion microscope (SHIM). In many cases electronic energy loss and electron emission are strictly related and KEE yields g (number of emitted electrons per incident ion) are found to be proportional to the electronic stopping power for slow light ions. Moreover, impact parameter dependent effects, such as electronic excitation in close atomic encounters, occur at impact energies above a threshold that is peculiar to the collision system and often promote electrons above the vacuum level, resulting in electron emission that produces features in the energy distributions and in the yield curve of emitted electrons.

In this work, we present energy distribution and yields of electrons emitted in the interaction of slow singly charged He ions with free electron metal surfaces (Al and Mg) as a function of incident ion energy in the range 0.1-10 keV. The role of each electron excitation mechanism in determining the behaviour of the total electron emission yields with incoming ion velocity will be discussed. We also discuss implications on the debate about electronic excitations and energy deposition, which is relevant to many fields, since helium ions are applied in the characterization and imaging of materials.

REFERENCES

- D. Primetzhofer et al. Phys. Rev. Lett. 107 (2011) 163201
- [2] M. Ahn San Zeb et al. Nucl. Instr. Meth. Phys. Res. B 303 (2013) 59
- P. Riccardi, A. Sindona, C.A. Dukes, Phys. Rev. A **93**, 042710 (2016)

Influence of cationic substitution on antibacterial activity of nanosised calcium phosphate

Wednesday, 24th March - 13:48: Flash Session 1 (Room 2) - Abstract ID: 267

Dr. Agnese Brangule¹, Dr. Ingus Skadiņš², Prof. Dace Bandere¹

1. Riga Stradiņš University, Department of Pharmaceutical Chemistry; Baltic Biomaterials Centre of Excellence, Headquarters at Riga Technical University, 2. Riga Stradiņš University, Department of Biology and Microbiology

Introduction

The structure of mammalian bones and teeth is often compared to the structure of apatites. The stoichiometric calcium hydroxyapatite (HAp), $\text{Ca}_{10}(\text{PO}_4)_6(\text{OH})_2$ is considered as an idealised bone and dental inorganic composition model.

Recent trends in biomaterials are focused on overcoming the limitations on biological apatites. One of the research directions is the study of substituted calcium phosphates.

To give calcium phosphate, several properties simultaneously, cation and anion substitution is performed.

Single or multiple ion-doped or substituted calcium phosphates can be used as bone-forming agents, microbial agents, and drug delivery carriers.

The present work describes the synthesis of silver Ag, copper Cu, zinc Zn and carbonate ions containing calcium phosphates. Special attention is paid on the quantitative characterisation of synthesised calcium phosphate depending on the type of doped ion and the ion concentration and on the qualitative in vitro characterisation depending on the type of doped ion and the ion concentration.

Methods

Amorphous carbonated calcium phosphates (ACCP) exhibiting single and multiple cations at different concentrations were synthesised by the wet precipitation method.

The powders were characterised by ED-XRF, FTIR and ICP-MS method to evaluate the structure and the effect of the different doping on the practical concentration in the ACCP structure.

The dried powders were in vitro tested on gram-positive and gram-negative bacteria cultures to determine the presence of bacteria and the degree of colonisation depending on the type of doped ion and the ion concentration in samples.

Results and Discussion

To overcome the matrix effect, with ED-XRF method were tested not only doped calcium phosphates but also mechanical mixtures containing ACCP and corresponding metal compounds. Effectiveness of cationic substitution and the influence of competitive cation was determined. Antibacterial properties of Zn, Cu, Ag and corresponding di-substituted HAP were evaluated.

The ion substituted calcium phosphates can have potential applications to their antibacterial activity and drug delivery carrier potential.

ACKNOWLEDGEMENTS. This project has received funding from the European Union's Horizon 2020 research and innovation programme under the grant agreement No 857287.

Hybrid Concept to Develop Next-Generation Energy-Storage Technologies

Wednesday, 24th March - 14:00: Flash Session 2 (Room 1) - Abstract ID: 151

***Ms. anukriti pokhriyal*¹, *Prof. Pedro Gómez-Romero*²**

1. Catalan Institute of Nanoscience and Nanotechnology (ICN2), CSIC and BIST Campus UAB, Bellaterra, 08193 Barcelona, Catalonia, Spain, 2. ICN2

Introduction

Energy storage technologies, especially batteries play an indispensable role in our current society. From smart hand-held communication devices to transportation and balancing power grids, they are essential in numerous applications. Therefore, it is imperative to find ways to make battery technology more efficient, long-lasting and low-cost.

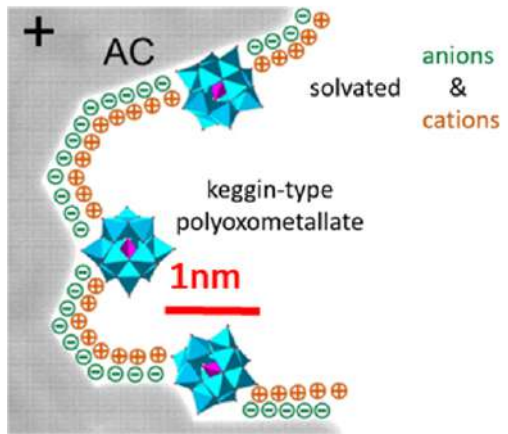
Our research aims to achieve this by exploring the concept of hybrid energy-storage. Hybrid materials have the potential to combine the advantages of high power density of capacitors and large energy density of batteries. That is, they could deliver high power in a short time as well as relatively high energy over a larger time period. This concept is key to develop a new generation of energy storage devices such as hybrid supercapacitors, making research of novel electroactive nano-materials crucial. The study explores the advantages and disadvantages of hybrid materials formed by electroactive Keggin-type polyoxometalates (POMs) adsorbed on nanocarbons and also takes a step beyond by synthesizing other hybrid electroactive materials such as decavanadate clusters on activated carbon (AC) to gain advantage over the current state of the art. Moreover, methods to improve cells are studied and adapted to these new materials and explore possible suitable applications such as frequency regulation in large-scale grids.

Methods

The hybrid materials are prepared through materials engineering and tested by a variety of experiments. Firstly, chemical synthesis of precursors, their adsorption on AC and sonication of electroactive materials (such as decavanadate clusters) with carbons such as Carbon SuperP and Multiwalled Carbon Nanotubes are used. Finally, the hybrid electrode materials are tested through Cyclic Polarizations (CPs) and Galvanostatic Cycling with Potential Limitation (GCPLs) in aqueous and organic electrolytes.

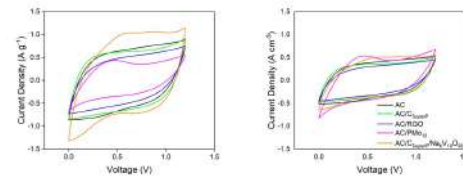
Results and Discussions

Preliminary results show improvement in capacitance by using hybrid materials. Integrating POMs with nanocarbon materials leads to hybrid electrodes with improved energy storage capabilities. It was observed that different nanocarbons are better suited for aqueous or organic electrolytes. Further, Decavanadate cluster ($[V_{10}O_{28}]^{6-}$) leads to better gravimetric capacitance given its lower molecular weight compared with Phosphomolybdate $[PMo_{12}O_{40}]^{3-}$. We are presently carrying out further work to improve charge transfer.



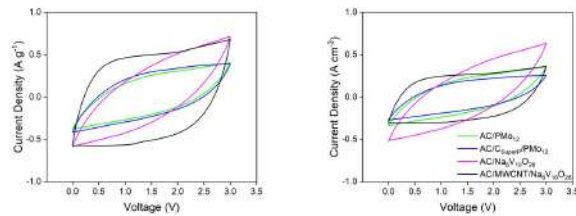
Activated carbon and keggin-type polyoxometallates.png

Cyclic Polarisation of Symmetric Hybrid Supercapacitors with 1M H_2SO_4



Cyclic polarisation of symmetric hybrid supercapacitors with 1m h2so4.jpg

Cyclic Polarisation of Symmetric Hybrid Supercapacitors with 1M TEABF_4 in Acetonitrile



Cyclic polarisation of symmetric hybrid supercapacitors with 1m teabf4 in acetonitrile.jpg

Enhancing the Perovskite Solar Cells Efficiency by Carbon Dots Integration into the PCBM Electron Transport Layer

Wednesday, 24th March - 14:03: Flash Session 2 (Room 1) - Abstract ID: 126

Ms. Melis Özge ALAŞ¹, Mr. Adem Mutlu², Prof. Emre Gür³, Prof. Ceylan Zafer², Dr. Rükan GENÇ ALTÜRK¹

1. Mersin University, Department of Chemical Engineering, **2.** Ege University, Solar Energy Institute, **3.** Atatürk University, Department of Solid State Physics

Perovskite solar cells (PSCs) have demonstrated rapid development over the past decade, with extremely low production costs achieved and high power conversion efficiencies of up to 27.3%, even better than commercialized polycrystalline silicon solar cells. However, problems such as long-term stability, lead-based toxicity, and hysteresis in PSCs continue to limit their potential as an alternative to conventional or plate-based cells^{1,2}. In recent years, carbon-based nanomaterials with enormous properties have been used in optimization studies in perovskite absorbent layer, interface, and device structure to overcome these problems in PSCs and have been shown to have positive effects³. Carbon nanodots (CDs) are new members of the luminescent carbon material family in the spherical form with graphene-like structural properties. Due to their intrinsic properties such as good absorption in UV area, wavelength-dependent emission, tunable optical and electronic properties, and photochemical stability, CDs have become particularly attractive for energy-focus scientific and technological areas such as energy storage and conversion (solar cells, supercapacitors, and batteries, etc.)^{4,5}. Herein, we attempted to enhance the perovskite solar cell performance by incorporating the environmentally friendly, multi-color fluorescent carbon quantum dots (Blue (B), green (G), and yellow (Y) emitting CDs) made up of a very cheap natural carbon source into PCBM film as an electron transporting layer for perovskite solar cells. The device was built as FTO/PEDOT:PSS/Perovskite/PCBM:CDs/Ca/Ag. Cell efficiency of 8.2% is achieved with a 32.3 % enhancement as compared to the reference solar cell of pure PCBM using blue-emitting CDs where both G-CDs and Y-CDs were also enhanced the device efficiency by 16.1% and 12.9%. CDs doping into the PCBM layer leads to enhanced electrical conductivity, electron mobility, and charge extraction efficiency. Moreover, we think that such CDs doping help prevents I⁻ ions from interface diffusing and thus enhances the stability of solar cells.

Acknowledgement

This study was supported by Mersin University Scientific Research Project Unit (Project No: BAP-2019-2-TP3-3599).

References

- 1 Y. Wen, G. Zhu and Y. Shao, *J. Mater. Sci.*, 2020, **55**, 2937–2946.
- 2 Q. Guo, F. Yuan, B. Zhang, et al., *Nanoscale*, 2019, **11**, 115–124.
- 3 M. Batmunkh, C. J. Shearer, M. J. Biggs and J. G. Shapter, *ACS Appl. Mater. interfaces*, 2017, **9**(23), 19945–19954.
- 4 M. O. Alas, A. Güngör, R. Genc and E. Erdem, *Nanoscale*, 2019, **11**, 12804–12816.
- 5 J. Jin, C. Chen, H. Li, Y. Cheng, et al., *ACS Appl. Mater. Interfaces*, 2017, **9**, 14518–14524.

Local heat sources based on Al-CuO_x multilayer structures: formation features and thermal properties

Wednesday, 24th March - 14:06: Flash Session 2 (Room 1) - Abstract ID: 148

Dr. Egor Lebedev¹, Ms. Larisa Sorokina¹, Mr. Roman Ryazanov², Mr. Artem Sysa²

1. National Research University of Electronic Technology - MIET; 2. Scientific-Manufacturing Complex "Technological Centre"

Introduction

Currently, progress in micro- and nanoelectronics is associated not only with a decrease in the topological dimensions of elements, but also with an increase in integration level. The development of technologies and methods for 3d-assemblies, system-on-crystal, micro- and nanoelectromechanical systems formation will allow for the transition to advanced technologies and systems. Development of methods for groups of components joining, incl. thermosensitive, using local heat sources is one of the promising universal approaches to solving the problem of a reliable joining formation of various surfaces. However, in order to create effective local heat sources with specified characteristics, it is necessary to solve the most important scientific problem - the determination and prediction of the energy properties of thermite materials, taking into account their chemical composition, size effects and properties of the surfaces to be joined. This paper presents the results of studying the features of the formation and research the thermal properties of multilayer thermite materials based on Al and CuO_x.

Methods

Multilayer structures with different thicknesses of individual layers were formed by alternate sputtering of Al and CuO_x targets by magnetron sputtering. Studies of the formed materials using energy-dispersive X-ray spectroscopy and stylus profilometry made it possible to reveal the dependences of the deposition rate and composition of copper oxide layers on the partial pressure of oxygen in the process of target sputtering. Thermal effects were measured by differential scanning calorimetry, and the propagation velocity of the wave combustion front was carried out using high-speed video camera.

Results

Figure 1 shows a cross-section photo of multilayer structure before and after combustion. After combustion the reagents melt and drops are formed from the reaction products – Al₂O₃ and Cu.

Figure 2 shows a storyboard of the initiation and combustion of a multilayer Al-CuO_x

structure. It is clearly seen, that wave combustion propagates uniformly from the point of initiation in all directions. The wave propagation speed was 6,6 m/s.

The experimental results obtained made it possible to optimize not only the formation process multilayer structures, but also its energetic properties.

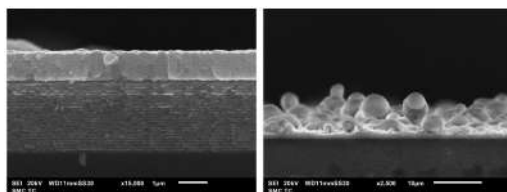


Figure 1 - sem images of cross-sections of multilayer al-cuox structures before left and after right combustion.jpg

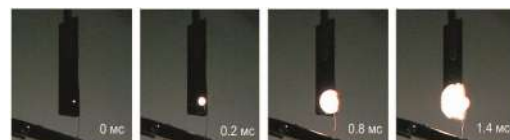


Figure 2 -storyboard of the combustion process of al-cuox.jpg

Optimization of eco-friendly synthesis of silver nanoparticles from leaves extract of *Alstonia angustiloba*.

Wednesday, 24th March - 14:09: Flash Session 2 (Room 1) - Abstract ID: 224

Mrs. NURHIDAYAH AB. RAHIM¹, Prof. MD AZMAN SEENI MOHAMED¹

1. Universiti Sains Malaysia

Silver nanoparticles have specific physical and chemical properties which contribute to high electrical conductivity, optical, thermal, electrical and biological activities, making it useful to apply in medical, consumer, food, healthcare and industrial purposes. Biological method is an eco-friendly approach to synthesize nanoparticles for biomedical application because of least toxic to living things, simple preparation, environmental friendly, cheaper and produce high yield. The study was carried out to identify potentiality of *A. angustiloba* leaves extract to acts as reducing and capping agents in the eco-friendly synthesis of silver nanoparticles. Different parameters such as concentration of extract and molarity of precursor was tested at different reaction times. The eco-friendly synthesized silver nanoparticles were called as *A. angustiloba*-AgNPs. The obtained yield was then characterized by UV-Vis spectrophotometer, scanning electron microscopy (SEM), transmission electron microscopy (TEM), Fourier-transform infrared spectroscopy (FTIR) and zeta potential analyzer. Gradually color changing from faint light to yellowish brown and finally to colloidal brown was initially observed after addition of leaves extract of *A. angustiloba* into 1 mM silver nitrate (AgNO_3) aqueous solution within 24 hours of reaction time. The UV-visible spectra of *A. angustiloba*-AgNPs revealed strong and broad surface plasmon resonance (SPR) at 445 nm. SEM micrograph revealed that the particles have spherical shaped, presence either in spread or aggregated form and ranged from 20 to 80 nm. The particles were primarily spherical form and well-dispersed with the average particle size of 15 nm and a size range from 1 nm to 84 nm. The mean of hydrodynamic size was 61.21 ± 3.96 nm with mean of polydispersity index was 0.514 ± 0.055 . Zeta potential value of the *A. angustiloba*-AgNPs was -18.67 ± 3.12 mV indicated that the particles have negatively charged on their surfaces and relatively stable because of the electrostatic repulsion. The FT-IR spectrum of *A. angustiloba*-AgNPs showed intensive peaks at 3228.99, 1518.76, 1600.69, 1280.07 and 1061.60 cm^{-1} . It is thus a prospective for *A. angustiloba* leaves to be applied in the synthesis of nanoparticles that can require further scale-up studies.

Atomically dispersed Fe in C₂N framework as sulfur host materials for Efficient Lithium-Sulfur Batteries

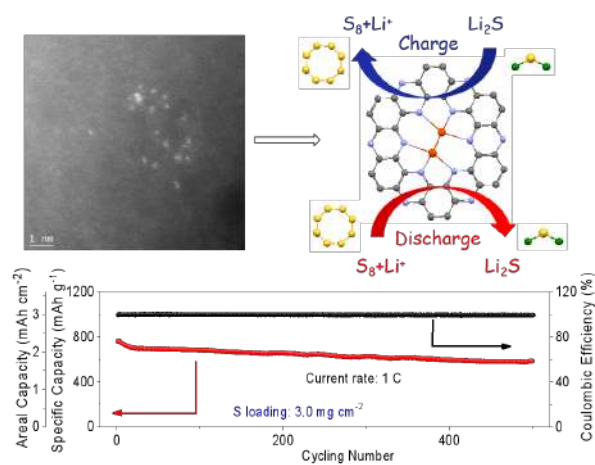
Wednesday, 24th March - 14:12: Flash Session 2 (Room 1) - Abstract ID: 68

Mr. Zhifu Liang¹, Mr. Dawei Yang², Dr. Pengyi Tang³, Dr. Jordi Llorca⁴, Dr. Marc Heggen³, Dr. Rafal E Dunin-Borkowski³, Dr. Yingtang Zhou⁵, Dr. Joan Ramon Morante², Dr. Andreu Cabot², Dr. Jordi Arbiol¹

1. Catalan Institute of Nanoscience and Nanotechnology (ICN2), CSIC and BIST Campus UAB, Bellaterra, 08193 Barcelona, Catalonia, Spain, 2. Catalonia Institute for Energy Research - IREC Sant Adrià de Besòs, Barcelona, 08930, Catalonia, Spain, 3. Ernst Ruska-Centre for Microscopy and Spectroscopy with Electrons and Peter Grünberg Institute Forschungszentrum Jülich GmbH 52425 Jülich, Germany, 4. Institute of Energy Technologies, Department of Chemical Engineering and Barcelona Research Center in Multiscale Science and Engineering Universitat Politècnica de Catalunya, EEBE, 08019 Barcelona, Catalonia Spain., 5. Key Laboratory of Health Risk Factors for Seafood and Environment of Zhejiang Province Institute of Innovation & Application Zhejiang Ocean University, Zhoushan, Zhejiang Province, 316022, China

In recent years, single-atom catalysts (SAC) have become one of the most research hot topics in heterogeneous catalysis. As it is known, both homogeneous and heterogeneous catalysts are important for the reactions used in chemical industry. In homogeneous catalysis, up to 100% of the atoms may remain active during reactions, while in the case of heterogeneous catalysts, only a small fraction of the metal atoms can be utilized due to the aggregation of the atoms when forming clusters. In this way, SACs have the benefits of homogeneous and heterogeneous catalysts. On the other hand, Lithium-sulfur batteries (LSBs) are considered as one of the most promising next generation energy storage systems due to their high energy density and low materials cost. However, some challenges still exist for the commercialization of LSBs, for example, the sluggish redox reaction kinetics and the shuttle effect of lithium polysulfides (LiPS). Here we report on a novel two-dimensional organic family of materials named C₂N, loaded with atomically dispersed iron as efficient sulfur host in LSB cathodes.[1] X-Ray absorption fine spectroscopy and density functional theory calculations proves the atomically dispersed Fe/C₂N catalysts to promote the reversible electrochemical conversion reaction and to immobilize LiPS to enhance the LSBs performance. As a result, our Fe/C₂N-based cathodes significantly improve the rate performance and long-term cycling stability. Fe/C₂N-based cathodes display initial capacities up to 1540 mAh g⁻¹ at 0.1 C and 678.7 mAh g⁻¹ at 5 C, while retaining 496.5 mAh g⁻¹ after 2600 cycles at 3 C with a decay rate as low as 0.013% per cycle. Even at a high sulfur loading of 3 mg cm⁻², Fe/C₂N-based cathodes deliver a remarkable specific capacity retention of 587 mAh g⁻¹ after 500 cycles at 1 C. Overall the present work provides a rational structural design strategy to inspire the development of high-performance cathodes based on atomically dispersed catalysts for the next generation LSBs.

[1] Z. Liang, et al., *Advanced Energy Materials*, DOI: 10.1002/aenm.202003507 (2021)



Zhifu liang icn2.png

Grewia tenax leaves extract mediated silver nanoparticles applications for antibacterial, antibiofilm and antifungal activity

Wednesday, 24th March - 14:15: Flash Session 2 (Room 1) - Abstract ID: 112

Mrs. Priyanka Yadav¹, Ms. Monisha Singhal¹, Dr. Surendra Nimesh², Dr. Sreemoyee Chatterjee¹, Dr. Nidhi Gupta¹

1. IIS (deemed to be University), 2. Central University of Rajasthan, Ajmer.

Abstract

Introduction- *Grewia tenax* plant possesses lots of medicinal qualities that can be utilized in arena of bio-nanotechnology in the form of biosynthesized silver nanoparticles. Biosynthesized silver nanoparticles from *Grewia tenax* leaves extract can be utilized in the pharmacological area as they are sustainable, cost effective and environment friendly.

Methods- The silver nanoparticles were prepared from 10 percent *Grewia tenax* disease free fresh leaves extract. The reduction of Ag^+ to Ag^0 was due to existence of bioactive agents present in the extract. The silver nanoparticles were first detected by observing the change in color from light yellowish brown to dark brown and then confirmed by UV-visible spectroscopy. In the current research, several physico-chemical parameters namely; time, temperature, concentration of AgNO_3 and ratio of extract to AgNO_3 were adjusted by using Box-Behnken design (BBD) by Design Expert, version 12 (State- Ease Inc., Minneapolis). UV-visible spectroscopy accompanied by dynamic light scattering technique (DLS) and Scanning electron microscopy (SEM) with Energy-dispersive X-ray spectroscopy (EDS) determine the size, morphological variations and chemical constituents of *Grewia tenax* silver nanoparticles (GT-AgNPs). Zeta potential, X-ray diffraction (XRD) and Fourier transform infrared spectroscopy (FTIR) were done to analyze GT-AgNPs by conferring their stability and excellent dispersion and the biomolecules in aqueous leaf extract liable for bio reduction of these silver particles.

Results- These biologically synthesized GT-AgNPs showed an excellent antibacterial action against Gram positive (*Staphylococcus aureus* and *Bacillus subtilis*) and Gram negative bacteria (*Pseudomonas aeruginosa* and *Escherichia coli*) which was observed by disc diffusion assay and estimated by the leaked protein and DNA levels in the cultural solution after being treated with GT-AgNPs. The antibiofilm proficiency of these Gram positive and Gram negative bacteria was effectively unveiled by Congo red agar plate (CRA) assay, microtiter plate assay and microscopic study using coverslip method. These studies displayed reduction in bacterial sustainability and formation of exopolysaccharide (responsible for blackening of colonies).

The antifungal competency against *Aspergillus niger* and *Candida albicans* was confirmed by disc diffusion assay and colony growth assay as these. SEM was performed for understanding intracellular breakage and morphological transformations in cell of gram positive bacteria and fungi after treatment with GT-AgNPs.

The current study therefore, enlightened applications of GT-AgNPs, as an active efficient antimicrobial agent and applicable substitute in pharmaceutical area. Their antifungal potency could be utilized as fungicides in agricultural zone.

Keywords: antibacterial, antibiofilm, antifungal, Box- Behnken design (BBD) version 12, *Grewia tenax*, silver nanoparticles

1D sp-carbon chains-based nanocomposites by laser ablation in polymeric solutions

Wednesday, 24th March - 14:00: Flash Session 2 (Room 2) - Abstract ID: 129

Dr. Sonia Peggiani¹, Dr. Pietro Marabotti¹, Dr. Anna Facibeni¹, Prof. Alberto Milani¹, Prof. Valeria Russo¹, Prof. Andrea Li Bassi¹, Prof. Carlo Casari¹

1. Politecnico di Milano - Department of Energy

Nowadays the request for biocompatibility, low-cost, high chemical and mechanical resistance have pushed the research towards new materials. Carbon-based fillers such as nanotubes or graphene have revolutionized the properties of nanocomposites. Finite 1D sp-carbon chains are interesting systems for future applications because of their structure-dependent opto-electronic properties [1]. Among the large variety of available synthetic methods, pulsed laser ablation in liquid (PLAL) is a scalable technique which mainly allows the synthesis of hydrogen-capped chains based on alternated single and triple bonds, the so-called polyynes. However, these molecules suffer from a limited stability [2], which can be improved by the encapsulation in a polymer matrix, therefore creating a new nanocomposite.

In the work here presented, we develop PLAL for *in situ* synthesis of polyynes directly in a polymer matrix. We ablate graphite in a liquid solution of poly(vinyl alcohol) (PVA) [3] or polymethylmethacrylate (PMMA) at different concentrations by Nd:YAG nanosecond pulsed laser at 532 nm. Ag nanoparticles are added to polyynes/polymer mixtures in order to structurally characterized by surface-enhanced Raman spectroscopy (SERS) both polymeric solutions and free-standing films (see **Figure 1**). Solutions have been then optically characterized by UV-Vis spectroscopy, while nanocomposites (**Figure 2**), obtained after solvent evaporation, have been morphologically analysed by scanning electron microscopy (SEM). Polyynes stability has been investigated by periodic SERS measurements.

We observed improvements both in the yield of sp-carbon chains by laser ablation in polymeric solutions and in the stability of these 1D nanostructures if embedded in PVA or in PMMA.

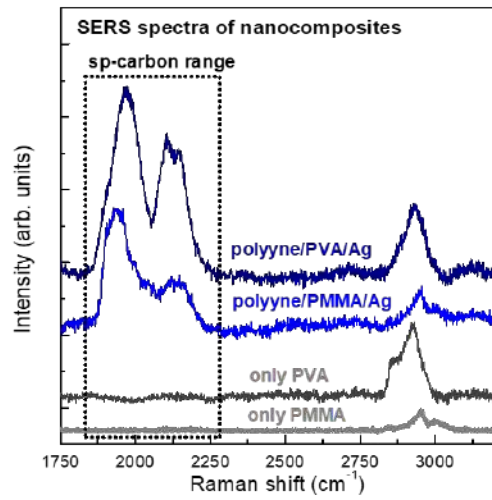
By this way, we here propose a novel strategy for the preparation of new functional materials for future industrial applications.

Acknowledgements

Authors acknowledge funding from the European Research Council (ERC) under the European Union's Horizon 2020 research and innovation program ERC-Consolidator Grant (ERC CoG 2016 EspLORE grant agreement No. 724610, website: www.esplore.polimi.it).

References

- [1] C.S. Casari and A. Milani, MRS Comm., 8, 207, 2018.
- [2] S. Peggiani et al., Chemical Physical Letters, 740, 137054, 2020.
- [3] S. Peggiani et al., Materials Advances, 1, 2729, 2020.



Picture1-sers spectra of the solid nanocomposites and of the polymeric matrices.png



Picture2-polyynes/pva/Ag nanocomposite.png

Development of chitosan/gelatin/ silver nanoparticles based bionanocomposite films for wound healing applications

Wednesday, 24th March - 14:03: Flash Session 2 (Room 2) - Abstract ID: 131

Ms. Isha Gupta¹, Dr. Sonia Gandhi², Prof. Sameer Sapra³

1. Metabolomics Research Facility, Division of Behavioural Neuroscience, Institute of Nuclear Medicine and Allied Sciences, Defence Research and Development Organization, Delhi, India and Department of Chemistry, Indian Institute of Technology, Delhi, India, 2. Metabolomics Research Facility, Division of Behavioural Neuroscience, Institute of Nuclear Medicine and Allied Sciences, Defence Research and Development Organization, Delhi, India, 3. Department of Chemistry, Indian Institute of Technology, Delhi, India

Introduction

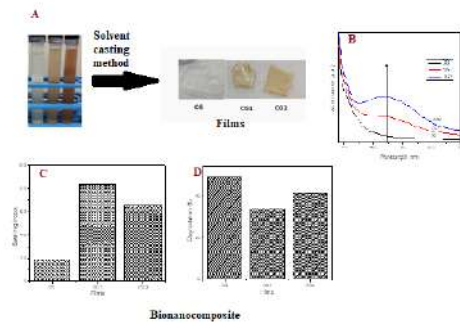
Nanocomposites are one of the branches of Nanoscience, being exploited for adsorption, sensors, and biomedicine. It is prepared by dispersing inorganic nanoparticles as a filler in the matrix of the polymer. If nanocomposites contain biopolymers such as chitosan, alginate, and gelatin, these are known as 'bionanocomposites'. Bionanocomposite is biocompatible, biodegradable, non-toxic, non-allergic and reduces the cytotoxicity of the nanoparticles. In this work, bionanocomposites of different formulations were prepared for dermal applications on the acute wounds.

Methods

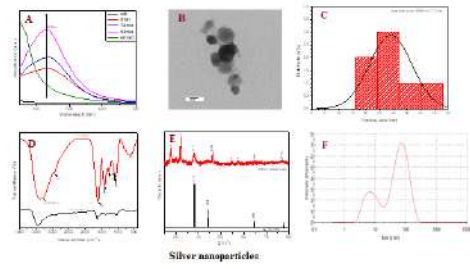
The concentrations of aqueous tulsi powder and silver salt were optimised for the green synthesis of silver nanoparticles. Then the particles were characterised by UV-Visible spectroscopy, Fourier Transform Infrared (FTIR) spectroscopy, Transmission electron microscopy (TEM), X-ray diffractometer (XRD) and Dynamic Light Scattering (DLS). The physical blending prepared the blend of chitosan-gelatin (r=1:1) with the above synthesised silver nanoparticles. Three bionanocomposites solutions CG, CGA₁, and CGA₂ have 0%, 1% and 2% (v/v %) concentration of silver nanoparticles. Glycerol (0.4%, v/v) was used as a plasticiser. Three films were prepared by casting on glass petri-dishes through the solvent casting method.

Results & Discussions

The reaction of silver nanoparticles was monitored with the help of UV-Visible spectroscopy. From TEM micrograph, particle size was found to be 28.95 ± 7.74 nm. The absorbance confirmed the presence of silver nanoparticles in the blend at 435 nm in UV-Visible spectra. Phytochemicals such as flavones, amino acids and proteins were found to be responsible for the synthesis of nanoparticles. The increase in the absorbance of the blend indicated the increase in the concentration of nanoparticles in the composites. Films with uniform thickness were obtained through solvent casting method. The other physical properties essential for accelerating wound healing such as swelling index and degradation properties were investigated. These properties confirmed the stable complex formation between polymers and silver nanoparticles. This study gave an alternative and eco-friendly approach for the synthesis of composite films for wound healing applications.



Bionanocomposite.png



Silver nps.png

Secondary Electron emission in the interaction of low Energy ions and electrons from graphene based materials

Wednesday, 24th March - 14:06: Flash Session 2 (Room 2) - Abstract ID: 109

Dr. pierfrancesco riccardi¹

1. Dipartimento di Fisica - Università della Calabria and INFN gruppo collegato di Cosenza

Two dimensional (2D) crystals are attracting interest in materials science as they can be the building blocks of more complex three dimensional (3D) hetero-structures with properties tailored to suit specific demands. On the other side, emerging facts and concepts about 2D materials can give new insight into the electronic properties of materials that have been widely investigated and applied, such as graphite. We use Angle resolved secondary electron emission (ARSEE) as a probe for excited states of 3D materials derived from 2D crystals. Spectra of electrons emitted under the impact of low energy ions and electrons with graphene on substrates show a fine structure related to the band structure of the unoccupied energy levels of the sample. Experiments of keV He⁺ ion impact show that excitation of valence electrons occur by electron promotion in close He-C collisions. This produces a high energy features that is attributed to the detection in vacuum of electrons promoted into conduction band states. In the case of electron impact, the fine structure is very sensitive to the crystalline quality of the sample and show several peaks, that reflect features in the density of conduction band states at corresponding energies above the vacuum level [1,2].

We can also use state of the art Density Functional Theory (DFT) [3] to calculate of the electronic band structure of our samples, focusing on the unoccupied energy levels up to 50 eV above the Fermi level [4]. The results of the calculations can be compared with available observations obtained in ARSEE experiment either performed by us or reported in the literature. ARSEE measurements show spectroscopic features that can be linked to energy states found in band structure calculations. The combined analysis of DFT calculations and ARSEE experiments can allow us to show how peculiar properties of the electronic structure of 2D crystals are reflected in 3D derived systems.

References:

1. P. Riccardi, A. Cupolillo, M. Pisarra, A. Sindona, L.S. Caputi Appl. Phys. Letters 97 (2010) 221909
2. Riccardi P, A. Cupolillo, M. Pisarra, A. Sindona, and L. S. Caputi Appl. Phys. Letters 101 (2012) 183102
3. M. Pisarra, A. Sindona, P. Riccardi, V.M. Silkin, J.M. Pitarke. New Journal of Physics, 16 (2014) 083003
4. M. Pisarra, P. Riccardi, A. Sindona, A. Cupolillo, N. Ligato, C.Giallombardo, L. S. Caputi

Carbon 77 (2014) 796

In-situ fabrication of ZnO-rGO nanomaterials and their photocatalytic performance

Wednesday, 24th March - 14:09: Flash Session 2 (Room 2) - Abstract ID: 145

Mrs. Aura Merlano¹, Dr. Ángel Salazar¹

1. Grupo de Óptica y Espectroscopía (GOE), Centro de Ciencia Básica, Universidad Pontificia Bolivariana, Cq 1 # 70-01, Medellín, Colombia.

According to previous studies, ZnO-graphene composites have many advantages like reduction of bandgap, enhancement of the surface area and reactive sites, improved separation of charge carriers, inhibition the photo-corrosion of ZnO, among others [1-3]. These properties make the coupling of nanocarbons and semiconductors one of the most promising strategies for development of robust and efficient photocatalysts [4-5]. In this context, this work focuses on the chemical, structural and photocatalytic analysis of ZnO-rGO nanomaterials with different ZnO morphology. The composites were synthesized using a microwave-assisted hydrothermal route and the zinc precursor concentration was varied. The results show possible variations in the kinetics of the crystal growth due to the zinc precursor concentration can change the final sizes and morphologies of the ZnO structures anchored in the composite. They were characterized by SEM, FTIR, XRD, Raman spectroscopy, XPS and UV-VIS DRS. Both composites presented high adsorption and photocatalytic degradation (ca. 100%) of aqueous methylene blue, which was explained in terms of the excellent coupling between the rGO sheets and the different ZnO morphologies.

References:

- [1] A. F. Ghanem, A. A. Badawy, M. E. Mohram, and M. H. Abdel Rehim, "Synergistic effect of zinc oxide nanorods on the photocatalytic performance and the biological activity of graphene nano sheets," *Heliyon*, vol. 6, no. 2, p. e03283, 2020, doi: 10.1016/j.heliyon.2020.e03283.
- [2] E. Albiter, A. S. Merlano, E. Rojas, J. M. Barrera-andrade, Á. Salazar, and M. A. Valenzuela, "Synthesis , Characterization , and Photocatalytic Performance of ZnO – Graphene Nanocomposites : A Review," pp. 1–40, 2021.
- [3] X. Liu *et al.*, "Graphene oxide-based materials for efficient removal of heavy metal ions from aqueous solution: A review," *Environ. Pollut.*, vol. 252, pp. 62–73, 2019, doi: 10.1016/j.envpol.2019.05.050.
- [4] X. Li, J. Yu, M. Jaroniec, and X. Chen, "Cocatalysts for selective photoreduction of CO₂ into solar fuels," *Chem. Rev.*, vol. 119, no. 6, pp. 3962–4179, 2019, doi: 10.1021/acs.chemrev.8b00400.
- [5] A. A. Yaqoob, N. Habibah, A. Serr, M. Nasir, and M. Ibrahim, "Advances and Challenges in Developing Efficient Graphene Oxide-Based ZnO Photocatalysts for Dye Photo-oxidation," *Nanomaterials*, vol. 10, no. 932, p. 24, 2020.

Regularities of the catalyst nanoparticles formation and the synthesis of CNTs in PECVD process

Wednesday, 24th March - 14:12: Flash Session 2 (Room 2) - Abstract ID: 254

Dr. Evgeniy Kitsyuk¹, Ms. Yulia Fedorova¹, Dr. Alexander Dudin²

1. Scientific-Manufacturing Complex «Technological Centre», 2. Institute of Nanotechnologies of Microelectronics, Russian Academy of Sciences

The catalytic synthesis of carbon nanomaterials is currently the only technological way to form nanostructures, such as nanotubes (CNTs) and graphene, at a given location of a functional element. In most cases, catalytic metals such as Ni, Co, Fe, Au can interact with common substrates. Ti and Si are most commonly used as a buffer layer and substrate, despite their interaction with the catalytic materials. Ti as a buffer layer in the synthesis is not a clear-cut solution of the problem, since such a system allows the diffusion of transition metal atoms into the depth of the buffer layer. Using the prior processing of the catalytic layer allows both increasing the efficiency of CNTs synthesis and controlling the characteristics of the synthesized array in some degree. In this work, we investigated the reaction of Ni catalyst on Ti buffer layer during prior oxidative and reductive processing, as well as their effect on the synthesis of CNTs.

The prior processing and the synthesis process were carried out in the «Nanofab 800 Agile» unit built on the «PlasmaLab System 100» platform (Oxford instruments, GB). Metallic films were formed by electron-beam sputtering. Further experiments were carried out with the film thicknesses of 10/2 and 25/10 Ti/Ni in order to determine the effect of the nickel mass on its behavior during decomposition into nanoparticles. The plan of experiments included the oxidation at 280° C and reduction processes of the samples with different time durations, as well as varying the reduction temperature: 500 or 680 °C.

Further processing in ammonia and hydrogen atmosphere leads to the reduction of nickel to metal. Titanium, as a result of the partially atomic displacement of oxygen, becomes oxynitride. It was determined that the formed nickel particles were partially immersed in titanium. In this case, only the reduction process affects on the height of nanoparticles. The duration of the treatments affects not only on the size of nanoparticles and their height, but also on their number. The prior processing duration affected not only on the distribution of nanoparticles, but defined the height, diameter, quality, and CNTs array density.

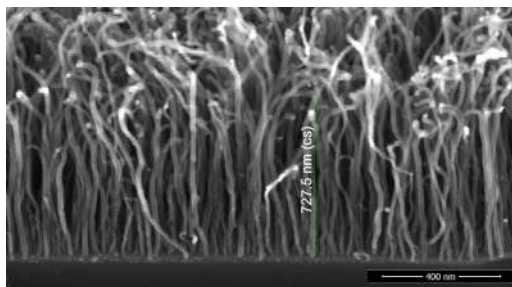


Figure 1. sem of pecvd cnt after 5 min oxidation and reduction of catalyst.jpg

Reduction process at 500 °C	Sample number	T _{ox} , °C	t _{ox} , min	T _{red} , °C	t _{red} , min	d, nm	h, nm	Q, pcs/mkm ²
	1	280°	1	500°	1	10-12	2	529
	2	280°	5	500°	1	7-9	8-9	525
	3	280°	10	500°	1	7-9	10	472
	4	280°	1	500°	5	7-9	4	718
	5	280°	1	500°	10	7-9	3	701
	6	280°	5	500°	5	7-9	7	466
	7	280°	10	500°	10	7-9	7	444
Reduction process at 680 °C	Sample number	T _{ox} , °C	t _{ox} , min	T _{red} , °C	t _{red} , min	d, nm	h, nm	Q, pcs/mkm ²
	8	280°	1	680°	1	10-12	12	283
	9	280°	5	680°	1	31-33	25	29
	10	280°	10	680°	1	32	35	17
	11	280°	1	680°	5	9, 14	8	183
	12	280°	1	680°	10	9	8	110
	13	280°	5	680°	5	28	25	80
	14	280°	10	680°	10	32	35	38

Table 1. process parameters and characteristics of nanoparticles for ti-ni 10-2 nm.jpg

Electron beam-plasma vacuum deposition of very thin carbon films on quartz and sapphire substrate for transmissive photocathode applications

Wednesday, 24th March - 14:15: Flash Session 2 (Room 2) - Abstract ID: 84

Dr. Jozef Huran¹, Dr. Nikolay Balalykin¹, Dr. Mikhail Nozdrin¹, Dr. Vlasta Sasinková², Mrs. Eva Kováčová³, Mr. Alexander Skrypnik¹, Dr. Alexander Kobzev¹, Dr. Grigory Shirkov¹

1. Joint Institute for Nuclear Research, 2. Institute of Chemistry, Slovak academy of Sciences, 3. Institute of Electrical Engineering, Slovak Academy of Sciences

Very thin carbon-based films were deposited on quartz and sapphire substrates by electron beam-plasma (EBP) vacuum deposition. In EBP system electrons emitted by the incandescent cathode are focused by the electrostatic lens and accelerated by the electric field between the cathode and the crucible filled with evaporated material. At an initial instant, the evaporated material is melted due to electron bombardment effect. An increase in electron beam energy (due to an increase in working voltage) incites material's evaporation. On achieving a certain vapor density (specific for each material), a non-independent discharge in material's vapor is developed within the anode-cathode gap (~6-10 mm). The directly heated cathode changes its purely thermo emission mode of operation into a combined - i.e. thermo- plus ion-electronic emission - mode. In our case the evaporated material was pyrolytic graphite. Substrate holder temperature during deposition was in the range 300-500 °C. Film thickness were in the range 15-30 nm. The concentration of elements in the films was determined by RBS and ERD analytical method. Raman spectroscopy was used for chemical structural features determination of carbon films. Elements concentration results were practically the same for the all samples: carbon - 93 at.%, nitrogen - 2 at.%, hydrogen - 2 at.%, oxygen - 3 at.%. Raman spectrum of very thin carbon film, which is typical for all samples, was deconvoluted. We used five peaks fitting for the range 1000-1800 cm⁻¹ and four peaks fitting for the range 2500-3300 cm⁻¹. Very thin carbon-based films contained several carbon phases. The photo-induced (pulsed laser –266 nm) electron emission properties of carbon-based very thin films were determined by the measurement of cathode bunch charge and calculate quantum efficiency of the prepared back-side illuminated transmissive photocathode. The photo-induced electron emission characteristics of carbon-based very thin films prepared by EBP vacuum deposition on quartz and sapphire substrate as back-side illuminated transmissive photocathode are discussed.

Pseudocapacitive electrodes: a journey from nano to micro

Wednesday, 24th March - 14:50: Oral Session 2-1 (Room 1) - Abstract ID: 168

Prof. Thierry Brousse¹

1. Institut des Matériaux Jean Rouxel de Nantes (IMN), Réseau sur le Stockage Electrochimique de l'Énergie (RS2E)

Electrochemical Capacitors, so called pseudocapacitors, are charge storage devices that can complement batteries in many applications which require high power density, long cycle life and moderate energy density. Apart from carbon based electrodes that are currently implemented in commercial devices, a lot of materials have been envisioned as potential electrodes for supercapacitors, from simple or multicationic oxides to nitrides, sulfides, etc. Unfortunately, only few compounds exhibit a true pseudocapacitive behavior (“looks like” capacitive). This electrochemical peculiarity seems to be related to the intrinsic structural/chemical properties of the desired material, which means that whatever the particle size, the electrode exhibits the same electrochemical signature. Other materials need to be finely divided to show such behavior which means this is some kind of extrinsic property, not depending on the material itself but rather on the design/architecture of the electrode material. Thus, the investigation of nano or micro-sized compounds as electrodes for supercapacitors involves the use of advanced in-situ or operando techniques that enables to discriminate between intrinsic or extrinsic pseudocapacitive behavior, and to further engineer materials for such energy storage devices.

Electrodeposition of metal-organic frameworks for energy and environment applications

Wednesday, 24th March - 15:20: Oral Session 2-1 (Room 1) - Abstract ID: 48

Dr. Xuan Zhang¹, Mr. Wei Guo¹, Mr. Sijie Xie¹, Prof. Jan fransaer¹

1. KU Leuven

Metal-Organic Frameworks (MOFs) have received a lot of attention due to their diverse structures and tunable properties (including pore size, metal center, functional linkers and post modification), which exhibit a broad potential for different applications. Some of the applications are generally based on MOFs as the powder (e.g. gas storage and drug delivery). But MOFs are preferably required in the form of surface layers/films for many other applications such as sensors, catalysis, electronic devices (including optoelectronic, electrochemical energy storage and conversion device) and membranes. Because of the demand for MOF films, several techniques have been developed in the past years, including seeded growth or secondary growth, Langmuir Blodgett layer-by-layer deposition or liquid phase epitaxy, dip coating, evaporation induced crystallization, spin coating, gel-layer synthesis, chemical vapor deposition and other similar methods. However, these methods often involve multi-step and complex processing procedures or high-cost techniques, leading to low reproducibility and they often are time- and resource-consuming. Moreover, some of these methods can only be used to prepare a few types of MOFs. Compared with the above methods, electrochemistry is considered as one of the most promising methods to prepare MOF films. On the one hand, electrochemical synthesis allows the large-scale production of MOFs in powder form, while it is also an effective method to synthesize thin films and coatings. Some of the salient features of the electrochemical deposition method are (i) there is no pre-treatment required except for simple cleaning of the substrate. (ii) the possibility to operate under milder conditions with short synthesis time (iii) the possibility to monitor the process in real time and continuously which is useful for industrial scale operations (iv) the self-closing ability of electrochemical deposition ensures high throwing power and less cracks in the film. More importantly, the parameters during electrochemical deposition can be easily and precisely controlled. Combined with the designable characteristics of MOFs, the highly controllable electrochemical deposition procedure is a promising strategy for the tailor-making of MOF films for desired applications. The salient features and advantages outlined above have evoked interest in the electrochemical deposition of MOFs and this research topic has seen explosive growth in recent years.

Eco-friendly synthesis of noble metallic nanoparticles: from theory to practice

Wednesday, 24th March - 15:35: Oral Session 2-1 (Room 1) - Abstract ID: 274

***Ms. Ana-Alexandra Sorescu*¹, *Dr. Alexandrina Nuta*², *Dr. Suica-Bunghez Ioana-Raluca*³, *Dr. Mariana Calin*⁴**

1. The National Research&Development Institute for Chemistry and Petrochemistry, 2. The National Research&Development Institute for Chemistry and Petrochemistry, 3. The Natio, 4. The National Research&Development Institute for Chemistry and Petrochemistry

Silver and gold nanoparticles, due to their unique size and antimicrobial characteristics, have a wide range of applications from the textile industry to the versatile nanomedicine. They can be chemically synthesized using either the bottom-up or the top-down approach but these routes involve the use of toxic chemicals, long reaction times, require high energy consumption and toxic by-products result. So, eco-friendly alternatives are constantly detaching from the conventional routes and they involve plants and their extracts, in a one-pot reproducible process. In the present research paper, we describe the eco-friendly synthesis of different sized silver (AgNPs) and gold nanoparticles (AuNPs) prepared under different temperature conditions. All the plants used were of up-most pharmacological importance to human health: Ramson, St Benedict's herb, Hyssopus, Wood avens, etc. In order to determine the bioactive compounds found in the aqueous extracts, qualitative screenings and quantitative determinations were performed. The eco-friendly prepared AgNPs and AuNPs were investigated by recording UV-Vis spectra in the range of 250 – 800 nm, their FTIR spectra revealed the different functional groups in their structure and DLS evaluated their size. Also, using the DPPH method, antioxidant activity was evaluated and preliminary antimicrobial screening were achieved against known Gram-positive and Gram-negative bacteria.

Preparation of TiO₂ thin films covered by plasmonic Ag nanoparticles by laser ablation technique for visible-light water splitting

Wednesday, 24th March - 15:50: Oral Session 2-1 (Room 1) - Abstract ID: 280

Dr. Martin Kostejn¹, Dr. Radek Fajgar¹, Dr. Vladislav Drinek¹, Dr. Vera Jandova¹, Dr. Jaroslav Kupcik¹, Dr. Snejana Bakardijeva²

1. Institute of chemical process fundamentals of the CAS, 2. Institute of Inorganic Chemistry of the CAS

Introduction

Water splitting using semiconductor photocatalysts is a potential process for production of hydrogen from renewable resources. Here we present preparation and characterization of water splitting system based on TiO₂ covered with plasmonic nanostructured silver.

Methods

The samples were prepared by ArF laser ablation of TiO₂ and silver targets. The ablation of the TiO₂ was carried out in vacuum using a focused laser beam to prepare a thin layer. The layer was covered by nanoparticles, prepared by ablation of Ag target at 4 Pa of inert gas. The deposits were grown on suitable substrates. The samples were heat treated at 500°C to crystallize both TiO₂ and AgNP. Both samples, as-prepared and annealed, were studied by microscopy (HRTEM), diffraction (ED, XRD) and spectroscopic techniques (UV-Vis, Raman and XPS). Photocatalytic activity towards water splitting was tested by a sweep voltammetry.

Results

As revealed by HRTEM (Fig.1), the as-prepared sample (Fig.1a) is composed of amorphous TiO₂ covered by AgNP with irregular shapes with the size 10 - 100 nm. In contrast, the annealed samples (Fig.1b) are composed of anatase TiO₂ thin film with homogeneously distributed spherical Ag nanoparticles with the size 20 – 40 nm. Heating to 500°C leads to crystallization of metal nanoparticles, but crystallinity of TiO₂ remains poor.

Plasmonic character of the deposited AgNP was proved by UV-Vis spectroscopy (Fig.2). The undoped TiO₂ layer exhibits high absorption under 330 nm in UV spectrum. AgNP absorption at 560 nm (as-prepared sample) and 400 nm (annealed sample) was recognized as a localized plasmon resonance. This absorption has a potential to improve photocatalytic properties of the deposit.

The XPS spectrum revealed prevailing Ag in the superficial layer of the as-prepared sample based on Ti 2p and Ag 3d regions. The annealed samples showed higher [Ti]/[Ag] atomic ratio.

Photoelectrochemical measurements (Fig.3) were conducted with deposits (blue - as-prepared, red - annealed) on FTO glass substrates. The sweep voltammetry was studied at bias potentials -0.1 to +1.3 V with Pt counter electrode and Ag/AgCl reference electrode in H₂SO₄. Under irradiation by visible light, H₂ on Pt and O₂ generation on working electrodes were visible.

Discussion

The samples displayed higher activities when exposed to light. The photochemical activity of the as-prepared sample was low under studied bias potentials, but satisfying activities of the annealed samples were observed, as expected from the intense LSP resonance at 400 nm.

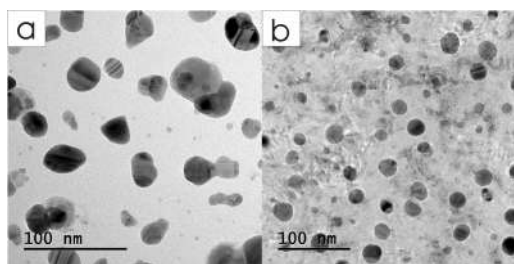


Fig 1 hrtem images.jpg

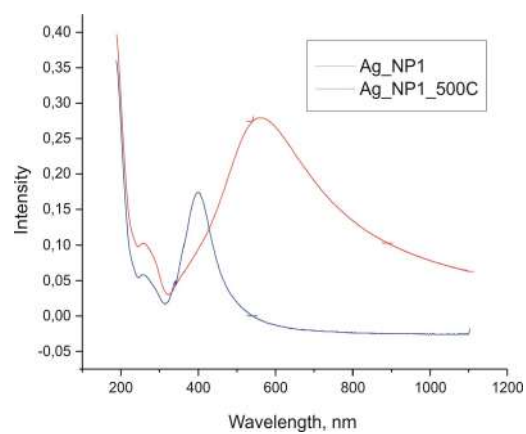


Fig 2 uv-vis spectra.jpg

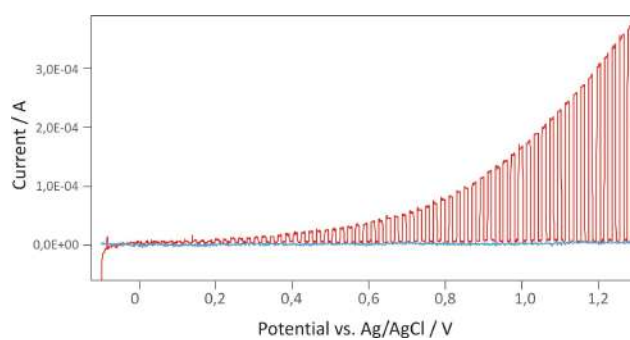


Fig 3 sweep voltammetry.jpg

Green Energy hybrid graphene device

Wednesday, 24th March - 16:05: Oral Session 2-1 (Room 1) - Abstract ID: 244

Dr. javier martinez¹

1. ISOM Institute of Optoelectronic Systems and Microtechnology

Graphene has attracted increasing attention in recent years due to its excellent mechanical, optical and electrical properties [1]. Its high theoretical specific surface area ($SSA = 2630 \text{ m}^2 \text{ g}^{-1}$) and high electrical conductivity make it an attractive material for many industrial applications [2,3]. Also, it is a flexible transparent material that can be used for solar cells, light emitting diodes (LEDs, OLEDs), touchscreens and LCD displays [4], and in the near future, its flexibility will let to create foldable and wearable devices. In particular, as a consequence of the increasing demand for more efficient, longer-lasting and more compact portable electronic devices, the use of graphene in energy storage devices is one of the most promising applications for this material [5].

We report on the precise fabrication of low cost, high-performance electrochemical supercapacitors with electrodes based in reduced graphene oxide(rGO)/polyaniline nanofiber composite electrode [5]. An infrared laser has been used to reduce the graphene oxide, converting the initial graphene oxide (GO) compact layer into a three dimensional open network of exfoliated graphene flakes (LrGO). This highly conducting porous structure is well suited for electrodepositing pseudocapacitive materials owing to its large surface area. Polyaniline nanofibers have been controllably electrodeposited [6] on the graphene flake network, not only extending further the electrode surface area and providing it with a strong pseudocapacitance but also preventing the restacking of the graphene sheets during the subsequent device processing and charge-discharge cycling.

The progress in silicon-heterojunction solar cells requires to develop new architectures of transparent front electrodes in order to generate and extract current in a more efficient way [7]. State-of-the-art contacts for this application are a wide variety of transparent conductive oxides (TCOs). Among them, the one most commonly used is an 80-nm-thick indium tin oxide (ITO) layer. But the cost and scarcity of indium and its rather limited sheet resistance, not below $100 \Omega/\text{sq}$ for such thicknesses, lead to the search of new strategies [8].

New architectures of indium-free TCO-based transparent electrodes incorporating one, two and three atomic graphene layers, respectively in different configurations were explored as possible approaches to improve silicon-heterojunction-cell front contacts. The results reveal that the transparent-electrode properties (Fig. 2) dramatically depend on the order in which the TCO and graphene layers have been deposited [9].

In conclusion, graphene can be used in energy generation and storage devices and it is possible to create a hybrid device that combine these two devices.

Acknowledgements:

This research was partially funded by the Spanish Ministry of Science & Innovation under the project DiGRAFEN, grant number (ENE2017-88065-C2-1-R) and (ENE2017-88065-C2-2-R) (MINECO/AEI/FEDER, UE) and A. V. FPU grant, as well as the Comunidad de Madrid through project NMat2D-CM (S2018/NMT-4511). J.P. acknowledges support from Spanish MINECO (Grant RyC-2015-18968). R.S.F. acknowledges support from European Union's Horizon 2020 Research and Innovation Programme under Marie Skłodowska-Curie Grant Agreement No 642688. And The authors A.L., M.F., I.A. acknowledge support from the EU under Horizon 2020's EIC SME Instrument, under grant agreement No 829644. The author I.A. also acknowledges funding provided by FEDER and the Spanish Ministerio de Ciencia, Innovación y Universidades – Agencia Estatal de Investigación, under project TEC2017-85529-C3-2-R (AEI/FEDER, UE).

Acknowledgements.jpg

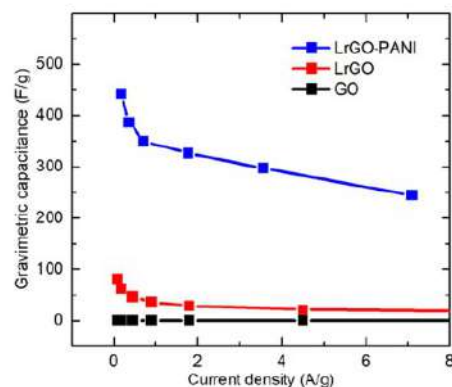
**Figure 1:** Gravimetric capacitance as a function of the current density for the GO, LrGO and PANI-LrGO electrodes.

Figure 1.jpg

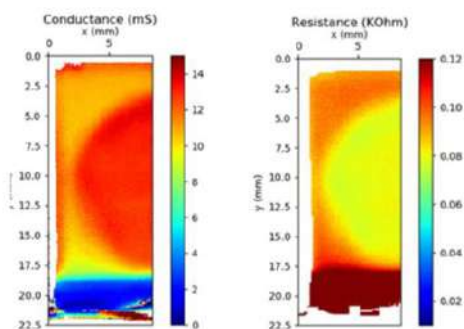
**Figure 2:** Conductance and resistance maps of three graphene layers transferred on top of the ITO/Si substrate system.

Figure 2.jpg

References:

- [1] Luo et al., *Small*, 8 (2012), 630
- [2] Stoller et al., *Nano Lett.*, 8(2008), 3498
- [3] Bosca et al., *Sci. Rep.*, 6(2015), 21676
- [4] Cao et al., *Small*, 7(2011), 3163
- [5] Ladrón de Guevara et al., *Appl. Surf. Sci.*, 467 (2019), 691
- [6] Pedrós et al., *J. Power Sourc.*, 317(2016), 35
- [7] Green, et al., *Prog. Photovolt.:Res. Appl.* 24(2016) 905.
- [8] Terasako, et al., *Surf. Coat. Technol.* 201(2007) 8924
- [9] Fernández et al., *Micromachines* 10 (2019) 402.

References.jpg

PCE-based additives enable the formulation of highly-loaded, high-performance ceramic inks for extrusion printing

Wednesday, 24th March - 14:50: Oral Session 2-2 (Room 2) - Abstract ID: 304

**Mr. Omid Akhlaghi¹, Mr. Amin Hodaiei¹, Mr. Can Akaoglu¹, Mr. navid Khani¹, Ms. Ferdows Afghah²,
Mr. Bahattin Koc¹, Ms. Ozge Akbulut³**

1. Sabanci University Nanotechnology Research and Application Centre, 2. Sabanci University, 3.

ozge.akbulut@sabanciuniv.edu

Additive manufacturing (AM) has shown its potential to print “functionality” along with “form”. Fabrication of ceramic objects/features has become one of the goals of AM since ceramics are hard to process with conventional methods. The capabilities of AM, however, are restricted by the availability of ceramics inks. Current formulations are highly-loaded suspensions of ceramic particles (at amounts 65–75 wt. % for direct-writing, 5–20 wt. % for ink-jet printing). The stability and viscosity-control of these suspensions are sustained through combinations of additives in large amounts (5–30 wt. %). There are two inter-related problems associated with these formulations: i) they utilize linear polyelectrolytes as dispersants and rely on electrostatic repulsion-based stability—the key role of steric hindrance for stability and rheological control of suspensions is ignored, ii) non-optimized chemicals rise a need for the use of many additives in high amounts leading to harder dimensional control and more defects. This conspicuous lack of systematic strategy for designing ceramic inks hinders the ultimate potential of AM.

Here, I will be describing the particle-specific design of poly(carboxylate ether)(PCE)-based single additives that can offer both stability and viscosity-control in extrusion-printing of ceramic inks. I will be underscoring the choice of co-monomers and side-chain density for three different particle systems—iron oxide, alumina, and zirconia, while demonstrating the clear difference between the performance of optimized and non-optimized inks. Through utilizing less than 1,5 wt.% PCE-based additives in ceramic inks, we are reaching almost theoretical loadings and these formulations can provide i) tighter dimensional control, ii) lower sintering temperatures, and iii) elimination of other additives and hence the complex burn-out step.

Tumor-Targeted Indocyanine Green-Loaded Ferritin Nanotracers for Intraoperative Detection of Cancer Tissue on an Orthotopic Murine Model of Breast Cancer

Wednesday, 24th March - 15:20: Oral Session 2-2 (Room 2) - Abstract ID: 269

Dr. Serena Mazzucchelli¹, Dr. Marta Sevieri¹, Dr. Leopoldo Sitia², Dr. Arianna Bonizzi¹, Dr. Raffaele Allevi¹, Dr. marta truffi³, Dr. Carlo Morasso³, Prof. Fabio Corsi³

1. Dipartimento di Scienze Biomediche e Cliniche "L. Sacco", Università di Milano, 2. Dipartimento di Scienze Biomediche e Cliniche "L. Sacco", università di Milano, 3. Istituti Clinici Scientifici Maugeri IRCCS, 27100 Pavia

Introduction: Indocyanine green (ICG) is a near infrared fluorescent tracer used in image-guided surgery to assist surgeons during resection. Despite it seems a very promising tool for surgical oncology, its employment is limited to lymph nodes mapping, since it lacks tumor targeting specificity. Recently, we proposed to nanoformulate ICG giving it tumor targeting specificity, in order to expand its employment in surgical oncology. This nanosystem is constituted by 24 monomers of H-Ferritin (HF_n), which self-assembles in a spherical cage structure enclosing ICG. This natural protein-based nanoparticle has been demonstrated to display tumor homing, thanks to the specific interaction between the HF_n nanocage and the transferrin receptor 1, which is overexpressed in most of tumor tissues.

Methods: ICG loaded HF_n nanocages (HF_n-ICG) were prepared exploiting the ability of HF_n to disassemble and reassemble its quaternary structure in response to changes in pH. We assessed their capability of recognition and uptake *in vitro* into different gastric, breast, and colo-rectal cancer cell lines. Finally, we evaluated HF_n-ICG tumor accumulation and off-target biodistribution in a preclinical model of breast cancer. 4T1 tumor-bearing mice were randomly divided into two groups and injected intravenously with HF_n-ICG or free ICG. Then mice were sacrificed after 6 or 24 hours after injection and analyzed in order to detect the fluorescent signal by coupling the use of the KARL STORZ NIR/ICG endoscopic system to the IVIS Lumina II system.

Results and discussion: Our study demonstrated that HF_n-ICG exhibits specific uptake into different cancer cell lines and is able to deliver ICG to the tumor more efficiently than the free dye in an *in vivo* model of breast cancer (Figure 1). In addition, the *ex vivo* comparison between the biodistribution of HF_n-ICG and free ICG clearly showed that ICG-related fluorescent signal is localized in the tumor mass of mice treated with HF_n-ICG 6 hours after injection and it is still detectable 24 hour after. Otherwise, mice injected with free ICG display a barely noticeable signal (Figure 2). Moreover, HF_n encapsulation modifies ICG biodistribution and significantly preserve ICG fluorescence by protecting it from rapid metabolism and degradation (Figure 3), improving its tumor accumulation. Our results support the suitability of HF_n-ICG as an *in vivo* nanotracer for fluorescence-guided intraoperative detection of tumors.

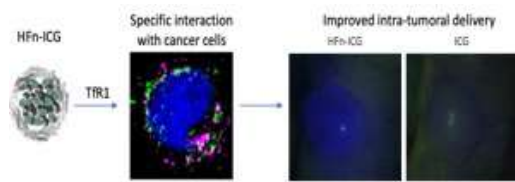


Figure1.jpg

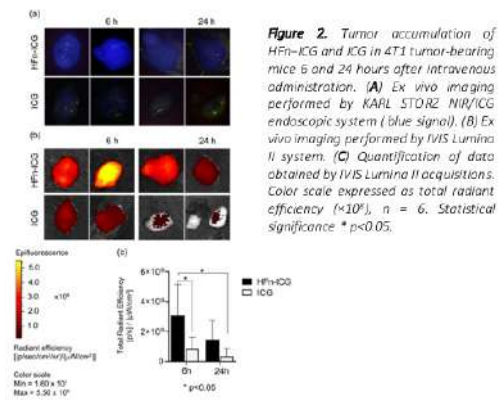


Figure2.jpg

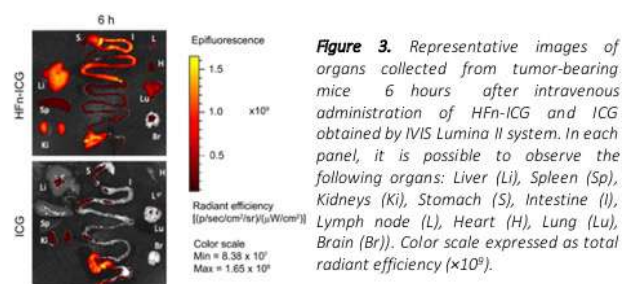


Figure3.jpg

A Nanotoxicology Study: The Impact of Size of Silver & Gold Nanoparticles on Lung Cells

Wednesday, 24th March - 15:35: Oral Session 2-2 (Room 2) - Abstract ID: 237

Ms. Hanouf Bafhaid¹, Dr. Zubair Ahmed¹, Dr. Youcef Mehellou², Dr. Hanene Ali-Boucetta¹

1. University of Birmingham, 2. Cardiff University

Introduction: Nanotoxicology studies are not conclusive about the cytotoxicity of nanoparticles (NPs) as the biological responses are predominately influenced by NPs' different physiochemical properties which are often are not well characterised. This study investigates the cytotoxicity of spherical silver (AgNPs) and gold (AuNPs) nanoparticles of different sizes (10,40 and 80nm) following their 24hrs exposure to normal lung fibroblasts (MRC-5) and lung adenocarcinoma (A549) cells.

Methods: The size and charge of the NPs were characterised using dynamic light scattering and transmission electron microscopy. The cytotoxicity effects of NPs were then studied using MTT, mLDH assays and the mechanism(s) of cell death investigated using Annexin-V/PI, reactive oxygen species (ROS) generation and glutathione depletion.

Result: On A549 cells, we found that CC50 (50% cytotoxic concentration) of Ag10 and Au10 after 24hrs are 11.7 and 42.2µg/ml respectively which suggests that AuNP are safer than AgNP. It was interesting to see that the smaller sizes (10,40nm) of AgNP and AuNP demonstrate more cytotoxicity in comparison to their bigger counterparts(80nm). Apoptotic cell death was observed in a size and concentration dependent manner following exposure to AgNP in both cell lines. Induction of oxidative stress was also found after 24hrs post- exposure to all sizes of AgNP on both cell lines, while AuNP showed an increase in ROS generation only at the highest concentration(40µg/ml). After 24hrs exposure to AgNP, the amount of reduced glutathione was significantly depleted in a size and dose-dependent manner with up to 80% decrease in reducing glutathione levels after A594 exposure to Ag10. AuNP illustrated a reduction effect on reduced glutathione in A549 and MRC-5 cells at the highest concentration which correlates with the detected ROS levels.

Discussion: Our findings demonstrate that the size of NPs can influence their interaction with cells. Smaller AgNPs sizes (10 and 40nm) show detrimental effects on both lung cell lines. AuNP demonstrated a good safety profile comparing to AgNP of the same size, emphasising that NPs composition has also an impact on their cellular toxicity. However, MRC-5 and A549 cells display similar trend of toxicity toward AgNP, which is associated with the release of silver ions. The toxicological profile of NPs may not only be influenced by their physiochemical properties (such as size) but also their chemical composition. It is therefore important that a systematic nanotoxicology framework is established to validate current nanotoxicology literature. This is crucial especially if these NPs are to be used in biomedicine.

Tunable hydrogel nanostructures by microfluidics to control Hydrodenticity effect for multimodal imaging applications

Wednesday, 24th March - 15:50: Oral Session 2-2 (Room 2) - Abstract ID: 139

Mr. Alessio Smeraldo¹, Prof. Enza Torino²

1. Department of Chemical, Materials Engineering & Industrial Production, University of Naples Federico II, Piazzale Tecchio 80, 80125 Naples, Italy, 2. Department of Chemical, Materials Engineering & Industrial Production, University of Naples Federico I. Center for Advanced Biomaterials for Health Care, CABHC, Istituto Italiano di Tecnologia, IIT@CRIB,

The possibility to obtain an accurate and reliable diagnosis is one of the main challenges in the clinical practice. For this reason, contrast agents are commonly used to improve the difference between normal and pathological districts and get important information from images. However, main limitations are a non-specific biodistribution, that leads to have low sensitivity in the investigated region, and a rapid clearance that allows only short imaging times. Recently, polymer nanoparticles have proven to be promising nanostructures to improve detection of several diseases thanks to a precise delivery to the target site. In order to achieve the desired signal in a specific body district, the rational design of the polymer nanoparticles is essential to affect the contrast agent pharmacokinetics. In this perspective, to finely tune nanoparticles physicochemical properties, microfluidics offers more advantages over batch processes. Within the microfluidic chip, diffusion and thermodynamic phenomena can be handled by tuning the process parameters. In the present work, ionotropic gelation via chitosan-sodium tripolyphosphate crosslinking followed by hyaluronic acid-chitosan complex coacervation has been implemented. The production of hybrid chitosan-hyaluronic acid nanoparticles has been carried out in a custom-designed microfluidic chip with a specific geometry tailored to achieve a hydrodynamic flow focusing condition. Results show the microfluidics' ability to control morphological properties of the nanovectors through the manipulation of flow rates, influencing their formation at molecular level. Moreover, the potentiality of these nanostructures has been proven through the encapsulation of a clinical used Magnetic Resonance Imaging contrast agent, Gd-DTPA, demonstrating their ability to improve relaxometric properties of the metal-complex. In fact, through the proper control of the structural properties of the nanovectors, a specific effect, called *Hydrodenticity*, can be reached. In addition, the encapsulation of Gd-DTPA and a dye for Optical Imaging is achieved in a one-step process, demonstrating the dual capability of the nanoparticles as a promising nanocarrier for multimodal imaging.

Fighting *Helicobacter pylori* with drug-free nanostructured lipid carriers (NLC)

Wednesday, 24th March - 16:05: Oral Session 2-2 (Room 2) - Abstract ID: 143

Ms. Rute Chitas¹, Dr. Catarina L. Seabra², Dr. Cláudia Nunes², Dr. Paula Parreira³, Prof. M. Cristina L. Martins¹

1. 1. INEB - Instituto de Engenharia Biomédica, Universidade do Porto | 2. i3S - Instituto de Investigação e Inovação em Saúde, Universidade do Porto | 3. ICBAS - Instituto de Ciências Biomédicas Abel Salazar, Universidade do Porto, 2. 4. LAQV-REQUIMTE, Departamento de Ciências Químicas, Faculdade de Farmácia, Universidade do Porto, 3. 1. INEB - Instituto de Engenharia Biomédica, Universidade do Porto | 2. i3S - Instituto de Investigação e Inovação em Saúde, Universidade do Porto

Introduction: *Helicobacter pylori*(Hp) is a gastric pathogen that infects around half of the world's population. Hp is responsible for the development of several gastric disorders, including gastric cancer [1]. The main treatments to counteract Hp infection consist in the administration of antibiotics and proton-pump inhibitors. These treatments are failing, mainly due to the increase of antibiotic resistance [2]. Drug-free nanostructured lipid carriers (NLC) have been studied for Hp eradication, showing bactericidal effect against Hp both *in vitro/vivo*[3,4,5]. This work aims to optimize NLC efficiency by fine-tuning its physicochemical characteristics, in order to achieve complete Hp eradication.

Methods: Two surfactants were tested in NLC preparation: Tween®60 and Tween®80. NLC were produced by hot homogenization followed by ultrasonication. The nanoparticles were optimized in terms of size by altering the ultrasonication parameters, namely time and amplitude of sonication. NLC characterization was done by dynamic light scattering (DLS) and electrophoretic light scattering (ELS), to determine size and charge, respectively. Concentration was measured by nanoparticle tracking analysis (NTA). For NLC with Tween®60 and Tween®80 the effect of dialysis in NLC activity was evaluated. Furthermore, the effect of size was assessed in NLC with Tween®60. All NLC were tested *in vitro* against Hp J99 strain.

Results: The nanoparticles with Tween®60 and Tween®80 had sizes between 140-486nm and 190-228nm, respectively. In terms of charge, both NLC were anionic with a surface charge between -25 to -30mV. All NLC stocks had a final concentration in 10¹³-10¹⁴ particles/ml range. The anionic NLC were tested against Hp J99. After 24h of incubation, both formulations had similar outcomes, achieving a bactericidal effect. Non-dialyzed and dialyzed NLC also showed the same bactericidal activity. Additionally, NLC with bigger sizes (>400 nm) showed a higher bactericidal effect.

Discussion: The NLC were successfully optimized in terms of size. Both formulations (Tween®60 and Tween®80) were effective against Hp and the dialysis didn't affect the NLC bactericidal activity. Additionally, preliminary results indicate that size can play a role in the NLC bactericidal activity.

Conclusion:Overall, these results further support the therapeutic potential of these nanoparticles for management of Hp gastric infection.

References:

- [1] Karkhah A. *et al.*, Microbiological Res, 218 (2019) 49-57.
- [2] Testerman T.L & Morris J., World J Gastroenterol, 20 (2014) 12781-12808.
- [3] Seabra C.L. *et al.*, Int J Pharm, 519 (2017) 128-137.
- [4] Seabra C.L. *et al.*, Eur J Pharm Biopharm, 127 (2018) 378-386.
- [5] Seabra C.L. *et al.*, Manuscript in preparation.

TBD

Wednesday, 24th March - 16:40: Plenary Session 2 (Room 1) - Abstract ID: 309

Dr. Steven George¹

1. University of Colorado

TBD

Plasmonic metal oxide nanocrystals

Wednesday, 24th March - 17:25: Plenary Session 2 (Room 1) - Abstract ID: 301

Prof. Delia Milliron¹

1. University of Texas at Austin

Metal oxide nanocrystals doped with a few percent of aliovalent dopants become electronically conducting and support strong light-matter interactions in the infrared due to localized surface plasmon resonance (LSPR). In the prototypical material tin-doped indium oxide ($\text{Sn:In}_2\text{O}_3$), we have found that the strength and spectrum of light absorption depend nontrivially on nanocrystal doping, size, and the radial distribution of dopants. Localizing tin dopants in the outer shell of the nanocrystals makes them more sensitive to changes in the refractive index of their surroundings. The associated compression of the near-surface depletion region also enhances conductivity in nanocrystal films. Doping with fluorine, as a substitutional dopant for oxygen, plays a dual role as an electron donor and a shape-directing agent, leading to well-faceted nanocrystal cubes. Co-doped $\text{F,Sn:In}_2\text{O}_3$ nanocrystals have strong coupling between the near-infrared LSPR of individual cubes in 2-D arrays. Overall, this new class of plasmonic nanomaterials offers opportunities for synthetic tuning of optical properties beyond what's possible with conventional metals. Emerging applications in sensing, smart windows, and catalysis may take advantage of their unique ability to concentrate and direct energy flow from infrared light.

TBD

Thursday, 25th March - 09:00: Plenary Session (Room 1) - Abstract ID: 310

Prof. Manish Chhowalla ¹

1. university of cambridge

TBD

Nanocrystals as chemical building blocks

Thursday, 25th March - 09:45: Plenary Session (Room 1) - Abstract ID: 299

Prof. Helmut Cölfen¹

1. University of Konstanz

Nanoparticles have interesting analogies to molecules. Recent research has revealed that nanocrystals can align and fuse to larger single crystalline units (Oriented Attachment) or build self-assembled superstructures with mutual crystallographic order (Mesocrystals). These examples suggest that it should be possible to establish chemistry with nanocrystals as chemical building blocks. Nanocrystals are similar to molecules concerning active reaction sites and ability for directed interactions. Oriented attachment is analogous to chemical bond formation, while mesocrystal formation is analogous to non-covalent bonds in complexes between molecules. Key for the defined nanocrystal activation as chemical building unit is the selective adsorption/desorption of specially designed molecules on pre-defined crystal faces. Examples for this concept will be given for gold nanoparticles.

Alternatively, interaction of the nanocrystal surface adsorbed molecules can be induced, leading to mesocrystal formation. Mesocrystals can combine typical nanocrystal properties like high surface area or effects like superparamagnetism, surface plasmon resonance, or quantum size effect with the good processability of micro- or macrocrystals and single crystal properties. In this presentation typical synthesis concepts for mesocrystals will be shown as well as the structure of mesocrystals. Also, some fascinating properties of mesocrystals will be presented like semiconducting properties of metal mesocrystals, conducting mesocrystals as well as catalytic properties. The spectrum of useful properties can potentially even be increased for binary mesocrystals with two chemically different building blocks. First examples of binary mesocrystals will also be given, combining the properties of chemically different nanocrystals.

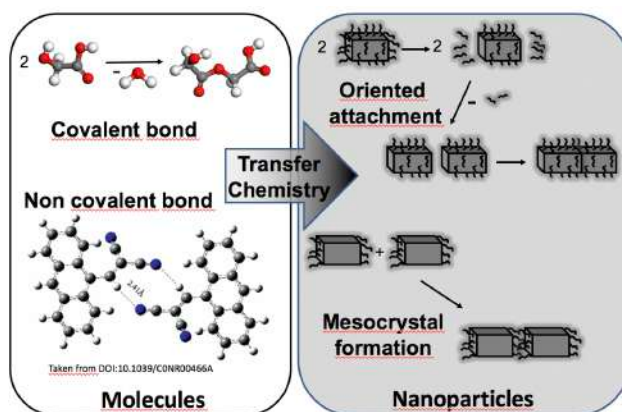


Image for abstract coelfen.png

TBD

Thursday, 25th March - 10:50: Oral Session 1-1 (Room 1) - Abstract ID: 311

Ms. Lianzhou Wang¹

1. univesity of quinsland

TBD

Hydroxyapatite Growth on the Carbon Dot entegrated TiO₂Nanoneedles in Simulated-Body-Fluids(SBF)

Thursday, 25th March - 11:20: Oral Session 1-1 (Room 1) - Abstract ID: 61

Mr. aziz rahman aylak¹, Dr. Rükan GENÇ ALTÜRK²

1. Ph.d. chemical engineering of mersin university, 2. Assoc. Prof. Dr. in university of mersin

In this study, TiO₂ nanoneedles (NNs) and TiO₂/CDot nano-composites were synthesized by the hydrothermal method. Investigation for the corresponding morphologies and detailed formation mechanisms of samples were conducted by X-ray diffraction pattern (XRD), Scanning electron microscope (SEM), Fourier transform infrared (FT-IR) spectroscopy, and Brunauer, Emmet, and Teller (BET) analysis. The surface areas of TiO₂ and TiO₂/CDot were found to be 45.55 and 224.74 m²/g, respectively. The presence of CDot on the TiO₂ structure increased the surface area more than 5 times. Further studies on the hydroxyapatite (HAP) deposition on the TiO₂/CDot (10 wt%) as compared to neat TiO₂ in simulated-body-fluid (SBF) after 1 and 2 weeks of incubation, an apparent improvement of HAP crystallization on the surface of TiO₂/CDot was observed. Moreover, XRD analysis of the samples showed enhancement of the peak intensities at $2\theta=32.17$ and $2\theta=46.71$ which belong to HAP, while the FTIR peaks located at around 560-640, 963, and 1028-1110 cm⁻¹ were attributed to the PO₄⁻³ ion of HAP were also demonstrated an improved deposition of HAP on to the TiO₂ surface after CDot integration.

Characterization and in-vitro hemolysis evaluation of carboxy methyl cellulose capped silver nano particles .

Thursday, 25th March - 11:35: Oral Session 1-1 (Room 1) - Abstract ID: 240

Ms. Archi Ghosh¹, Dr. Mahua Ghosh Chaudhuri², Dr. Prasanta Kumar Maiti³, Prof. Kumkum Bhattacharyya⁴

1. Institute of Post-Graduate Medical Education & Research, Kolkata, India, 2. Jadavpur University, Kolkata, 3. IPGME&R and SSKM Hospital Kolkata, 4. Institute of Post Graduate Medical Education & Research, Kolkata, India

Introduction:

The search for resistant-proof, non-traditional antibacterial agents are gaining importance in view of dwindling of antibiotic development and increasing irrational antibiotic therapy in recent time. Silver nanomaterials are increasingly being used as antimicrobial agents. This study will assess the in vitro hemolytic potential of silver nano particles in human blood determining physical and chemical particle properties that contribute to mechanisms of red blood cell (RBC) damage.

Methods:

The colloidal silver nano-particles had been prepared from silver nitrate by Carboxy Methyl Cellulose (CMC) as source of capping agents and glucose as reducing agents & characterized for physical and antimicrobial properties .

The diluted RBC suspension (0.3 ml) were mixed with Ag-NP suspensions in PBS (1.2 ml) at various concentrations (final hematocrit, 5%). RBC suspension in PBS (1.2 ml) without AgNPs were used as a control. The final combined suspensions were gently mixed and incubated at room temperature at 1 hour intervals upto 4 hours. Heparinized human blood were diluted with $\text{Ca}^{2+}/\text{Mg}^{2+}$ -free DPBS and added to solutions of undiluted silver nano particles. After 3.5-h incubation in 37 °C water bath, the tubes were centrifuged at 800 x g for 15 min at room temperature. The supernatants were mixed in a 1:1 ratio with CMH reagent and were analyzed at 540 nm. The concentration of cell-free hemoglobin in each sample were assessed from the hemoglobin standard curve and by accounting for the 16-fold dilution factor for the samples and controls. The percent hemolysis was obtained by dividing each sample's cell-free hemoglobin concentration by the total hemoglobin concentration (10 mg/ml). Poly ethylene glycol was used as a negative control and Triton X-100 was used as a positive control.

Results:

Prepared CMC capped silver nanoparticles showed average size of 9.5 nm, with triangular shape. Their UV-absorption spectrum were 409 nm. Zeta potential values of prepared silver nano particle were -28 mV.

The antimicrobial efficacy of the AgNPs were between 8192 to 32,768 folds.

The silver nano particles did not cause any hemolysis even at the highest concentration which indicate the test material does not cause any damage to RBCs and safe for systemic use.

Discussion:

Silver nanoparticles present numerous interactions with blood components as RBCs, platelets and a coagulation system. For the development of nanomedicines from a hemocompatibility perspective, the hemolysis analysis may be useful for first-in-human exposure and for identifying appropriate safety margins.

Table: Anti-microbial enhancement of CMC capped silver nanoparticles by shifting MIC following nano conversion :

AgNPs	Organism	MIC of colloidal AgNP	MIC of AgNO ₃ solution with equivalent silver	Antimicrobial efficacy
CMC Capped AgNPs (10.8 mg / L Silver from 17 mg AgNO ₃ / L)	<i>S aureus</i> ATCC 43300	1/32768 dL	1/2 dL	16384- fold
	<i>S. aureus</i> MDR	1/32768 dL	1/2 dL	16384- fold
	<i>E. coli</i> ATCC 25922	1/32768 dL	1/2 dL	16384- fold
	<i>E. coli</i> MDR	1/32768 dL	1/2 dL	16384- fold
	<i>P. aeruginosa</i> ATCC 27833	1/32768 dL	1/8 dL	8192- fold
	<i>P. aeruginosa</i> MDR	1/32768 dL	1/4 dL	8192- fold
	<i>C. albicans</i> ATCC 10251	1/35536 dL	1/2 dL	32768- fold
	<i>C. albicans</i> MDR	1/35536 dL	1/2 dL	32768- fold

Table final.jpg

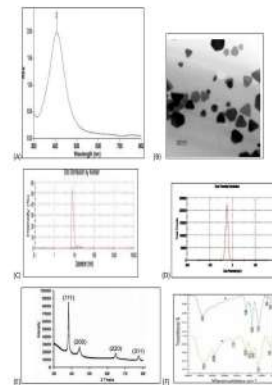


FIGURE (A) UV absorption spectrum of carboxymethyl cellulose capped silver nanoparticles at 400 nm and narrow distribution; (B) TEM image of triangular carboxymethyl cellulose capped silver nanoparticles; (C) Size distribution obtained from DLS measurements of carboxymethyl cellulose capped silver nanoparticles; (D) Zeta potential of carboxymethyl cellulose capped silver nanoparticles; (E) FTIR spectrum of pure carboxymethyl cellulose; (F) FTIR spectrum of carboxymethyl cellulose capped silver nanoparticles.

Figure final.jpg

GREEN BIOSYNTHESIS OF MULTIFUNCTIONAL NANOMATERIALS

Thursday, 25th March - 11:50: Oral Session 1-1 (Room 1) - Abstract ID: 91

Prof. Malik Maaza¹

1. UNISA

•Up to recently, the various nanomaterials were synthesized via 2 major methodologies: Physical or chemical. While the physical methodologies are energy-intensive, the chemical ones are waste exhaustive. Lately, green bio-nano synthesis, based on the usage of natural extracts as effective chelating agents is gaining momentum. This fast-growing topic, obeying the 12 commandments of green chemistry, cements further the fields of Phytochemistry, biosciences & drug design. This contribution reports on a series of functional nanomaterials bio-engineered using natural extracts of various indigenous plants such as Hoodia Gordonii (Khoisan hoodia), Agathosma betulina (Buggu) or aspalathus linearis(Rooibois) or Calistemon viminalis (bottlebrush)or Moringa among others. Likewise, we report on their efficiency as anti-microbial & anti-viral, anti-cancer & cosmetics responses.

Optical Properties of Layered Hybrid Perovskites: Nano @ Bulk

Thursday, 25th March - 10:50: Oral Session 1-2 (Room 2) - Abstract ID: 303

***Prof. Angshuman Nag*¹**

1. Indian Institute of Science Education and Research (IISER) Pune

Hybrid perovskites like $(\text{C}_4\text{H}_9\text{NH}_3)_2\text{PbI}_4$ have fascinating layered crystal structure with periodic nanoscale interfaces between the inorganic $\{\text{PbI}_4\}^{2-}$ and organic $\text{C}_4\text{H}_9\text{NH}_3^+$ layers. Because of these interfaces, electron and hole are confined in atomically thin $\{\text{PbI}_4\}^{2-}$ inorganic well layers. Therefore, these layered perovskites are considered as electronically 2D systems, irrespective of their crystallite sizes.^{1,2} Importantly, the crystal structure is flexible, allowing a number of combinations of different organic cations and inorganic anions. So a rational design of the nanoscale interfaces, and hence, tunable optoelectronic properties are feasible. For example, excitonic binding energy can be controlled over an order of magnitude from a few tens of meV to a few hundreds of meV, with simple variation of composition of organic cations. So for solar cell and photocatalytic applications, one can choose the composition with lower excitonic binding energies, whereas for LED, higher excitonic binding energy is preferred. Interestingly, chiral organic cations can impart optical non-linearity and chiral optoelectronic properties. In this talk, I will discuss about how controlling nanoscale interface between organic and inorganic layers can yield interesting optical and optoelectronic properties. Furthermore, we observe signatures of interactions between adjacent $\{\text{PbI}_4\}^{2-}$ inorganic wells.³ Does it mean that the layered perovskites deviates from the perceived model of electronically 2D quantum well? Well, the story is not so simple, and I will discuss the role of layer edges.

References:

1. Sheikh, T.; Shinde, A.; Mahamuni, S.; Nag, A. Possible Dual Bandgap in $(\text{C}_4\text{H}_9\text{NH}_3)_2\text{PbI}_4$ 2D Layered Perovskite: Single-Crystal and Exfoliated Few-Layer. *ACS Energy Lett.* **2018**, *3*, 2940.
2. Chakraborty, R.; Nag, A. Dielectric Confinement for Designing Compositions and Optoelectronic Properties of 2D Layered Hybrid Perovskites. *Phys. Chem. Chem. Phys.* **2021**, *23*, 82.
3. Sheikh, T.; Nawale, V.; Pathoor, N.; Phadnis, C.; Chowdhury, A.; Nag, A. Molecular Intercalation and Electronic Two Dimensionality in Layered Hybrid Perovskites. *Angew. Chem. Int. Ed.* **2020**, *59*, 11653.

Hybrid luminescent systems on the base of PbS nanocrystals and freestanding porous silicon microcavities in the near-infrared range

Thursday, 25th March - 11:20: Oral Session 1-2 (Room 2) - Abstract ID: 236

Ms. Irina Kriukova¹, Dr. Pavel Samokhvalov², Prof. Igor Nabiev³

1. LRN-EA4682, Université de Reims Champagne-Ardenne, Reims, France; LNBE, NRNU MEPhI, Moscow, Russian Federation, 2. LNBE, NRNU MEPhI, Moscow, Russian Federation, 3. LRN-EA4682, Université de Reims Champagne-Ardenne, Reims, France; LNBE, NRNU MEPhI, Moscow, Russian Federation; Sechenov University, Moscow, Russian Federation

Light-matter interaction in hybrid systems made of fluorophores embedded in a microcavity (MC) attracts much attention [1]. Depending on the coupling strength between the components, either photoluminescence (PL) enhancement or hybridization of luminophore energy levels with the MC eigenmode resulting in two hybrid energy states occurs in these systems. This effect can be used in various practical applications for accelerating chemical reactions, enhancing Raman scattering, increasing conductivity, obtaining Bose-Einstein condensates at room temperature, etc. [1]. Hybrid structures emitting in near infrared (NIR) range can be used in biomedical applications for exciting and detecting radiation within the transparency window of biological tissues.

We have developed hybrid photoluminescent structures based on porous silicon photonic crystals (PhCs) and PbS quantum dots (QDs) emitting in the NIR range. PhC-based MCs obtained by electrochemical etching of monocrystalline Si comprise two Bragg mirrors (sequences of alternating layers of high and low porosities) with a cavity layer of double thickness between them. The PhCs were exfoliated from monocrystalline Si by electrochemical polishing to obtain free-standing samples. Comparison of the PhC reflectance spectra before and after exfoliation showed a 100-nm blue shift of the photonic band gap due to partial oxidation, the other parameters, including the eigenmode width (~10 nm) and Q-factor (~200), being unchanged. Hence, our exfoliation routine does not significantly affect the MC properties. For stabilizing the MC optical properties of and reducing the number of de-excitation channels for embedded QDs, the samples were thermally oxidized before QD deposition, which resulted in a further blue shift of the reflectance spectrum and an increase in the eigenmode width due to a decreased contrast of refractive indices.

After embedding QDs by drop-casting, we observed narrowing of their PL spectrum compared to the QD solution. We attribute this to suppression of QD PL outside the MC eigenmode due to the Purcell effect [2]. This clearly indicates weak coupling between the QD exciton and MC eigenmode.

Thus, our hybrid structures display weak light-matter coupling in the NIR range, which provides the basis for new nanophotonic biosensor systems. In addition, they are freestanding, thus offering prospects for designing sensors with the option of pumping analytes through the porous structure.

[1] DOVZHENKO, D. S., RYABCHUK, S. V., RAKOVICH, Y. P., NABIEV, I.R. 2018. Light-matter interaction in the strong coupling regime: configurations, conditions, and applications. *Nanoscale*, 10, 3589-3605.

[2] PURCELL, E. M. 1946. Spontaneous emission probabilities at radio frequencies. *Phys Rev*, 69, 681.

Morphologically controlled synthesis of Ag@S where S= CZTS, PbS based hybrid nanostructures

Thursday, 25th March - 11:35: Oral Session 1-2 (Room 2) - Abstract ID: 132

Ms. Anchal Yadav¹, Prof. Bart Follink², Dr. Alison Funston¹

1. Monash University, ARC Centre of Excellence in Exciton Science, 2. Monash University

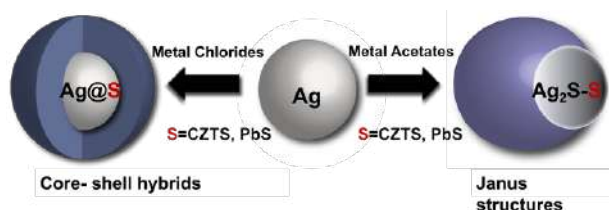
Compared with the single component, the multicomponent nanostructures known as hybrid nanostructures synthesized by combining two or more chemically distinct components to generate various hybrid nanostructure offers the unconventional properties and has the potential to lead to useful applications in the field of electronic and various optoelectronic devices.

However, due to the different composition, it is difficult to obtain the growth of one material onto the other material and several parameters such as the lattice mismatch, crystal structure, surface reactivity of the materials need to be considered. With metal-semiconductor hybrid nanostructures, the lattice mismatch between the two is quite large due to which it is difficult to grow semiconductor shells uniformly or epitaxially onto metals, and they often end up self-nucleating instead of growing on it. The complexity further increases with plasmonic metal such as silver as it has a lattice mismatch of about 50% with the semiconductor. Despite this, silver has been an area of great interest because of the advantage of being able to tune the plasmon resonance into the blue, with generally a higher quality plasmon resonance when compared to the gold.

However, there are only a few reports published so far with silver and semiconductor nanostructures because of the high ionic mobility and chemical reactivity of Ag^+ ions due to which silver nanoparticles tend to be oxidized and sulfurized during the synthesis

A large number of reports published so far focuses mainly on changing the morphology of the nanostructures by varying the ratios of precursor concentration added or by controlling the temperature kinetics. In this work, we have developed a general strategy for the synthesis of hybrid Ag@Semiconductor core-shell hybrid nanostructures and Ag_2S -SJanus nanostructures valid for PbS and CZTS semiconductor by changing the surface chemistry of the metal nanoparticles added in the solution by changing the metal precursors shown in the image. This is achieved via injection of metal nanoparticles into the solution containing metal precursors such as metal chlorides and metal acetates along with the long-chain primary alkylamine and TOPO.

The chloride ions are playing an important role in forming the Ag concentric cores, resulting in Ag-Semiconductor core-shell hybrid nanostructures whereas changing the counterions from chlorides to acetate forms semiconductor Ag_2S instead of metallic Ag resulting in Ag_2S -Semiconductor Janus nanostructures. Consequently, we expect that this approach could provide a broader platform to rationally tailor the synthesis of various other semiconductor-Ag based systems.



Schematic showing hybrid structures synthesized by controlling the counterions in the synthesis.png

Implementation of disordered hyperuniform micro and nano architectures via nano-imprint lithography of metal oxides

Thursday, 25th March - 11:50: Oral Session 1-2 (Room 2) - Abstract ID: 257

Dr. Zeinab CHEHADI¹, Dr. Mohammed Bouabdellaoui¹, Mrs. Mehrnaz Modaresialam¹, Prof. David Grosso¹, Dr. Marco Abbarchi¹

1. Nova Team, Institut Matériaux Microélectronique et Nanosciences de Provence, (IM2NP) -UMR CNRS 7334, Aix-Marseille Université, Faculté des sciences de Saint Jérôme, 13397 Marseille Cedex 20, France.

Fabrication and scaling of disordered hyperuniform materials remain hampered by the difficulties in controlling the spontaneous phenomena leading to this novel kind of exotic arrangement of objects. Here we demonstrate a hybrid top-down/bottom-up approach based on sol-gel dip-coating and nano-imprint lithography for the faithful reproduction of disordered hyperuniform metasurfaces in metal oxides. Nano- to micro-structures made of silica and titania can be directly printed over several cm² on glass and on silicon substrates. First, we describe the polymer mould fabrication starting from a hard master obtained via spontaneous solid state dewetting of SiGe and Ge thin layers on SiO₂. Then we address the effective disordered hyperuniform character of the master and of the replica. Thus, we study the role of the initial thickness of the sol-gel layer on the metal oxide replicas. Finally, as a potential application, we show the anti-reflective character of titania structures on silicon. Our results are relevant for the realistic implementation over large scales of disordered hyperuniform nano- and micro-architectures made of metal oxides thus opening their exploitation in the framework of wet chemical assembly.

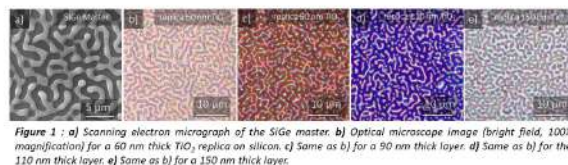


Figure 1 : a) Scanning electron micrograph of the SiGe master. b) Optical microscope image (bright field, 100X magnification) for a 60 nm thick TiO₂ replica on silicon. c) Same as b) for a 90 nm thick layer. d) Same as b) for the 110 nm thick layer. e) Same as b) for a 150 nm thick layer.

Figure annic 2021.jpg

Quantum Dots dimers: fabrication and insight on interaction mechanisms

Thursday, 25th March - 12:05: Oral Session 1-2 (Room 2) - Abstract ID: 196

Mr. Carlo Nazareno Dibenedetto¹, Prof. Elisabetta Fanizza¹, Dr. Liberato De Caro², Dr. Rosaria Brescia³, Dr. Annamaria Panniello⁴, Prof. Raffaele Tommasi¹, Dr. Chiara Ingrosso⁴, Dr. Cinzia Giannini², Prof. Angela Agostiano¹, Prof. Maria Lucia Curri¹, Dr. Marinella Striccoli⁴

1. University of Bari "Aldo Moro", 2. CNR - Istituto di Cristallografia, 3. IIT- Istituto Italiano di Tecnologia, 4. CNR - Istituto per i Processi chimico Fisici

Introduction:

Design of colloidal quantum dots (QDs) molecular assemblies and investigation of interaction with each other's and with the close chemical-physical environment are of great interest for improving the performances of QD-based optoelectronic devices. In particular, the coupling taking place when only a few QDs are assembled at a short interparticle distance is relevant to better promote the electron/energy transfer processes arising in such molecular assemblies, for new technological applications.

Methods:

Hetero and homo dimers have been fabricated as follows. Firstly, QDs ($5 \cdot 10^{-7}$ M) have been treated by means of BUA ($2.5 \cdot 10^{-2}$ M in hexane) at BUA:QD molar ratio of 500:1. The addition of the dithiols ($1.7 \cdot 10^{-4}$ M in hexane) was further carried out at DT:QD molar ratio of 50:1, under stirring for 5 min. Spectroscopic characterization such as UV-Vis absorption, PL and TR-PL ($\lambda_{ex} = 485$ nm), together with morphological analysis have been carried out. Samples were diluted to 1:60 in hexane for TEM grid preparation and statistical analysis of the Dimer Yield (DY).

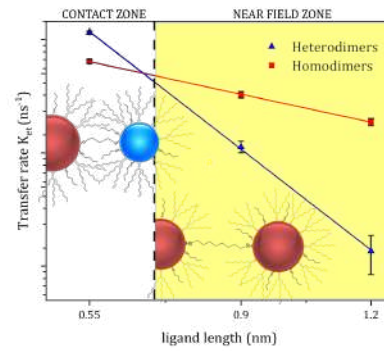
Results and Discussion:

Heterodimers composed by CdSe QDs of two different sizes,[1] and analogous homodimers formed by QDs of the same size,[2] connected by short alkyl chain dithiols, are fabricated in solution. Varying the chain length of the bifunctional linker from sub-nanometer to nanometer range is possible to fine-tuning the interparticle distance. From the crystallographic analysis, it can be evinced that the nearest surfaces involved in the linking of the QDs are the (101) faces. An exhaustive spectroscopic investigation allows to rationalize the interaction mechanism between the QDs, ranging from charge transfer/wavefunction delocalization to energy transfer, depending on their separation distance, QDs size, and energetic levels position. The findings evidence the potential of the heterodimers in terms of transfer rate in application where a high charge transfer/wavefunction delocalization is required, taking advantage from the cascade-like energetic levels in the contact zone. On the other hand, FRET architectures would strongly benefit from the use of homodimers that are able to couple more efficiently by means of energy transfer mechanism, thanks to quasi iso-energetic electronic levels.

[1] Dibenedetto, C.N., et al., *Quantum dot heterodimers in solution: insight on interaction mechanisms*. Chemistry - A European Journal, 2021. Submitted.

[2] Dibenedetto, C.N., et al., *Coupling effects in QD dimers at sub-nanometer interparticle distance*. Nano Research, 2020. **13**(4): p. 1071-1080.

This work is financially supported by the H2020 FET project COPAC (Contract agreement n.766563). The MIUR PRIN 2015 n. 2015XBZ5YA is acknowledged.



Logarithmic plot of transfer rates calculated from exciton lifetimes versus ligand length for both the series of homodimers and the heterodimers.png

Detailed calorimetric analysis of micelle formation from aqueous binary surfactant mixtures for design of nanoscale drug carriers

Thursday, 25th March - 13:30: Oral Session 2-1 (Room 1) - Abstract ID: 8

Dr. Ádám Juhász¹, Mr. László Seres¹, Dr. Edit Csapó¹

1. Department of Physical Chemistry and Materials Science, H-6720 Szeged, Rerrich B. sqr. 1.

Introduction: The present work describes a calorimetry-founded characterization and design of a potential surfactant based colloidal drug delivery system. However, numerous research groups have published their outcomes according to the thermodynamic characterization of mixed micelle formation but only a few articles provide deeper information on the temperature and composition dependence micellization in mixed surfactant systems combining the advantages of both aspects. For self-assembled surfactant systems, the most important parameter is the critical micelle concentration (cmc) value, which quantifies the tendency to associate and gives the value of Gibbs energy of micellization. Several techniques are known for determining cmc, but the isothermal titration calorimetry (ITC) deserves special attention in comparison to other procedures. The calorimetry gives an absolute basic thermodynamic characterization in a single experiment, includes cmc and binding enthalpy and this is it does not require other label material such as fluorophore, chromophore etc. as heat is a universal signal. In contrast these advantages an important shortcoming of the procedure is that, while there are several commercial software solutions for processing calorimetric data of receptor-ligand-type interactions, the modeling of self-assembled colloidal systems must be solved by self-developed computational methods.

Results and Discussion: According to the calorimetric profiles of the dilution of aqueous surfactants and their mixtures, the cmc values were determined at different temperatures and compositions. In the investigated temperature range and whole micelle mole fractions interval, we found some state where the cmc is lower than the ideal mixing model calculated value. These equimolar binary surfactant mixtures showed higher solubilization capacity for poorly water-soluble drugs than their individual compounds. Thus, the rapid and fairly accurate calorimetric analysis of mixed micelles can lead to the successful design of a nanoscale drug carrier. Thanks to the spreadsheet implementation of ITC analysis, our evolution method does not require any user input other than the ITC data in integrated and normalized form and the thermodynamic parameters can be predicted using the estimation protocol developed by our researchers.

Methods: Outcomes of the calorimetric investigation of self-assembling process were evaluated using a spreadsheet-edited routine developed for handling ITC data. Thermodynamic parameters of mixed micelle formation were obtained from the nonlinear modelling of temperature- and composition dependent enthalpograms. Further the value of thermodynamic parameters the uncertainty of these data is also very important, in this way, a weighted resampling “jackknife” procedure was used for calculation of the standard deviations of the fitting parameters.

Local Administration of Nanoparticles for Chronic Lung Fibrotic Disorders

Thursday, 25th March - 13:45: Oral Session 2-1 (Room 1) - Abstract ID: 15

Dr. Laura Pandolfi¹, Ms. Vanessa Frangipane¹, Ms. Roberta Fusco², Mr. Marco Giustra³, Dr. Rosanna Di Paola², Prof. Jorge Distler⁴, Dr. Veronica Codullo¹, Prof. Miriam Colombo⁵, Dr. Sara Bozzini¹, Dr. Monica Morosini¹, Prof. Davide Prosperi⁵, Prof. Salvatore Cuzzocrea², Prof. Federica Meloni¹

1. IRCCS Fondazione Policlinico San Matteo, 2. University of Messina, 3. University of Milano-Bicocca, 4. University Hospital Erlangen, 5. University of Milano - Bicocca

Introduction:

The most common and studied application of nanoparticles in medicine involves the use of nanodevices for cancer treatment through the intravenous administration. However, nanomedicine can be useful for many other diseases exploiting different routes of administration. For instance, our research group is trying to design the best nanovehicle to deliver drugs directly inside lungs through inhalation to obtain a non-invasive and non-toxic therapy for patients affected by chronic lung fibrotic disorders.

Methods:

We studied the efficiency of gold nanoparticles (GNP) functionalizing their surface with a specific antibody against CD44 (GNP-HC), a glycoprotein highly expressed by fibrotic cells to preserve healthy epithelial cells. We tested GNP-HC loaded with Imatinib (GNP-HCIm), an anti-fibrotic drug impossible to administer locally inside lung, on two different mouse models: heterotopic tracheal transplantation (HTT) as bronchiolitis obliterans syndrome (BOS) model, the major clinical phenotype of chronic lung allograft dysfunction; and bleomycin-induced pulmonary fibrosis. In both models, GNP-HCIm were administered locally up to 28 days: in HTT model GNP-HCIm were perfused into tracheal grafts by an Alzet pump and in bleomycin-induced pulmonary fibrosis model GNP-HCIm were tracheally instilled.

Results:

We demonstrated that GNP-HCIm decreased significantly all the key features of HTT BOS model: reduced tracheal lumen obliteration ($p < 0.05$), decreased rate of cells in apoptosis ($p < 0.05$) and TGF- β -positive signal in surrounding tissue ($p < 0.05$). Moreover, GNP-HCIm significantly reduced leucocytes infiltration ($p < 0.05$). Regarding bleomycin-induced pulmonary fibrosis model, GNP-HCIm reduced significantly lung fibrotic changes and collagen deposition ($p < 0.05$). By TEM analysis we observed an important accumulation of GNP-HCIm in alveolar macrophages.

Discussion:

Our results demonstrate that local administration of nanoparticles by inhalatory route could be very promising option to vehicle those drugs that might be difficult to use in chronic lung disorders due to their systemic toxicity. However, it is very important to choose the right material-basing nanoparticle to avoid nanoparticle side effects. In fact, we move our study onto more biocompatible nanovehicle: liposomes conjugated with hyaluronic acid, the physiologic ligand of CD44

Complexation of glycogen with magnetic nanoparticles towards the formulation of biocompatible nanocarriers

Thursday, 25th March - 14:00: Oral Session 2-1 (Room 1) - Abstract ID: 130

Dr. Maria Karayianni¹, Dr. Stergios Pispas², Dr. Evangelia D. Chrysina¹

1. Institute of Chemical Biology, National Hellenic Research Foundation, 2. Theoretical and Physical Chemistry Institute, National Hellenic Research Foundation

Introduction: The demand for biofunctional nanoparticles for medical applications has led to the utilization of macromolecules of biological origin, that are intrinsically biocompatible, biodegradable, and nontoxic. One such example is glycogen, which is a highly branched polysaccharide of glucose, structured into roughly spherical nanoparticles with increased water solubility. Polysaccharides have been extensively researched in biomedical applications related to drug, protein, or gene delivery systems, as well as nanoprobe for cellular and tissue imaging; however, there are only a few studies concerning glycogen.

Methods: In this work we examine the complexation of glycogen (Glyc) (from oyster) with CoFe_2O_4 magnetic nanoparticles (MNPs), which bear a hydrophilic anionic organic coating (Fig. 1). We employed dynamic and electrophoretic light scattering in order to investigate the solution behaviour, size, structure and effective charge of the formed complexes in aqueous milieu, at different MNPs concentrations. The magnetophoretic behaviour of the formed complexes was monitored via magnetophoresis experiments in solutions using a UV-Vis spectrophotometer and a neodymium permanent magnet. Fluorescence spectroscopy measurements were also performed, using pyrene as a probe of the microenvironment polarity and hence an indicator of the magnitude of hydrophobic domains within the complexes.

Results: According to the results of our study the size (hydrodynamic radius about 170 nm, Fig. 2), structure, and stability of the Glyc/MNPs complexes proved to be dependent on the MNPs concentration. Additionally, the formed complexes seem to have a rather loose conformation and are considered to be decorated with Glyc molecules. The complexes exhibit a rather slow response to the magnetic field, with their magnetophoretic behaviour being affected by the MNPs concentration (Fig. 3). Pyrene fluorescence revealed the presence of hydrophobic domains and even crowding conditions (excimer formation) in some cases.

Discussion: Stable complexes between Glyc and inorganic MNPs have been developed. These functional nanostructures are characterized by innate biocompatibility, have a size in the nanometre range suitable for prolonged blood circulation, and can respond to external magnetic field. All these properties give them great potential to be exploited as novel theranostic nanocarriers.

Acknowledgement: Authors acknowledge financial support by the project “INSPIRED-The National Research Infrastructures on Integrated Structural Biology, Drug Screening Efforts and Drug target functional characterization” (MIS 5002550), which is implemented under the Action “Reinforcement of the Research and Innovation Infrastructure”, funded by the Operational Programme “Competitiveness, Entrepreneurship and Innovation” (NSRF 2014-2020) and co-financed by Greece and the European Union (European Regional Development Fund).

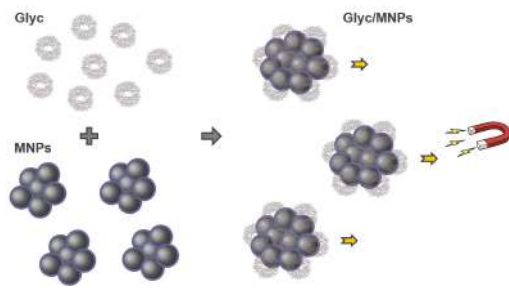


Fig.1 complexation scheme.jpg

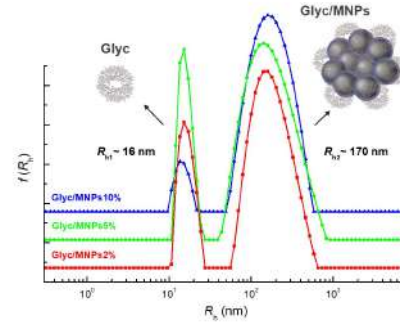


Fig.2 distribution functions.jpg

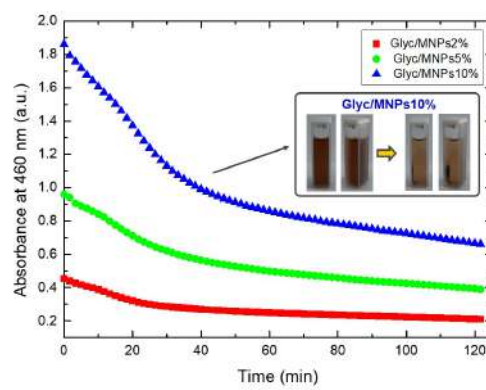


Fig.3 magnetophoresis.jpg

The bittersweet symphony of Pexiganan-A grafted chitosan microparticles & *Helicobacter pylori*

Thursday, 25th March - 14:15: Oral Session 2-1 (Room 1) - Abstract ID: 141

Ms. Diana R. Fonseca¹, Ms. Ana Moura², Dr. Cátia Teixeira³, Dr. Catarina Leal Seabra², Dr. Victoria Leiro², Dr. Berta Estevinho⁴, Prof. Paula Gomes³, Dr. Paula Parreira², Prof. M. Cristina L. Martins⁵

1. 1.Instituto de Engenharia Biomédica, Universidade do Porto | 2. i3S, Instituto de Investigação e Inovação em Saúde, Universidade do Porto | 3.Faculdade de Engenharia, Departamento de Engenharia Metalúrgica e de Materiais, Universidade do Porto, 2. 1.Instituto de Engenharia Biomédica, Universidade do Porto | 2. i3S, Instituto de Investigação e Inovação em Saúde, Universidade do Porto, 3. 5. LAQV-REQUIMTE, Departamento de Química e Bioquímica, Faculdade de Ciências, Universidade do Porto, 4. 4. LEPABE, Departamento de Engenharia Química, Faculdade de Engenharia da Universidade Do Porto, 5. 1.Instituto de Engenharia Biomédica, Universidade do Porto | 2. i3S, Instituto de Investigação e Inovação em Saúde, Universidade do Porto | 6. ICBAS, Instituto de Ciências Biomédicas Abel Salazar, Universidade do Porto

Helicobacter pylori (*Hp*) colonizes the gastric mucosa of 50% of the worldwide population. It is associated to several gastrointestinal diseases, accounting for 90% of non-cardia gastric cancer cases¹. *Hp* is one of the 16 bacteria that raises the highest concerns regarding antibiotic resistance¹. Antimicrobial peptides (AMPs) are an interesting alternative to antibiotics due to their low propensity to induce bacterial resistance. MSI-78A, an analogue of Pexiganan, is one of the few reported bactericidal AMPs against *Hp*². AMPs immobilization onto biomaterials is an advocated strategy to overcome some of the AMPs weaknesses *in vivo*, namely proteolytic degradation and aggregation with proteins³.

This work aims the development of biocompatible chitosan microspheres decorated with MSI-78A (AMP-ChMic) that, after oral administration, will cross the gastric mucosa and kill *Hp* at the surface of epithelial gastric cells, where most of the bacteria are found.

Chitosan (Ch) was chosen as biomaterial since it has been widely studied against *Hp*⁴. Ch (acetylation degree of 6%) was purified and crosslinked with genipin (2.5 mM) to prevent its dissolution in gastric acidic conditions. Ch microspheres (ChMic) were produced by spray drying (size distribution between 2 and 7 µm). Afterwards, a heterobifunctional spacer (NHS-PEG-MAL) was grafted onto the ChMic to further allow the immobilization of the MSI-78A modified with a terminal cysteine on the C-terminal (MSI-78A-SH) in a controlled orientation.

AMP-ChMic were successfully engineered, as shown by Fourier Transform Infrared analysis. The yield of the immobilization reaction was 74% and was accessed by UV-Vis spectrophotometry. The developed AMP-ChMic were able to retain their integrity in acidic and neutral pH, proving their pH-resistance and validating this approach for gastric settings. AMP-ChMic efficacy against *Hp* J99 strain (human highly pathogenic strain) was demonstrated in a concentration dependent manner. Bactericidal effect was seen as soon as 2h and it was maintained up to 6h, with a decrease of at least 3logs (from 10⁷ to 10³ CFU/mL). This result indicates that MSI-78A can retain its activity when immobilized onto ChMic.

Overall, AMP grafting onto ChMic was successfully achieved. This strategy promotes AMP exposure and interaction with *Hp*, boosting its bactericidal performance. AMP-ChMic demonstrated high potential for *Hp* infection management and should be further explored within the scope of non-antibiotic therapeutic strategies.

1. Rawla *et. al.* Gastroenterol., 14(2019)26–38
2. Neshani *et. al.* Helicobacter. 24(2019)
3. Bassegoda *et. al.* Appl. Microbiol. Biotechnol., 102(2018)2075–2089
4. Gonçalves *et. al.* Expert Rev. Anti. Infect. Ther., 12(2014)981–992

Acknowledgments: PTDC/CTM-BIO/4043/2014 & SFRH/BD/146890/2019

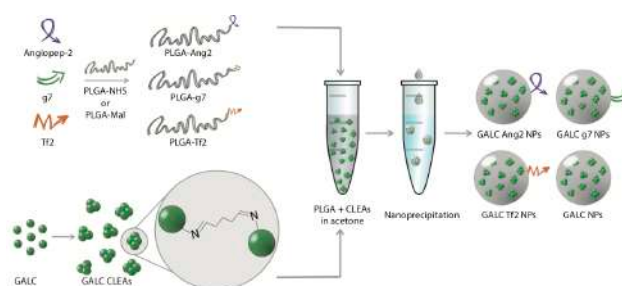
Brain-targeted nanoparticles for enzyme replacement therapy in neuropathic lysosomal storage disorders: application to Krabbe disease.

Thursday, 25th March - 14:30: Oral Session 2-1 (Room 1) - Abstract ID: 10

Dr. Ambra Del Grosso¹, **Dr. Marianna Galliani**², **Ms. Lucia Angella**¹, **Dr. Melissa Santi**², **Dr. Ilaria Tonazzini**¹, **Mr. Gabriele Parlanti**¹, **Dr. Giovanni Signore**³, **Dr. Marco Cecchini**¹

1. NEST, Istituto Nanoscienze-CNR and Scuola Normale Superiore, Piazza San Silvestro 12, 56127 Pisa, Italy., **2.** NEST, Istituto Nanoscienze-CNR and Scuola Normale Superiore and Center for Nanotechnology Innovation@NEST, Piazza San Silvestro 12, 56127 Pisa, Italy., **3.** NEST, Istituto Nanoscienze-CNR and Scuola Normale Superiore, Piazza San Silvestro 12, 56127 Pisa, Italy and Fondazione Pisana per la Scienza ONLUS, 56017 Pisa, Italy.

Lysosomal storage disorders (LSDs) are a large group of metabolic diseases, individually rare but collectively common (1:5,000 live births). Usually, they result from an enzyme deficiency within lysosomes, which ultimately causes accumulation of undegraded substrates. The most clinically applied method to treat LSDs is the systemic administration of the missing enzyme. This approach, however, is not effective in the case of LSDs that involve the central nervous system (CNS); the presence of the blood brain barrier (BBB), in fact, forbids translocation of big molecules into the brain. Here, a new enzyme delivery system based on the encapsulation of cross-linked enzyme aggregates (CLEAs) into poly-(lactide-co-glycolide) (PLGA) nanoparticles (NPs) functionalized with brain targeting peptides (Ang2, g7 or Tf2) is demonstrated for Krabbe disease (KD or Globoid cell leukodystrophy; OMIM #245200), an inherited neurodegenerative LSD caused by the genetic deficiency of the enzyme galactosylceramidase (GALC; EC 3.2.1.46). We firstly synthesize and characterize Ang2, g7 and Tf2-targeted GALC CLEA NPs. Then, we study NP cell uptake and trafficking, assessing their capability to reinstate enzymatic activity in vitro. Finally, we successfully test our NP formulations in the Twitcher mouse, the spontaneous murine model of KD. We report enzymatic activity measurements in the nervous system and in typical accumulation districts upon NP intraperitoneal injections, demonstrating GALC activity recovery in the brain up to the level of unaffected control mice. In addition, the presence of targeted NPs in the brain was confirmed by confocal microscopy. Taken together, these results open new therapeutic perspectives for KD, and for all LSDs with major involvement of the CNS.



Brain-targeted GALC CLEA nanoparticles synthesis. Peptide-modified PLGA was produced by covalent linking of each peptide to a previously activated form of PLGA. GALC CLEAs were obtained by precipitation of GALC in acetone in the presence of glutaraldehyde, resulting in Schiff base formation between enzyme molecules. Last, targeted GALC CLEA NPs were obtained by nanoprecipitation. [Del Grosso et al. "Brain-targeted enzyme-loaded nanoparticles: A breach through the blood-brain barrier for enzyme replacement therapy in Krabbe disease." *Science advances* 5.11 (2019): eaax7462.]

Fig. annic.png

Isobaric labeling proteomics allows an easy and high-throughput investigation of protein corona orientation

Thursday, 25th March - 14:45: Oral Session 2-1 (Room 1) - Abstract ID: 184

Dr. Nara Liessi¹, Dr. Luca Maragliano¹, Dr. Valentina Castagnola¹, Dr. Mattia Bramini², Prof. Fabio Benfenati¹, Dr. Andrea Armirotti¹

1. Istituto Italiano di Tecnologia, 2. University of Granada

INTRODUCTION

The formation of biomolecular corona represents a crucial factor in controlling the biological interactions and trafficking of nanomaterials. In this context, the availability of key epitopes exposed on the surface of the corona, and able to engage the biological machinery, is important to define the biological fate of the material. While the full biomolecular corona composition can be investigated by conventional bottom-up proteomics, the assessment of the spatial orientation of proteins in the corona in a high-throughput fashion is still challenging.

METHODS

In this work, we propose a novel, easy and high throughput methodology to investigate the protein corona orientation. Given the involvement of our group in the Graphene Flagship, we used two graphene-based materials (with distinct surface chemistries, graphene oxide and pristine graphene) as models for a proof-of-concept test of our approach. This approach exploits isobaric labeling of proteins, followed by conventional bottom-up proteomics, to derive information on the spatial orientation of a given peptide directly from the list of identified proteins.

RESULTS

In this work, we show that labeling corona proteins with isobaric tags in their native conditions and analyzing MS/MS spectra of tryptic peptides allows an easy and high-throughput assessment of the inner/outer orientation of the corresponding proteins in the original corona. We first put our results in the context of what is currently known of the protein corona of graphene-based nanomaterials and we then explored the orientation data we obtained directly from our proteomics experiments. Our conclusions are in line with previous data and were also confirmed by *in silico* calculations.

DISCUSSION

This work represents a proof-of-concept study highlighting an innovative strategy to simultaneously investigate the composition *and* the orientation of the proteins forming the biomolecular corona onto nanomaterial surfaces. In addition to conventional bottom-up proteomics experiments for protein corona, this approach is: 1) fast: a few additional hours of work are required, 2) easy to perform, 3) cheap, and 4) non-invasive toward post-translational modification analysis (several tens of phosphorylation sites were identified in our data). The workflow we developed could be routinely implemented into protein corona proteomics studies, and it would represent a valuable tool in line with the great efforts for nanomaterials biointeractions screening and classification promoted by worldwide nanosafety projects.

Reference: Isobaric Labeling Proteomics Allows a High-Throughput Investigation of Protein Corona Orientation. Liessi N, Maragliano L, Castagnola V, Bramini M, Benfenati F, Armirotti A. *Anal Chem.* 2021 Jan 19;93(2):784-791.

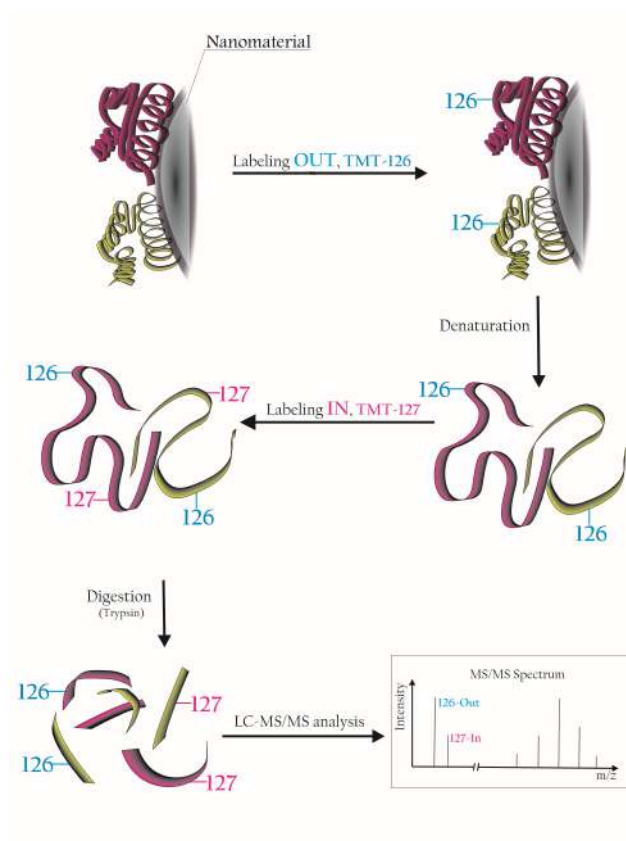


Figure 1.png

Quantum mechanics and Molecular dynamics investigations on carbon-based nanofluidic device

Thursday, 25th March - 13:30: Oral Session 2-2 (Room 2) - Abstract ID: 251

Dr. Alia Mejri ¹, Dr. Guillaume Herlem ¹, Dr. Fabien Picaud ¹

1. Laboratoire de Nanomédecine, Imagerie et Thérapeutique, Université Bourgogne-Franche-Comte (UFR Sciences et Techniques), EA 4662, Centre Hospitalier Universitaire de Besançon, 16 route de Gray, 25030 Besançon, France.

The development of nanofluidics over the past years has shown a great interest for the design of smart devices aiming at understanding and controlling the water and ion transport in order to open-up a large field of engineering applications [1].

A current challenge nowadays in nanofluidics is to actively control and understand the motion of water and ions inside these narrow nanochannels and to identify the influence of the geometric parameters (diameter and length) on the fluid circulation.

In this study, a special attention has been paid to single walled carbon nanotubes as promising framework for water and ions transport due to their simple composition, remarkable chemical and mechanical properties, smooth walls for fast motion of liquid flow and important surface charge that can be controlled in such devices [2,3]. DFT-MD calculations were conducted to look into the reactivity of the carbon surface toward dissociated and undissociated water molecule (with or without salt) under an electric bias (figure 1)[3].

Then classical MD simulations of the system (figure 2) are performed to different tube diameters and lengths in order to account the ionic conductance behavior as a function of the geometric parameters of the pore.

Key words: carbon nanotube, nanofluidic devices, OH⁻/H⁺ adsorption, conductance behavior.

This work was funded by Agence Nationale de la Recherche (ANR-18-CE09-0011-01 "IONESCO")

References :

1. Xiao, K.; Jiang, L.; Antonietti, M. Ion transport in nanofluidic devices for energy harvesting. *Joule* 2019, 3, 2364–2380. [CrossRef] 31. Ye, J.; Simon, P.; Zhu, Y. Designing ionic channels in novel carbons for electrochemical energy storage. *Natl. Sci. Rev.* 2019, 7, 191–201.
2. Werkhoven, B.L.; van Roij, R. Coupled water, charge and salt transport in heterogeneous nano-fluidic systems. *Soft Matter* 2020, 16, 1527–1537.
3. Grosjean, B. Pean, C. Siria, A. Bocquet, L. Vuilleumier, R. and Bocquet, M.-L. The Journal of Physical Chemistry Letters 2016, 7, 4695.
1. Mejri, A. ; Herlem, G.; Picaud, F. From Behavior of Water on Hydrophobic Graphene Surfaces to Ultra-Confinement of Water in Carbon Nanotubes. *Nanomaterials*. 2021, 11(2), 306.



Supercapacitor electrodes based on carbon nanostructures

Thursday, 25th March - 13:45: Oral Session 2-2 (Room 2) - Abstract ID: 253

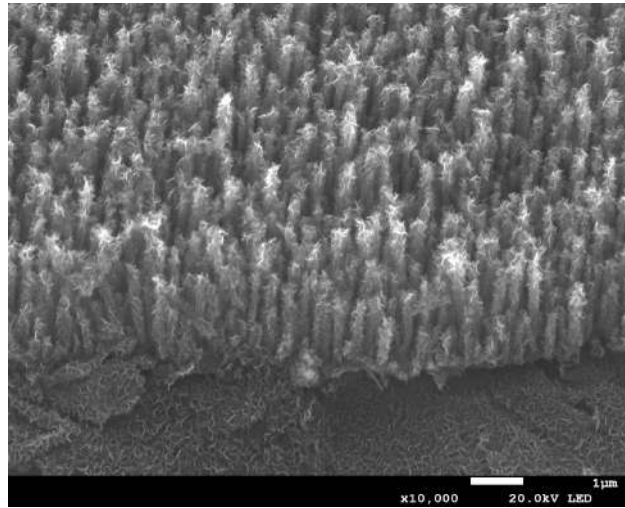
Dr. Roger Amade Rovira¹, Mr. Joan Martí Gonzalez¹, Mr. Islam Alshaikh¹, Prof. Esther Pascual¹, Dr. Jose Luis Andújar¹, Prof. Enric Bertran Serra¹

1. ENPHOCAMAT Group, Department of Applied Physics, Universitat de Barcelona

Carbon nanostructures have been intensively studied due to their outstanding features such as strength, chemical inertness and temperature stability. In particular, they are commonly used as electrode materials for electrochemical energy storage devices due to their large surface area, high conductivity, variety of morphologies and structural robustness. Among the different energy storage devices supercapacitors have been pointed out as advantageous because of their high power density, rapid charge-discharge, high cycling stability, safe working and low-cost. Supercapacitors can be classified as EDLC (electrochemical double layer capacitors) and pseudocapacitors. The charge-storage mechanism being almost entirely based on electrostatic interactions for the former and due to electrochemical surface redox reactions for the latter.

Here, we present results related to the growth and synthesis of carbon nanostructures on flexible and conductive substrates using chemical vapour deposition activated by plasma at low pressure. Vertically aligned carbon nanotubes (CNTs), graphene nanowalls (GNWs) or a combination of both have been obtained and characterized by electron microscopy and Raman spectroscopy. Furthermore, the surface of the carbon nanostructures can be functionalized by electrodepositing active metal oxides such as manganese dioxide to increase the electrochemical performance of the electrodes. Cyclic voltammetry, galvanostatic charge/discharge and impedance spectroscopy techniques are used to determine the capacitance, cycling stability and electrochemical series resistance of the electrodes.

MnO₂/Carbon nanostructures composites show a 5-fold increase in capacitance with respect to bare MnO₂ layer. In addition, these composites present high cycling stability up to about 10,000 cycles, high coulombic efficiency and electrochemical series resistances in the range of $1 \Omega \cdot \text{cm}^2$. Thus, these carbon-based nanostructured composites are promising candidates for electrodes materials with novel properties and enhanced performance.



Cntcnwx10t2.jpg

Multicomponent suspensions for electrophoretic deposition of composites with carbon nanotubes

Thursday, 25th March - 14:00: Oral Session 2-2 (Room 2) - Abstract ID: 228

Mr. Aleksey Alekseyev¹, Dr. Egor Lebedev², Prof. Dmitry Gromov², Mrs. Svetlana Pereverzeva³, Mr. Roman Ryazanov³, Dr. Alexander Dudin⁴

1. National Research University of Electronic Technology, 2. National Research University of Electronic Technology - MIET, 3. Scientific-Manufacturing Complex "Technological Centre", 4. Institute of Nanotechnologies of Microelectronics, Russian Academy of Sciences

Electrophoretic deposition (EPD) is the shaping of an electrode coating out of particles suspended in a certain solvent when an electric field is applied. This method is economically effective and suitable for many materials and their combinations. Nonetheless, the process of authentic insertion and uniform distribution of nanosized particles in the volume of CNT matrix is rather challenging, while controlled morphology is extremely important. A stable suspension is required to obtain high quality, uniform coatings. In this work, we consider approaches to the creation of suspensions with the aim of forming composite layers of CNTs and transition metal compounds as functional material for electrodes of electrochemical energy storage devices.

To obtain CNTs, chemical vapor-phase deposition is used, as well as treatment in oxidizing agents for the functionalization. Substrates for the deposition are being prepared in two ways: liquid treatment of a Ni foil and magnetron sputtering of Ni onto non-conductive substrate followed by laser scribing. For suspensions, mixtures of components and solvents are being set to ultrasonic treatment, then placed in studio box for sedimentation analysis. Electrophoretic deposition comes into play next. Inspection of EPD films is carried out by means of scanning electron microscopy, focused ion beam, energy dispersive X-ray spectroscopy, thermogravimetric analysis, differential scanning calorimetry. Electrochemical energy storage device properties are evaluated through cyclic voltammetry, galvanostatic cycling and impedance spectroscopy.

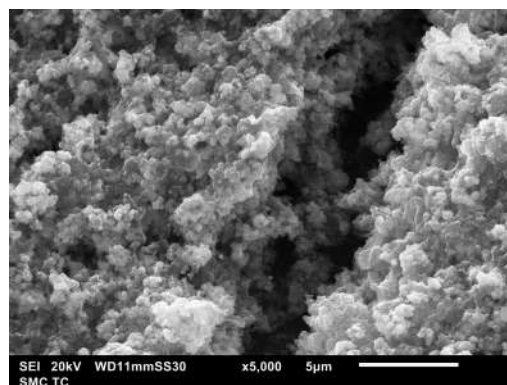
In principle, suspensions with or without an electrolyte (i.e. charger salt) are to be considered. In the first case, transition metal hydroxide can be formed directly on CNTs during the EPD with subsequent annealing. In the second - metal oxide is added into the suspension presynthesized. To add stability to the suspension dispersing agents can be introduced, e.g. hydroxypropyl cellulose (HPC). But this may be controversial, because their presence in the composite is detrimental, so carbonization by thermal treatment should be used. Researches for optimal temperature and environment were held.

Solvent for the suspension greatly affects its stability and the EPD character. In general, it depends on the ratio of dielectric permittivity and viscosity. Acetone has one of the highest ratios and is quite accessible. Besides, in the presence of iodine ions, it can produce hydrogen ions, which can be used to drive particles to the electrode in times, when their surface charge is too low otherwise. Solvent's properties can be tuned by adding another solvent.

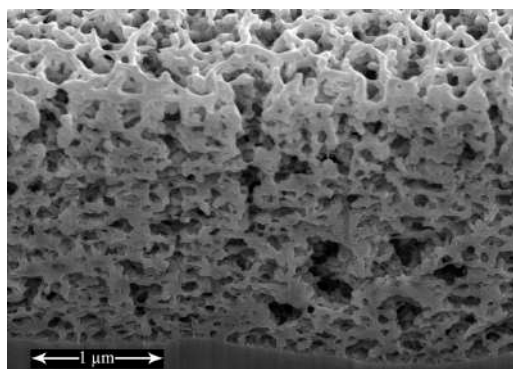
Funding: The reported study was funded by RFBR, project number 20-38-90245



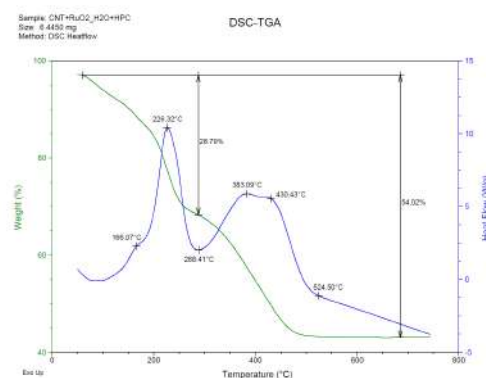
Cnt-ruo2 h2o suspensions based on acetone with left and without right the addition of hpc after 2 weeks.png



Electrophoretically deposited film of cnt-ruo2 h2o-hpc before annealing.jpg



Fib crossection of electrophoretically deposited film of cnt-niohx-hpc before annealing.png



Results of dsc and tga of cnt-ruo2 h2o-hpc composite on air.png

Bioinspired Polymer Nanocomposites Providing Scalable Solution for Thermal Management

Thursday, 25th March - 14:15: Oral Session 2-2 (Room 2) - Abstract ID: 154

Dr. George Stiubianu¹, Dr. Maria Cazacu¹, Dr. Carmen Racles¹, Dr. Mihaela Dascalu¹, Dr. Alexandra Bargan¹, Dr. Adrian Bele¹, Dr. Codrin Tugui¹, Dr. Cristian Ursu¹

1. Petru Poni Institute of Macromolecular Chemistry Iasi

Introduction

Thermal management is important for technologies such as buildings, electronics, and clothing. The animal kingdom provides multiple sources of inspiration for development of new materials and methods for thermal management. Thus, for bioinspired nanocomposites, the fast dynamic optical color changing capabilities of organelles found on the abdomen of the mirror comb-footed spider has provided inspiration for new polymer nanocomposite materials with application in thermal management. Since thermal management involves controlling infrared radiation, we developed materials replicating the capability of aforementioned animals to change the reflectance and transmittance of light in the infrared wavelength range. Overall, the nanocomposites developed by our team are safe for human use, can be prepared without use of volatile organic solvents, and are scalable for commercial-scale application.

Methods

The new polymer nanocomposites work for thermal management by bringing together the advantages of passive thermal control, such as low cost, easily scalable implementation, and efficiency in terms of on/off switching ratio, with active thermal control advantages, such as on-demand control of temperature. The procedure (Figure 1) can be scaled up by using current metal layer deposition and polymer spraying.

Results and Discussion

Our team developed the polymer nanocomposites taking advantage of the versatile chemistry of silicone and styrene polymers, obtaining nanocomposites that can actively manage up to 50 W/m² and could lower the energy load for cooling and heating in buildings, while also providing thermal comfort if integrated into clothing. The dynamic capability for managing the thermal flux can be controlled either mechanically or electrically, with a mechanical input of <3 W/m². In an office building over 60% of the heat exchange between the human body and the environment takes place through infrared radiation, and the nanocomposite materials in unactuated state can reflect infrared radiation as well as the space blanket developed by NASA in 1960, while under mechanical or electrical actuation the nanocomposites can dynamically modulate more than 70% of the heat flux emitted by the human body, with possible application in clothing. With such capabilities the polymer nanocomposites could be scaled for use in buildings, containers clothing and electronics of such nanocomposites, and it would provide significant energy savings amounting to ~3% of worldwide energy consumption (Figure 2).

Acknowledgements: This work was supported by a grant of the Romanian Ministry of Education and Research, CCCDI - UEFISCDI, project number PN-III-P2-2.1-PED-2019-1885, within PNCDI III (Contract 463PED/2020).

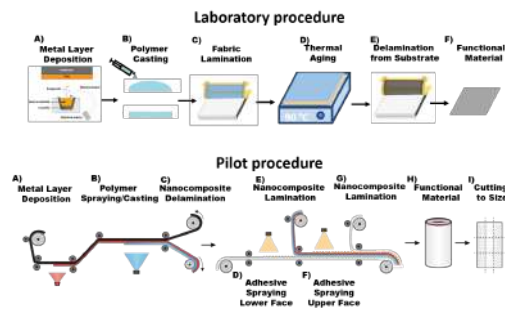


Figure 1.png

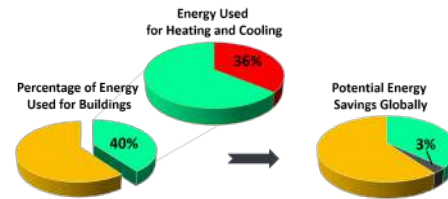


Figure 2.png

Microstructural properties and electrochemical performance of electrospun Ge-doped Fe₂O₃ nanofibers as anode material in sodium-ion batteries

Thursday, 25th March - 14:30: Oral Session 2-2 (Room 2) - Abstract ID: 203

Dr. Beatrix Petrovicova¹, Dr. Chiara Ferrara², Dr. Gabriele Brugnetti², Dr. Clemens Ritter³, Dr. Martina Fracchia⁴, Dr. Paolo Ghigna⁴, Dr. Pollastri Simone⁵, Dr. Claudia Triolo¹, Dr. Lorenzo Spadaro⁶, Prof. Riccardo Ruffo², Prof. Saveria Santangelo¹

1. Dipartimento di Ingegneria Civile, dell'Energia, dell'Ambiente e dei Materiali (DICEAM), Università Mediterranea di Reggio Calabria, 89122 Reggio Calabria, Italy, 2. Dipartimento di Scienza dei Materiali, Università di Milano Bicocca, 20125 Milano, Italy, 3. Institut Laue-Langevin - 71 avenue des Martyrs CS 20156, 38042 Grenoble, Cedex 9, France, 4. Dipartimento di Chimica, Università degli studi di Pavia, 27100, Pavia, Italy, 5. Elettra-Sincrotrone Trieste, 34149, Basovizza, Trieste, Italy, 6. Istituto di Tecnologie Avanzate per l'Energia (ITAE) del Consiglio Nazionale delle Ricerche (CNR), 98126 Messina, Italy

Affordable and clean energy is one of the 17 sustainable development goals (SDGs) adopted by the United Nations General Assembly in 2015. Although this SDG will most likely not be achieved by the agreed date (2030), thanks to the impressive advances of renewable energy sources (RESs), access to electricity in poorer Countries is speeding up. However, the sustainability of energy production systems still represents a challenge. Electrochemical energy storage (EES) technologies are gathering growing attention due to the numerous initiatives aimed at improving efficiency and management of the RESs. The development of cost-effective materials allowing improving power density and cyclability is a key point both for more mature and developing EES devices. Presently, research on post-lithium batteries (pLIBs) is focused on nanostructured materials. Among them, those produced by electrospinning, suitable for production at the large-scale and able to meet requirements of a wide range of EES applications, have been broadly investigated as active components in pLIBs.

In this scenery, sodium-ion batteries (SIBs), even if not commercialized at the large scale yet, probably represent the technology with the highest maturity and sustainability level. The development of highly performing SIB anode materials is one of the crucial tasks. Transition metal oxides have been extensively evaluated as anode materials as they offer low costs combined with high theoretical reversible capacities. Iron(III) oxide that stores sodium ions via the $\text{Fe}_2\text{O}_3 + 6 \text{Na}^+ + 6 \text{e}^- \rightarrow 3 \text{Na}_2\text{O} + 2 \text{Fe}^0$ conversion mechanism are featured by large abundance, environmental friendliness and non-toxicity. Incorporating tetravalent impurities in the Fe_2O_3 lattice is a commonly adopted strategy to enhance the oxide conductivity.

This work deals with the effects produced by germanium doping on the microstructure, crystalline phase and electrochemical activity as anode material in SIBs of electrospun Fe_2O_3 nanofibres (NFs). The microstructural analysis performed on Ge-doped Fe_2O_3 NFs evidences the germanium incorporation in the iron oxide lattice mainly as a dopant impurity. It favors the formation of α - and γ -phases of the iron oxide along with an amorphous component. Ge^{4+}

ions occupy tetrahedral sites of the maghemite ($\gamma\text{-Fe}_2\text{O}_3$) lattice and the defective hematite ($\alpha\text{-Fe}_2\text{O}_3$) surface sites. The Ge-doped Fe_2O_3 NFs exhibit excellent rate capability (still delivering 140 mAh g^{-1} at 2 A g^{-1}) and good specific capacity (320 mAh g^{-1}

at 50 mA g^{-1}), but a constant specific capacity decrease of 0.75 mAh g^{-1} per cycle over 180 cycles at 70 mA g^{-1} .

Microfluidic synthesis of PLGA nanocarriers for the controlled delivery of bioactive compounds in plants of agronomic interest

Thursday, 25th March - 14:45: Oral Session 2-2 (Room 2) - Abstract ID: 108

Dr. Laura Chronopoulou¹, Ms. Francesca Portoghesi¹, Dr. Elisa Brasili², Dr. Giulia De Angelis², Dr. Anastasia Orekhova³, Dr. Giovanna Simonetti², Prof. Gabriella Pasqua², Prof. Cleofe Palocci¹

1. Department of Chemistry, University of Rome La Sapienza, **2.** Department of Environmental Biology, University of Rome La Sapienza, **3.** Dipartimento di Sanità Pubblica e Malattie Infettive, University of Rome La Sapienza

Nanotechnologies are foreseen to play a crucial role in the development of new crop management techniques in the near future. In fact, nanoscale particles have properties which can allow to increase the agrochemical efficiency of pesticides, fertilizers and genetic material, delivering them in a controlled and sustained manner. Nanodelivery would significantly reduce the indiscriminate use of conventional pesticides and ensure their safe application. However, detailed knowledge of the interaction of nanosize materials with crop plants and their ultimate fate in the environment is lacking. Scientific evaluations of benefits and risks for future developments in agriculture are necessary. Such information will help the establishment of a regulatory framework for their commercialization.

We developed and optimized a continuous flow microfluidic reactor that allows to precisely control some characteristics that are crucial for NPs applications as controlled size, morphology and reproducibility. PLGA-based NPs were synthesized using the solvent-displacement or nanoprecipitation technique and the effect of different fluidodynamic conditions as well as PLGA molecular weight and concentration on NPs features (dimensions, polydispersion, morphology, stability) was studied. DLS, SEM and TEM techniques were employed to characterize the NPs. Fluorescent NPs were used to test their ability to penetrate inside plants of agronomic interest (*Vitis vinifera*) and some common pathogenic fungi (*Botrytis cinerea*, *Aspergillus niger*, and *Aspergillus carbonarius*) in fluorescence microscopy experiments, both *in vitro* and *in vivo*. Also, we entrapped in PLGA NPs some model drugs (i.e. ribavirin, methyl jasmonate, fluopyram) and studied the cytotoxicity and biochemical effects of such nanocarriers on different plant species and fungi.

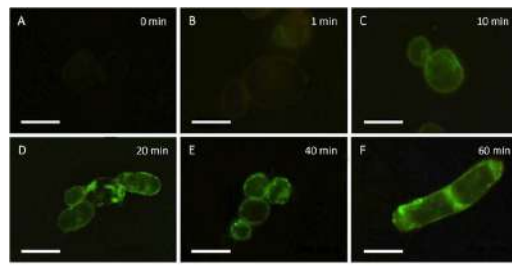
The optimization of the operating conditions of the microfluidic reactor allowed us to obtain spherical monodisperse NPs with controllable and tunable dimensions in the range from 25 to 300 nm [1]. By using NPs with different dimensions, we highlighted the role of the cell wall and membrane in NP size selection. We also confirmed that the uptake of PLGA NPs in plant cells follows mainly the clathrin independent endocytic pathway, without entering the lytic compartment, where they would be degraded [2]. In fact, the different bioactives loaded in PLGA NPs were able to penetrate cells, they were efficiently released and produced the expected biochemical effects, that were generally stronger, earlier and more durable than free formulations [3,4].

[1] Journal of Nanoparticle Research 2014, 16, 2703-2713.

[2] Plant Cell Reports 2017, 36(12), 1917-1928.

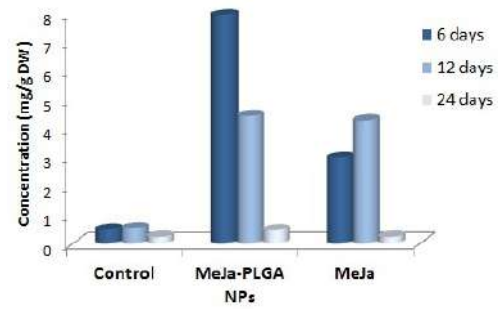
[3] Scientific reports 2019, 9, 1-9.

[4] Molecules 2019, 24, 2070-2084.



Time-dependent uptake of 50 nm fluorescent PLGA NPs by *Vitis vinifera* cell suspensions. Scale bars=50 μ m.

Uptake.jpg



Stilbene concentrations in *V. vinifera* cv. Malvasia cell cultures subjected to different treatments.

Stilbenes production.jpg

Understanding the pathological versus physiological effects of Sr^{2+} on bone by substitution in biomimetic apatite

Thursday, 25th March - 15:20: Oral Session 3-1 (Room 1) - Abstract ID: 285

Dr. Camila Tovani¹, Dr. Alexandre Gloter², Dr. Thierry Azaïs¹, Mr. Mohamed Selmane¹, Dr. Ana P Ramos³, Dr. Nadine Nassif¹

1. Sorbonne Université, 2. Université Paris-Saclay, 3. Universidade de São Paulo

Clinical reports of pathological mineralization are described for excess of Sr^{2+} whereas it is a widely used element in treatments of osteoporosis. These contradictory effects strengthen the need of clarifying the effect of Sr^{2+} on bone formation. To address these shortcomings, we describe herein a simple and versatile procedure to study the Sr^{2+} incorporation in bone mineral. Our strategy consists in using bioinspired conditions close related to that observed during the bone remodelling process. A set of Sr^{2+} substituted biomimetic apatite that combines the major features of bone mineral such as size, morphology, crystalline structure and CO_3^{2-} substitution was obtained reaching the content of Sr^{2+} described for human bone. The increase of Sr^{2+} concentration leads to the disruption of the hexagonal structure of hydroxyapatite stabilizing an unexpected amorphous phase (Sr-ACP). Interestingly, instead of the formation of pure Sr-apatite when the degree of Sr^{2+} substitution reached 100% in the starting solution, we observed the formation of a Sr-phosphate salt. These results may explain the development of skeletal diseases such as osteomalacia in rats treated with high doses of Sr^{2+} . As expected for the lower Sr^{2+} doses, the products presented lower crystallinity and expanded cell parameters in comparison to the pure apatite. This finding can be correlated to the increase in the bone rigidity in osteoporotic patients treated with pharmacological doses of Sr^{2+} . A mechanism that involves differences in the Ca^{2+} and Sr^{2+} concentration at the surface and the core of the particles was proposed. These results offer a new strategy towards the understanding of the different Sr^{2+} impacts in the bone mineral.

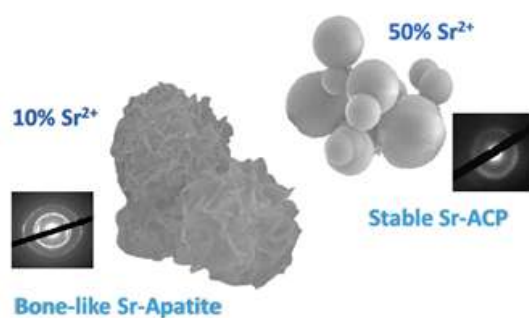


Image1.png

Designing functionalized polyelectrolyte microcapsules for cancer-cell-targeting and cancer treatment

Thursday, 25th March - 15:35: Oral Session 3-1 (Room 1) - Abstract ID: 183

Mrs. Daria Kalenichenko¹, Dr. Galina Nifontova¹, Dr. Alyona Sukhanova², Prof. Igor Nabiev³

1. LRN-EA4682, Université de Reims Champagne-Ardenne, Reims, France, LNBE, NRNU MEPhI, Moscow, Russian Federation, **2.** LRN-EA4682, Université de Reims Champagne-Ardenne, Reims, France, **3.** LRN-EA4682, Université de Reims Champagne-Ardenne, Reims, France, LNBE, NRNU MEPhI, Moscow, Russian Federation, Sechenov University, Moscow, Russian Federation

Introduction. Development of controlled and targeted delivery systems for anticancer therapy is a challenging task of personalized treatment of tumors. Controlled transportation and release reduce the side effects and toxicity of anticancer drugs for normal cells. Polyelectrolyte microcapsules (PMCs) are promising candidate delivery systems combining these functions. PMCs are prepared by layer-by-layer (LbL) adsorption of oppositely charged polyelectrolytes onto the template surface. This method allows fabricating core, core/shell, and shell PMCs and their functionalization with anticancer agents (e.g., doxorubicin) [1], metal (e.g., plasmon and magnetic) nanoparticles, and fluorescent labels (e.g., fluorescent nanocrystals (quantum dots (QDs)) or organic dyes) [2].

Modification of the PMC surface by attaching various recognition molecules, e.g., monoclonal antibodies (mAbs) or their fragments (mAbFr), proteins, small molecules (e.g., folic acid, galactose) can provide targeted delivery to cancer cells [3,4]. The small and compact mAbFr (F(ab)₂/Fab) comparable to full-size antibodies in antigen-binding affinity are characterized by a high stability and enhanced tissue diffusion, thus representing promising vector molecules for PMC functionalization to ensure their specific and selective interaction with cancer cells [4].

Methods. PMCs were fabricated using LbL deposition of PAH/PSS polyelectrolytes onto homemade CaCO₃ microparticles. The designed microcapsules were functionalized with doxorubicin by coprecipitation and spontaneous loading. The PMC shell was encoded with QDs to ensure fluorescent imaging [2,3]. The doxorubicin encapsulation efficiency, release kinetics at pH values corresponding to those of normal human tissues and tumors, particle dispersity, and morphology were evaluated. The PMC surface was modified using a heterobifunctional crosslinker with N-hydroxysuccinimide ester, maleimide groups, and a 12-unit PEG spacer to ensure coupling of the recognition molecules.

Results & discussion. The prepared PMCs were 2–3 μm in size. The doxorubicin encapsulation efficiency was 50.6 ± 3.2% in the case of spontaneous loading and 31.74 ± 0.99% in the case of coprecipitation. The possibility prolonged release of doxorubicin from PMCs of various designs at normal (physiological) and tumor microenvironment pH was determined. An approach to PMC surface activation using the heterobifunctional crosslinker preserving PMC dispersity and enabling a recognition molecules coupling efficiency of at least 50% was developed. The results pave the way to further development of novel functionalized PMC-based delivery systems for cancer-cell-targeted delivery and controlled release of anticancer agents.

References:

- [1] V. Kozlovskaya, et al., *Langmuir*, 34:39(2018), 11832-11842
- [2] G. Nifontova, et al., *ACS Appl.Mater.Inter.*, 12:32(2020), 35882-35894.
- [3] G. Nifontova, et al., *Front.Chem.*, 7(2019).
- [4] G. Rousserie et al., *Anal.Biochem.*, 10:8(2014), 1701-1709.

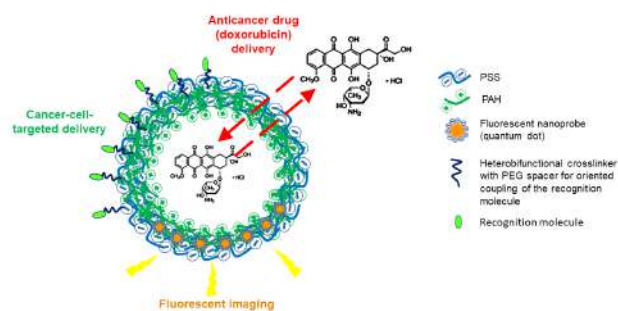


Figure 1. Designing functionalized polyelectrolyte microcapsules for cancer-cell-targeting and cancer treatment.

Figure 1. designing functionalized polyelectrolyte microcapsules for cancer-cell-targeting and cancer treatment..png

Hybrid Nanoparticle-Doped Polyelectrolyte Microcapsules with Controlled Photoluminescence for Bioimaging Applications

Thursday, 25th March - 15:50: Oral Session 3-1 (Room 1) - Abstract ID: 194

Dr. Galina Nifontova¹, Dr. Victor Krivenkov², Ms. Mariya Zvaigzne², Dr. Anton Efimov³, Mr. Evgeny Korostylev⁴, Mr. Sergei Zarubin⁴, Prof. Alexander Karaulov⁵, Prof. Igor Nabiev⁶, Dr. Alyona Sukhanova⁷

1. LRN-EA4682, Université de Reims Champagne-Ardenne, 51100 Reims, France, LNBE, National Research Nuclear University MEPhI (Moscow Engineering Physics Institute), 115409 Moscow, Russian Federation, 2. LNBE, National Research Nuclear University MEPhI (Moscow Engineering Physics Institute), 115409 Moscow, Russian Federation, 3. V.I. Shumakov National Medical Research Center of Transplantology and Artificial Organs, 123182 Moscow, Russian Federation, 4. Moscow Institute of Physics and Technology (State University), Dolgoprudny, Moscow Region, 141701 Russian Federation, 5. Sechenov University, 119146 Moscow, Russian Federation, 6. LRN-EA4682, Université de Reims Champagne-Ardenne, 51100 Reims, France, LNBE, National Research Nuclear University MEPhI (Moscow Engineering Physics Institute), 115409 Moscow, Russian Federation, Sechenov University, 119146 Moscow, Russian Federation, 7. LRN-EA4682, Université de Reims Champagne-Ardenne, 51100 Reims, France

Introduction. Fluorescent imaging is widely used in diagnostics and tracking of distribution, interaction, and transformation processes at molecular, cellular, and tissue levels. To be detectable delivery systems should exhibit a strong and bright fluorescence. Quantum dots (QDs) are highly photostable fluorescent semiconductor nanocrystals with wide absorption spectra and narrow, size-tunable emission spectra that make them suitable fluorescent nanolabels to be embedded within the microparticles used as bioimaging and theranostic agents [1-3]. Layer-by-layer (LbL) deposition allows designing fluorescent self-assembled microcapsules demonstrated as perspective tools for visually controlled stimuli-responsive delivery and release by entrapment of magnetic nanoparticles (MNPs) along with fluorescent dyes. LbL approach allows entrapping QDs and obtaining bright fluorescent microcapsules with a versatile surface charge and properties, size, and rigidity [4].

Methods. For microcapsule encoding water-soluble, PEGylated core/shell QDs using ligand exchange and solubilization approaches were prepared. Hybrid, nanoparticle-doped microcapsules were assembled by alternation of oppositely charged polyelectrolytes, QDs, and carboxylated MNPs onto calcium carbonate microtemplates. Particle surface charge and size distribution were analyzed using dynamic light scattering and laser Doppler electrophoresis. Nanoparticle-doped microcapsules were characterized by fluorescent, electron, and scanning probe microscopy. Photoluminescence (PL) study was performed using a self-made irradiation setup.

Results&Discussion. Here, we report on the results of preparation of water-soluble QDs, designing of the microcapsules with obtained QDs and additionally doped with MNPs, assessment of the structural, and photoluminescent characteristics of the microcapsules (Figure 1). The effects of nanoparticle spatial arrangement within the polyelectrolyte shell, the total shell thickness, surface charge of the microcapsules, on their PL characteristics during prolonged irradiation were investigated. The obtained data will allow further sophistication of the functionality of the imaging tools based on QD-encoded microcapsules. The designed hybrid, QD-, MNP-doped polyelectrolyte microcapsules are perspective stimuli-controlled agents to be used as tools for continuous fluorescence visualization.

This study was supported by the Ministry of Science and Higher Education of the Russian Federation, the Grant Program of the President of the Russian Federation for support of young Russian scientists (№ MK-3433.2021.3). A.S. and I.N. acknowledge support of the French Ministry of Higher Education, Research and Innovation, and the University of Reims Champagne-Ardenne. G.N. was supported by the Metchnikov Fellowship.

[1] G. Nifontova, et al. *Nanoscale Res. Lett.*, 13:30 (2018), 1-12.

- [2] G. Nifontova, et al. *Front. Chem.*, 7:34 (2019), 1-11.
[3] R. Bilan, et al. *Sci. Rep.* 7:44668 (2017), 1-10.
[4] G. Nifontova, et al. *ACS Appl. Mat. Interf.*, 12 (2020), 35882–35894.

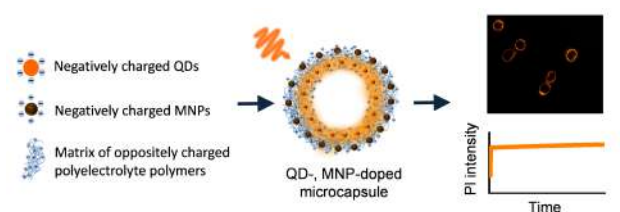


Figure 1. designing of hybrid nanoparticle-doped polyelectrolyte microcapsules with controlled photoluminescence for bioimaging applications.png

Theranostic Hyaluronic Acid Nanoparticles (Thera-ANG-cHANPs) for Dual Targeting and Boosted Imaging of Glioma Cells

Thursday, 25th March - 16:05: Oral Session 3-1 (Room 1) - Abstract ID: 158

Mrs. ANGELA COSTAGLIOLA DI POLIDORO¹, Dr. Laura Mezzanotte², Prof. Enza Torino³

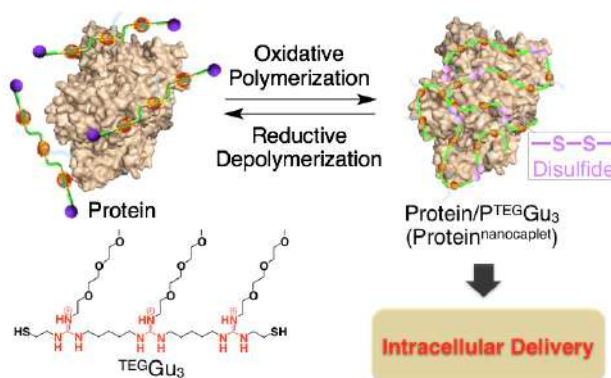
1. University of Naples Federico II, Department of Chemical, Materials and Production Engineering (DICMaPI), 80125, Naples, Italy, **2.** Erasmus Medical Center, Molecular Genetics, 3015 CN Rotterdam, The Netherlands, **3.** Department of Chemical, Materials Engineering & Industrial Production, University of Naples Federico I. Center for Advanced Biomaterials for Health Care, CABHC, Istituto Italiano di Tecnologia, IIT@CRIB,

Glioblastoma multiforme (GBM) is the most aggressive malignant brain tumour. The presence of the Blood-Brain Barrier (BBB) and the highly heterogeneous tumour microenvironment pose many hurdles to the transport of active agents, both for diagnosis and therapy, that are unable to reach the tumour cells at relevant concentrations. Indeed, the chemotherapeutic agent Temozolomide (TMZ), which in combination with radiotherapy constitutes the first line treatment for GBM, still fails in improving patient prognosis significantly that remains very poor with a mean survival of only 15 months. The intravenous injection of polymer nanoparticles has demonstrated great potential in improving pharmacokinetics of these molecules and in modulating their transport properties. In this regard, hydrogels and particularly Hyaluronic Acid (HA), are among the most promising candidates as naturally occurring polymer of the ECM. Recent evidence are showing the key role that HA plays in modulating the interaction of delivered agents with glioma cells through CD44 receptors abundantly expressed by stem-like glioma cells and mediators of cell adhesion and invasion. In addition, by the effect of *Hydrodenticity*, hydrogel matrices boost relaxometric properties of gadolinium (Gd) chelates as Gd-DTPA, the most common contrast agent used in clinical T1-weighted MRI, the gold standard for GBM diagnosis and monitoring.

In our work, crosslinked Hyaluronic Acid Nanoparticles encapsulating gadolinium-diethylenetriamine pentaacetic acid (Gd-DTPA) and the chemotherapeutic agent Irinotecan (Thera-cHANPs) are presented as an innovative theranostic nanosystem with improved MRI capacities. Irinotecan has been selected since many clinical trials demonstrate its potential as alternative treatment with respect to the poorly effective TMZ. In addition, the surface of nanoparticles has been decorated with Angiopep-2 (Thera-ANG-cHANPs), a dual-targeting peptide interacting with LRP-1 receptors overexpressed by endothelial cells of the BBB and by glioma cells. Results showed that *Hydrodenticity* is preserved in ANG-cHANPs and that the peptide is able to improve the uptake of NPs in U87 cells and patient-derived glioblastoma cell culture, compared to untargeted cHANPs by increasing both NP uptake rate and duration. Thera-ANG-cHANPs uptake mechanism has been elucidated and an active mechanism involving Angiopep-2 has been demonstrated. Finally, we proved that multifunctional Thera-ANG-cHANPs improved the therapeutic potential of Irinotecan, showing a cytotoxic effect within 24h. Overall, results contribute to the increasing evidence that specific design choices confer a specific biological identity to the carrier that is directly impacting its interaction with the biological target.

*Dr. Hashim P.K*¹

Many of the disaster diseases considered as undruggable by small molecule drugs, instead designed macromolecules such as nucleic acid or proteins can be used as therapeutic drug for the disease treatment due to high specificity towards target gene. However, stability of macromolecules in blood is very low and quickly degrades by enzymes or proteases. Nanotechnology-based medicine that consists of a protective carrier encapsulating therapeutic agent can dramatically enhance the blood stability and efficacy of drugs [1]. However, most of the carrier/drug conjugates resulted in a larger hydrodynamic size, and hence the construction of carrier/drug conjugates smaller than 10 nm that may behave, as ‘small molecule drugs’ remains a big challenge. We recently developed a ‘template polymerization’ approach to prepare a uniform polymer layer (nanocaplet) on a small interfering RNA (siRNA) surface [2]. In the present study, we successfully prepared protein-nanocaplets using protein ‘templates’ (BSA, Cytochrome C, *b*-galactosidase). In the case of BSA, a water-soluble $^{152}\text{Eu}^{3+}$ monomer bearing two thiol termini adheres to carboxylate anion present in the protein surface via ‘salt-bridge’ interaction. Upon addition of oxidizing agent, disulfide polymerizations at the protein surface generate a nanocaplet coat that has a collective hydrodynamic size of ~10 nm as observed by transmission electron microscopy (TEM). BSA-nanocaplet showed responsiveness to reducing agent such as dithiotritol (DTT) and efficiently internalizes into cancer cells [3]. Because of ultra-small size, the nanocaplets have potential to use for delivery applications at remote areas such as brain that usually restricts the passage of larger nanocarrier (30–300 nm) across blood brain barrier (BBB).



104

Bottom-up Synthesis of Layered Metal Chalcogenides: Chemical Routes to New 2D Materials

Thursday, 25th March - 15:20: Oral Session 3-2 (Room 2) - Abstract ID: 170

Prof. David Lewis¹

1. The University of Manchester

Layered bulk materials have attracted much attention for various technological applications including tribology and catalysis [1]. One of the most recent applications is in their study in the two-dimensional limit i.e. atomically thick materials such as graphene. Inorganic graphene analogues such as few layer molybdenum disulphide, black phosphorus and main group chalcogenides have also been the subjects of much intense research as two-dimensional semiconductors that would be complementary to graphene in a future electronics industry [2]. We have devised top-down routes to 2D black phosphorus [3] and tin(II) sulphide [4] both of which have layer dependent band gaps. However, these top-down processes suffer from a major drawback: often commercially available layered bulk crystals are used as feedstock and this inherently limits the palette of two-dimensional materials available for study without resorting to expensive processing via CVD.

As a solution to this, we have devised new routes based on solventless thermolysis of metal-organic precursors that can produce layered materials in bulk at relatively low temperatures and in relatively high purity. Because the precursors used are on the molecular scale, we can control the extent of doping or alloying of materials and this then widens range of layered materials available for exfoliation. I will present the synthesis of layered MoS₂, MoO₃ [5] MoWS/MoWSO alloys[6] and PbSnS alloys [7], the latter studied as post-processed 2D materials as an example of this new processing route toward bespoke 2D materials.

[1] Tedstone et al, Chem. Mater., 2016, 28, 1965-1974

[2] Tedstone et al Nanoscience: Volume 4 (RSC Specialist Periodical Reports), 2017, 4, 108-141

[3] Brent et al, Chem. Commun., 2014, 50, 13338-13341

[4] Brent et al J. Am. Chem. Soc. 2015, 126, 9413-9424

[5] Zeng et al, Chem. Commun. 2019, 55, 99-102;

[6] Zeng et al, Chem. Mater. 2020, 32, 7895-7907.

[7] Norton et al, Chem. Sci. 2019, 10 (4), 1035-1045.

Synthesis and Optimization of Magnetic Polymer Nanocomposites for Biomedical Applications

Thursday, 25th March - 15:35: Oral Session 3-2 (Room 2) - Abstract ID: 133

Mr. Eoin McKiernan¹

1. University College Dublin

The unique magnetic properties of iron oxide nanoparticles (IONPs) combined with the materials excellent biocompatibility make them attractive candidates for biomedical applications.¹ Potential theragnostic applications of these particles arise from their response to applied magnetic fields. Under constant field particles show strong and reversible magnetization, allowing them to be used as efficient magnetic resonance imaging (MRI) contrast agents.² When exposed to an alternating magnetic field, particles may act as potent heating mediators, allowing them to be exploited for therapeutic applications such as thermally triggered drug release and hyperthermia cancer treatment.³ However, preventing NP aggregation in biological environments remains an important challenge.⁴

Careful selection of the appropriate combination of NP and stabilizing ligand is required to maintain colloidal stability, biocompatibility and the magnetic properties of the NPs. In this work we present a facile and effective method for the steric stabilization of multicore iron oxide NPs using a biocompatible polymer (Polyethylene glycol, PEG). This PEGylation approach provides excellent long-term aqueous stability while preserving the NPs magnetic properties for magnetic hyperthermia and MR imaging applications, promising in-vivo results are observed.

Finally, the impact of phase transfer from aqueous to bulk polymer media on the magnetic properties of multicore nanoparticles will be presented. It is found that by controlling interparticle interactions, the emergent magnetic properties of the polymer composites can be modulated. This allows for optimization of nanocomposite responses for bio-medical applications both as bulk materials and as components in micron-scale printed structures. These advances will be described.

References:

- [1] A. S. Labbe, C. Bergemann, H. Riess, F. Schriever, and D. Huhn, *Cancer Res*, 1996, **56**, 4686-4693.
- [2] B. Bonnemain, *Journal of Drug Targeting*, 1998, **6**, 167-174.
- [3] V. I. Shubayev, T. R. Pisanic and S. Jin, *Adv Drug Deliv Rev*, 2009, **61**, 467-477
- [4] L. Gutiérrez, L. de la Cueva, M. Moros, G. Salas, *Nanotechnology*, 2019, **30**, 112001-112015

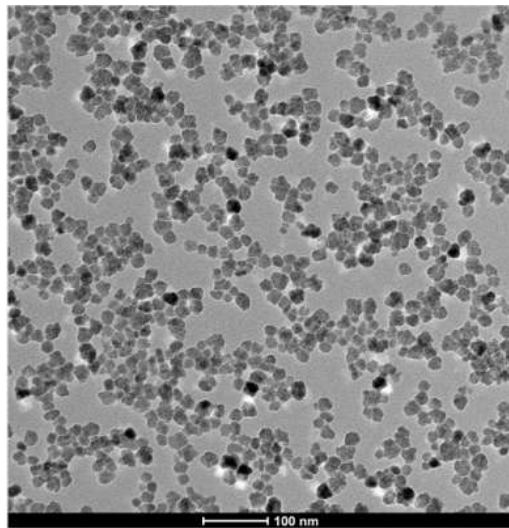


Figure 1 transmission electron microscopy images of multi-core ionps.png

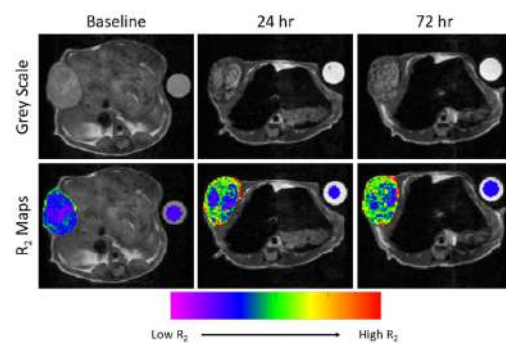


Figure 2 mri slices with r2 heat maps of tumour implanted mice post injection of pegylated multicore nanoparticles.png

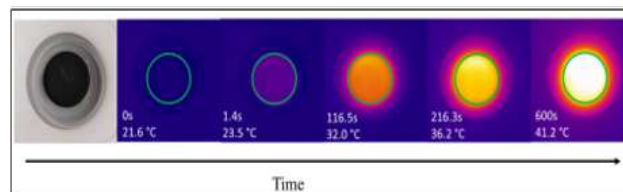


Figure 3 time resolved thermography of amf stimulation of bulk magnetic polymer nanocomposite.png

Indium-Filled Porous Silicon Formed by Electrochemical Deposition

Thursday, 25th March - 15:50: Oral Session 3-2 (Room 2) - Abstract ID: 70

Mr. Nikita Grevtsov¹, Dr. Eugene Chubenko¹, Dr. Vitaly Bondarenko¹, Dr. Ilya Gavrilin², Dr. Alexey Dronov², Dr. Sergey Gavrilov²

1. Belarusian State University of Informatics and Radioelectronics, 2. National Research University of Electronic Technology

Introduction

While electrodeposition of indium and other fusible metals on flat conductive substrates is generally well described in literature, investigations regarding the filling of porous nanostructures (namely, porous silicon (PS)) with said metals are nearly non-existent. Presumably, structures of such a nature could serve as a prominent matrix for acquiring semiconductor/metal nanostructures and alloys by utilizing the electrochemical liquid-liquid-solid (ec-LLS) growth mechanism, where each deposited metal particle acts both as a microscopic cathode and a growth medium for the precursor material present in the electrolyte. However, to maximize the efficiency of such a process, a more or less uniform level of fusible metal distribution throughout the porous layer may be required.

Methods

In this study PS was formed by anodizing monocrystalline (100)-oriented heavily-doped (0.01 Ohm×cm) n-type silicon wafers in a 9 wt.% HF aqueous solution at a current density of 70 mA/cm² for 30 s. Indium was then electrochemically deposited into the pores from a water solution of In₂(SO₄)₃, (0.001 M) and Na₂SO₄(0.003 M).

Results

The SEM and EDX data suggest that indium deposits assemble in cylindrical shapes along the pore channels. The number of pores filled with indium increases with current density. Additionally, partially oxidizing PS beforehand substantially limits the current distribution in its uppermost areas, localizing the deposition deeper inside the pores (figure 1). Due to accumulating diffusion limitations attributed to the pores' small lateral sizes the heights of these cylindrical structures get smaller the deeper they are into the pores.

Discussion

Presumably, deposition is initiated when a local breakdown of the oxide layer on the pores' sidewalls occurs. The number of these breakdown points increases with current density due to a higher voltage being applied. Nucleation may also take place at various surface defects that locally reduce the surface barrier and with it the breakdown voltage. Formation of initial indium nuclei leads to voltage redistribution, and any further deposition takes place on the formed indium clusters that continue to grow into cylindrical structures along the pore channels (figure 2). Preliminary oxide formation may also additionally assist the deposition process by increasing the wettability of the pores' side walls and reducing the negative effect of diffusion limitations. By varying all the parameters listed above, an optimal level of indium distribution can be achieved, suitable for efficiently carrying out the ec-LLS process.

Acknowledgements

This work was financially supported by the Russian Science Foundation (project no. 20-19-00720).

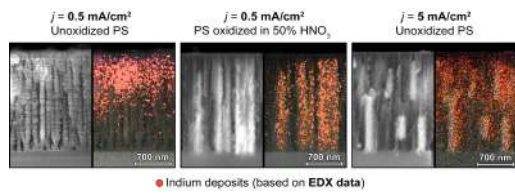


Figure 1.png

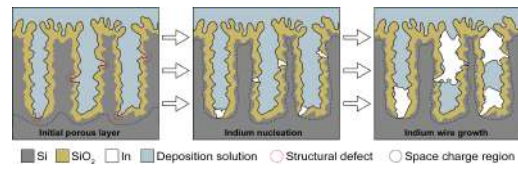


Figure 2.png

ZnO nano tetrapods based coatings and their application

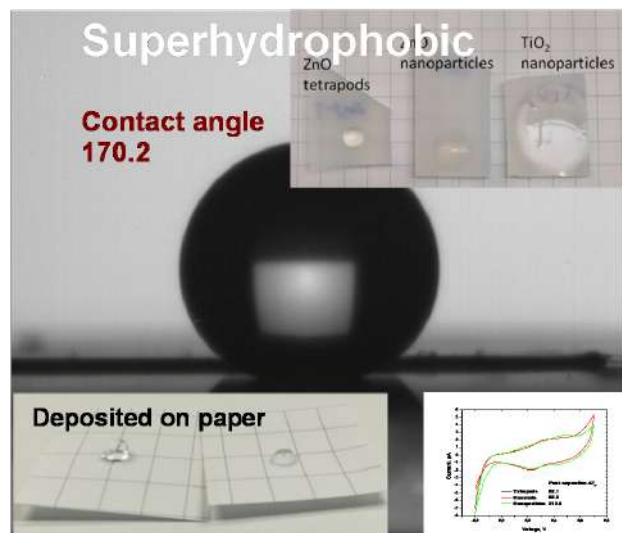
Thursday, 25th March - 16:05: Oral Session 3-2 (Room 2) - Abstract ID: 138

**Dr. Rasa Mardosaite¹, Dr. Agne Sulciute¹, Mr. Mindaugas Ilickas¹, Mr. Paulius Laurikenas¹,
Dr. Simas Račkauskas¹**

1. Kaunas University of Technology

The majority of the nanowire (NW) synthesis methods utilize catalyst particles to guide the nanowire geometry. In contrast, catalyst-free methods are attractive for facile fabrication of pure nanowires without the need for catalyst preparation. Zinc oxide nanostructures have received broad attention due to their distinguished performance in electronics, optics, gas sensing and piezoelectronics. Zinc oxide tetrapod (ZnO-T) is one of these structures, consisting of 4 nanowires, is especially interesting for its simple synthesis, however growth mechanism is not thoroughly understood.

Here, we propose a simple non-catalytic one-step process method for an efficient and rapid synthesis of ZnO tetrapods by Zn vapor oxidation under air environment and application for multifunctional coatings and fast UV sensors.



11.png

Spatially Controlled Atomic Layer Deposition within Polymer Templates for Multi-Material Nanorods Fabrication

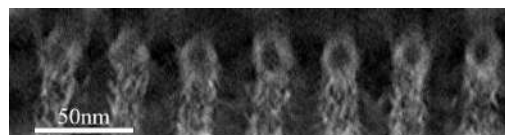
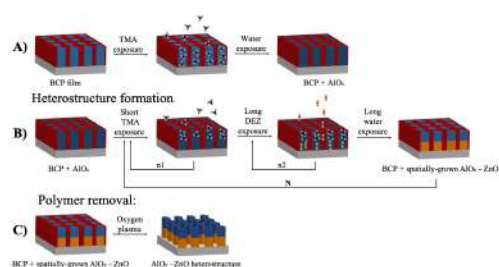
Thursday, 25th March - 16:20: Oral Session 3-2 (Room 2) - Abstract ID: 201

Ms. Rotem Azoulay¹, Dr. Neta Shomrat¹, Ms. Inbal Weisbord¹, Dr. Galit Atiya², Dr. Tamar Segal Peretz¹

1. Department of Chemical Engineering, Technion, 2. Department of Materials Science and Engineering, Technion

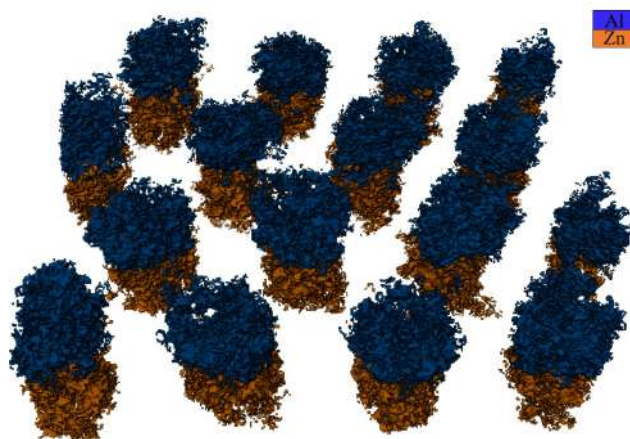
Today's nanofabrication techniques require multistep and costly processes in order to fabricate complex, multi-materials nanostructures. Performing atomic layer deposition (ALD) within polymeric templates can offer a simple solution for nanostructure fabrication. In this process, named sequential infiltration synthesis (SIS), high partial pressures and long exposures times lead to inorganic materials growth within polymers. Sequential polymer removal results in polymer-templated inorganic nanostructure. While SIS shows great potential in fabricating large variety of structures, it is currently limited to a single material growth process.

In this research, we demonstrated, for the first time, multi-material SIS process with control over the spatial location of each material and fabricate heterostructure nanorods. We studied SIS within self-assembled block copolymer (BCP) films and developed multi-material SIS, where two metal oxides are grown together in a single process, with precise control over their location within the polymer template. We used cylinder forming poly(styrene-block-methyl methacrylate) (PS-b-PMMA) films as the polymeric template and DEZ (diethyl zinc) and TMA (trimethyl aluminum) as the organometallic precursors. We achieved control over the growth location of each metal oxide by tuning the organometallic precursors diffusion time, forming heterostructures after polymer removal. A short exposure of the first precursor resulted in a limited growth only at the upper part of the polymer, while a long exposure of the second precursor enabled it to reach the full depth of the polymer besides the section which was already occupied by the first precursor. An exposure to water completed the cycle. We demonstrated this process on BCP films to achieve AlOx-ZnO nanorods arrays (Figure 1). We performed structural characterization using scanning and transmission electron microscopy (SEM and TEM, respectively) to characterize nanorods as well as three-dimensional characterization scanning TEM (STEM) tomography and energy-dispersive X-ray spectroscopy (EDS) STEM tomography in order to probe the structure and the chemical composition in 3D (Figure 2,3). This research opens new pathways for multi-materials nano scale structure fabrication through ALD-based growth within polymers.



Cross sectional view from haadf-stem tomography figure 2 .jpg

Spatially controlled sis process figure 1 .jpg



Perspective view obtained from visualization of the stem-eds tomography figure 3 .jpg

Metal halide perovskites: a journey through structure, properties and stability

Thursday, 25th March - 16:55: Plenary Session 2 (Room 1) - Abstract ID: 317

Dr. Ana Flavia Nogueira¹

1. University of Campinas (UNICAMP)

TBD

Supported metallic heterogeneous catalysts in light of density functional theory calculations: from single atoms to subnanometric clusters

Thursday, 25th March - 17:40: Plenary Session 2 (Room 1) - Abstract ID: 12

Dr. Céline Chizallet¹

1. IFP Energies nouvelles

Platinum-based sub-nanometric particles and platinum single atoms supported on alumina play a prominent role in heterogeneous catalysis, in particular for catalytic reforming, alkane dehydrogenation and pollution abatement. The identification of the structure and the electronic properties of their active sites is an important challenge. The combination of density functional theory calculations, of X-Ray absorption spectroscopies and of electronic microscopy is fruitful. Pt clusters supported on chlorinated alumina exhibit a diameter close to 0.9 nm (Figure b)),^[1] which makes Pt₁₃ models relevant. 20% of the reduced platinum is in the form of single atoms.^[1] DFT models have been developed that take into account the effect of the particle size,^[2, 3] the hydroxylation and chlorination of the support,^[2, 4] and of the reaction atmosphere (hydrogen,^[3, 5, 6] oxygen,^[3, 7] carbon monoxide, hydrocarbons^[8, 9]). Reconstruction effects are revealed, that strongly depend on all these parameters. These models also made possible the assignment of in situ HERFD-XANES (Fig a)).^[6] Recently, thanks to HR-HAADF-STEM, the preferential location of the particles at the edges of alumina platelets was established,^[1] whereas ¹H NMR combined to DFT concluded that chlorine also preferentially sites at the edges.^[1] The impact of bimetallicity upon alloying with Sn was also taken into account in the DFT models (Fig. c)),^[10] which shows a crucial role of the ductility of the clusters on the hydrogen adsorption properties. Ductility also plays a role in the stabilization of reaction intermediates by the platinum sub-nanometric particles, involved in the dehydrogenation of methylcyclohexane into toluene.^[9] The role of Pt single atoms (arrows in Fig. b)) in dehydrogenation catalysis is still questioned, whereas we showed that in oxidant conditions, single atoms are most stable than clusters, the reverse holding true in reducing conditions.^[3]

[1] A.T.F. Batista et al., *ACS Catal.*,**2020**, *10*, 4193.

[2] C.H. Hu et al., *J. Catal.*,**2010**, *274*, 99.

[3] C. Dessa et al., *Nanoscale*,**2019**, *11*, 6897.

[4] C. Mager-Maury et al., *ACS Catal.*,**2012**, *2*, 1346.

[5] C. Mager-Maury et al. , *ChemCatChem*,**2011**, *3*, 200.

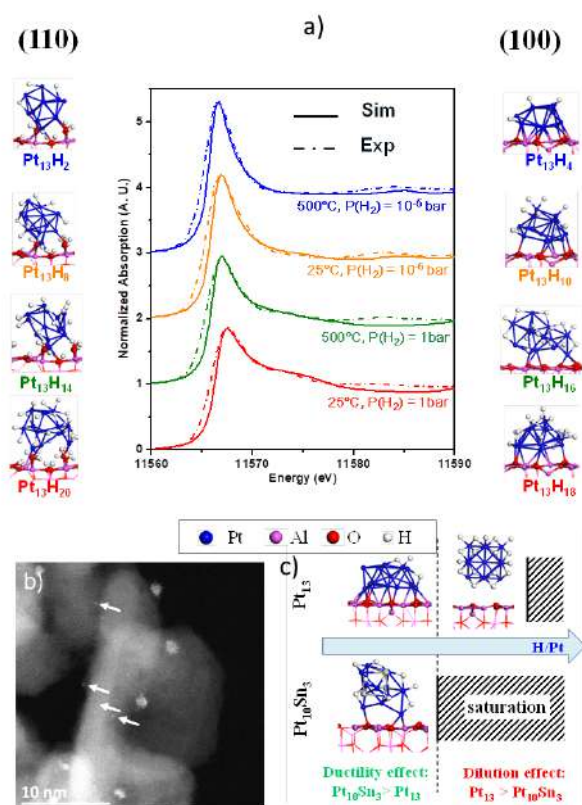
[6] A. Gorczyca et al., *Angew. Chem., Int. Ed.*,**2014**, *53*, 12426.

[7] A. Sangnier et al., *J. Phys. Chem. C*,**2018**, *122*, 26974.

[8] P. Raybaud et al., *J. Catal.*,**2013**, *308*, 328.

[9] W. Zhao et al., *J. Catal.*,**2019**, *370*, 118.

[10] A. Gorczyca et al., *ChemCatChem*,**2019**, *11*, 3941; A. Jahel et al., *J. Phys. Chem. C*,**2012**, *116*, 10073.



Clusters-pt-alumina.png

TBD

Friday, 26th March - 09:00: Plenary Session 1 (Room 1) - Abstract ID: 314

***Prof. Kimberly Dick Thelander*¹**

1. Lund University

TBD

TBD

Friday, 26th March - 09:45: Plenary Session 1 (Room 1) - Abstract ID: 315

Prof. Rainer Haag¹

1. *Institut für Chemie und Biochemie, Freie Universität Berlin, Takustr. 3, 14195 Berlin*

TBD

Anisotropic Plasmonic Nanoparticles with Wide Range Resonance Tunability

Friday, 26th March - 10:50: Oral Session 1-1 (Room 1) - Abstract ID: 302

Dr. Supriya Atta¹, **Dr. Ted Tsoulos**², **Ms. Kaleigh Ryan**³, **Prof. Laura Fabris**³

1. Duke University, 2. EPFL, 3. Rutgers University

Anisotropic plasmonic nanoparticles can display exceptional field enhancement properties and tunable resonant modes that can be leveraged in several fields, from imaging to catalysis. Among these nanoparticles, gold nanostars have emerged as extremely promising, in particular as it concerns the creation of effective imaging tags, phototherapeutic agents, and hot electron-based photocatalysts. In my talk, I will discuss our concerted computational/experimental approach to design and synthesize six-branch gold nanostars with high shape anisotropy. These particles combine the unique advantages of nanostructures fabricated from the top-down and those synthesized from the bottom-up, showcasing a unique plasmonic response that remains largely unaltered on going from the single particle to the ensemble. These nanostars display multiple, well-separated, narrow resonances, the most intense of which extends in space much farther than that observed before for any plasmonic mode localized around a colloidal nanostructure. Importantly, the unique close correlation between morphology and plasmonic response leads the resonant modes of these particles to be tunable between 600 and 2000 nm, a unique feature that could find relevance in cutting edge technological applications. Along with the fundamental properties of the bare nanostars, I will discuss the synthetic protocols we have developed to coat them with thin semiconductor shells, further extending their applicability in spectroscopy and catalysis.

Plasmonic mesoporous silica coated copper sulfide nanoparticles as near infrared absorbing photothermal agents

Friday, 26th March - 11:20: Oral Session 1-1 (Room 1) - Abstract ID: 271

Prof. Elisabetta Fanizza¹, **Ms. Orietta Pugliese**², **Ms. Rita Mastrogiacomo**², **Dr. Luciano De Sio**³, **Dr. Alexa Guglielmelli**⁴, **Dr. Federica Rizzi**², **Mr. Pierluigi Lasala**², **Dr. Maria Principia Scavo**⁵, **Dr. Gennaro Gentile**⁶, **Dr. Rachele Castaldo**⁶, **Prof. Angela Agostiano**¹, **Dr. Marinella Striccoli**⁷, **Dr. Nicoletta Depalo**⁸, **Prof. Maria Lucia Curri**¹

1. University of Bari "Aldo Moro", 2. Chemistry Department, Università degli Studi di Bari, Via Orabona 4, 70126 Bari, Italy, 3. Department of Medico-Surgical Sciences and Biotechnologies, University of Rome Sapienza, Corso della Repubblica 79, 04100 Latina (LT), 4. Department of Physics, University of Calabria, 87036, Arcavacata di Rende, Cosenza, 5. Personalized Medicine Laboratory, National Institute of Gastroenterology "S. De Bellis" Research Hospital, Via Turi 27, Castellana Grotte, Bari, 6. CNR- Institute for Polymers, Composites and Biomaterials Via Campi Flegrei 34, 80078 Pozzuoli(NA), 7. CNR-IPCF, 8. CNR-Istituto per i Processi chimico Fisici (CNR-IPCF), SS Bari, Via Orabona 4, 70126 Bari, Italy

The impact of cancer in human life pushes translational research towards development of unconventional nanosystems for cancer diagnosis and therapy.¹⁻² Photothermal therapy (PTT), based on conversion via photothermal transducer of light into heat represents a precise and minimally invasive modality for the treatment and management of tumors. The exploitation of the second NIR (NIR-II) light (1000–1700 nm), which penetrates deeper into tissue and has decreased photoscattering is more suitable for deep PTT, enabling high therapeutic efficacy, deep therapeutic window, minimizing side effects. Efficiency of a properly designed PTT agent (PTTA) depends on its stability in biological media and its ability to absorb and convert the NIR light into heat, sustaining laser irradiation without undergoing to decomposition. Many preclinical studies demonstrate the efficacy of PTTA highly improved if used in combination with both radio and chemotherapeutic agents.³

Organic capped plasmonic Cu_{2-x}S NPs, showing a plasmon band in the NIR II region, are here selected as potential PTTA, thanks to their demonstrated activity in PTT, as well as reactive oxygen species generation, photoacoustic, magnetic resonance and positron emission tomography imaging.¹ Here, Cu_{2-x}S NPs, synthesized by hot injection approach⁴ are encapsulated into an optically transparent hydrophilic mesoporous silica shell (Cu_{2-x}S@MSN), templated by surfactants, with loading/selective release capability. Different key aspects regarding structure, chemistry at the interface and property must be tackled: (i) control over Cu_{2-x}S NP geometry and stoichiometry, thus plasmonic properties⁴ (ii) development of a functionalization protocol to homogeneously coat Cu_{2-x}S NPs with a mesoporous hydrophilic silica shell, keeping the size in the sub-micrometre regime (iii) formation of a high surface area and tunable porous structures suitable for drug delivery.

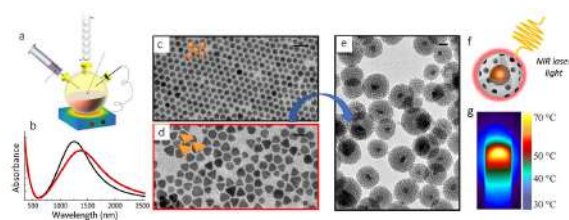
Core-shell Cu_{2-x}S@MSN of nearly 50 nm presenting a plasmon band centred at 1250 nm are synthesised and their light-to-thermal energy conversion proved by investigating the photothermal response, upon excitation with laser light at 810 nm. A temperature increase up to nearly 70°C is attained after short-term exposure (60 sec) being the photothermal response reversible. These properties may ensure local/repeatable thermal treatment of tumour tissue with low damage to the surrounding healthy tissues, highlighting the potential of the Cu_{2-x}S@MSN as effective PTTA and reliable drug delivery system.

1. Y. Liu et al. Mol. Pharmaceutics 2019, 16, 3322

2. H. Sun et al. ACS Appl. Mater. Interfaces 2020, 12, 30145

3. F. Vischio et al J. Phys. Chem. C 2019, 123, 23205

4. M. Giancaspro et al. Mater. Chem. Front. 2021, DOI. 10.1039/D0QM00596G



Synthesis and properties of copper sulfide-mesoporous silica core-shell structures as drug delivery systems with photothermal property.jpg

Size, shape and phase modulation of colloidal plasmonic copper sulphide nanocrystals

Friday, 26th March - 11:50: Oral Session 1-1 (Room 1) - Abstract ID: 256

Ms. Mariangela Giancaspro¹, Dr. Teresa Sibillano², Ms. Francesca Panzarea¹, Dr. Cinzia Giannini³, Ms. Silvia Schmitzer¹, Mr. Fabio Vischio⁴, Dr. Nicoletta Depalo⁴, Prof. Angela Agostiano⁵, Prof. Maria Lucia Curri⁵, Dr. Marinella Striccoli⁶, Prof. Elisabetta Fanizza⁵

1. Chemistry Department, Università degli Studi di Bari, Via Orabona 4, 70126 Bari, Italy, **2.** CNR-Istituto di Cristallografia (CNR-IC), Via Amendola, 122/O, 70126 Bari, Italy, **3.** CNR - Istituto di Cristallografia, **4.** CNR-Istituto per i Processi chimico Fisici (CNR-IPCF), SS Bari, Via Orabona 4, 70126 Bari, Italy, **5.** University of Bari "Aldo Moro", **6.** CNR-IPCF

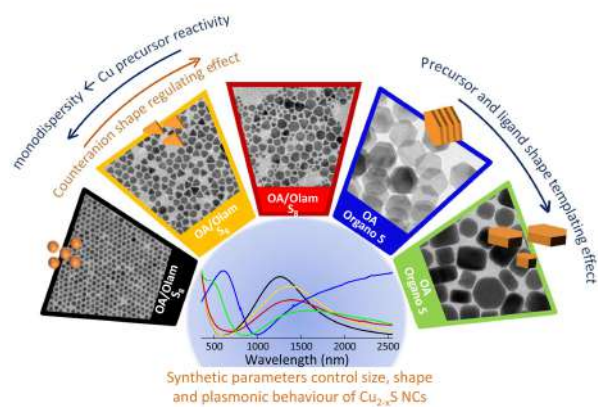
Self-doped copper sulphide Cu_{2-x}S nanocrystals (NCs) are p-type semiconductors with intriguing near infrared (NIR) plasmonic properties explored in a wide variety of applications such as catalysis, energy conversion, sensing and biomedicine.^{1,2} Due to their stoichiometry-, size- and shape- dependent properties, the NCs design is crucial to yield high performances devices. Even though, at the present stage of the research, advances in terms of controlled geometry and optical properties are made in Cu_{2-x}S NCs synthesis by hot injection, unexpected sizes and shapes and broad polydispersity still represent critical issues, responsible of unpredictable optical response and undesirable broadening of the spectroscopic feature. This work aims to tackle such limitations by rationalizing the influence of reactants on Cu_{2-x}S NCs size, shape and phase modulation.

A systematic morphological, structural and spectroscopic analysis of Cu_{2-x}S NCs samples prepared by hot-injection methods using various conventional copper precursors (i.e. CuCl , CuCl_2 , $\text{Cu}(\text{AcAc})_2$, $\text{Cu}(\text{AcO})_2$), sulphur reactants (i.e. S_8 , tert-dodecanthiol (tDT) or dibutyldisulfide (DBDS)) and coordinating solvents (oleic acid, OA and oleylamine, Olam), have been carried out. The reactivity of copper salt precursors, considered with respect to metal ion valence and type of counterions, and the strength of ligand bindings to NP surface, have been evaluated on the base of Hard Soft Acid Base theory (HSAB).

The $\text{CuCl} > \text{CuCl}_2 > \text{Cu}(\text{AcO})_2 > \text{Cu}(\text{AcAc})_2$ order of reactivity has been directly related to the rate of monomer release controlling the size and shape monodispersity; type of counterions, balanced by the ligand composition, have demonstrated to define the final NC shape when S_8 is used as sulfur precursor, while hexagonal discotic micellar structures of chloride Cu-tDT liquid crystalline phase templated the formation of hexagonal monodispersed thin NPLs in the case of alkanethiol. The intrinsic poor reactivity of organosulphur, injected *in situ* provides the djurlite $\text{Cu}_{1.94}\text{S}$ while S_8 , decomposed *ex situ* in coordinating reducing solvent, has led to digenite $\text{Cu}_{1.8}\text{S}$ NCs. Overall, this work has successfully contributed to the fundamental understanding of the complex mechanism behind the formation of Cu_{2-x}S NCs, providing an effective toolbox, based on precursors and reactants and chemical considerations, to achieve NCs with controlled structural and morphological characteristics and well defined plasmonic response, thus suited for future technological applications.

References:

1. Y. Liu, et al. The Journal of Physical Chemistry C, 2017, **121**, 13435-13447
2. S. Goel, et al. Small, 2014, **10**, 631-645
3. M. Giancaspro et al., Mater Chem. Front., 2021, DOI. 10.1039/D0QM00596G



A chemical toolbox for the production of copper sulphide nanocrystals with controlled structural and morphological characteristics and well defined plasmonic behavior.jpg

Plasmonic biocatalysis: using light for the regulation of enzyme activity on plasmonic nanoparticles

Friday, 26th March - 12:05: Oral Session 1-1 (Room 1) - Abstract ID: 92

***Dr. Heloise Ribeiro de Barros*¹, *Prof. Pedro Camargo*², *Prof. Susana Inés Cordoba de Torresi*¹, *Prof. Fernando López-Gallego*³, *Prof. Luis Liz-Marzán*³**

1. São Paulo University, 2. University of Helsinki, 3. CIC Biomagune

Introduction

The light-driven regulation of enzyme functions at the interface with plasmonic nanoparticles (PNPs) has fostered innovative opportunities in the emerging field of plasmonic biocatalysis. PNPs can be applied to manipulate enzyme functionality, in particular by the effects resulted from the localized surface plasmon resonances (LSPR) excitation. The incident light can trigger energetic processes (*i.e.*, temperature and electronic effects) for the PNPs, which can affect the properties of the enzyme immobilized on the surface of the PNPs. In the present study, we explored the plasmonic effects on the biocatalysis of the lipase from *Candida antarctica* fraction B (CALB) conjugated on Au nanospheres (AuNSp) and nanostars (AuNSt) upon an 808 nm near-infrared (NIR) laser excitation. We herein investigated the enhancement of the enzyme activity, and the fundamental mechanistic and kinetic understanding about the plasmonic effects in the interface of the enzyme-PNPs. The results obtained in this study enabled to explore the plasmonic effects for the precise and remote regulation of the enzyme activity, using light as an external stimulus.

Methods

CALB was conjugated on AuNSp and AuNSt by chemical adsorption. AuNSp were obtained by the Turkevitch method, and AuNSt were obtained by the seed-mediated growth method. CALB immobilized on AuNSp (LSPR at 525 nm) and AuNSt (LSPR at 700 nm) were excited by NIR laser. CALB activity was monitored toward the hydrolysis of nitrophenyl palmitate by UV-vis spectroscopy.

Results and Discussion

Enzyme activity of CALB was significantly enhanced under NIR laser irradiation when immobilized on AuNSt (up to 58%) than on AuNSp (up to 13%) (Figure 1A). The higher yield for the AuNSt corresponds to the resonance effects between the LSPR and the NIR laser irradiated. We investigated the enzyme activity, the plasmonic properties of PNPs, the conformational properties of CALB, and the parameters governing the molecular interactions. To decipher the fundamental mechanisms responsible for the LSPR-enhanced biocatalysis, we investigated whether the light affects the product release or the chemical hydrolysis step during the reaction in presence of the AuNSt. Data obtained from the biocatalysis kinetic recorded in PBS buffer (Figure 2B), viscous conditions (Figure 2C), and solvent isotope effect in D₂O (Figure 2D) revealed the NIR laser favored the product release rather than the chemical hydrolysis step. Therefore, we concluded the localized photothermal heating promoted from the LSPR excitation of AuNSt enabled the enhanced CALB biocatalysis as a model system, which can be extended to other combinations of PNPs-enzyme hybrids.

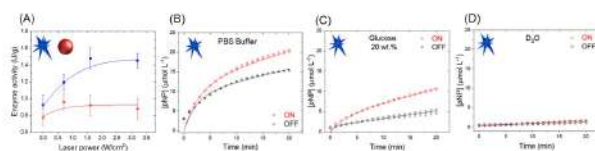


Figure 1. (A) Effect of NIR laser irradiation in the biocatalysis of CALB on the AuNSi (blue data) and AuNSp (red data). (B-D) Monitoring of biocatalysis of CALB on AuNSi under NIR laser irradiation on (3.2 W/cm²) and off in PBS buffer (B), glucose 20 wt% (C), and D₂O (D) media.

Figure abstract annic2021.jpg

From whole blood to isolated extracellular vesicles: SERS for efficient cancer diagnostics

Friday, 26th March - 10:50: Oral Session 1-2 (Room 2) - Abstract ID: 313

Dr. Tatu Rojalin¹, Ms. Hanna Koster¹, Prof. Randy Carney¹

1. University of California, Davis

Recently it has been demonstrated that cancer pathology is dramatically mediated by cellular vesicle transport machinery via a number of key proteins, lipids, small molecules, and non-coding RNAs trafficked in exosomes and related nanoscale extracellular vesicles (EVs). Sensitive and specific detection of the cell-specific biomaterials recruited and packaged in EVs has the potential to revolutionize identification and monitoring of cancer. However, current methods for detecting and analyzing EVs released into circulation cannot readily distinguish tumor-associated from healthy vesicles. Surface-enhanced Raman spectroscopy (SERS) represents a promising tool to address current limitations, but are challenging to implement in minimally-purified whole biofluids, which would be most useful for clinical adoption.

We demonstrate that SERS techniques represent an ideal tool to assess and measure the high heterogeneity of EVs isolated from clinical samples in an inexpensive, rapid, and label-free assay. Compared to whole biofluids, EVs perform notably better for cancer specificity. However, observe a major loss of specificity for ovarian and endometrial cancer following enzymatic cleavage of EVs' extraluminal domain, suggesting its critical significance for diagnostic platforms.

Functionalized drug loaded H-Ferritin nanocages target Cancer Associated Fibroblasts in vitro and in vivo

Friday, 26th March - 11:20: Oral Session 1-2 (Room 2) - Abstract ID: 234

Dr. Leopoldo Sitia¹, Dr. Arianna Bonizzi¹, Dr. Serena Mazzucchelli¹, Dr. Sara Negri², Dr. Cristina Sottani², Dr. Elena Grignani², Dr. Maria Antonietta Rizzuto³, Prof. Davide Prosperi⁴, Dr. Luca Sorrentino⁵, Dr. Carlo Morasso², Dr. Raffaele Allevi¹, Dr. Marta Sevieri¹, Dr. Filippo Silva¹, Dr. marta truffi², Prof. Fabio Corsi²

1. Dipartimento di Scienze Biomediche e Cliniche "L. Sacco", Università di Milano, **2.** Istituti Clinici Scientifici Maugeri IRCCS, 27100 Pavia, **3.** Department of Biotechnology and Biosciences, University of Milan-Bicocca, 20126 Milan, **4.** University of Milano - Bicocca, **5.** Colorectal Surgery Unit, Fondazione IRCCS Istituto Nazionale dei Tumori di Milano, 20133 Milan

Cancer-associated fibroblasts (CAFs) are considered promising therapeutic targets as they promote cancer progression, metastasis formation, and induce drug resistance. Engineered nanoparticles has shown a great potential as targeted delivery agents of cytotoxics with high specificity for CAFs (Truffi et al. 2019). Here, we loaded navitoclax into H-ferritin nanocages (HFn) with navitoclax (Nav), we functionalized them with fibroblast activation protein (FAP) antibody fragments and we evaluated their potential use as drug carriers to target and eradicate CAFs in vitro and in vivo (Sitia et al. 2021).

HFn were functionalized with anti-FAP antibody fragments, by a two-step reaction using NHS-PEG-Mal as a heterobifunctional linker. Navitoclax (Nav) was loaded by exploiting the metal ions affinity method, using Cu(II) as a complexing agent, as already described by our group (Bonizzi et al. 2019). Drug loading and HFn functionalization were evaluated by UPLC-MS/MS, SDS-PAGE, Raman Spectroscopy, Transmission Electron Microscopy and Dynamic Light Scattering. Binding, uptake and cytotoxicity were evaluated on FAP⁺ (CAFs and myofibroblasts (HMF)) and FAP⁻ (4T1 and MDA-MB-231) tumor cell lines by cytofluorimetry, UPLC-MS/MS, MTS and by studying Nav mechanisms of action (PARP cleavage and BAX activation). Finally, biodistribution and CAF targeting were studied by in vivo and ex vivo imaging, and by immunofluorescence confocal microscopy.

First, we optimized functionalization by comparing two different NHS-PEG-Mal molecules (5 and 10 kDa MW) finding that the 10 kDa induced the highest preferential binding with FAP⁺ cells as compared with FAP⁻ cancer cells. Then, we loaded HFn-FAP with Nav, a very promising experimental pro-apoptotic drug, characterized by a strong hydrophobicity and systemic toxicity (thrombocytopenia), that limit its clinical development. We proved that the cytotoxicity of the drug was significantly higher in CAFs after its loading into functionalized HFn (HNav-FAP) as compared to non-functionalized HNav and that the mechanisms of action of the drug were maintained after encapsulation. Moreover, this was correlated with a higher intracellular Nav uptake only in FAP⁺ cells, confirming the efficacy of our functionalization strategy. Finally, we studied HFn-FAP biodistribution in a mouse model of triple negative breast cancer and we found that the functionalized nanocages are able to accumulate in the tumor and target CAFs after intravenous administration.

Our results prove that HNav-FAP promote selective drug delivery into CAFs. If confirmed by further efficacy studies, this could open the way to the development of innovative anticancer therapeutic strategies, that combine well-established chemotherapeutic regimens with innovative approaches that target tumor microenvironment.

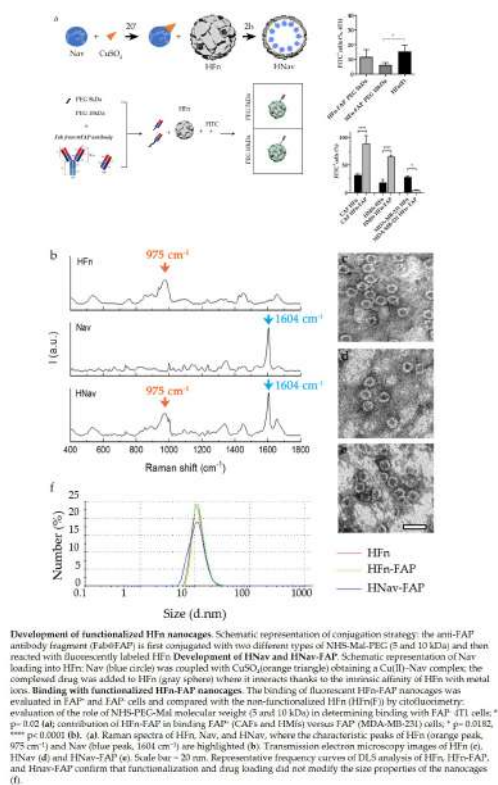


Figure 1.jpg

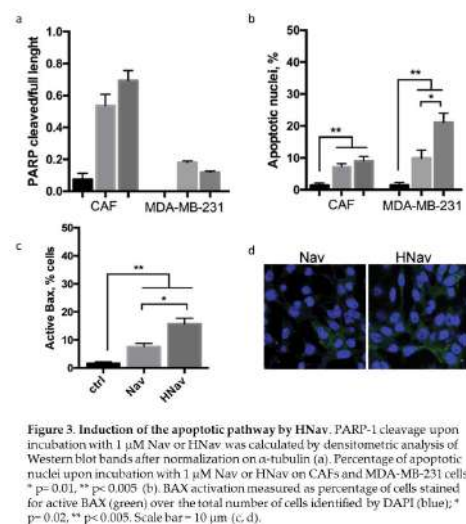


Figure 3.jpg

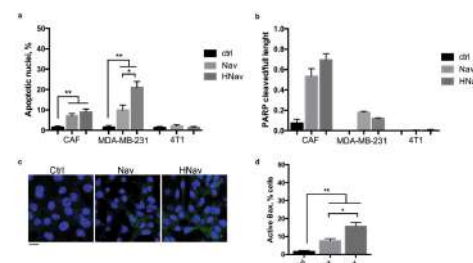


Figure 2.jpg

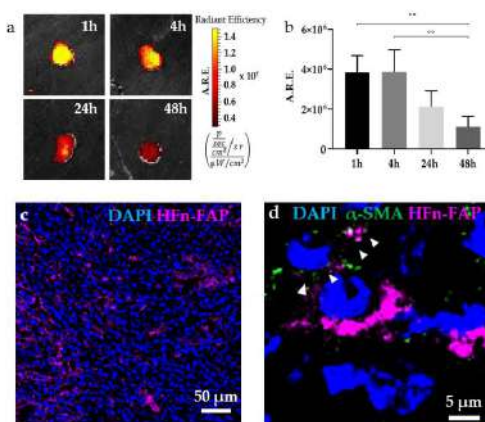


Figure 4.jpg

Dissecting how cells internalize and process nano-sized drug carriers for nanomedicine applications

Friday, 26th March - 11:35: Oral Session 1-2 (Room 2) - Abstract ID: 283

Ms. Anna Salvati¹

1. University of Groningen

Introduction

Nano-sized materials are used in nanomedicine to deliver drugs more efficiently to their site of action. In order to improve their efficacy and fully exploit nanomedicine potential, a better understanding of how cells internalize and process nano-sized materials is required.

Methods

To this aim, we have combined the use of transport inhibitors and RNA interference with proteomic-based methods to identify the cell surface receptor interacting with nano-sized materials and characterize the subsequent mechanisms of uptake by cells.^{1,2} Additional efforts have been focused on developing *in vitro* endothelial cell barriers more closely resembling the barriers nanomedicines encounter *in vivo*.³ Uptake and distribution of nanoparticles have also been studied in precision cut tissue slices from the major organs in which nanoparticles distribute, such as the liver, lungs and kidneys, as an advanced *ex vivo* 3D model.⁴

Results

Our results show that the same cells process nanoparticles in different ways when they are developed into an endothelial cell barrier rather than at different degrees of cell density, as commonly applied for *in vitro* studies.³ Furthermore we show that nanoparticles are internalized *ex vivo* in liver tissue slices, and more specifically, higher uptake is observed in the Kupffer cells, the liver macrophages.⁴ Importantly, the corona molecules adsorbing on the nanoparticle surface once applied in serum or plasma can interact with specific cell receptors and in this way affect the mechanism by which cells internalize the nano-sized drug carrier.⁵ Based on these findings, we used liposomes of different composition to modulate the corona forming in serum and identify proteins associated with higher or lower uptake by cells.⁶

Discussion

These results show that advanced models for *in vitro* testing are required to better resemble the *in vivo* environment and cell barriers that nanomedicines encounter. Additionally, the biological fluid in which nano-sized drug carriers are applied strongly affect the interactions of nanocarriers with cells. Thus, nanocarriers design can be tuned in order to modulate the corona forming in serum and in this way affect cell receptor interactions and nanocarrier uptake efficiency, which both affect nanomedicine targeting and efficacy.

References

¹Montizaan et al, Nanomedicine NBM, 2020, 30, 102300

²Francia et al, Nanomedicine 2019, 14 (12), 1533

³Francia et al, Nanoscale 2018 10 (35), 16645

⁴Bartucci et al, Small, 2020, 1906523

⁵Francia, et al, ACS nano 2019 13 (10), 11107

⁶Yang et al, Acta Biomaterialia, 2020, 106, 314

Hybrid diatomite-based nanocarriers for release and intracellular monitoring of Galunisertib to colorectal cancer cells.

Friday, 26th March - 11:50: Oral Session 1-2 (Room 2) - Abstract ID: 220

Ms. Chiara Tramontano¹, Ms. Giovanna Chianese², Dr. Luca De Stefano², Dr. Anna Chiara De Luca³, Dr. Stefano Managò³, Dr. Enza Lonardo⁴, Dr. Donatella Delle Cave⁴, Dr. Ilaria Rea²

1. University of Naples Federico II, Department of Pharmacy, Via Domenico Montesano 49, 80131, Naples; **Institute of Applied Science and Intelligent System (ISASI), National Research Council of Naples, Via Pietro Castellino 111, 80131, Naples.,** **2.** Institute of Applied Science and Intelligent System (ISASI), National Research Council of Naples, Via Pietro Castellino 111, 80131, Naples., **3.** Institute of Biochemistry and Cell Biology (IBBC) National Research Council, Via Pietro Castellino 111, 80131 Naples, **4.** Institute of Genetics and Biophysics (IGB), National Research Council of Naples, Via Pietro Castellino 111, 80131, Naples

Cancer metastasis is a complex process in which cells break out the primary tumor mass by invading and colonizing new vital organs. When patients are diagnosed with metastatic cancer, such as colorectal cancer (CRC), metastasis has already spread to another part of the body and conventional therapies fail to target cancer cells. In the last years, the oral small-molecule Galunisertib has been approved for the treatment of metastatic CRC thanks to its ability to block the Transforming Growth Factor- β (TGF- β) pathway. However, the systemic administration of Galunisertib can cause severe toxicity and painful undesired effects. In this scenario, the controlled delivery of Galunisertib to CRC through nanoparticle-based approaches can be a valid strategy to increase the drug concentration at the tumor site and reduce toxicity to healthy cells.

It has been shown that -due to the high rate of glycolysis and lack of functional lymphatic drainage systems- cancer cells produce large amounts of lactate causing an acidic extracellular environment. In this study, the different pH-value of malignant and non-malignant cell microenvironment is the key element for the development of hybrid pH-responsive biosilica NPs able to release Galunisertib to the tumor microenvironment. To this aim, we modified the surface of porous biosilica NPs obtained by diatomite (DNPs), a fossil constituted by shells of diatoms made of Food and Drug Administration (FDA)- approved biosilica. Hybrid pH-responsive NPs were fabricated by decorating the surface of DNPs with gold nanoparticles (AuNPs) and loading the small molecule Galunisertib in DNP porous ultrastructure. Finally, the surface of the nanoplatfrom was covered by a thin layer of gelatin that was in situ crosslinked via click chemistry. The loading capacity of the hybrid nanoplatfrom calculated by High-Performance Liquid Chromatography was 2 ± 0.1 %. The presence of AuNPs on the surface of hybrid pH-responsive DNPs enabled to monitor the release profile of Galunisertib in living cells via Surface-Enhanced Raman Scattering (SERS) technique (Fig.1). Hybrid pH-responsive DNPs showed both a pH and time-dependent release profile that was investigated by HPLC and SERS techniques. The tightly folded gelatin matrix blocked the release of Galunisertib from the nanosystem in physiological conditions (7.4), whereas the relaxation of the gelatin chains promoted the drug release in a more acidic environment (5.5). In vitro tests performed on CRC cell line confirmed that the nanoparticle-based therapy of Galunisertib showed a therapeutic effect stronger than conventional administration of the drug.

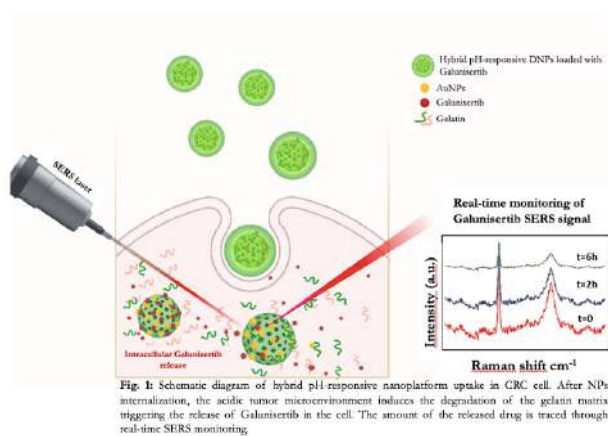


Fig.1.png

Towards low-cost metal-enhanced fluorescence biosensor based on 3D bio-responsive hydrogels

Friday, 26th March - 12:05: Oral Session 1-2 (Room 2) - Abstract ID: 273

Mr. Bruno Miranda¹, Dr. Rosalba Moretta², Dr. Selene De Martino³, Dr. Ilaria Rea², Dr. Principia Dardano¹, Dr. Carlo Forestiere⁴, Dr. Luca De Stefano²

1. 1) Institute of Applied Sciences and Intelligent Systems, National Research Council, Napoli, Italy. 2) Department of Electrical Engineering and Information Technology, University of Naples "Federico II", Italy, 2. 1) Institute of Applied Sciences and Intelligent Systems, National Research Council, Napoli, Italy., 3. 3) Materias s.r.l., via Protopisani 50, Naples, Italy, 4. 2) Department of Electrical Engineering and Information Technology, University of Naples "Federico II", Italy

Localized Surface Plasmon Resonance (LSPR) and Metal-Enhanced Fluorescence (MEF)-based optical biosensors provide unique advantages compared to other sensing technologies to design point-of-care (POC) diagnostic tools. These devices exploit the capability of noble-metal nanoparticles of absorbing light at a well-defined wavelength, which can be combined with excitation/emission spectra of fluorescent dyes to achieve high MEF signals. An optical platform based on spherical gold nanoparticles (AuNPs) embedded in varying molecular weight poly(ethylene glycol) diacrylate (PEGDA) hydrogels is proposed. As a hydrogel, PEGDA represents a biocompatible, flexible, transparent polymeric network to design wearable and 3D MEF biosensors for the multiplexed detection of targets with different molecular weights for the early diagnosis of disease (Figure 1).

Citrate-stabilized AuNPs (~65 nm) were synthesized via seeded-growth method, embedded in PEGDA (700 Da and 10 kDa) pre-polymer solutions, and polymerized by UV light exposure. Citrate-displacement via cysteamine, biotin interaction, and Cy3*-streptavidin conjugation were performed by soaking the PEGDA/AuNPs nanocomposite in the prepared solutions. LSPR signal was monitored via transmission mode customized setup and MEF signal was detected via Fluorescence and Confocal Microscopes.

AuNPs exhibiting a distribution of 65 ± 20 nm were embedded in PEGDA 700 Da and 10 kDa, respectively. The patches were used as volumetric 3D biosensors both in LSPR and MEF sensing modes. PEGDA700/AuNPs nanocomposites exhibit good Sensitivity to refractive index variation (~110 nm/RIU) for LSPR sensing. This nanocomposite was exploited to detect Biotin concentration down to a limit of detection of 25 μ M, a significant value for a small molecule (Figure 2). PEGDA10000/AuNPs, exhibiting a higher swelling capability, was used as a MEF biosensor to detect Biotin-Streptavidin interaction down to 60 nM concentration, as confirmed by the preliminary fluorescence measurements. From the preliminary data reported in Figure 2, it is evident that a lower concentration of Streptavidin can be easily detected, as also confirmed by the specificity test. To demonstrate that the obtained epifluorescence signal was due to a volumetric 3D contribution of streptavidin within the samples, confocal microscopy was performed. The results show a uniform distribution of Streptavidin within the polymeric network, thus improving the surface-to-volume ratio and the sensitivity of the platform. We aim to provide this platform with microelectronics, consisting of miniaturized LED and photodetector to achieve a Point-of-Care testing platform and a wearable sensor for the rapid diagnosis of a disease directly on the patient.

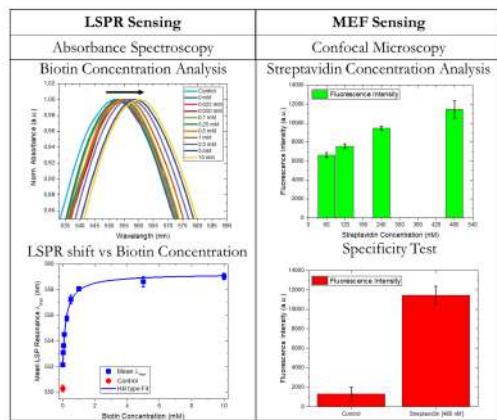


Figure2.png

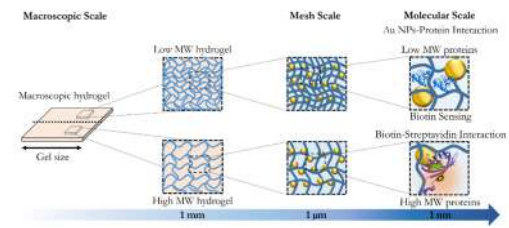


Figure1.png

Inexpensive and Scalable Production of High Performance Thermoelectric Materials through Solution Methods

Friday, 26th March - 10:50: Oral Session 1-3 (Room 3) - Abstract ID: 312

Prof. Maria Ibáñez¹

1. IST Austria

The conversion of thermal energy to electricity and vice versa through solid-state thermoelectric devices is exceptionally appealing for many applications. Not only because thermal waste energy is generated in many of our most common industrial and domestic processes but also because thermoelectric devices can be used for temperature sensing, refrigeration, etc. However, their extended use has been seriously hampered by the relatively high production cost and low efficiency of thermoelectric materials. The problem is that thermoelectric materials require high electrical conductivity (σ), high Seebeck coefficient (S), and low thermal conductivity (κ); three strongly interrelated properties.

After decades of research, promising material candidates that are Earth-abundant and low cost have been identified; among them, SnSe. In fact, since the material was “re-discovered” in 2014, SnSe has become the most studied thermoelectric material due to its extraordinary performance in its single crystal form with up to 2.8 values in the figure of merit ($ZT = \sigma S^2 T \text{ K}^{-1}$). However, the high cost and stagnant production of single crystals and their poor mechanical properties limit the large-scale production of SnSe-based thermoelectric devices. Therefore, a great deal of attention has been placed in replicating the single crystal charge and thermal transport properties in its polycrystalline counterpart to produce cost-effective materials with enhanced mechanical stability. To date, this has been proven difficult due to the easy oxidation of small crystalline domains, the partial loss of anisotropy, and the difficulty to control the doping level finely. Herein, we present a scalable, low-cost, and environmentally friendly methodology to produce SnSe nanocomposites with outstanding performance. In particular, we synthesize SnSe nanoparticles in water and modify their surface before consolidation to finely tune its electronic structure and its charge and phonon scattering properties to achieve figures of merit up to 2.4. These results are of high promise to introduce waste heat recovery through thermoelectric devices into the market.

Variable angle spectroscopic ellipsometry characterization of turbostratic CVD-grown bilayer and trilayer graphene

Friday, 26th March - 11:20: Oral Session 1-3 (Room 3) - Abstract ID: 216

Mrs. Grazia Giuseppina Politano¹, Dr. Carlo Vena¹, Dr. Giovanni Desiderio¹, Prof. Carlo Versace¹

1. Università della Calabria, dipartimento di Fisica

Introduction

We report a Variable Angle Spectroscopic Ellipsometry (VASE) characterization of the surface of CVD-grown bilayer and trilayer graphene produced by multiple transfer on SiO₂/Si and polyethylene terephthalate (PET) substrates. Silicon and PET substrates were chosen for different reasons. Silicon substrate covered by 300 nm of SiO₂ ensures a better graphene visibility, increasing the contrast due to interference enhancement. PET substrate, which is a transparent plastic commonly used for food packaging applications, in combination with graphene, has been studied for the development of next-generation flexible electronics and wearable devices.

Methods

Some commercially available samples of bilayer and trilayer graphene on SiO₂/Si (doped P/Boron) and PET, bought from Graphenea Co., were investigated. Graphene was grown via CVD method. The bilayer and trilayer graphene products consist of CVD layers produced by multiple transfer on SiO₂/Si and PET substrates. The resulting stacking orientation is random.

The optical characterization of the samples was carried out by using VASE. Spectra of the ellipsometric angles ψ and Δ were acquired in the [0.38 -5.2] eV photon energy in the case of bilayer and trilayer graphene on SiO₂/Si and in the range between [4-5.2] eV in the case of graphene samples on PET substrates.

Results and discussion

The behavior of the dispersion laws of bilayer and trilayer graphene on SiO₂/Si is described by two Lorentz oscillators and a pole. The oscillator energy at 4.4 eV in bilayer graphene is assigned to the peak due to a van Hove singularity in the density of states of graphene. This peak is red-shifted from 4.6 eV in monolayer graphene to 4.4 eV in bilayer graphene, even in non-AB stacked graphene, in accordance with previous reports. The absorption peak at 3 eV in bilayer and trilayer graphene on SiO₂/Si, which is not reported in other SE research works, may also be explained considering e-h interaction effects.

The behavior of the dispersion laws of monolayer, bilayer and trilayer graphene samples on PET is described by two Lorentz oscillators. The oscillators at 4.6 eV can be assigned to the peak due to the van Hove singularity in the density of states of graphene. Interestingly, it is not observed the red-shift of this peak, which was instead observed on bilayer graphene on SiO₂/Si.

[1] G.G. Politano, C. Vena, G. Desiderio, C. Versace, Variable angle spectroscopic ellipsometry characterization of turbostratic CVD-grown bilayer and trilayer graphene, *Opt. Mater. (Amst.)* 107 (2020) 110165. <http://www.sciencedirect.com/science/article/pii/S0925346720305085>.

Perspectives for Human Angiotensin I-Converting Enzyme registration by the Surface Enhanced Raman Spectroscopy

Friday, 26th March - 11:35: Oral Session 1-3 (Room 3) - Abstract ID: 195

***Dr. Irina Boginskaya*¹, *Dr. Olga Kost*², *Mrs. Natalia Nechaeva*³, *Dr. Victoria Tikhomirova*², *Dr. Olga Kryukova*², *Dr. Naida Bulaeva*⁴, *Dr. Elena Golukhova*⁴, *Dr. Ilya Ryzhikov*¹, *Dr. Ilya Kurochkin*³, *Mr. Konstantin Afanasev*¹, *Dr. Valery Evdokimov*⁵**

1. Institute for Theoretical and Applied Electromagnetics RAS, 125412, Moscow, Russia, 2. Faculty of Chemistry, M. V. Lomonosov Moscow State University, 119234, Moscow, Russia, 3. Emanuel Institute of Biochemical Physics RAS, 119334, Moscow, Russia, 4. Bakoulev Center for Cardiovascular Surgery, 119049, Moscow, Russia, 5. Prokhorov General Physics Institute of the Russian Academy of Sciences, 119991, Moscow, Russia

Angiotensin I-converting enzyme (ACE) is a glycoprotein, consisting of two homologous domains within a single polypeptide chain. The exact 3D-structure of the two-domain ACE is still unknown. ACE produced in different cells is differently glycosylated which may alter some enzyme characteristics. ACE concentration in the blood is an important parameter of clinical observation, its increase or decrease may accompany various pathologies. Of special interest, however, could be the possibility to distinguish ACE in the blood coming from different organs in certain diseases, even in small amounts. Application of surface-enhanced Raman spectroscopy (SERS) provides the qualitative and quantitative analysis of many compounds, including proteins. This is why we tried to provide a method for defining very small amounts of ACE by its SERS spectra. For this purpose, we used special nanostructured matrices based on thin silver films obtained by electron beam evaporation in a vacuum. For the first time, stable SERS spectra of native and thermo-denatured ACE from seminal fluid were obtained and their complete interpretation was carried out. The measurements were carried out at excitation laser wavelength 785 nm, accumulation time of one spectrum 60 sec, and laser power 64 mW. The reproducibility of the spectra was checked by assessing the value of the root-mean-square deviation over the entire spectrum. Putative ACE degradation during long-term measurements of SERS spectra on the matrices was prevented due to a certain ratio of the root-mean-square roughness of the silver film and its thickness. Based on SERS spectra of native ACE, we characterized the region on the ACE molecule in contact with the silver matrix and demonstrated the model of the two-domain ACE. It appears the C-domain is located in such a way that its long axis is parallel to the silver matrix and the N-domain is almost perpendicular to the long axis of the C-domain. It was found that ACE denaturation led to a significant increase of SERS spectra intensity and to bands shifting. Deglycosylation of denatured ACE resulted in SERS spectra change. The results demonstrate the opportunity to define ACE SERS spectra of native and denatured enzyme forms, as well as deglycosylated ACE, which could form the base for the detection of tissue-specific ACE. Thus, we took a step towards the development of an interdisciplinary direction using SERS on functional nanoplasmonic materials for accurate detection of the enzyme for the purpose of further medical diagnostic methods.

Excitable cells activity detection through graphite-patterned diamond biosensors

Friday, 26th March - 11:50: Oral Session 1-3 (Room 3) - Abstract ID: 263

***Ms. Veronica Varzi*¹, *Mr. Pietro Aprà*¹, *Mrs. Giulia Tomagra*¹, *Prof. Andrea Marcantoni*¹, *Prof. Alberto Pasquarelli*², *Prof. Paolo Olivero*¹, *Prof. Valentina Carabelli*¹, *Dr. Federico Piccolo*¹**

1. UNIVERSITY OF TORINO, 2. University of Ulm

To better understand neuronal signalling behind brain activity, a proper detection of both electrical and chemical signals is essential. Indeed, action potentials (APs) generation and synaptic quantal release of neurotransmitters play a fundamental role in the cellular mechanisms underlying brain functions, being at the basis of information transmission and signal communication in neuronal microcircuits.

In the present work, we present the employment of diamond-based micro-patterned graphitic biosensors to extracellularly record the activity of excitable cells, to resolve APs waveforms and neurotransmitter release [1-2]. The multi-electrode-array sensors were fabricated using a three-dimensional patterning process by means of MeV He ion-beam-based lithography on an artificial-type-IIa single-crystal monocrystalline diamond sample (4.5×4.5×0.5 mm³), thus creating 16 independent graphitic electrodes embedded in its matrix. Being electrically conductive, the micro-channels of the sensors were used to investigate the *in-vitro* neuron activity both in terms of electrical signals generation (APs firing) and neurotransmitter secretion (quantal exocytic events).

The diamond biocompatibility allowed neuronal cells to be plated directly over the diamond device. Potentiometric measurements of APs generation were recorded from cultured hippocampal neurons, while quantal secretory events were amperometrically recorded from plated mouse dopaminergic neurons [3]. The electrical activity of an intact mouse sinoatrial node directly placed on the sensor was also recorded.

These results demonstrated the usability of diamond-based biosensors as promising devices for the simultaneous multi-parametric *in-vitro* detection of both electrical and chemical signals, representing in perspective a further step for a better understanding of brain functioning.

[1] Piccolo, F. et al. Anal. Chem. 88, 7493–7499 (2016).

[2] Tomagra, G. et al. Front. Neurosci. 13, 288 (2019).

[3] Tomagra, G. et al. Carbon 152, 424-433 (2019).

Nanomaterial-based Dual Luminescence Aptasensor for Pathogen Detection

Friday, 26th March - 12:05: Oral Session 1-3 (Room 3) - Abstract ID: 113

***Dr. Milad Torabfam*¹, *Dr. Hasan Kurt*², *Dr. Mustafa Kemal Bayazit*³, *Prof. Meral Yüce*³**

1. Sabanci University, Faculty of Engineering and Natural Sciences, 2. Department of Biomedical Engineering, School of Engineering and Natural Sciences, Istanbul MedipolUniversity, 34810, Istanbul, Turkey, 3. Sabanci University Nanotechnology Research and Application Centre

A highly specific dual-excitation luminescence biosensor for simultaneous screening of bacterial pathogens, namely *Escherichia coli* and *Salmonella typhimurium* was assembled in this report Stokes emission profile of quantum dots (QDs) and Anti-Stokes emission profile of upconversion nanoparticles (UCNPs). The developed sensor principle is based on the luminescence resonance energy transfer (LRET) between aptamer-coupled gold nanostructures as capture probes and complementary single-stranded DNA-coupled luminescent nanoparticles as the signal probes. For the characterization of the provided sensing probes, UV-Visible Spectroscopy, Dynamic Light Scattering, and Circular Dichroism spectroscopy were utilized. The CdSe/ZnS core/shell QDs were excited with UV radiation at 350 nm, and the excitation of NaYF₄:Yb, Er upconverting nanoparticles was achieved at the near-infrared region of 980 nm. Thus, the possible signal cross-talk between QDs and UCNPs was minimized. The dual system's detection limit was calculated as 8 and 10 CFU mL⁻¹ for *E. coli* and *S. typhimurium*, respectively. The biosensor was also evaluated for simultaneous detection of the spiked bacteria in local lake samples. By using numerous UCNPs and QDs with distinct luminescence emission profiles, the suggested LRET-based biosensor may be utilized to detect a wide range of analytes at the same time, posing good application prospects in various fields ranging from food safety analysis to environmental applications.

Variable Angle Spectroscopic Ellipsometry Characterization of Reduced Graphene Oxide Stabilized with Poly(Sodium 4-Styrenesulfonate)

Friday, 26th March - 13:30: Flash Session 1 (Room 1) - Abstract ID: 207

Mrs. Grazia Giuseppina Politano¹, Dr. Carlo Vena¹, Dr. Giovanni Desiderio¹, Prof. Carlo Versace¹

1. Università della Calabria, dipartimento di Fisica

Introduction

In this work, we report a Variable Angle Spectroscopic Ellipsometry (VASE) characterization of GO thin films dip-coated on SiO₂/Si substrates and thermally reduced GO films in the [0.38-4.1] eV photon energy range. Moreover, the optical properties of RGO stabilized with poly(sodium 4-styrenesulfonate) (PSS) films dip-coated on SiO₂/Si substrates are studied in the same range for the first time. The Lorentz optical models fit well the experimental data. In addition, the morphological properties of the samples were investigated by Scanning Electron Microscopy (SEM) analysis.

Methods

The dip-coating process was employed to deposit GO and PSS-functionalized RGO on SiO₂/Si (SiO₂ ≈ 2 nm) substrates with a homemade apparatus at a speed of 0.33 mm/s. The samples were prepared using commercial dispersions in H₂O of GO (4 mg/mL) and PSS-functionalized RGO (10 mg/mL) that were bought from Sigma-Aldrich. The solutions were sonicated for 30 min using an ultrasonic bath. GO films on SiO₂/Si were eventually heated at 400 °C for 20 min in an Ar atmosphere furnace. SEM analysis was accomplished with a FEI Quanta FEG 400 F eSEM microscope. The optical characterization of the samples was carried out by using VASE. Spectra of the ellipsometric angles ψ and Δ were acquired using a V-Vase (J.A. Woollam) ellipsometer in the 0.38–4.1 eV photon energy range at 65°, 70°, and 75° incident angles at room temperature.

Results and discussion

The behavior of the dispersion laws of GO films is described using three Lorentz oscillators at around 2.8 eV, 3.2 eV and 3.9 eV, while the dispersion laws of thermally reduced GO films were modeled using three Lorentz oscillators at around 2.1 eV, 3.17 eV and 4 eV.

In addition, we report for the first time the optical properties of PSS-functionalized RGO films dip-coated on SiO₂/Si in the same range.

The dispersion laws of PSS-functionalized RGO films on SiO₂/Si substrates is described by a Lorentz oscillator and a pole.

Our GO, RGO, and PSS-RGO models provide accurate complex refractive index values that are useful especially in the extended near-infrared and mid-infrared spectral range, where they had not been reported before.

[1] G. Politano, C. Vena, G. Desiderio, C. Versace, Variable Angle Spectroscopic Ellipsometry Characterization of Reduced Graphene Oxide Stabilized with Poly(Sodium 4-Styrenesulfonate), *Coatings*. (2020) 743. <https://doi.org/https://doi.org/10.3390/coatings10080743>.

Synthesis of 2D nanomaterials (h-BN, Bi₂Te₃, MoS₂) by top-down techniques

Friday, 26th March - 13:33: Flash Session 1 (Room 1) - Abstract ID: 252

Mr. Jesús Javier Castellanos González¹, Dr. Antonio Esau Del Río Castillo², Dr. Ana Laura Martínez Hernández¹, Dr. Carlos Velasco Santos¹

1. Tecnológico Nacional de México campus Querétaro, 2. IIT- Istituto Italiano di Tecnologia

The 2D materials are stacked on layers attracted each other by Van der Waals forces, there are a large range of materials in this category with properties and possible applications which haven't been researched deeper yet. An example of these materials are: Boron nitride (BN) with a graphene alike hexagonal configuration, Bismuth telluride (Bi₂Te₃), whose single layer composition is a five layer stack of alternating Bismuth and Tellurium, Molybdenum disulfide (MoS₂), whose monolayer is a sandwich-type arrangement with a thickness of 3 atoms. BN and Bi₂Te₃ possess a high heat conductivity, but different electric properties, BN is an insulator (Bhimanapati, Glavin, & Robinson, 2016), Bi₂Te₃ has a low voltage activation semi-conductor properties (Li, Ren, & Luo, 2011), while MoS₂ has interesting electronic applications as a semi-conductor (Xiao Li & Zhu, 2015). In this work are analyzed two Top-Down obtention methods for 2D materials. The 2D material synthesis is developed by a liquid phase exfoliation and Wet-Jet Milling processes, (Del Río et al; 2018). Morphology is compared of the resulting materials by Transmission Electron Microscopy. The bandgap of the materials of each method was obtained of the UV-Vis spectroscopy results applying Tauc plot approaches. The obtained 2D materials can be objects of other studies with a view to different possible applications.

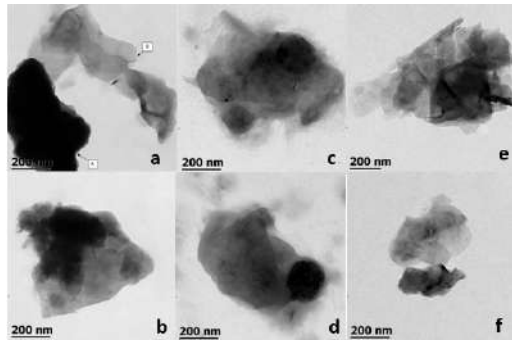
Bhimanapati, G. R., Glavin, N. R., & Robinson, J. A. (2016). 2D Boron Nitride: Synthesis and Applications. Semi-conductors and Semimetals, 95(1). 101–147 (ed. Francesca Iacopi, John J. Boeckland Chennupati Jagadish) in 2D materials semiconductors and semimetals, Elsevier Science, <https://doi.org/10.1016/bs.semsem.2016.04.004>

Del Río Castillo, A., et al; 2018. High-yield production of 2D crystals by wet-jet milling. Materials Horizons, 5(5), 890–904. <https://doi.org/10.1039/c8mh00487k>

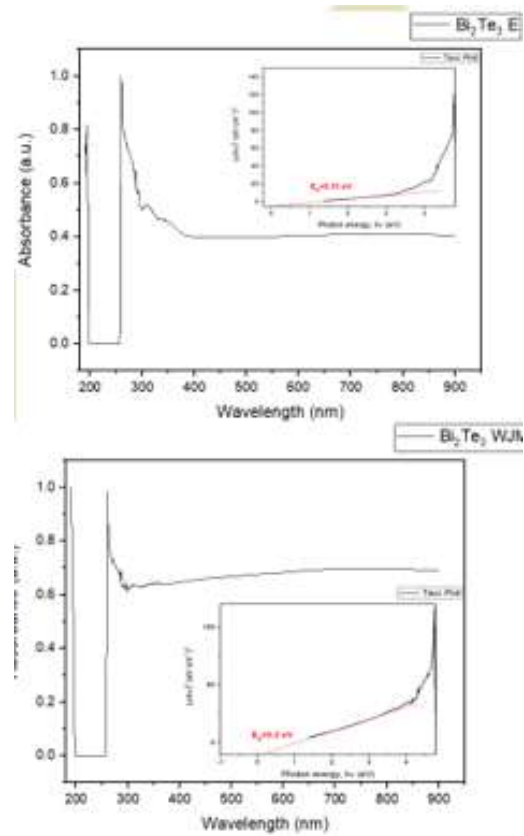
Li, Xiao, & Zhu, H. (2015). Two-dimensional MoS₂: Properties, preparation, and applications. Journal of Materials, 1(1), 33–44.

<https://doi.org/10.1016/j.jmat.2015.03.003>

Li, X., Ren, H., & Luo, Y. (2011). Electronic structure of bismuth telluride quasi-two-dimensional crystal: A first principles study. Applied Physics Letters, 98(8), 2011–2014. <https://doi.org/10.1063/1.3556654>



Tem images of different boron nitride processes -
bulk exfoliated wet yet milling.png



Uv-vis and tauc plot of bismuth telluride
exfoliated and wet yet milling .png

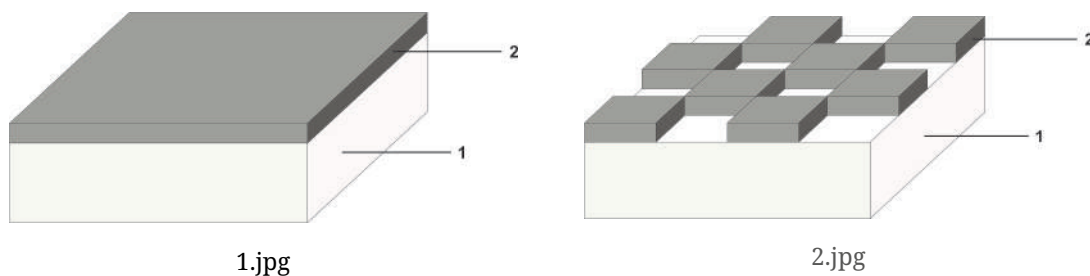
Surface layer thickness determination in case of “island” structure by X-ray Photoelectron Spectroscopy

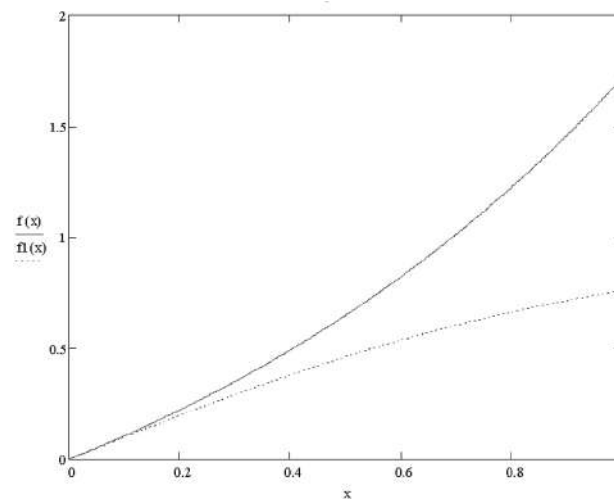
Friday, 26th March - 13:36: Flash Session 1 (Room 1) - Abstract ID: 96

Dr. Viktor Afanas'ev¹, Mr. Daniil Selyakov¹

1. National Research University «Moscow Power Engineering Institute», 111250, Moscow, Russia

Surface layer (film) thickness determination is an important application of X-ray Photoelectron Spectroscopy (XPS). The method is based on measurement of substrate and film peak intensities and assumes the presence of a plane-parallel film (Fig. 1, 1 is a silicon substrate, 2 is a gold film) on a semi-infinite flat substrate. We will consider how the XPS signal changes if the film is not a flat homogeneous layer but constitute an island (cluster) structure, which may be energetically favorable for the atoms of the film. Such structures are typical of gold in submonolayer configurations. XPS spectra were measured for three samples (gold films of different thicknesses located on top of silicon substrates) at five different angles and have been interpreted by the straight line approximation model. The effect of a decrease in the value of the effective average coating thickness (d) with a detecting angle increase was observed, when signal is interpreted within flat homogeneous layer coating model. Considering the configuration of an island (cluster) surface coverage (the simplest model when the half of the silicon surface is covered with plane-parallel islands with a thickness of $2d$ (Fig. 2)) we can compare the behavior of the theoretical curves showing the dependence of the signal intensity ratio for island and uniform coverage and see that if the flux of photoelectrons is detected at grazing angles, the curves will coincide (Fig. 3, $f(x)$ is the ratio of intensities assuming the model of plane surface, $f_1(x)$ – of an island structure, x is inversely proportional to the cosine for a detecting angle measured from the normal). The value of the critical angle at which curves coincidence will be determined by the shape of the islands. The presence of an island surface coating can be confirmed by XPS measurements with an angular resolution and will be accompanied by a decrease in the layer thickness values determined by traditional XPS methodology as the detecting angles approach the grazing angle. The average value of the film thickness (the thickness of an equivalent homogeneous layer) is determined by detecting the XPS signal at angles exceeding the critical angle determined by the island morphology. The simplest model of an island coating makes it possible to qualitatively interpret the effect of a decrease of the effective average coating thickness observed in XPS experiments with an angular resolution.





3.png

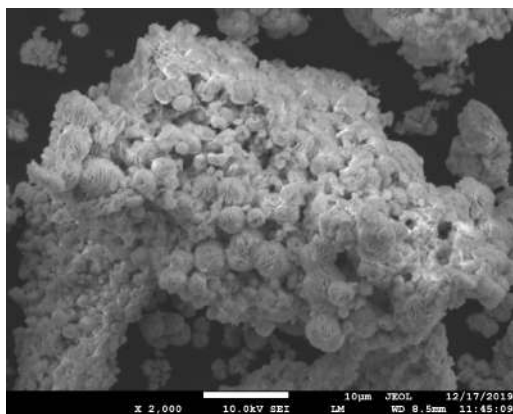
Nanocomposites of PMMA and rose-like BiOCl nanostructure: Synthesis and characterization

Friday, 26th March - 13:39: Flash Session 1 (Room 1) - Abstract ID: 28

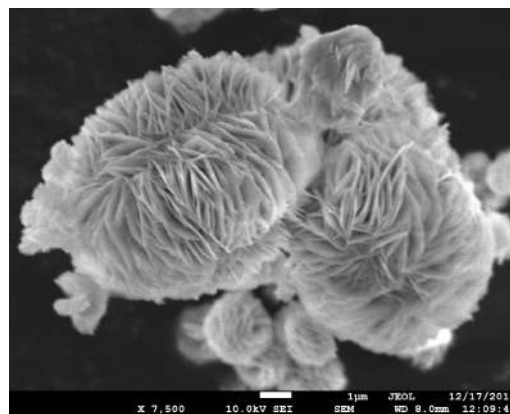
Ms. Sakshi Sharma¹, Dr. Aman Deep Acharya¹

1. Department of Physics, Lovely Professional University, Phagwara, Punjab, India-144411

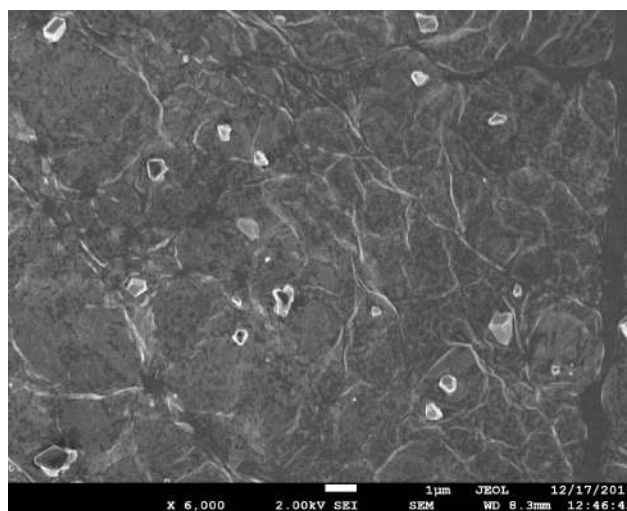
Nanocomposites of PMMA: BiOCl with different concentrations of BiOCl (5, 10, 15 wt%) were prepared by using simple solution cast technique. Prepared nanocomposites as well as BiOCl nanostructure characteristics were examined by using XRD, FESEM and EDAX. Morphology reveals that the developed nanostructure of the filler (BiOCl) is of rose like geometry, which composed of dozens rapidly grown nanosheets of thickness 53nm. Uniform distribution and tight adherence of nanoparticles with PMMA matrix has also been confirmed through FESEM images. It is witnessed that the surface morphology changes from smooth to rough with increase in weight ratio of filler might be due to particle-particle interaction dominance over matrix-particle interactions. Further the newly emerged sharp peaks in the XRD pattern confirm the presence of nano-BiOCl crystallites within the polymeric matrix. The obtained results reflect that the properties of polymer nanocomposites depend upon the type of nanomaterial such as shape, concentration, size, and interaction with polymer matrix, which find its application in optical devices, fuel cells, and chemical sensors.



Sem image 1 of rose like biocl morphology.jpg



Sem image 2 of rose like biocl morphology.jpg



Pmma-biocl nanocomposite.jpg

Wearable Graphene-Kapton Sensor for Blood Toxicity Monitoring

Friday, 26th March - 13:42: Flash Session 1 (Room 1) - Abstract ID: 260

Mr. Mohamed Bouherour¹, Dr. Nabila Aouabdia¹, Prof. Azzedine Bellet¹

1. Laboratoire des Etudes de Matériaux d'Electronique pour Applications Médicales (LEMEAMED), Faculté des Sciences de la Technologie, Université Frères MENTOURI Constantine

Wearable biosensors draw in huge interest for their abilities in real-time monitoring of patient wellbeing status. Expanded researches are oriented towards fast monitoring of human health, a wide scope of wearable sensors are being created for real-time monitoring.

Figure 01 presents the miniaturized Graphene_kapton sensor which is designed and intended for blood lead contamination detection applications, the proposed sensor uses appropriate dimensions presented in table 01 of a rectangular patch to get the most optimal results, the design is basic, minimized, and simple to manufacture. The simulation results from the software (HFSS 13.0) which is based on the finite element methods are highly suitable. The proposed sensor shows the ability to clearly detect even the smallest traces of lead in blood and demonstrates a better response of parameter S11 compared to all that was proposed in the previous works and high efficiency due to the extraordinary properties of the materials that have been chosen for its construction. To support what we say we present figure 02 where are presented the reflection coefficients S11 of the sensor without superstrate, with a drop of blood, and with the same drop of blood infected with two lead particles of different sizes from 79000 nm and we decreased up to 690 nm what gives us a different response for each size, the sensor clearly detects the two nanoparticles by showing a relative error of frequency between pure blood and infected blood of 0.79%, showing that the proposed sensor is a promising candidate for incorporation into wearable systems.

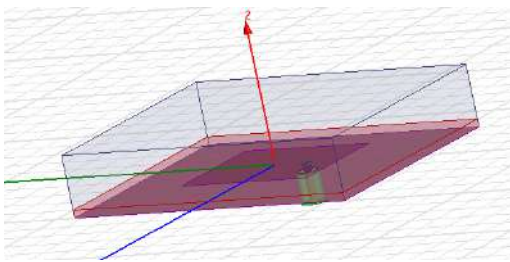


Figure 01 grephene-kapton sensor structure.png

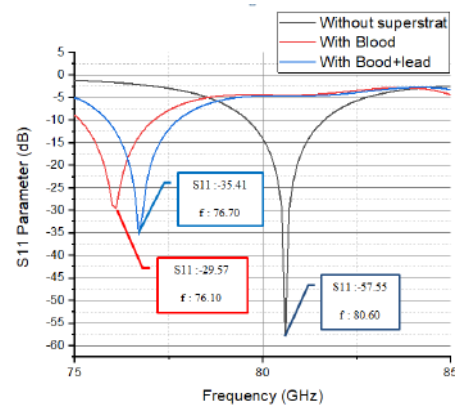


Figure 02 biosensor graphene-kapton response parameter s11without superstrat with blood and with blood lead.png

Parameters	Value
substrate length	5 mm
substrate width	4 mm
substrate height	0.125 mm
patch length	2.29 mm
patch width	1.9 mm
Frequency solution	125 GHz
Graphene conductivity	650737705 S/m

Table 01 sensor s important parameters.png

Electrical Properties of Epoxy Composites Containing Carbon Black and Carbon Nanotube

Friday, 26th March - 13:45: Flash Session 1 (Room 1) - Abstract ID: 123

Dr. Raja Nor Raja Othman¹, Mr. Afham Zaim¹

1. Universiti Pertahanan Nasional Malaysia

Epoxy have been usually used in construction, machinery, aerospace and other related fields due to their low cost, excellent bonding performance, outstanding mechanical properties, easy processability, superior thermal and chemical resistance. The disadvantages of epoxy is the high density, large internal stress, brittle, low dielectric constant and poor impact resistance¹ of the epoxy resins after curing that prevent the other good properties of epoxy to be limited. This is the reason why the epoxy needs to improve its dielectric constant by combining with conductive fillers such as Carbon Black (CB) and Carbon Nanotubes (CNT). In this work CB and CNT are added into epoxy composites are prepared in this work to improve the dielectric and electrical properties of the. Different loadings of conductive carbon fillers have been applied to the epoxy to improve the dielectric constant of epoxy composites. First, CB was dispersed within the epoxy matrix at various loading. It can be observed that there was an increase in the dielectric constant, k , between 3 wt.% (27.17) and 4 wt. % CB loading, at $f = 100$ Hz. It was observed that k increases, from $k = 27.17$ to $k = 134.57$. This indicate that the conducting network that was formed within the particles in the composite also increased as the carbon black filler added to epoxy resin. When the carbon black is well dispersed, the large surface area of tiny carbon black aggregates serve as the electrode surfaces of numerous small capacitors. The capacitor network within the composite can thus give a large capacitance and dielectric constant. CNT was also added to the CB at a weight ratio of 1:1 wt.%, as a way to assess the effects of employing high aspect ratio conductive filler, such as CNT in influencing the formation of dielectric network. It can be observed that there was an increase in the value of k for 6 wt.% hybrid loading (3 wt. % CB + 3 wt.% CNT), compared to 6 wt. % CB loading. At 15 kHz of frequency, the value of k for 3 wt. % CB + 3 wt.% CNT epoxy composite was recorded to be 303.12, which was higher than that containing 6 wt. % CB alone, which was 171.74. The effects of employing dual fillers was demonstrated in this work, where the values of k increases tremendously by incorporating CNT together with CB, at the same weight loading.

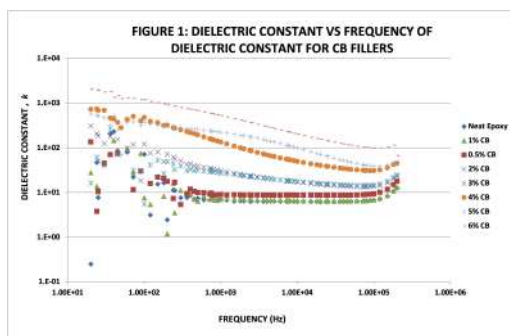


Figure 1.jpg

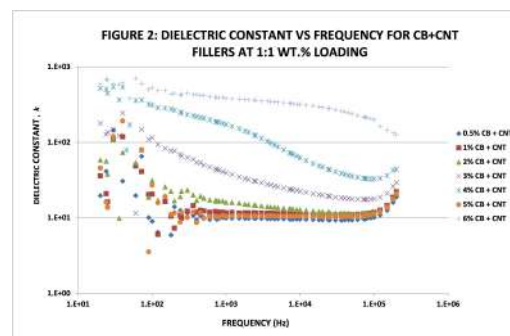


Figure 2.jpg

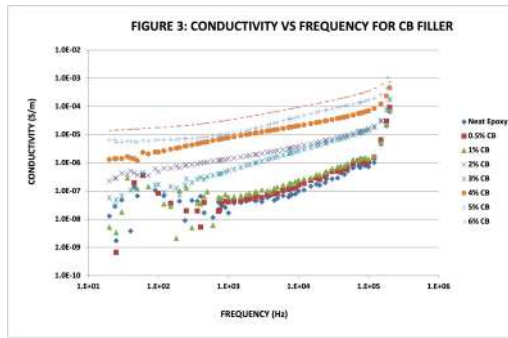


Figure 3.jpg

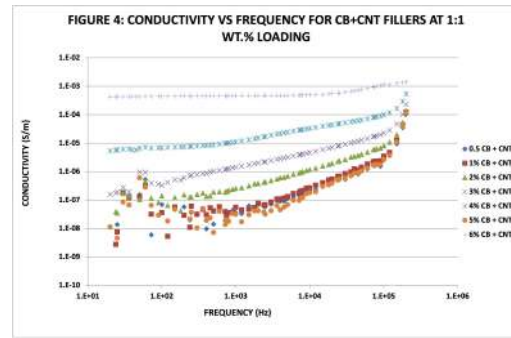


Figure 4.jpg

A comparison Study in Synthesis of Aluminum and Copper Nanoparticles using Pulsed Laser Ablation in Liquid

Friday, 26th March - 13:48: Flash Session 1 (Room 1) - Abstract ID: 54

***Dr. Ridha Hamdi*¹, *Dr. Tahani Felemban*², *Mr. Hassan Al-khabbaz*¹, *Dr. Alheshibri Alheshibri*², *Dr. SULTAN AKHTAR*², *Prof. Khaled A Elsayed*²**

1. Imam Abdulrahman Bin Faisal University, 2. Imam Abdulrahman Bin Faisal University

Nanoparticles (NPs) provide a higher surface to volume ratio and zero-dimensional confinement compared to other nanostructures, due to them being able to perform a profusion of applications such as detectors, catalysis, optoelectronic technologies, and medical devices. Various methods have been developed to synthesize NPs; however, the environmental concern becomes crucial into account during the designing of novel materials. Pulsed Laser Ablation in Liquid (PLAL) is the most common, simple, and efficient technique to synthesize NPs. In this work, pure Aluminum (Al) and Copper (Cu) targets are located inside a liquid ambient. A Nd:YAG Laser of 1064 nm wavelength and 10 Hz pulse repetition is used at different pulse energies of 30, 50, 70, and 90 mJ. We approach a comparative and superlative study of the formation of Al-NP and Cu -NP using the techniques of the zeta potential, UV-Vis spectroscopy, Transmission Electron Microscope (TEM), Scanning Electron Microscopy (SEM) with energy-dispersive X-ray spectroscopy (EDX), and spectroscopy Fourier transform infrared (FT-IR). The influence of laser energy on the size of NPs is investigated. The size of NPs increases firstly when the laser power varies from 30mJ to 70mJ irrespective of the metallic target, and then decreases. In addition, the degree of oxidation is high in Al-NP compared to Cu-NP. These results demonstrate that the size of NPs and their degree of oxidation produced by laser ablation in liquid media is mainly governed not only by the laser power but also by the nature of the material.

Cedar essential oil - β -cyclodextrin nanocomplex formation for the effective inhibition of acetylcholinesterase

Friday, 26th March - 13:30: Fash Session 1 (Room 2) - Abstract ID: 137

Ms. Annita Katopodi¹, Ms. Ioanna Pitterou¹, Ms. Georgia Petridou¹, Ms. Rafaella Spanou¹, Dr. Eleni Kavetsou¹, Prof. Anastasia Detsi¹

1. National Technical University of Athens (NTUA)

Introduction

The cedar (*Juniperus phoenicea*) essential oil (CEO) possesses antimicrobial, antioxidant and neuroprotective activities. Acetylcholinesterase (AChE) inhibition is of utmost importance in the pursue of Alzheimer's Disease (AD) treatment, since it increases acetylcholine levels and improves the cognitive function of AD patients. Despite the significant therapeutic profile of CEO, its volatility, hydrophobicity, and light, air or heat sensitivity remain a challenge for its effective use in industrial applications. However, complexation of EOs with cyclodextrins consists a well-known and very promising technique for their protection, aqueous solubility improvement and controlled release.

In this content, we present the formation and characterization of supermolecular complexes of Cedar essential oil derived from a Greek region with β -cyclodextrin, along with their ability to inhibit acetylcholinesterase *in vitro*.

Methods

CEO- β -CD inclusion complexes (ICs) were prepared using the co-precipitation method and were characterized by Dynamic Light Scattering (DLS), NMR and FT-IR spectroscopy and Differential Scanning Calorimetry (DSC) and Thermogravimetric Analysis (TGA) methods. Their acetylcholinesterase inhibition activity was evaluated using Ellman's method and their release profile was studied at 37 °C and pH 7.4.

Results and Discussion

CEO- β -CD inclusion complexes (ICs) presented sizes ranging from 315.9 nm to 769.6 nm, while exhibiting moderate size distribution values from 0.396 to 0.604. ¹H Nuclear Magnetic Resonance (NMR) studies indicated the successful formation of the ICs. The release study revealed a sustained release profile, with an initial burst effect at the first 5 h, while the kinetic modelling studies indicated that the Higuchi equation model best fitted the release data. Finally, the CEO of the current study presented significantly higher AChE inhibitory activity (IC₅₀ 37 μ g/mL) than CEO from different regions that have been reported so far, while a prolonged anti-AChE potency was observed for CEO- β -CD-ICs (IC₅₀ 50 μ g/mL after 24 h).

Acknowledgments

A. K. gratefully acknowledges State Scholarships Foundation (IkY). This research is co-financed by Greece and the European Union (ESF) through the Operational Programme (Human Resources Development, Education and Lifelong Learning) in the context of the project "Strengthening Human Resources Research Potential via Doctorate Research" (MIS-5000432), implemented by the State ScholarshipsFoundation (IkY).

References

- Kotronia, M. et al. (2017). Encapsulation of Oregano (*Origanum onites* L.) essential oil in β -cyclodextrin (β -CD): Synthesis and characterization of the inclusion complexes. *Bioengineering*, 4(3), 74.
- Kavetsou, E. et al. (2019). Encapsulation of *Mentha pulegium* essential oil in yeast cell microcarriers: an approach to environmentally friendly pesticides. *Journal of agricultural and food chemistry*, 67(17), 4746-4753.

Development of solid lipid nanoparticles (SLNs) and nanostructured lipid carriers (NLCs) for the encapsulation and sustained release of the flavonoid naringin

Friday, 26th March - 13:33: Fash Session 1 (Room 2) - Abstract ID: 155

Ms. Ioanna Pitterou¹, Ms. Annita Katopodi¹, Dr. Eleni Kavetsou¹, Prof. Anastasia Detsi¹

1. National Technical University of Athens (NTUA)

Introduction: Naringin is a flavanone 7-O-glycoside and a basic ingredient of citrus fruits, mainly found in grapefruit. Naringin exerts a variety of pharmacological effects such as antioxidant, anti-inflammatory and anticancer activity. However, its health benefits can be limited due to its low water solubility, leading to its low bioavailability. Various nanoparticle systems have been investigated to counter this problem and to enhance its functional properties.

Methods: In this study, naringin was encapsulated in solid lipid nanoparticles (SLNs) and nanostructured lipid carriers (NLCs), which consist the new generation lipid carriers. The SLNs and NLCs were prepared by the emulsification and solvent evaporation technique. The physicochemical characteristics of the nanoparticles were analyzed by DLS, FT-IR and TGA methods. The release rate of naringin from the lipid carriers was determined in pH 7.4 and 5.5 at 37 °C.

Results and Discussion: The developed SLNs and NLCs showed a mean particle size of 128.9 and 118.2 nm, zeta potential values of -20.3 and -40.9 mV and a narrow size distribution with the encapsulation efficiency of SLNs and NLCs being 85 ± 4 and $91 \pm 1\%$, respectively. Naringin was released in a sustained manner from both drug delivery systems, while the kinetics study in different pH demonstrated the Fickian diffusion release mechanism of the flavonoid from the nanocarriers.

References

- Anastasia Detsi, Eleni Kavetsou, Ioanna Kostopoulou, Ioanna Pitterou, Antonella Rozaria, Nefeli Pontillo, Andromachi Tzani, Paris Christodoulou, Aristeia Siliachli and Panagiotis Zoumpoulakis. (2020) Nanosystems for the Encapsulation of Natural Products: The Case of Chitosan Biopolymer as a Matrix; a Review. *Pharmaceutics*, 12(7), 669.
- Kesente, M., Kavetsou, E., Roussaki, M., Blidi, S., Loupassaki, S., Chanioti, S., Siamandoura, P., Stamatogianni, C., Philippou, E., Papaspyrides, C., Vouyiouka, S., & Detsi, A. (2017). Encapsulation of olive leaves extracts in biodegradable PLA nanoparticles for use in cosmetic formulation. *Bioengineering*, 4(3), 75.

Topical Formulation with AS1411-Gold Nanoparticles as Cervical Cancer Drug Delivery System

Friday, 26th March - 13:36: Fash Session 1 (Room 2) - Abstract ID: 157

Ms. Jéssica Nunes¹, Ms. Ana S. Agonia², Mr. Tiago Rosado³, Dr. Eugénia Gallardo¹, Dr. Rita Palmeira-de-Oliveira⁴, Dr. Ana Palmeira-de-Oliveira⁴, Prof. José Martinez-de-Oliveira⁵, Dr. José Fonseca-Moutinho⁴, Dr. Maria Paula Cabral Campello⁶, Dr. António Paulo⁷, Prof. Andrew D. Ellington⁸, Dr. Carla Cruz⁹

1. CICS-UBI Centro de Investigação em Ciências da Saúde, Universidade da Beira Interior, Av. Infante D. Henrique, 6200-506 Covilhã, Portugal, 2. Labfit - HPRD Health Products Research and Development, Lda, Edifício UBIMEDICAL Estrada Municipal 506, 6200-284 Covilhã, Portugal, 3. 1CICS-UBI Centro de Investigação em Ciências da Saúde, Universidade da Beira Interior, Av. Infante D. Henrique, 6200-506 Covilhã, Portugal, 4. CICS-UBI Centro de Investigação em Ciências da Saúde, Universidade da Beira Interior, Av. Infante D. Henrique, 6200-506 Covilhã, Portugal, 5. CICS-UBI Centro de Investigação em Ciências da Saúde, Universidade da Beira Interior, Av. Infante D. Henrique, 6200-506 Covilhã, Portugal; Centro Hospitalar Universitário Cova da Beira, Covilhã, Portugal, 6. 6Centro de Ciências e Tecnologias Nucleares, Instituto Superior Técnico, Universidade de Lisboa, Estrada Nacional 10 (km 139,7), 2695-066 Bobadela LRS, Portugal, 7. 6Centro de Ciências e Tecnologias Nucleares, Instituto Superior Técnico, Universidade de Lisboa, Estrada Nacional 10 (km 139,7), 2695-066 Bobadela LRS, Portugal, 8. Department of Molecular Biosciences, The University of Texas at Austin, Austin, TX 78712, USA., 9. CICS-UBI – Centro de Investigação em Ciências da Saúde, Universidade da Beira Interior, Covilhã

Introduction: Cervical cancer is one of the most common cancers in women and is usually treated with surgery, radio-, and chemotherapy. However, the conventional anticancer therapies present low specificity, causing several side effects. DNA aptamers, able to adopt G-quadruplex structures, are more stable and can improve the selectivity of different anticancer therapeutic strategies. These aptamers bind to specific targets, such as AS1411 that binds to nucleolin, a protein overexpressed in cancer cells, namely in cervical cancer cells. AS1411 was already tested in clinical trials, but due to its low response rates and suboptimal pharmacokinetics, those ended in phase II. This aptamer is able to selectively deliver anticancer drugs, increasing their efficacy and reducing the cytotoxicity in healthy cells. Moreover, the conjugation of AS1411 with gold nanoparticles (AS1411-AuNPs) increases the anticancer effect of the aptamer. The use of AS1411-AuNPs as drug carriers may therefore be a potential approach for the selective delivery of anticancer drugs to cervical cancer cells.

Methods: Citrate gold nanoparticles were functionalized with AS1411 and, then, loaded with potential anti-cancer drugs (C8 e Imiquimod) via supramolecular assembly. The resulting nanoparticles were characterized by dynamic light scattering, transmission electron microscopy and their drug release profile was determined. Afterward, nanoparticles internalization and their effect in cellular viability was evaluated by MTT, flow cytometry and confocal microscopy in cancer (HeLa) and normal (NHDF) cell lines. Finally, the nanoparticles were incorporated in a topical formulation and its permeation in Franz cells studies (in porcine vaginal epithelia) was quantified using a HPLC-FLD method.

Results/ Discussion: The final nanoparticles presented suitable properties for pharmaceutical applications, such as small size (around 15-20 nm), negative charge and favourable drug release properties. The nanoparticles were efficiently internalized mainly by cancer cells. Moreover, they presented higher toxicity in cancer cells. The nanoparticles were incorporated into a gel formulation of polyethylene glycol suitable for topical application in the female genital tract, and Franz cells studies revealed promising tissue retention properties in the porcine vaginal epithelia after HPLC-FLD quantification. These findings suggest that these nanoparticles were able to improve selectivity for cancer cells, increase their cellular uptake, and enhance their toxicity in a cervical cancer cell line, making them promising drug carriers for cervical cancer therapy.

Acknowledgements: Jéssica Lopes-Nunes acknowledges the doctoral fellowship grant from the FCT – Founda-

tion for Science and Technology ref. 2020.05329.BD. This work was supported by UTAustin FCT project DREAM ref. UTAP-EXPL/NTec/0015/2017.

Biodegradable lipid-polymer nanoparticles with predictable in vivo miRNA delivery activity

Friday, 26th March - 13:39: Fash Session 1 (Room 2) - Abstract ID: 159

***Ms. Felicia Roffo*¹, *Prof. Enza Torino*²**

1. Department of Chemical, Materials Engineering & Industrial Production, University of Naples Federico II, Piazzale Tecchio 80, 80125 Naples, ITA, 2. Department of Chemical, Materials Engineering & Industrial Production, University of Naples Federico I. Center for Advanced Biomaterials for Health Care, CABHC, Istituto Italiano di Tecnologia, IIT@CRIB,

A significant effort in the microfluidic research was focused on the understanding of the thermodynamics of liposomes and polymer nanoparticles, separately. Because of the limitations affecting the nanostructures as standalone nanocarriers, a *new generation* of hybrid vehicle, lipid-polymer NPs, has been outlined. However, the conventional batch methods to produce them strongly prevent the achievement of tunable and on-demand properties, which are essential to predict their performance in clinical translation. Since the thermodynamics of hybrid nanoparticle, polymer and liposomes, in a microfluidic production process has not been investigated yet, this latter represents a fundamental aspect to deepen. In this work, innovative usage of the hydrodynamic flow focusing to produce lipid-polymer nanoparticles for multimodal imaging applications is presented. This finding is in agreement with the observations made in the analysis of the hybrid NPs using Transmission Electron Microscopy (TEM) and confocal microscope. We develop a method for the engineering of monodisperse population of NPs, in which Gd-DTPA and ATTO633 compounds are co-encapsulated. The results show stable hybrid nanoparticles that can be used both for MRI and for optical applications. Additionally, preliminary results about the NPs structural integrity and storage stability in different dispersants are reported. The biological efficacies in miRNA delivery and superior biocompatibility of nanoparticles produced by microfluidic device are examined in vitro.

Chitosan covered calcium phosphate particles as a vehicle for ocular drugs

Friday, 26th March - 13:42: Fash Session 1 (Room 2) - Abstract ID: 202

***Mrs. Ekaterina Popova*¹, *Dr. Victoria Tikhomirova*¹, *Mrs. Olga Beznos*², *Mrs. Natalia Chesnokova*²,
*Dr. Olga Kost*¹**

1. Faculty of Chemistry, M. V. Lomonosov Moscow State University, 119234, Moscow, Russia, 2. Helmholtz National Medical Research Center of Eye Diseases

The pathological processes within eye are preferably treated by local drug intake. However, topical application of the drug, although sparing for the patient, is less effective for the treatment of the diseases, which include inner structures of the eye, due to the poor transport (less than 5%) of the drug into the eye due to tear drainage and the cornea barrier. The effectiveness of the drug can be increased by its encapsulation into nano- and micro particles, but for low molecular drugs, it is still a challenging task.

We demonstrate the perspectives of the use of inorganic biocompatible, biodegradable and nontoxic calcium phosphate particles as vehicles for such drugs on example of the inhibitor of angiotensin-converting enzyme, enalaprilat, which is known to lower intraocular pressure (IOP) and improve the hydrodynamics of the eye. Since the mucin layer over the corneal epithelium has a negative charge, we covered the particles with positively charged polysaccharide, chitosan, to increase the affinity of the particles to the eye surface. For this purpose, we used two different chitosans, low molecular (about 5 kDa) chitosan and glycol chitosan (72 kDa). Particles containing enalaprilat and coated with 5 kDa chitosan were characterized by a hydrodynamic diameter 180 nm and ζ potential +7 mV, while particles coated with glycol chitosan were characterized by a hydrodynamic diameter 260 nm and ζ potential +16 mV. Both types of particles exhibited high stability at 4°C and very high capacity in relation to enalaprilat, enalaprilat incorporation into the particles being about 70%. The experiments *in vivo* on rabbits demonstrated that topical enalaprilat incorporated in the calcium phosphate particles coated with two types of chitosan retained on the anterior eye surface twice as long as free enalaprilat and caused a more significant decrease of IOP in normotensive rabbits than aqueous solution of enalaprilat in eyedrops. Moreover, IOP decrease was observed remarkably longer in case of enalaprilat-containing particles. Thus, such formulations could be very effective for the treatment of eye diseases, accompanied by high IOP, including glaucoma.

Double polymer shell liposomes for oral delivery of curcumin

Friday, 26th March - 13:45: Fash Session 1 (Room 2) - Abstract ID: 270

Ms. Anna Maria Maurelli¹, Dr. Vincenzo De Leo¹, Dr. Fulvio Ciriaco¹, Dr. Roberto Comparelli², Prof. Angela Agostiano¹, Prof. Lucia Catucci¹

1. Department of Chemistry, University of Bari Aldo Moro, Via Orabona 4, 70126 Bari, Italy, 2. CNR-Istituto per i Processi chimico Fisici (CNR-IPCF), SS Bari, Via Orabona 4, 70126 Bari, Italy

Introduction

Numerous studies confirmed the beneficial antioxidants, anti-inflammatory, antimicrobial properties of curcumin. However, it has poor bioavailability and biostability^[1].

To prepare a nanostructured drug-delivery system suitable for oral-delivery of curcumin, liposomes with a double polymer shell were prepared. To gain mucus penetrating and bile salts^[2] resistant features, liposomes have been covered with a first polymer shell of PEG-2000. Then liposomes have been covered with a second shell of Eudragit-S100, a gastro-resistant polymer with pH-dependent solubility which protects vesicles from the acidic gastric pH and intestinal enzymes, while releasing them at neutral-alkaline pH conditions, near the absorption site in the colon region. These liposomes have been morphologically characterized through TEM. Some investigations have been conducted to optimize the encapsulation efficiency (EE%) and the loading capacity (LC%) of the curcumin. The optimization is based on the application of a second-degree polynomial interpolation with two variables to the experimental data, which allowed to predict the values of lipidic and curcumin concentration which maximize EE% and LC%.

Materials and Methods

Liposomes have been made of Lipoid-S100, Cholesterol and PEG-2000-PE and loaded with curcumin by the sonication-extrusion method, using membranes with a porosity of 80 nm. Then they have been covered with Eudragit-S100, through a pH-jump method as previously described^[3]. Encapsulation efficiency (EE) and loading efficiency (LE) were maximized by in silico data elaboration performed in *Phyton*. Curcumin quantification was assessed by UV-vis absorption measurement, while vesicle morphology was evaluated by TEM microscopy.

Results and Discussion

Nanostructured curcumin-liposomes (about 80 nm) with a homogeneous and brush-like coating of PEG were obtained by sonication-extrusion method. Curcumin content was varied in the range 5-20 μ M and that of lipids in the range 1-8 mg/mL. Based on the results of single-factor experiments, the preparation technology was optimized by applying a two-variable second-degree polynomial interpolation to the experimental data, which allowed to predict the values of lipid concentration and curcumin for which the values of EE and LE were maximized. TEM images demonstrated the vesicle encapsulation in Eudragit-S100. Prepared cargo proved to be stable in an acidic environment, while it released its content at pH > 7.0.

References

- [1] P. Anand et Al., *Molecular Pharmaceutics* **2007**, *4*, 807-818.
- [2] H. He et Al., *Acta Pharmaceutica Sinica B* **2019**, *9*, 36-48.
- [3] a) V. De Leo et Al. *Coatings*, **2020**, *10*, 114; b) V. De Leo et Al., *Molecules* **2018**, *23*, 739.

Redox-responsive mesoporous silica nanoparticles for cancer therapy

Friday, 26th March - 13:48: Fash Session 1 (Room 2) - Abstract ID: 238

Dr. Rosemeyre Cordeiro¹, **Ms. Ana Maria Carvalho**², **Prof. Luísa Durães**³, **Dr. Henrique Faneca**⁴

1. Center for Neuroscience and Cell Biology - University of Coimbra, **2.** aCenter for Neuroscience and Cell Biology - University of Coimbra, **3.** Chemical Process Engineering and Forest Products Research Centre - University of Coimbra, **4.** Center for Neuroscience and Cell Biology - University of Coimbra

Introduction

Mesoporous silica nanoparticles (MSNs) have been considered as promising anticancer drug delivery systems, improving the efficacy of conventional chemotherapy treatments. They present a very high surface area and an extraordinary surface-to-volume ratio, which imparts a great loading capacity, with a highly interesting potential as drug delivery systems. Stimuli-responsive drug delivery MSNs provide a triggered release of the drug. Redox potential stimulus takes advantage of the significant difference in the reduced glutathione (GSH) concentration between the extracellular (2-20 μ M) and intracellular (8-10 mM) environments. Besides, the intracellular levels of GSH in most tumor cells can be 4-fold higher than those in normal cells. In this work, we developed a novel and effective redox-responsive MSNs to carry an anticancer drug.

Methods

Tetrasulfide-based mesoporous silica nanoparticles (TMSNs) were prepared using bis[3-(triethoxysilyl)propyl]tetrasulfide (BTESPT) and tetraethyl orthosilicate (TEOS) as silica precursors. TMSNs were posteriorly functionalized with (3-aminopropyl)triethoxysilane (APTES) (TMSNs-NH₂) through silane chemistry (Figure 1).

For the drug loading, nanosystems were suspended in an epirubicin (Epi) solution and stirred in the dark for 24 h. In the release studies, Epi-loaded TMSNs were dispersed in PBS with or without 10 mM of GSH, and at different pH values (5.5 and 7.4).

The cytotoxicity of unloaded and Epi-loaded nanosystems, and free Epi was evaluated in HepG2 cell line by Alamar blue assay.

Results and discussions

The obtained TMSNs had a mean diameter of 165 ± 21 nm and an average pore diameter of 2.3 nm. The presence and homogeneous distribution of sulfur throughout the TMSNs framework were confirmed through STEM-EDS (Figure 2), as well as CHNS elemental analysis, which revealed that about 32 mol% of BTESPT was integrated into the nanoparticle structure.

TMSNs were successfully functionalized with amine groups using an eco-friendly post-synthetic grafting process. The success of the APTES grafting process was confirmed through zeta potential analysis. In addition, the developed nanosystems were evaluated as anticancer drug delivery systems, using epirubicin as a model drug to study their drug loading and release profiles, which confirmed their responsive release.

Finally, the cytotoxicity studies demonstrated an efficient drug release from nanosystems, leading to the death of up to 94% of HepG2 cancer cells (Figure 3).

In conclusion, it was developed a redox-responsive system with potential for cancer treatment.

Acknowledgements

This work was financed by the ERDF, through the COMPETE 2020 program (Operational Program for Competitiveness and Internalization), and Portuguese national funds via FCT-[POCI-01-0145-FEDER-30916 and UID/NEU/04539/2019].

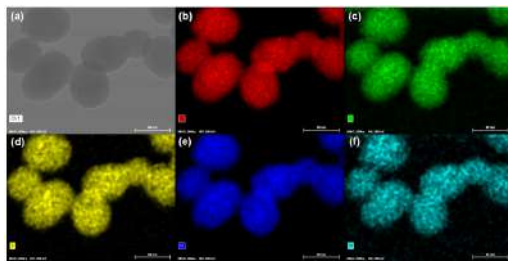


Figure 2.jpg

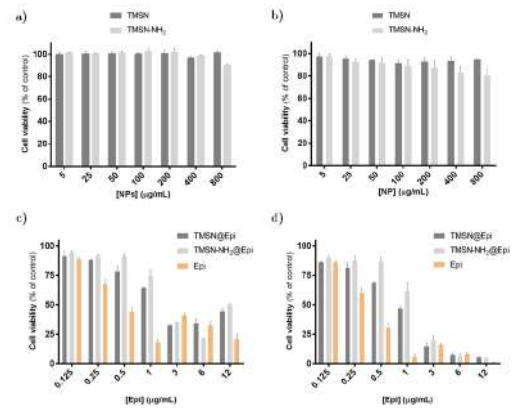


Figure 3.jpg

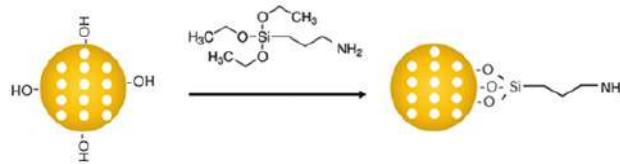


Figure 1.jpg

Photophysical Probing of Squaraine Nanoenvironment, Diffusion Dynamics and Energy Transfer in Conjugated Polymer Nanoparticles

Friday, 26th March - 13:30: Flash Session 1 (Room 3) - Abstract ID: 160

Ms. Clara Zehe¹, Prof. Gareth Redmond¹

1. University College Dublin

Introduction

Conjugated polymer nanoparticles have gained significant attention due to their bright emission characteristics, good tuneability, biocompatibility and straightforward manufacturing methods. Doping these particles with suitable organic dyes is a promising route to improve and tune their photophysical properties and to study the internal particle environment through spectroscopic techniques.¹ Squaraine dyes are desirable dopants due to their bright narrow-band emission in the red to NIR spectral region,² which is favorable to achieve good colour purity in fluorescence applications. Their sensitivity to local polarity makes them promising candidates as molecular microenvironment probes.³

Methods

Polyfluorene nanoparticles were doped with 0-5 wt% of two squaraine dyes respectively. Aqueous nanoparticle suspensions with hydrodynamic radii of 30-60 nm were prepared through reprecipitation. The effect of squaraine concentration on the photophysics of the nanoparticles, energy transfer and response of dye encapsulated in the particles were investigated by steady state absorption and fluorescence spectroscopy combined with time-correlated single-photon counting techniques to extract fluorescence lifetimes and time-resolved emission anisotropies of both the polymer matrix and squaraine dopants. The energy transfer process was quantified through FRET overlap and efficiency calculations.

Results

Energy-transfer from the polyfluorene matrix to both squaraine dopants was observed despite small spectral overlap and lack of through-bond interactions following non-covalent dye encapsulation. This was confirmed by selective photoluminescence acquisition and lifetime studies, which yielded observable quenching of the fluorescent polymer with increasing dopant concentration accompanied by growing sensitisation of the dye emission.

Moderate fluorescence colour-tuning with rising dopant concentration was observed. A significant increase of the rotational relaxation time and a small hypsochromic shift of the squaraine emission in doped particles indicated encapsulation of the dye and interaction with the polymer matrix. The anisotropic response of the squaraine molecule was described by a two-step lateral diffusion and wobble-in-cone model.

Discussion

Successful non-covalent doping of polyfluorene nanoparticles with two squaraine dyes and the effects on the nanoparticle photophysics are demonstrated in this study. Potential applications and limitations of squaraines for molecular probing and FRET applications towards fluorescence imaging and sensing are further highlighted. Improved colour tuneability and microenvironment sensitivity may be achieved through optimized matching between components in future research.

(1) Wang, S. et al. *J. Phys. Chem. C* **2018**, 122 (12), 6900–6911.

(2) Wu, I. C. et al. *J. Am. Chem. Soc.* **2015**, 137 (1), 173–178.

(3) Laia, C. A. T.; Costa, S. M. B. *Phys. Chem. Chem. Phys.* **1999**, 1 (18), 4409–4416.

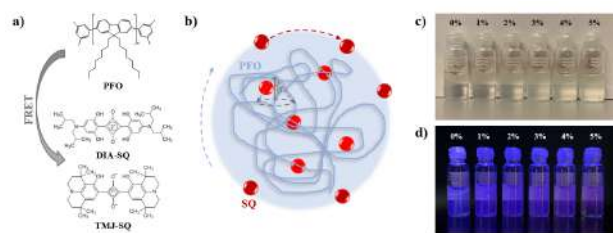


Figure 1 a) Molecular structures of the polyfluorene (PFO) and squaraines (DIA-SQ, TMJ-SQ) used in this study. **b)** Schematic representation of the assumed morphology of a doped nanoparticle displaying motions contributing to the anisotropy decay according to the wobble-in-cone model. **c)** Images of the nanoparticle suspensions with 0-5wt% DIA-SQ dopant under normal and **d)** UV irradiation showing a gradual colour change.

Cz fig1 schematics of squaraine-doped pfo nps.png

Hydrogen Production and Degradation of Antibiotics Using Silver-Based TiO₂ and ZnO Catalysts

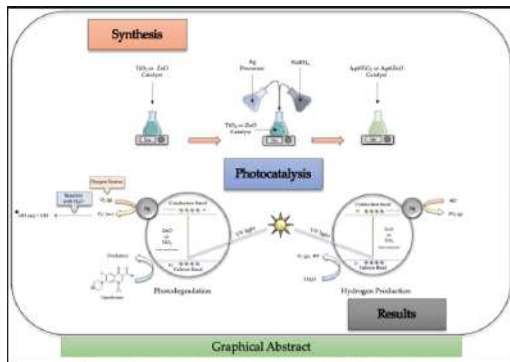
Friday, 26th March - 13:33: Flash Session 1 (Room 3) - Abstract ID: 161

Mr. Carlos A. Valentin¹, Dr. Loraine Soto-Vázquez², Dr. Abniel Machin³, Mr. Kenneth Fontánez⁴, Dr. Francisco Márquez¹, Ms. Carla Colón-Cruz¹, Mr. Gerardo Claudio¹, Dr. Edgard Resto², Dr. Carmen Morant⁵, Dr. Florian I. Petrescu⁶

1. Nanomaterials Research Group, School of Natural Sciences and Technology, Universidad Ana G. Méndez-Gurabo Campus, Gurabo 00778, Puerto Rico, 2. Materials Characterization Center, Molecular Sciences Research Center, University of Puerto Rico, San Juan 00926, Puerto Rico, 3. Arecibo Observatory, Universidad Ana G. Méndez-Cupey Campus, San Juan 00926, Puerto Rico, 4. Department of Chemistry, University of Puerto Rico-Río Piedras, San Juan 00925, Puerto Rico, 5. Department of Applied Physics, Autonomous University of Madrid and Instituto de Ciencia de Materiales Nicolas Cabrera, 28049 Madrid, Spain, 6.

IFTToMM-ARoTMM, Bucharest Polytechnic University, 060042 Bucharest, Romania

Multiple environmental challenges have been presented in the last century. One of them, is the continuous injection of CO₂ into the atmosphere due to the burning of fossil fuels for energy generation. Is for that reason that one of the focus of the 21st century is to develop clean and renewable sources of energy. One of the candidates that have been proposed as a replacement of fossil fuels is hydrogen. Currently, the production of hydrogen is mainly derived from fossil fuels which release carbon dioxide and other gases to the atmosphere. Another major problem is the continuous pollution of our water resources with organic pollutants such as antibiotics. This not only cause and environmental problem, but also create a health issue. For these reasons, different Ag@TiO₂ and Ag@ZnO catalysts, with nanowire (NW) structure, were synthesized containing different amounts of silver loading (1, 3, 5, and 10 wt.%) and characterized by FE-SEM, HRTEM, BET, XRD, Raman, XPS, and UV-vis. The photocatalytic activity of the composites was studied by the production of hydrogen via water splitting under UV-vis light and the degradation of the antibiotic ciprofloxacin. The maximum hydrogen production of all the silver-based catalysts was obtained with a silver loading of 10 wt.% under irradiation at 500 nm. Moreover, 10%Ag@TiO₂ NWs was the catalyst with the highest activity in the hydrogen production reaction (1119 µmol/hg), being 18 times greater than the amount obtained with the pristine TiO₂ NW catalyst. The most dramatic difference in hydrogen production was obtained with 10%Ag@TiO₂-P25, 635 µmol/hg, being 36 times greater than the amount reported for the unmodified TiO₂-P25 (18 µmol/hg). The enhancement of the catalytic activity is attributed to a synergism between the silver nanoparticles incorporated and the high surface area of the composites. In the case of the degradation of ciprofloxacin, all the silver-based catalysts degraded more than 70% of the antibiotic in 60 min. The catalyst that exhibited the best result was 3%Ag@ZnO commercial, with 99.72% of degradation. The control experiments and stability tests showed that photocatalysis was the route of degradation and the selected silver-based catalysts were stable after seven cycles, with less than 1% loss of efficiency per cycle. These results suggest that the catalysts could be employed in additional cycles without the need to be resynthesized, thus reducing remediation costs.



Graphical abstract.png

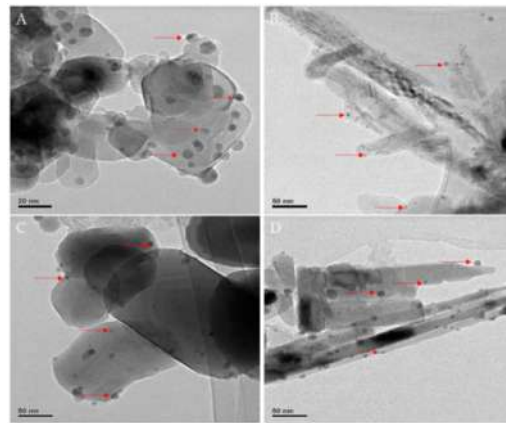


Figure 1: High-Resolution Transmission Electron Microscopy images for: A. 10%Ag@P-25, B. 10%Ag@TiO₂ NWs, C. 10%Ag@ZnO Commercial, and D. 10%Ag@ZnO NWs. The red arrows point towards the present silver nanoparticles.

Figure 1.png

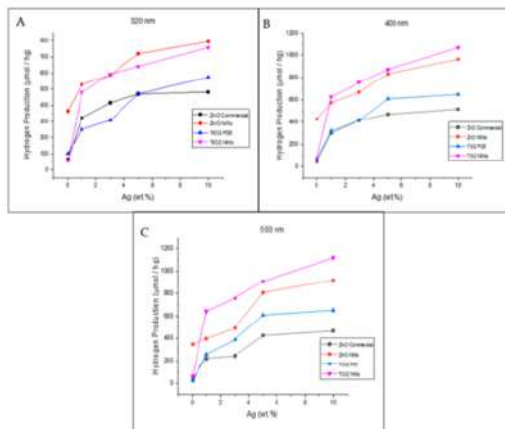


Figure 2: Photocatalytic hydrogen production of the different silver-based catalysts under A. 320nm, B. 400nm, and C. 500nm of irradiation.

Figure 2.png

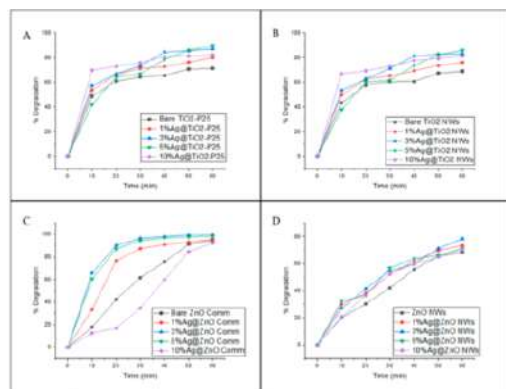


Figure 3: Degradation percentage of Ciprofloxacin in A. Ag@TiO₂ (P-25), B. Ag@TiO₂ NWs, C. Ag@ZnO Commercial, and D. Ag@ZnO NWs catalysts.

Figure 3.png

Amine assisted synthesis of dual metal shells on semiconductor nanostructures

Friday, 26th March - 13:36: Flash Session 1 (Room 3) - Abstract ID: 162

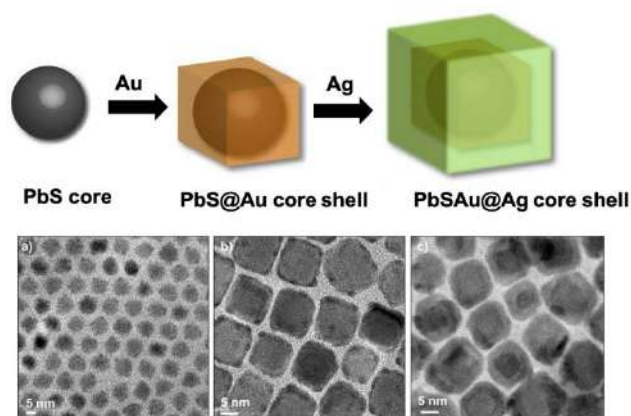
Ms. Anchal Yadav¹, Prof. Bart Follink², Dr. Alison Funston¹

1. Monash University, ARC Centre of Excellence in Exciton Science, 2. Monash University

The absorption of light by semiconductor materials generates a coupled electron-hole pair in the material, known as an exciton. Similarly, the use of plasmonic nanoparticles especially gold, silver and aluminium are also being extensively investigated due to their strong interaction with the resonant photons through excitation of surface plasmon resonance (SPR) which is intended to improve the absorption efficiency of the array. The combination of these two components is generated by growing metals on semiconductor allows tailoring of the band alignment and the system's potential generating possibilities to use them in (chemical and biological) and optoelectronic applications.

We have developed and investigated a seed-mediated growth strategy for depositing metal shells on pre-synthesized semiconductor nanostructures. So far, there are only a few reports outlining the successful deposition of a full and uniform metal shell on semiconductor nanostructures. Indeed, more commonly, metals often form separate islands or deposits on the sides or on defect sites present at the surface of semiconductor nanocrystals. Keeping the mentioned variables into account, a slow injection methodology was developed, where the metal precursors are reduced directly on the surface of pre-synthesized semiconductor nanoparticles, by controlling the rate of injection we are able to control the nucleation of metal onto the semiconductor nanocrystals (PbS, CZTS) and consequently end up forming a thin shell of gold enclosing the semiconductor nanostructure. This is then further shelled with silver to produce the final morphology as shown in the image.

Several factors important for achieving a uniform shell such as the injection rate, concentration of the precursors are investigated and reported. It is also found that the alkylamines such as DDA are important precursor to achieve the full shelling on semiconductors providing better colloidal stability. We have also observed a shape change upon the metal deposition which is also investigated and discussed in this work.



Schematic and tem images showing the formation of hybrid nanostructures after the depoistion of metal shells on semiconductors.jpg

Fluorescence enhancement and cetuximab-conjugation of nanodiamonds for drug delivery

Friday, 26th March - 13:39: Flash Session 1 (Room 3) - Abstract ID: 230

Mr. Pietro Aprà¹, Mr. Mirko Sacco², Ms. Veronica Varzi¹, Dr. Valentina Boscaro², Prof. Margherita Gallicchio², Prof. Alessandro Barge², Dr. Federico Piccolo¹

1. University of Torino, Department of Physics, 2. University of Torino, Department of Drug Science and Technology

Introduction

Currently, a strong interest has been focused on the employment of nanoparticles as promising tools in biomedical research, diagnostics and therapy. In this frame, Nanodiamonds (NDs) earned a solid reputation due to their interesting features, such as inertness, fluorescence, biocompatibility and the possibility of modifying their surface termination [1]. Aim of the work is the realization of diamond-based drug delivery systems which are optically trackable during *in-vitro* experiments, by exploiting the fluorescence properties deriving from the Nitrogen-Vacancy (NV) lattice defects [2]. By mean of ion-beam damaging, more defects can be introduced in the crystal lattice, thus creating new NV centers and enhancing the fluorescence.

Methods

The first part of the work was focused on the physical enhancement of the NDs fluorescence yield, thanks to the creation of new NV centers by mean of 2 MeV proton-beam irradiation. Raman and Photoluminescence (PL) spectroscopies were employed to quantify the ion-implanted NDs fluorescence. The second part has been oriented to develop a protocol for treating pristine NDs and controlling their surface chemistry, in order to allow a proper functionalization with cetuximab (NDs-Ctx), a monoclonal antibody specific for EGFR receptors expressed on colon-rectal cancer cells membrane. NDs surface was therefore chemically modified and made suitable for cetuximab covalent linking. The successful surface grafting attempt was assessed by Thermogravimetric Analysis. NDs-Ctx were then administrated to cultured DiFi rectal cancer cells and their internalization degree (compared to a control sample of unmodified NDs) was observed by confocal microscopy.

Results

PL spectra of proton-irradiated samples showed an increase of two orders of magnitude in fluorescence with respect to the unirradiated samples. Secondly, from the analysis of the acquired confocal microscopy images, a high uptake level was observed in the platelets of NDs-Ctx treated DiFi cells, while weak or no NDs fluorescence signal was appreciated inside the cells in the case of unmodified NDs administration.

Discussion

Results showed how post-synthesis treatments and proton-beam irradiation were effective in strongly enhancing NDs fluorescence yield. Cetuximab was successfully grafted on NDs surface and the uptake-inducing properties of the system were observed on DiFi cell line. These results reinforce the suitability of NDs as promising nano-tools both for biolabeling and drug delivery applications, worthy of further investigations in order to combine these two potentials.

[1] Mochalin et al., *Nat. Nanotech.*, 7, 11-23, (2012)

[2] Waldermann et al., *Dia. Rel. Mat.*, 16, 1887-1895, (2007)

A sustainable bottom-up synthetic approach for carbon dots

Friday, 26th March - 13:42: Flash Session 1 (Room 3) - Abstract ID: 235

Mr. Gianluca Minervini¹, Dr. Marinella Striccoli², Prof. Elisabetta Fanizza³, Prof. Angela Agostiano³, Prof. Maria Lucia Curri³, Dr. Annamaria Panniello⁴

1. Polytechnic University of Bari, **2.** CNR-IPCF, **3.** University of Bari "Aldo Moro", **4.** CNR - Istituto per i Processi chimico Fisici

INTRODUCTION

Carbon dots (CDs) are novel photoluminescent nanoparticles that have emerged in the last few years as greener and cost saving alternatives to semiconductor quantum dots and other heavy metal-containing luminescent compounds [1]. Their carbon-based chemical composition and the promising photoluminescence properties are making them progressively attractive for many fields of application.

METHODS

In a recently proposed bottom-up approach to prepare CDs, a surfactant precursor, cetylpyridinium chloride (CPC), was simply added to concentrated NaOH solutions in mild reaction conditions, yielding green-yellow emitting CDs [2, 3]. Motivated by the energy and cost-effectiveness of such synthetic method, we investigated the process of the CDs formation, exploring new synthetic practices aimed to achieve an even easier and faster production of CDs. Namely, we prepared CDs varying reaction conditions such as the precursor-to-NaOH concentration ratio, reaction temperature and time and we thoroughly characterized optically and morphologically the resulting CDs. Furthermore, we gave specific attention to the isolation and purification of the final products, and to the identification of intermediate species, contributing to the overall emission of the CDs samples [4].

RESULTS

In particular, we recognized that 2-pyridone molecular fluorophores are formed in the first steps of the reaction and then they are consumed as the reaction proceeds. This outcome inspired us to describe a two-step reaction mechanism, in which the 2-pyridones are firstly formed and then consumed while contributing to the formation of the final CDs. Furthermore, we find that the kinetics of the process can be regulated by mildly heating the reaction vessel. Notably, since the full conversion of all reaction intermediates to CDs requires a very long time (varying from tens of hours to days [3]) if performed at room temperature, this can be used to further advance the efficiency of the synthetic approach. Indeed, increasing the reaction temperature at 70°C, the complete carbonization of CPC occurs in only 20 min and CDs with well-defined morphological and optical properties are obtained.

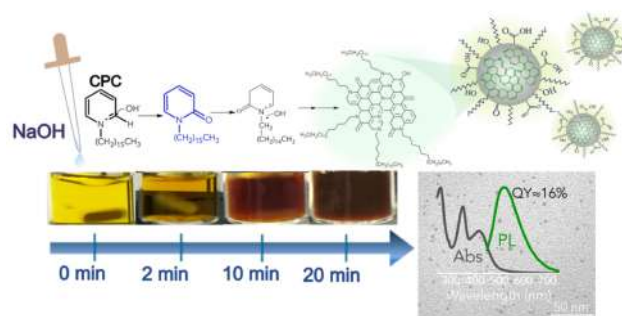
[1] Sciortino, A., *et al.*, *C***2018**, 4, 67

[2] Minervini, G., *et al.*, *Materials***2020**, 13, 3716; Kozák, O., *et al.*, *J. Phys. Chem. C***2013**, 117, 24991-24996; Deng, T., *et al.*, *Part. Part. Syst. Char.***2018**, 35, 1800190

[3] Zheng, B., *et al.*, *RSC Adv.***2015**, 5, 11667-11675

[4] Sharma, A., *et al.*, *J. Phys. Chem. Lett.***2017**, 8, 1044-1052

This work has been financially supported by the Italian MIUR PRIN 2017 Candl² Project Prot. n. 2017W75RAE.



Schematic overview of cds synthesis and properties.png

NOTEWORTHY THERMAL CONDUCTIVITY ENHANCEMENT IN Ag-GRAPHENE/ ETHYLENE GLYCOL BASED NANOFLUID

Friday, 26th March - 13:45: Flash Session 1 (Room 3) - Abstract ID: 169

Prof. Malik Maaza¹

1. University of Bath

•In terms of heat transfer, the thermal conductivity of graphene is demonstrated to be within the range of 3,000–5,000 Wm⁻¹ K⁻¹ at room temperature which is an exceptional figure when compared to the thermal conductivity of pyrolytic graphite (2000 W m⁻¹ K⁻¹ at room temperature), and surpasses even the highest value of natural diamond (895–1,350 Wm⁻¹ K⁻¹) as well as that of standard Cu (384.1 Wm⁻¹ K⁻¹). Hence, graphene would be an ideal candidate for use in nanofluids applications especially when decorated with additional metallic nanoparticles. This contribution reports on the synthesis and enhanced thermal conductivity of stable Ag-decorated 2-D graphene nanocomposite in ethylene glycol based nanofluid by laser liquid solid interaction. A surfactant free nanofluid of Ag nanoparticles anchored onto the 2-D graphene sheets were synthesized using a two-step laser liquid solid interaction approach. In order to understand a pulsed Nd:YAG laser at the fundamental frequency ($\lambda = 1,064$ nm) to ablate Ag and graphite composite target submerged in ethylene glycol (EG) to form AgNPs decorated 2-D GNs-EG based nanofluid. From a heat transfer point of view, it was observed that the thermal conductivity of this stable Aggraphene/EG is significantly enhanced by a factor of about 32.3%; this is highest reported value for a graphene based nanofluid.

Quantum oscillations in topological insulator microwires contacted with superconducting leads

Friday, 26th March - 14:00: Flash Session 2 (Room 1) - Abstract ID: 64

Dr. Leonid Konopko¹, **Prof. Albina Nikolaeva**¹, **Prof. Tito Huber**²

1. Ghitu Institute of Electronic Engineering and Nanotechnologies, MD-2028 Chisinau, Moldova, 2. Howard University, Washington, DC, 20059 USA

Introduction

Recent efforts to detect and manipulate Majorana fermions in solid state devices have employed topological insulator (TI) nanowires proximity coupled to superconducting leads (SC). This combination holds some promises for the fundamental physics and applications. We studied the transverse magnetoresistance of Bi_2Te_3 and $\text{Bi}_{0.83}\text{Sb}_{0.17}$ TI microwires contacted with superconducting In_2Bi leads. Bi_2Te_3 has a simple band structure with a single Dirac cone on the surface and a large non-trivial bulk gap of 300 meV. The semiconducting alloy $\text{Bi}_{0.83}\text{Sb}_{0.17}$ is a strong topological insulator due to the inversion symmetry of bulk crystalline Bi and Sb.

Methods

The polycrystal microwire samples of n -type Bi_2Te_3 with a glass coating were manufactured by liquid phase casting in a glass capillary using an improved Taylor technique. The single-crystal $\text{Bi}_{0.83}\text{Sb}_{0.17}$ microwire samples were prepared by the high frequency liquid phase casting in a glass capillary using an improved Ulitovsky technique; they were cylindrical single-crystals with (1011) orientation along the wire axis. For investigation TI/SC interface we have prepared Bi_2Te_3 and $\text{Bi}_{0.83}\text{Sb}_{0.17}$ glass coated microwire samples using superconducting alloy In_2Bi ($T_c=5.6$ K) for making contacts with copper leads.

Results and Discussion

The equidistant in transverse magnetic field (up to 1 T) magnetoresistance (MR) oscillations at the TI/SC interface have been observed at various temperatures (4.2 K – 1.5 K) both in Bi_2Te_3 and in $\text{Bi}_{0.83}\text{Sb}_{0.17}$ samples. The oscillations almost disappear when the measurement temperature reaches the superconducting transition temperature in In_2Bi . The amplitude of the MR oscillations also decreases with increasing magnetic field; in magnetic fields of $B > 0.6$ T at $T = 1.5$ K, oscillations are not visible. Possibly, the observed oscillations can be the Aharonov-Bohm oscillations of the magnetic flux quantization. In this case, a closed trajectory is formed at the edge states of the TI/SC interface. The oscillation period $\Delta B = (h/e)/S$ where h/e is flux quantum, S - cross-sections area of closed trajectory; for Bi_2Te_3 microwire the effective trajectory diameter should be about 500 nm, while for $\text{Bi}_{0.83}\text{Sb}_{0.17}$ microwire - about 300 nm. In both cases, these diameters are much smaller than the corresponding microwire diameters. Different assumptions about the nature of the observed effect are discussed.

Acknowledgements

This work was supported by the Moldova State Project # 20.80009.50007.02, NSF through STC CIQM 1231319, the Boeing Company and the Keck Foundation.

One-step microwave synthesis of functionalized magnetic nanoparticles

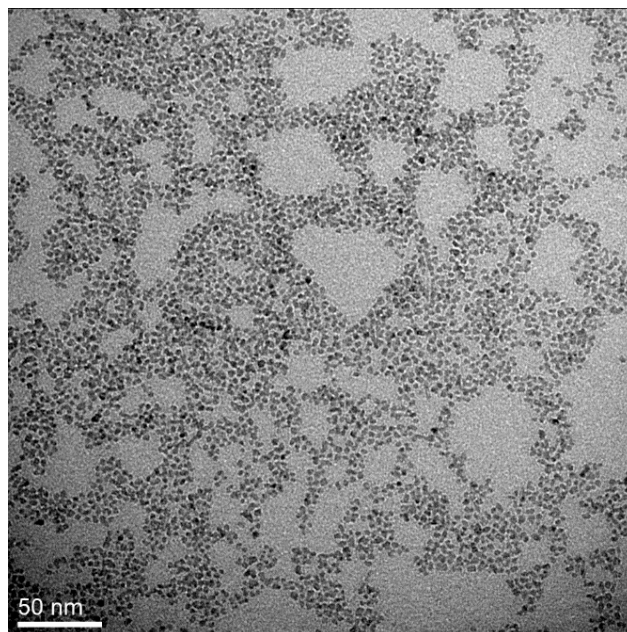
Friday, 26th March - 14:03: Flash Session 2 (Room 1) - Abstract ID: 82

Mr. Thomas Girardet¹, Ms. Amel Cherraj¹, Dr. Franck Cleymand¹, Dr. Solenne Fleutot¹

1. IJL - UMR CNRS 7198, Université de Lorraine, Nancy, France

Functionalized superparamagnetic iron oxide nanoparticles have been synthesized according to a one-step process with the aim to produce stable water-dispersible nanoparticles with a well-crystallized spinel structure. Microwave technology is implemented here to fulfill this objective considering method's ease, speed and reproducibility¹. This technique is more and more used in organic chemistry and it begins to develop for the synthesis in inorganic chemistry. Several parameters have been modified and optimized (temperature, synthesis time, stirring, ratio molar between iron and ligands, volume of basis, power of microwave). The obtained nanoparticles are characterized by TEM, DLS, XRD, FTIR, TGA and magnetic measurements to understand the relations between the size, the shape, the composition and the magnetic properties. The functionalization efficiency (by citrate in standard conditions) is demonstrated using several complementary techniques. This functionalization *in-situ* is showing that is the main element to obtain nanoparticles without aggregation and stable in water. Magnetic measurements indicate the superparamagnetic behavior of nanoparticles with high saturation magnetization. The properties of stable water-dispersible iron oxide nanoparticles combined with the potential for use and modification of functionalized layer make these hybrid systems, developed in one-step in water, prime candidates for future healthcare and environmental applications.

(1) Venturini, P.; Fleutot, S.; Cleymand, F.; Hauet, T.; Dupin, J.; Ghanbaja, J.; Martinez, H.; Robin, J.; Lapinte, V. Facile One-Step Synthesis of Polyoxazoline-Coated Iron Oxide Nanoparticles. *ChemistrySelect* **2018**, 3 (42), 11898–11901.



Micrograph tem of iron oxide nanoparticles obtained via the microwave heating.png

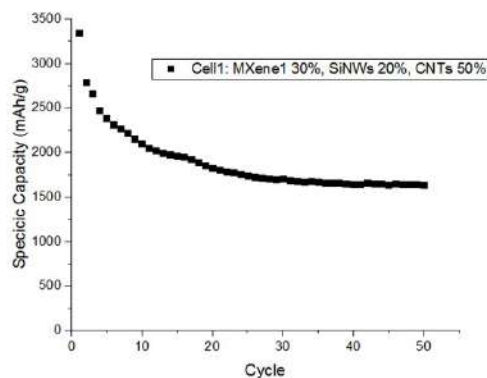
2D-Composites for the Development of Miniaturized Lithium Ion Batteries

Friday, 26th March - 14:06: Flash Session 2 (Room 1) - Abstract ID: 90

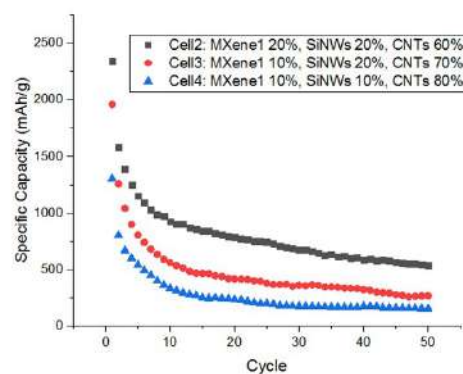
Ms. Carla Colon-Cruz¹, Dr. Abniel Machin², Dr. Maria Cotto¹, Dr. Carmen Morant³, Dr. Francisco Marquez¹

1. Nanomaterials Research Lab at Universidad Ana G. Mendez, Gurabo Campus, **2.** Arecibo Observatory, Universidad Ana G. Méndez-Cupey Campus, San Juan 00926, Puerto Rico, **3.** Universidad Autónoma de Madrid

The limitations of Li-ion batteries while being applied in certain medical devices, consumer electronics, transportation technologies and military/defense equipment is the size of the battery. Hence, the search for batteries with increasingly smaller sizes, high efficiency and high recyclability is at demand. Much of the behavior of the LIBs batteries is due to the high surface area that this material possesses and that offer electrochemical active sites for the storage of ions. This behavior establishes two-dimensional channels for the rapid transportation of ions. In view of this, four anodes were evaluated with electrochemical characterization using an Arbin potentiostat at room temperature. For this, four electrodes were prepared using proportions of MXene (30%, 20%, 10%), SiNW's (20% and 10%) and SWNT's (50%, 60%, 70% and 80%). Through the preliminary studies of these materials, the most stable specific capacity was seen with the proportions of 30% MXene, 20% SiNWs and 20% SWNTs. This result has led us to determine that the higher the amount of MXene material, the higher the stability of the battery. This preliminary work demonstrates that the search for the most stable proportion that sustain the most cycling stability can be achieved using a smaller number of materials. New strategies are being explored for further research by evaluating more varied proportions and extending the amount of cycling stability for the design of more efficient electrodes in batteries composed of metal-ion materials.



Cell 1.jpg



Cells 2 3 4.jpg



Objectives.jpg

Quantum size effect and surface state of “topological insulator” in $\text{Bi}_{1-x}\text{Sb}_x$ wires near the gapless state

Friday, 26th March - 14:09: Flash Session 2 (Room 1) - Abstract ID: 142

Prof. Albina Nikolaeva¹, Dr. Leonid Konopko², Prof. Tito Huber³, Mr. Ivan Popov², Ms. Oxana Botnari²

1. Ghitu Institute of Electronic Engineering and Nanotechnologies, 2. Ghitu Institute of Electronic Engineering and Nanotechnologies, MD-2028 Chisinau, Moldova, 3. Howard University, Washington, DC, 20059 USA

Introduction

Topological insulators (TI), with a gapless topological surface state define a new quantum phase of matter. The characteristic features of TI originate from the existence of topologically protected gapless surface state, which give rise to anomalous transport phenomena. Due to low electron effective masses and high anisotropy of the Fermi surface, Bi and $\text{Bi}_{1-x}\text{Sb}_x$ semimetal is the best material for studying quantum transport in low - dimensional systems and a very promising material for electronic and thermoelectric applications.

We present the experimental results the temperature dependences the resistance (Fig. 1), magnetoresistance and Shubnikov de Haas oscillations (SdH) (Fig. 2) in $\text{Bi}_{1-x}\text{Sb}_x$ wires near the gapless state with different diameter in temperature range 2-300 K.

Methods

The single crystal Bi-8at%Sb wire in glass cover with (1011) orientation along the wire axis and different diameter were prepared by the using high frequency liquid phase casting.

Results and Discussion

It was establish that the energy gap ΔE essential increase (\approx in 3 time) at decrease of the wire diameter from 2000 nm to 200 nm, that considerable exceeded value on similar semi- conductor $\text{Bi}_{1-x}\text{Sb}_x$ wires with diameter to 90 nm.

The increase ΔE at decrease wire diameter d occurs for the quantum size effect $\Delta E = \pi^2 \hbar^2 / md$.

Such abnormal increase of the energy gap at reduction of the wire diameter can be occur at reduction the cyclotron mass m of carriers charge at the linear dependences of energy from pulse. It is characteristic both for gapless state and for surface state of topological insulator.

The SdH oscillation analysis has shown, that the oscillation are characteristic for energy dispersion law type of “Dirac cone”.

This analysis can be extended to other nanowire systems and topological insulators to provide valuable information regarding Fermi energy for use in controlling and optimizing nanowire properties for specific applications in microelectronic and thermoelectricity.

Fig. 1 Temperature dependences of the relative resistance $\Delta R/R(T)$ for $\text{Bi}_{0.92}\text{Sb}_{0.08}$ nanowires with different diameters wires: 1. $d = 2.2 \mu$, 2. $d = 0.5 \mu$, 3. $d = 0.3 \mu$, 4. $d = 0.14 \mu$. Inset: dependence of the energy gap ΔE from wire diameter.

Fig. 2 Derivatives of transverse magnetoresistance $\partial R / \partial H(H)$ ($H \parallel C_3$ point B and $H \parallel C_2$ point A) at 4.2 K. Inset: dependences of the quantum number n - the SdH oscillation plotted vs. H^{-1} .

Acknowledgement

This work was supported by the Moldova State Project # 20.80009.50007.02, NSF through STC CIQM 1231319, the Boeing Company and the Keck Foundation.

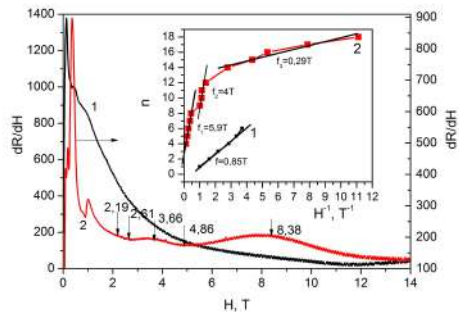


Fig2.jpg

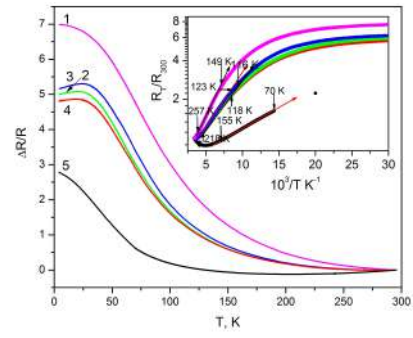


Fig1.jpg

Kinetics of the electrochemical precipitation of lead on FTO substrate at different temperatures

Friday, 26th March - 14:12: Flash Session 2 (Room 1) - Abstract ID: 53

Dr. Ridha Hamdi ¹, Dr. Amani Rached ², Dr. Amor BEN Ali ¹

1. Imam Abdulrahman Bin Faisal University, 2. Imam Abdulrahman Bin Faisal University

We report the electrochemical deposition of lead (Pb) onto fluorine-doped tin oxide (FTO) electrodes in a sodium nitrate bath (0.4M NaNO₃) at constant potential conditions. The kinetics electrodeposition processes have been *in situ* monitored for advanced nucleation stages by chronoamperometry for various temperature at fixed concentration of Pb²⁺, that is 0.1M. The microstructure and morphological characteristics of the deposit layers were investigated by X-ray diffraction (XRD), scanning electron microscopy (SEM) and energy dispersive X-Ray EDX techniques. The results show that the current density as well as the deposits density strongly depend on the temperature. The correlation between the experimental results and the theoretical process of the lead deposits was discussed and verified.

On quantum dynamics of magnetic dipoles in diamagnetic crystals

Friday, 26th March - 14:15: Flash Session 2 (Room 1) - Abstract ID: 100

Dr. Mikhail Kucherov¹

1. School of Space and Information Technologies, Siberian Federal University, 660074, Krasnoyarsk, Russia

We study correlation effects in the dynamics of magnetic dipoles forming magnetic environment of the tagged spin-bearing atom in the high-temperature approximation and rigid limit. The projectors of magnetic dipoles are the tensor products of individual spin-one-half projectors at neighboring sites. The interactions base on the effective Hamiltonian obtained from the truncated dipolar one. By using a symmetry-adapted basis operator set, [1] the overall density matrix equation was decoupled into finite number of equations for the time-resolved isochromat components, the sum of which yields the observed signal. The appropriate Liouville equation is solved by an eigenfunction expansion. [2]

As an extension of the above approach, for the first time the solid-echoes in a many-body system of interacting spins are described in the terms of the ensemble-averaged isochromats. Following the direct-product formalism for calculating magnetic resonance signals in many-body systems of interacting spins, the line shape expression in the thermodynamic limit is obtained. In general, we find that the correlations produces slower dynamics (many spectral components with low frequencies, “pedestal”) accompanied by an enhancement of mean local fields. It results in curves with peaks flatter than the tops of Gaussian curves with equal area and the same maximum value. As expected, only a relatively small number of atoms, the nearest and next-nearest neighbors of a tagged atom, are involved in creating the correlations in diamagnetic compounds. It constitutes a useful approach to treat multi-quantum statistical systems. References: [1] A. A. Nevzorov, J. H. Freed, J. Chem. Phys. 115, 2401 (2001), [2] M. M. Kucherov and O. V. Falaleev, J. Phys.: Conf. Ser. 987(1), 012043 (2018).

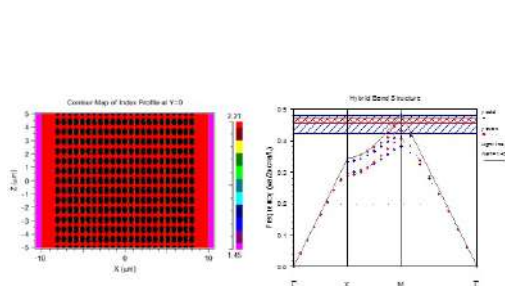
optimisation of the coupling length of magneto photonic slab waveguide based on a square lattice

Friday, 26th March - 14:18: Flash Session 2 (Room 1) - Abstract ID: 295

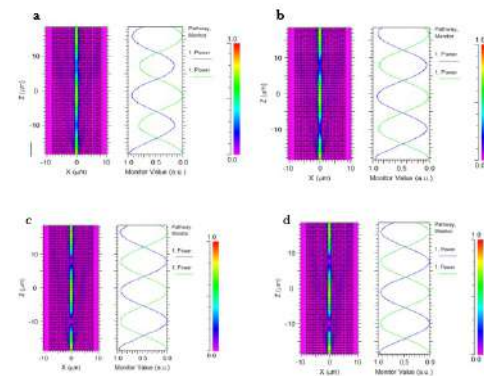
Dr. Salim ghalem¹, Dr. lebbal mohamedredha¹, Prof. Bouchemat mohamed¹, Prof. Boumaza-Bouchemat Touraya¹

1. Laboratoire Microsystemes et Instrumentation Département d'Electronique

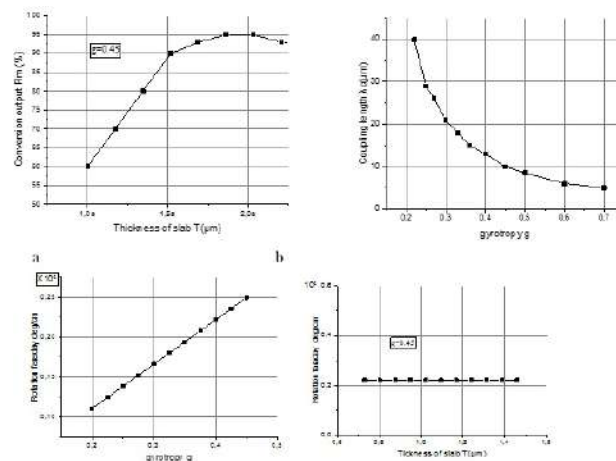
The concept of an integrated isolator is based on the conversion between the non-reciprocal TE-TM mode, the non-reciprocal coupling between the modes is due to a magneto-optical phenomenon, called Faraday rotation. in this paper, we propose to study this phenomenon, by the simulation of a magneto-photonic crystal (MPC) waveguide slab, this structure is formed by a square lattice of circular air holes in a garnet medium of yttrium iron substituted for cerium (Ce-YIG), grown on a silica substrate SiO₂, in this structure, we report a theoretical study of the conversion mode, and we study the effect of the thickness (T) and gyrotropy parameter (g), using a two-dimensional beam propagation method (BPM).



1.jpg



2.jpg



3.jpg

Enhancing the antioxidant activity of the natural coumarin daphnetin and its substituted analogues by their encapsulation in Solid Lipid Nanoparticles

Friday, 26th March - 14:00: Flash Session 2 (Room 2) - Abstract ID: 140

Ms. Annita Katopodi¹, Ms. Kyriaki Safari¹, Ms. Aikaterini Spanou¹, Dr. Eleni Kavetsou¹, Prof. Anastasia Detsi¹

1. National Technical University of Athens (NTUA)

Introduction

Daphnetin (7,8-dihydroxy-2H-chromen-2-one) is a naturally occurring coumarin derivative exhibiting a wide spectrum of biological activities, such as antioxidant and anti-inflammatory. Thus, several analogues of daphnetin have been synthesized and assessed for their pharmacological properties, even though compounds bearing a catechol moiety in their structure, can easily undergo air or light oxidation and generally possess low bioavailability. Nanoencapsulation consists a very promising technique for the protection of sensitive compounds from air or light oxidative degradation, the improvement of their aqueous solubility and their sustained release. Solid Lipid Nanoparticles (SLNs) have been extensively investigated as drug carriers for the encapsulation of both hydrophilic and hydrophobic compounds, while they present low toxicity and excellent bioavailability and biodegradability.

Methods

Hence, in this study, the preparation and characterization of SLNs of daphnetin (**a**), 7,8-dihydroxy-4-methyl-3-(4-hydroxyphenyl)-coumarin (**b**) and 7,8-dihydroxy-4-phenyl-coumarin (**c**) are reported. Trimyristin, extracted from nutmeg, was used as a lipid and Tween80 and phosphatidylcholine as emulsifiers using the solvent emulsification-evaporation method combined with ultrasonication. The antioxidant activity of the coumarins and the nanoparticles was evaluated using the DPPH radical scavenging assay. SLNs were characterized using Dynamic Light Scattering (DLS), FT-IR spectroscopy, Differential Scanning Calorimetry (DSC) and Thermogravimetric Analysis (TGA) methods.

Results and Discussion

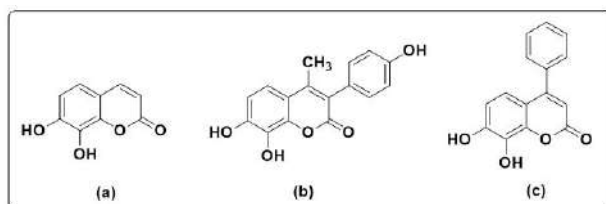
The nanoparticles exhibited sizes of 250 nm, PdI of 0.4 and zeta potential values ranging from -26 mV to -40 mV, approximately, indicating the high stability of the aqueous dispersions. Encapsulation process greater enhanced the DPPH radical scavenging activity of daphnetin (**a**) (IC_{50} 9 μ M) and its 3-aryl-analogue (**b**) (IC_{50} 13 μ M) presenting IC_{50} values of 5 μ M and 7 μ M, respectively. Finally, the coumarin analogues exhibited a sustained release profile (35 °C and pH 5.5), with the release kinetics being better fitted on the Higuchi model.

Acknowledgments

A. K. gratefully acknowledges State Scholarships Foundation (IkY). This research is co-financed by Greece and the European Union (ESF) through the Operational Programme (Human Resources Development, Education and Lifelong Learning) in the context of the project "Strengthening Human Resources Research Potential via Doctorate Research" (MIS-5000432), implemented by the State Scholarships Foundation (IkY).

References

- Detsi, A., Kontogiorgis, C., & Hadjipavlou-Litina, D. (2017). Coumarin derivatives: an updated patent review (2015-2016). *Expert opinion on therapeutic patents*, 27(11), 1201-1226.
- Detsi, A., Kavetsou, E., Kostopoulou, I., Pitterou, I., Pontillo, A. R. N., Tzani, A., ... & Zoumpoulakis, P. (2020). Nanosystems for the encapsulation of natural products: The case of chitosan biopolymer as a matrix. *Pharmaceutics*, 12(7), 669.



Chemical structures of the coumarin derivatives.jpg

A targeted delivery nanosystem to mediate a combined antitumor strategy to HCC

Friday, 26th March - 14:03: Flash Session 2 (Room 2) - Abstract ID: 279

Ms. Dina Farinha ¹, Dr. Michael Migawa ², Dr. Anabela Sarmento ³, Dr. Henrique Faneca ⁴

1. Center for Neuroscience and Cell Biology and Institute for Interdisciplinary Research (IIIUC), University of Coimbra, 3030-789 Coimbra, Portugal, **2.** Ionis Pharmaceuticals Inc, Carlsbad, CA 92010, USA, **3.** Center for Neuroscience and Cell Biology, **4.** Institute for Interdisciplinary Research (IIIUC), University of Coimbra, 3030-789 Coimbra, Portugal

Introduction: Hepatocellular carcinoma (HCC) is one of the main causes of cancer-related death. Sorafenib, which is the first-line therapy for this disease, is associated to reduced therapeutic efficacy, mainly due to drug resistance that could be minimized by combining sorafenib with selumetinib. However, both chemotherapeutic agents have lack of specificity to tumor cells and consequent inherent toxicity that leads to highly undesirable side effects. Therefore, the main goal of this work was to develop a hybrid nanosystem (HNP) capable of specifically and efficiently deliver both drugs into HCC cells. The new formulation consists of a PLGA polymeric core coated by a lipid bilayer containing the targeting ligand GalNAc.

Methods: The physicochemical characterization of HNP and their components was performed by dynamic light scattering, zeta potential, matrix-assisted laser desorption/ionization time-of-flight mass spectroscopy, and transmission electron microscopy. Cellular binding, uptake and specificity were evaluated through flow cytometry and confocal microscopy. The therapeutic activity was evaluated namely through: cell viability by Alamar Blue assay; cell death and mitochondrial membrane potential by flow cytometry; caspases activity by luminescence; and molecular targets levels by Western blot.

Results/Discussion: The obtained data show that these hybrid nanosystems present high stability and loading capacity of both drugs, and suitable physicochemical properties, namely a mean diameter of 194 nm and a zeta potential of -21 mV. Moreover, our results demonstrate that this new formulation allows to circumvent drug resistance and present high specificity for HCC cells, promoting higher cell death in HCC cell lines, but not in non-tumor cells, when compared to the administration of the same amount of free drugs. This potentiation of the antitumor effect mediated by HNP was shown to be carried out by increasing the programmed cell death, demonstrated not just by a strong reduction in the mitochondrial membrane potential, but also by a significant increase in the activity of caspases 3/7 and caspase 9, and much greater number of annexin V-positive cells. A synergistic antitumor effect of the two drugs when encapsulated in the new hybrid nanosystems was verified not only in 2D cell cultures but also in 3D ones, where it was observed an almost total death of the tumor mass with drugs loaded in nanosystems. This study demonstrates that this new drug formulation presents a high translational potential to improve the therapeutic approach against HCC.

Acknowledgements

This work was financed by the ERDF, through the COMPETE program, and Portuguese national funds via FCT [POCI-01-0145-FEDER-30916 and UID/NEU/04539/2019].

Title: Development of flexible nanovesicles for transdermal drug delivery of Azilsartan medoxomil

Friday, 26th March - 14:06: Flash Session 2 (Room 2) - Abstract ID: 259

Ms. aparanjitha r ¹

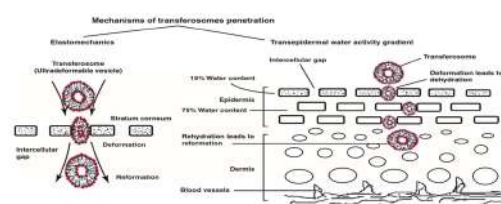
1. kakatiya university

Introduction: Transdermal drug delivery is more suitable for small molecules, lipophilic drug and highly impermeable to macromolecules and hydrophilic drugs. The incorporation of nanocarriers helps to overcome the drawbacks of transdermal formulation. Among the nanocarriers, transferosomes are capable of delivering wide variety drugs through transdermal route. Due to its high deformability it gives a better penetration. Anti-hypertensive drugs with less bioavailability and high first pass metabolism were selected for the present study. Azilsartan medoxomil acts by blocking angiotensin II receptor (ARB) helps in management of hypertension. The drug suffers from very less solubility and poor oral bioavailability due to first pass metabolism.

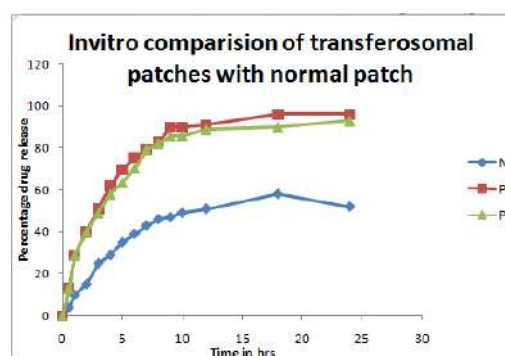
Methods: Transferosomes were formulated with the help of soyalecithin and surfactant (labrosol, Tween 80, Span 80) acts as edge activator. The morphology, entrapment efficiency, diameter and Zeta potential of the transferosomes were evaluated. The optimized transferosomes were further made into patch with the help of HPMC 5cps and PVP using water as solvent by solvent evaporation.

Results and Discussion : The prepared patches were evaluated for Folding endurance, thickness, drug content, invitro and ex-vivo studies. The *invitro* drug release of transferosomal patches (82.4%) after 24 h was higher than normal transdermal patches (68%). The Optimized transferosomal patches had excellent permeation rate through pork skin ($780.69 \mu\text{g}/\text{cm}^2/\text{h}$). A potential transferosomal transdermal system was successfully developed and from the research it is inferred that transferosomes are prominent carriers for transdermal drug delivery systems.

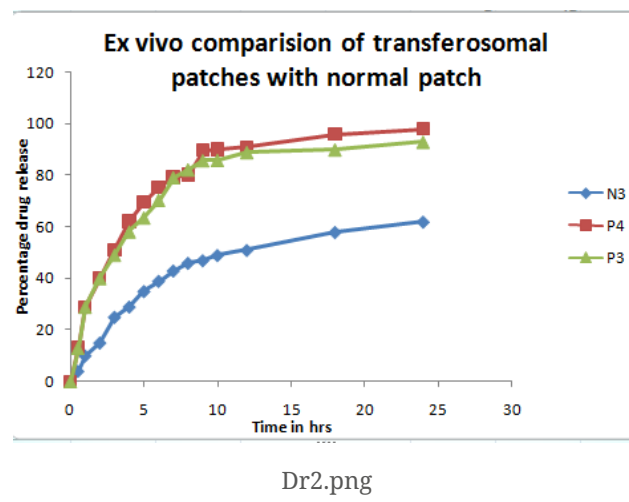
v♦♦♦m♦♦♦



Tr1.png



Dr 1.png



Bacteriophage T7 single-stranded DNA-binding protein displays template-catalyzed recycling

Friday, 26th March - 14:09: Flash Session 2 (Room 2) - Abstract ID: 144

Dr. Jordi Cabanas-Danes¹, Mr. Longfu Xu¹, Mr. Matthew Halma¹, Dr. Sarah Stratmann², Prof. Antoine van Oijen³, Prof. Erwin Peterman¹, Prof. Gijs Wuite¹

1. Vrije Universiteit Amsterdam, 2. University of Groningen, 3. University of Wollongong

Bacteriophage T7 single-stranded DNA-binding protein (gp2.5) is an essential component of the phage replication machinery. During DNA replication, gp2.5 binds and protects transiently exposed regions of single-stranded DNA (ssDNA) while dynamically interacting with other proteins of the replication complex. Here, we use optical tweezers combined with confocal fluorescence microscopy to investigate the real-time binding dynamics of gp2.5 to ssDNA. Our data show that bound gp2.5 reduces the contour length of ssDNA, in well agreement with structural data proposing a DNA binding cleft capable of sandwiching nucleotide triplets between aromatic residues. Also, we demonstrate that increasing the tension on the DNA template reduces gp2.5 binding significantly, thereby supporting a binding model that requires mechanical bending of the DNA, as nucleotide triplet stacking would imply. Next, we report two major trends that hint a binding model relying, at least partially, on the formation of hydrogen bonds between the protein and the ssDNA template. On the one hand, the protein exhibits a more stable binding on GC-rich than on AT-rich DNA sequences, in agreement with the intrinsic stability of DNA base pairs. On the other hand, we observed that if gp2.5 binds to ssDNA in absence of secondary structures, which can arise from base pairing, their formation is prevented in comparison to bare ssDNA. Lastly, we found evidence that re-association after unbinding is enhanced with regards to direct protein binding from solution, which would lead to an efficient spatial redistribution of gp2.5 during synthesis of successive Okazaki fragments. Together, our findings provide a more defined molecular picture of the role of gp2.5 during DNA replication.

Encapsulation of Dopamine and L-DOPA in various biodegradable nanosystems

Friday, 26th March - 14:12: Flash Session 2 (Room 2) - Abstract ID: 98

***Ms. Ioanna Pitterou*¹, *Mr. Isidoros Stamatiou*¹, *Dr. Eleni Kavetsou*¹, *Dr. Eleni Alexandratou*¹, *Prof. Anastasia Detsi*¹**

1. National Technical University of Athens (NTUA)

Introduction: Parkinson's disease (PD) is a progressive neurodegenerative disorder that depletes dopamine (DA) levels in the central nervous system (CNS). L-3,4 Dihydroxyphenylalanine (L-DOPA) is a precursor for dopamine synthesis and a mainstay treatment for PD. Various drug delivery systems, including cyclodextrin (CD) inclusion complexes, chitosan (CS) and polymeric nanoparticles, have been widely developed and provide an attractive alternative for the targeted and controlled delivery of therapeutic agents for the treatment of CNS disorders.

Methods: Inclusion complexes (ICs) of DA and L-DOPA in β -CD, hydroxypropyl- β -CD and methyl- β -CD were synthesized using the kneading method. In order to obtain a more sustained release profile, the DA- β -CD ICs were coated with chitosan (CS- β -CD-DA NPs) using the ionic gelation method. The obtained NPs were characterized using DLS, TGA and FT-IR, UV-Vis, NMR and fluorescence spectroscopies. Phase solubility studies were conducted, and the stoichiometry of ICs was established using Job's plot. The release profile of the DA and LD from the various nanocarriers was studied at pH 7.4 and 37 °C. The antioxidant activity of DA/LD nanosystems was precisely investigated using DPPH assay.

Results and Discussion: The developed nanosystems presented a mean particle size ranging from 326.7 to 372.8 nm, PdI values from 0.301 to 0.399 and zeta-potential values for ICs from -18.7 to -40.4 mV. On the other hand, the CS- β -CD-DA NPs showed positive surface charge with zeta-potential value of $+18.3 \pm 1.5$ mV, indicating the successful coating of the β -CD-DA ICs with chitosan. The DA- β -CD ICs showed a "burst release" of DA during the first 20 minutes (approximately 60%). However, the release profile of DA from the CS- β -CD-DA NPs was significantly different: during the first 20 minutes only 16% of DA was released reaching the maximum release after 24h (77%). Thus, the CS- β -CD-DA NPs can be used as a promising biodegradable carrier for sustained release of DA. The results of the DPPH assay revealed that the HP- β -CD ICs possess enhanced DPPH free radical scavenging activity compared to free DA and LD (IC₅₀(μ M) at 20 min: DA: 0.7, DA-HP- β -CD ICs: 0.2 and LD: 3.0, LD-HP- β -CD ICs: 1.9).

References

Chatzidaki, M., et al. (2020). β -Cyclodextrin as carrier of novel antioxidants: A structural and efficacy study. *Colloids and Surfaces A: Physicochemical and Engineering Aspects*, 603, 125262.

pre-miR-149 G-quadruplex as a molecular recognition agent of Nucleolin

Friday, 26th March - 14:15: Flash Session 2 (Room 2) - Abstract ID: 80

Mr. Tiago Santos¹, **Mr. André Miranda**¹, **Mr. Lionel Imbert**², **Dr. Gilmar Salgado**³, **Prof. Eurico Cabrita**⁴, **Dr. Carla Cruz**¹

1. CICS-UBI – Centro de Investigação em Ciências da Saúde, Universidade da Beira Interior, Covilhã, 2. Univ. Grenoble Alpes, CNRS, CEA, Institut de Biologie Structurale (IBS), F-38044 Grenoble, 3. Univ. Bordeaux, ARNA Laboratory, INSERM, U1212, CNRS UMR 5320, IECB, F-33600, Pessac, 4. UCIBIO, REQUIMTE, Faculdade de Ciências e Tecnologia, Universidade Nova de Lisboa, Caparica

Introduction: In recent years, the structural insights and potential application of precursor microRNA (pre-miRNA) in cancer therapeutics and diagnosis have spurred the interest of researchers. Under certain solution conditions, such as the presence of salts and/or ligands, it is possible to control the secondary structure that some pre-miRNAs can adopt. Previously, pre-miRNA 149 was demonstrated to adopt a G-quadruplex structure in the presence of salt and ligands. RNA sequences with the potential to form G4s are attractive molecular recognition agents, and cell surface nucleolin has been reported as a target of the G-quadruplex motif of pre-miRNA 149 (5'-GGGAGGGAGGGACGGG-3'). Nucleolin is an important multifunctional protein, overexpressed at the surface of cancer cells, that are involved in pre-miRNA biogenesis.

Methods: The pre-miR-149 sequence was designed without 10 nucleotides in the 5'- terminus, to circumvent a structural hindrance in that region (5'- GAGCUCUGGCUCCGUGUCUUCACUCCCGUGCUUGUCCGAGGAGGGAGGGAGGGACGGGGCUGUGCUGGGCAGCUGGA - 3'). In order to evaluate the formation and stabilization of pre-miR-149 G-quadruplex sequence by K⁺, we employed circular dichroism (CD) and UV spectroscopy. Thereafter, the stabilization of the pre-miRNA 149 through ligand binding was assessed by CD melting experiments. The formation of pre-miRNA/nucleolin and pre-miRNA/ligand/nucleolin complexes was checked by PAGE. The binding affinity of nucleolin towards pre-miRNA-149 and pre-miRNA-149/ligand complex was determined by means of Surface Plasmon Resonance (SPR). Finally, the ability of pre-miRNA-149 to detect and capture nucleolin was evaluated through a microfluidic platform based on fluorescence.

Results/Discussion: Our results suggested that pre-miRNA 149 G-quadruplex formation is K⁺ dependent. The stability of the pre-miRNA 149 G-quadruplex structure could be significantly improved ($\Delta T_m > 30$ °C) by adding well-known G4 ligands such as, acridine orange and phenanthroline derivatives. In this work, we explored the preliminary evidence and proved that pre-miRNA 149 G-quadruplex that binds with high affinity to nucleolin (K_D in nM range). The fluorescence of the microfluidic channel increases with nucleolin concentration demonstrating that pre-miRNA 149 has the ability to detect and capture nucleolin.

Acknowledgements: Tiago Santos acknowledges FCT for the doctoral fellowship PD/BD/142851/2018, PTNMR PhD Programme (PD/00065/2013). André Miranda acknowledges the fellowship grant (PINFRA/22161/2016-B4). This work was supported by MIT Portugal FCT project BIODEVICE ref. MITEXPL/BIO/0008/2017, PESSOA programme ref. 5079, project ref. IF/00959/2015 and PTNMR Network (ROTEIRO/0031/2013-PINFRA/22161/2016). The authors also acknowledge Jérôme Boisbouvier. This work benefited from access to the Cell Free Expression Platform of IBS - Institut de Biologie Structurale - Grenoble / France, an Instruct-ERIC centre. Financial support was provided by Instruct-ERIC (PID: 10168).

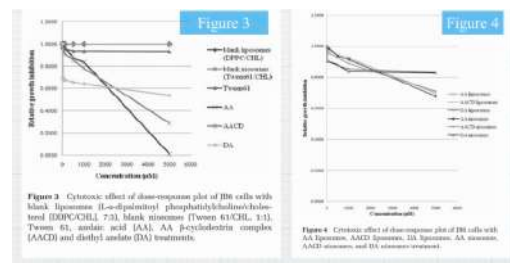
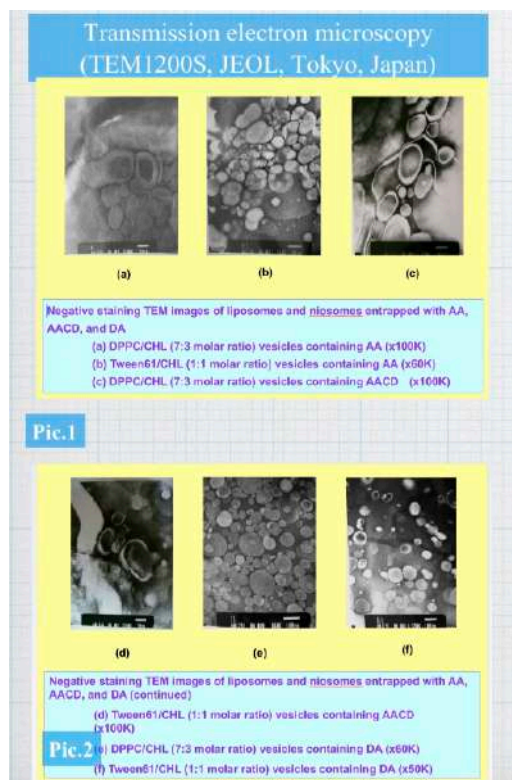
Effectiveness of azelaic acid inclusion complex and its derivative selection in nanovesicles on cell lines

Friday, 26th March - 14:18: Flash Session 2 (Room 2) - Abstract ID: 121

***Dr. Atchara Panyosak*¹**

1. School of Pharmaceutical Sciences University of Phayao

Liposomes and niosomes are nanovesicles which have been widely used as drug carriers. The encapsulation of drugs in these vesicular systems offers several advantages, including the modification of the lipophilicity and hydrophilicity, decreasing of toxicity, increasing of stability in circulation time and absorption of the drug. The azelaic acid (AA) nanovesicles and its derivatives composed of AA was modified by complexing AA with hydroxypropyl- β -cyclodextrin (AACD) and AA was improved to diethyl azelate (DA) by esterification with Fischer reaction for pharmaceutical was determined. AA AACD and DA were incorporated in liposomes and niosomes with the compositions of L- α -dipalmitoyl phosphatidylcholine/cholesterol and Tween 61/cholesterol. AA, AACD and DA and AA, AACD and DA in nanovesicles, using MTT assay in three cancer cell lines (HeLa, KB and B₁₆F₁₀) comparing with vincristine, were investigated. AACD showed the highest potency comparing to AA in HeLa, KB and B₁₆F₁₀ AA entrapped in liposomes more potent than the free AA, and less potent than vincristine. When entrapped in bilayer vesicles, DA and AACD were more effective than AA in killing cancer cells. AACD entrapped in liposomes gave the highest anti-proliferation activity in HeLa cell lines with the IC₅₀ more potent than vincristine and AA. DA in liposomes demonstrated the IC₅₀ less potent than vincristine in KB cell lines, while in B₁₆F₁₀ AACD in niosomes showed the IC₅₀ less potent than vincristine. This study has suggested that the modification of AA by derivatization and complexation as well as the entrapment in bilayer vesicles can enhance its therapeutic efficacy. However, the cytotoxicity of AA and its derivatives incorporated nanovesicular formulations on mouse epidermal cell lines (JB6, normal cell lines), using the SRB assay was modest when compared with cisplatin. Plain liposomes and niosomes gave no growth inhibitory effect. AA incorporated nanovesicles has been proved has antiproliferative effect in cancer cell lines. Furthermore, the safety of AA and its derivatives when incorporated in nanovesicles has been showed no toxicity to normal cell lines.



274409e7-7bf8-437f-92f8-472de9e8db15.jpeg

3d0aa446-5428-4ecc-bbc7-c45376d4f100.jpeg

Optical Properties Analysis of Local Structural Change Induced by Gamma Irradiation in $\text{Al}_{1.9}\text{Eu}_{0.1}\text{Sr}_6\text{Cs}_2(\text{PO}_4)_6(\text{OH})_2$

Friday, 26th March - 14:00: Flash Session 2 (Room 3) - Abstract ID: 125

Mr. Ayumu Masuda¹, Dr. Shinta Watanabe¹, Dr. Masahiko Nakase¹, Prof. Kenji Takeshita¹

1. Tokyo Institute of Technology

Huge amount of wastes containing radioactive Cs, Sr and minor actinide such as Am were generated due to Fukushima Daiichi Nuclear Power Plant Accident in 2011. Immobilization method of such radioactive nuclides is needed for volume reduction of the radioactive waste and safe disposal. Therefore, we focused on apatite materials due to some merits such as their long-term chemical durability, high thermal stability and radiation resistance. Furthermore, the apatite materials can accommodate multivalent cations stably in the structure by chemical interaction and hydrogen gas production can also be minimized because of the lack of hydrated waters if the heating step is applied in synthetic scheme. Recently, we successfully synthesized the apatite-type materials containing Cs, Sr and aluminum such as $\text{Al}_2\text{Sr}_6\text{Cs}_2(\text{PO}_4)_6(\text{OH})_2$ by solid-state reaction. As expected, the site occupancy of multivalent cations and the structural change in local site by gamma irradiation were not clearly detected by powder XRD though the slight color change was observed. To investigate the radiation effect in detail, we synthesized the Eu^{3+} doped apatite material, $\text{Al}_{1.9}\text{Eu}_{0.1}\text{Sr}_6\text{Cs}_2(\text{PO}_4)_6(\text{OH})_2$. Eu^{3+} was used as surrogate element of Am^{3+} and also as the fluorescent probe to detect the slight change in the local structure. Figure 1 presents nano to microcrystals of $\text{Al}_{1.9}\text{Eu}_{0.1}\text{Sr}_6\text{Cs}_2(\text{PO}_4)_6(\text{OH})_2$ after heating at 700 °C for 5 hours. Figure 2 shows emission spectra of $\text{Al}_{1.9}\text{Eu}_{0.1}\text{Sr}_6\text{Cs}_2(\text{PO}_4)_6(\text{OH})_2$ with increase in radiation dose up to 1000 kGy. With increase in radiation dose, decrease in luminescence intensities via Eu^{3+} f-f transitions were observed, indicating an increase in local structural defects such as anionic vacancies and nonradiative pathways to the excited state of Eu^{3+} . It was also noteworthy that the intensity ratio of $^5\text{D}_0 \rightarrow ^7\text{F}_2$ transition to $^5\text{D}_0 \rightarrow ^7\text{F}_1$ transition decreased gradually with increase in the radiation dose from Figure 3. Generally, Eu^{3+} f-f transitions are insignificantly affected by local environment, and an asymmetric ratio defined as a ratio of intensity of electric dipole $^5\text{D}_0 \rightarrow ^7\text{F}_2$ and magnetic dipole $^5\text{D}_0 \rightarrow ^7\text{F}_1$ transitions can be used to evaluate the environmental change. As a result of gamma irradiation, the increase of structural defects and the decrease of asymmetric ratio depending on local site symmetry of Eu^{3+} were clearly detected by luminescence spectra and the result may suggests the transformation of hydroxyl group surrounding trivalent cation in hydroxyapatite materials.

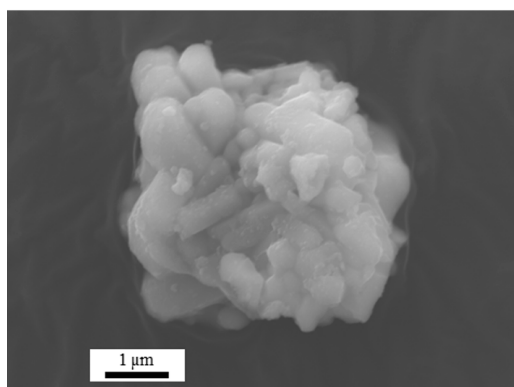


Figure 1. sem image of al1.9eu0.1sr6cs2 po4 6 oh 2 nano to microcrystals.png

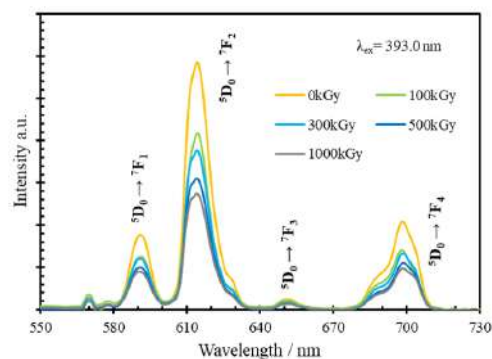


Figure 2. emission spectra of gamma irradiated al1.9eu0.1sr6cs2 po4 6 oh 2 at 393.0 nm excitation.png

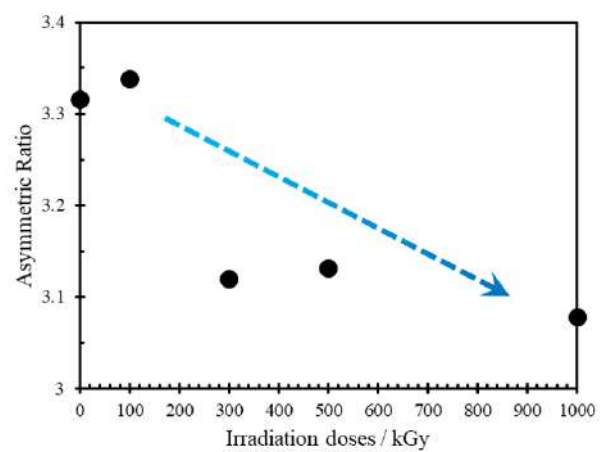


Figure 3. asymmetric ratios of gamma irradiated al1.9eu0.1sr6cs2 po4 6 oh 2.png

Nano-domain patterning by focused ion beam in nonpolar-cut MgOLN and PMN-PT single crystals covered by artificial dielectric layer

Friday, 26th March - 14:03: Flash Session 2 (Room 3) - Abstract ID: 278

Ms. Elena Pashnina¹, Mr. Dmitry Chezganov², Ms. Alla Nuraeva², Prof. Vladimir Shur²

1. School of Natural Sciences and Mathematics, Ural Federal University, Ekaterinburg, Russia e-mail: elena.pashnina@urfu.ru,

2. School of Natural Sciences and Mathematics, Ural Federal University, Ekaterinburg, Russia

The periodically poled lithium niobate (LN) crystals are widely used for light frequency conversion in the bulk and waveguide devices. The $\text{Pb}(\text{Mn}_{1/3}\text{Nb}_{2/3})\text{O}_3\text{-PbTiO}_3$ (PMN-PT) crystals with tailored domain structure can be considered as a potential candidate for such application. A comparative study of domain patterning in uniaxial LN and multiaxial PMN-PT crystals is important. The switching on nonpolar cuts allows to study the stage of the forward domain growth which is crucial for precise periodical poling with nanometer reproducibility of the domain wall position [1]. The irradiation by focused ion beam (i-beam) controlled by the lithographic system is a promising method for nanoscale domain patterning [2].

The irradiated surfaces of (100)-cut PMN-PT and Y-cut MgO-doped LN (MgOLN) single crystals were covered by AZ nLOF 1505 (Microchemicals GmbH, Germany) photoresist layer. The opposite surface was covered by solid Cu electrode. The SEM-FIB Auriga Crossbeam Workstation (Carl Zeiss NTS) equipped with i-beam lithography system Elphy Multibeam (Raith GmbH) was used for i-beam irradiation. The piezoresponse force (PFM) and scanning electron microscopy (SEM) were used for domain imaging.

We have shown that the surface coating by the dielectric layer improves significantly the domain structure homogeneity and reduces the irradiation dose due to high charge localization in the dielectric layer [2]. Isolated dot irradiation resulted in growth of the wedge-like domains in polar directions (Figure 1(a,b)). The stages of domain formation and growth were studied and discussed. We have shown that the dose increase led to nonlinear increase of the domain length (Figure 1(c)).

The model based on the kinetic approach was applied for explanation of the domain formation and growth under the action of i-beam irradiation [3]. The forward domain growth is considered as a result of step generation under the action of the field produced by injected charge and kink motion in the field produced by charged kinks.

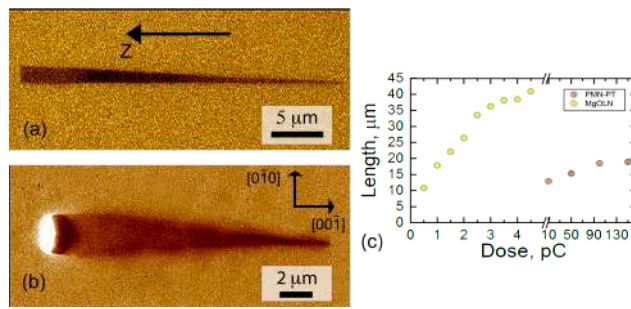
The obtained results can be used for the development of domain engineering methods for periodical poling to create the non-linear optical frequency converters with sub-micron periods.

The equipment of the Ural Center for Shared Use "Modern nanotechnology" Ural Federal University was used. The research was made possible by the Russian Science Foundation (grant № 19-72-00091).

[1] P. Mackwitz, M. Rüsing, G. Berth., Appl. Phys. 108, 152902 (2016).

[2] D.S. Chezganov, E.O. Vlasov, et al., Ferroelectrics, 559, 66 (2020).

[3] V.Ya. Shur. Journal of Materials Science, 199, 41 (1) (2006).



Pic.png

Local and non-local charge transfer of slow alkali ions at surfaces

Friday, 26th March - 14:06: Flash Session 2 (Room 3) - Abstract ID: 149

Dr. pierfrancesco riccardi¹

1. Dipartimento di Fisica - Università della Calabria and INFN gruppo collegato di Cosenza

Electronic interactions of charged particles with surfaces are important in a wide variety of research areas and applications, ranging from spectroscopic analysis of surface and nanomaterials, microscopy, gas discharge and the space environment. The neutralization of scattered alkali-metal ions offers a novel method to investigate surface electronic properties of nanoclusters [1]. However, despite decades of investigation, a detailed knowledge of the neutralization behavior of alkali ions at surfaces is still largely lacking, even for the simplest metals. For example, a substantial deviation from the prediction of the model of neutralization at a jellium surfaces has been recently reported for the ion fraction of sodium ions impinging on aluminum surfaces [2,3], and ascribed to the formation of extra Na^+ ions due to the Auger decay of projectiles' excited states [4], formed in collisions with Al atoms. These collisional excitations are generally described within a molecular orbital (MO) model, that describes the collision systems as transient quasi-molecules in which some MOs are promoted to higher energies [4]. For atomic collisions in a solid environment, it is commonly accepted that excitation results from promotion of one electron into the continuum of conduction band states. Here, we show that such a commonly accepted view of electron promotion in atomic collisions in solids is quite far from reality. To achieve our goal, we discuss the Auger decay of $2p$ excitations in the projectiles, produced by electron promotion in close atomic encounters with target atoms, which occurs when singly charged sodium and neon ions are scattered off an Al surface. In the following, we demonstrate that the electrons promoted in collisions of slow sodium projectiles with Al target atoms are located into atomic outer shells, rather than being transferred into the empty conduction states of the metal surface.

1) G. F. Liu, Z. Sroubek, and J. A. Yarmoff, Phys. Rev. Lett. **92**, 216801 (2004).

2) P. Liu et al. PHYSICAL REVIEW A **101**, 032706 (2020)

3) M. Wei et al. Nuclear Inst. and Methods in Physics Research B **478** (2020) 239–243

4) P. Riccardi, F. Cosimo, A. Sindona Phys. Rev. A **97** 032703 (2018)

UV photodetector based on Zn_{1-x}Mg_xO thin films

Friday, 26th March - 14:09: Flash Session 2 (Room 3) - Abstract ID: 106

Mr. Vadim Morari¹, Dr. Rusu Emil¹, Dr. Ursachi Veaceslav², Prof. Tighineanu Ion²

1. Ghitu Institute of Electronic Engineering and Nanotechnologies, 2. National Center for Materials Study and Testing, Technical University of Moldova

Introduction

ZnO semiconductor is regarded as a potential candidate for UV devices due to its several advantages, such as large exciton binding energy (60 meV), good resistance to irradiation with high-energy particles, low-cost, simple preparation and low-temperature growth. However, solid solutions are required to control the bandgap of the material and the spectral sensitivity range [1]. The Zn_{1-x}Mg_xO alloy system covers a wide ultraviolet (UV) spectral range between the direct bandgaps of 3.36 eV for ZnO and 4.2 eV with wurtzite structure.

Methods

ZnMgO thin films were prepared by aerosol deposition method. Solutions containing Zn(CH₃CO₂)₂ and Mg(CH₃CO₂)₂ acetates with Mg/Zn ratio from 0 to 2/3 were dissolved in ethyl alcohol 0.35M. The solutions prepared in an ultrasonic bath for 30 minutes at a temperature of 60°C were sprayed using a homemade sprayer onto the substrate heated at the temperature of 500 °C.

Results and Discussion

The structure of the photodetector with Schottky Ag-Zn_{0.65}Mg_{0.35}O barrier and with a gradient of the band gap in the detector active region is shown in (Fig.1). The energy diagram of the structure with two oxide compound layers, forming a gradient of the band gap (Fig. 2). The discontinuity in the valence band (VB) and the conduction band (CB) between the p-Si support and the oxide layer is 2.63 eV and 0.1 eV respectively. The difference between the band gaps of the Zn_{0.85}Mg_{0.15}O and Zn_{0.65}Mg_{0.35}O layers equals 0.5 eV. The electron affinity is 4.35 eV, 4.15 eV, and 3.80 eV for ZnO, Zn_{0.85}Mg_{0.15}O, and Zn_{0.65}Mg_{0.35}O, respectively, which results in discontinuity of the CB of 0.35 eV at the Zn_{0.85}Mg_{0.15}O/Zn_{0.65}Mg_{0.35}O interface. The thickness of the optical absorber layer is 500-600 nm, while the window layer has a value of 200-250 nm. The photodetector is practically insensitive to the IR radiation, and it demonstrates a low sensitivity to radiation from the visible range of the spectrum (Fig.3). The maximum photoresponse is located in the UV range of the spectrum. The experimentally measured responsivity (R) and detectivity (D*) of the detector were found to be equal to 460 mA/W and 1cmHz^{1/2}W⁻¹, respectively, at a direct 5V bias.

Acknowledgements. This work was supported financially by the National Agency for Research and Development, Republic of Moldova, through grant No. 20.80009.5007.02.

References

[1] J L. Yang., et al. Recent progress of ZnMgO ultraviolet photodetector, Chin. Phys. B 26, 047308 (2017). Doi:10.1088/1674-1056/26/4/047308.

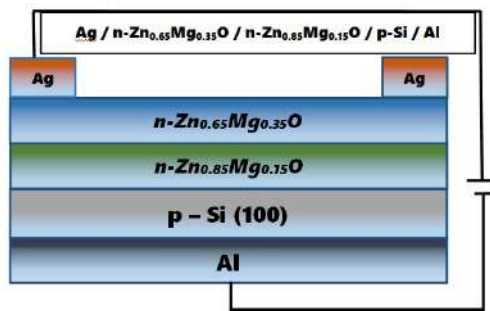


Figure 1.jpg.jpg

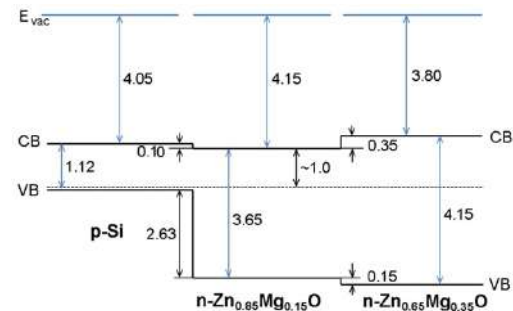


Figure 2.jpg.jpg

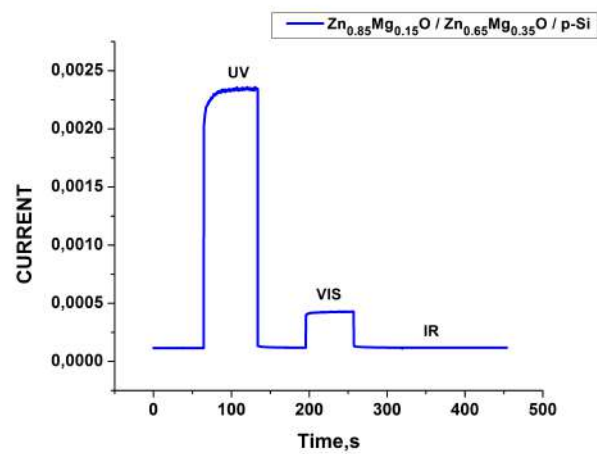


Figure 3.jpg.jpg

Performance and electrochemical studies of lithium ion hybrid supercapacitor

Friday, 26th March - 14:12: Flash Session 2 (Room 3) - Abstract ID: 18

Ms. Sarah Alshehri¹, Prof. Gregory G. Wildgoose¹, Dr. John Fielden¹

1. UEA

To meet our growing energy requirements in a sustainable manner, new energy storage materials are urgently required. Faradaic capacitive materials are promising for high capacitance, high power density supercapacitors. In this work, we developed hybrid battery /supercapacitor based on anthraquinone/lithium for use in hybrid-diffusional battery devices. The combination of anthraquinone with lithium was studied by different electrochemical methods including galvanostatic (charge-discharge), electrochemical impedance spectroscopy, cyclic voltammetry and electrochemical quartz crystal microbalance (EQCM). The effect of lithium ion during the titration process shifted the redox potential to more positive values. The hybrid battery /supercapacitor combines high capacitance with excellent life cycle stability. The anthraquinone/lithium system shows specific capacitance of 317 F.g^{-1} compared to 158 F.g^{-1} for a symmetric anthraquinone -carbon fibre (AQ-CF) supercapacitor.

Spectroscopic investigation of water soluble QDs with Proteinase K: FRET Approach

Friday, 26th March - 14:15: Flash Session 2 (Room 3) - Abstract ID: 272

Mr. Mallikarjun Patil¹, Dr. Sanjeev R. Inamdar¹, Dr. Kotresh M.G², Mr. Tilakraj T.S¹, Mr. Vighneshwar S Bhat¹, Mr. Vikram S Pujari¹

1. Laser Spectroscopy Programme, Department of Physics, Karnatak University, Dharwad 580003, India., 2. Department of Physics, Vijayanagara Sri Krishnadevaraya University, Ballari-583 105, Karnataka, India

- **Introduction:** Semiconductor quantum dots (QDs) are well-recognized fluorophores for biosensing applications because of their unique optical and photophysical properties. Size and/or materials confinement of the QDs leads to tuning of absorption and emission bands. Optical and photophysical properties of QDs can be controlled by their material composition, surface ligands, size, shape and thickness of shell. QDs are frequently used in various biological applications such as diagnostics, cellular imaging etc. The chief advantage of using QDs in bioanalysis is their broad absorption, high extinction coefficients, narrow emission bands, high stability and brightness. Herein, we report Fluorescence Resonance Energy Transfer (FRET) between Proteinase K and water soluble semiconductor QDs (CdSeS/ZnS and CdTe) employing steady-state and time-resolved (TR) fluorescence measurements.
- **Methods:** Absorption spectra were recorded by using dual beam UV-VIS-NIR spectrophotometer (JASCO, Model V-670). The fluorescence spectra were obtained by using Fluoromax-4 spectrofluorometer (JY Horiba, Model Fluoromax-4). Fluorescence lifetime measurements were performed using DeltaPro™ (HORIBA Scientific) TCSPC spectrometer with a 290 nm pulsed diode laser for exciting Proteinase K molecules and the decays were analyzed on DAS-6 decay analysis software.
- **Results and Discussion**

Figure 1. Overlap of normalized PL spectrum of Proteinase K and absorption spectra of QDs.

Figure 2. Steady-state emission spectra of Proteinase K with CdSeS/ZnS 490.

Fig.1 illustrates the ample overlap between normalized fluorescence spectrum of Proteinase K and absorption spectra of QDs. In Fig. 2 decrease in fluorescence intensity of proteinase K and enhancement in the fluorescence of CdSeS/ZnS 490 QDs suggest that proteinase K acts as donor (D) and QDs as acceptor (A). The quenching of fluorescence intensity and reduction in the fluorescence life time of Proteinase K in presence of QDs (CdSeS/ZnS and CdTe) provides that FRET is responsible for non-radiative energy transfer (ET). Obtained values of ET efficiency are 38.43% and 36.10% for CdSeS/ZnS 490 and CdSeS/ZnS 525 QDs, and 57.21% and 58.18% for CdTe 520 and CdTe 530 QDs. For both CdSeS/ZnS and CdTe QDs the FRET efficiency decreases with decrease in spectral overlap. These two FRET pairs are expected to open up exciting applications in fields ranging from photonics to biomedicine.

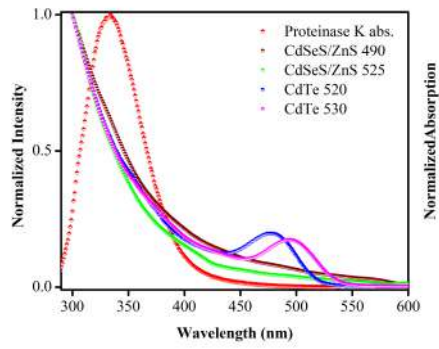


Figure 1.jpg

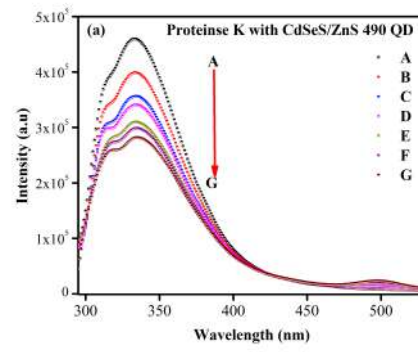


Figure 2.jpg

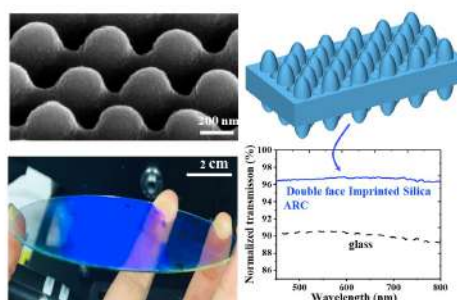
Methylated Silica Surfaces Having Tapered Nipple-Dimple Nanopillar Morphologies as Robust Broad-Angle and Broadband Antireflection Coatings

Friday, 26th March - 14:18: Flash Session 2 (Room 3) - Abstract ID: 266

Mrs. Mehrnaz Modaresialam¹, Dr. Marco Abbarchi², Prof. David Grosso², Dr. Jena-Benoit Claude¹

1. IM2NP univeristy aix-marseille, **2.** Nova Team, Institut Matériaux Microélectronique et Nanosciences de Provence, (IM2NP) -UMR CNRS 7334, Aix-Marseille Université, Faculté des sciences de Saint Jérôme, 13397 Marseille Cedex 20, France.

In this work, mechanically, chemically, and thermally resistant broadband and broad-angle antireflection coatings were prepared on 10 cm diameter glass substrates combining sol-gel deposition with nanoimprint lithography. The coatings are composed of water-repellent methylated silica ($\text{Si}_4\text{O}_7\text{Me}_2$) and exhibit a transverse refractive index gradient created by tapered, nipple-dimple, subwavelength nanostructures, featuring a record vertical aspect ratio of 1.7. The structure is composed of hexagonal arrays of nanopillars (200 nm height, 120 nm width) and holes (50 nm depth, 100 nm width) with a 270 nm pitch. The corresponding effective refractive index is between 1.2 and 1.26, depending on the fabrication conditions. Total transmission for double-face nanoimprint wafers reaches 96–97% in the visible range; it is limited by specular reflection and mostly by the intrinsic diffusion of the glass substrate. The antireflective effect is effective up to an 60° incidence angle. We address the robustness of the inorganic-based coating in various realistic and extreme conditions, comparing them to the organic perfluoropolyether (PFPE) counterpart (master reference). The sol-gel system is extremely stable at high temperature (up to 600 °C, against 200 °C for the polymer reference). Both systems showed excellent chemical stability, except in strong alkaline conditions. The inorganic nanostructure showed an abrasion resistance of more than 2 orders of magnitude superior to the polymer one with less than 20% loss of antireflective performance after 2000 rubbing cycles under an 2 N cm⁻² pressure. This difference springs from the large elastic modulus of the sol-gel material combined with an excellent adhesion to the substrate and to the specific nipple-dimple conformation. The presence of holes allows maintaining a refractive index gradient profile even after tearing out part of the nanopillar population. Our results are relevant to applications where transparent windows with broadband and broadangle transmission are needed, such as protective glasses on photovoltaic cells or C-MOS cameras.



Toc final .jpg

Nanostructured ceria-titania photocatalysts for environmental and energy-related applications

Friday, 26th March - 14:50: Oral Session 2-1 (Room 1) - Abstract ID: 41

Prof. Elisa Moretti¹

1. Department of Molecular Sciences and Nanosystems, Ca' Foscari University of Venice, Via Torino 155, 30172 Venezia

One of the main technological challenges that we are facing is the ability to provide a sustainable supply of clean energy and, among all renewable sources, solar energy displays the greatest potential. Converting solar energy into chemical energy through hydrogen generation is one of the most interesting approaches, since H₂ is the ideal energy carrier.

Among the most suitable materials for photo-assisted H₂ production, titania, TiO₂, is the most widely studied and applied, nevertheless it suffers from two well-known drawbacks: the wide band gap and the high recombination rate of electron-hole pairs.

A growing interest has recently emerged on photoenergy applications of ceria, CeO₂, due to its unique redox properties¹ and an experimental band gap very close to that of TiO₂. The development of novel synthetic strategies has led to the preparation of nanostructured materials displaying unique properties compared to the bulk counterpart systems, with controlled and tunable morphologies, able to enhance the activity and selectivity of a catalytic/photocatalytic process.

This talk will discuss the importance of tuning the morphological/textural features of a catalyst as a strategy to improve the catalytic activity, focusing on how rationally designing ceria-based materials can lead to obtain morphologies and micro- nanostructures suitable to enhance the catalytic performance. The talk will discuss some energy and environmental applications that can be addressed by copper-ceria and ceria-titania nanosystems², focusing on their structure-reactivity relationship. In particular, thermal and photocatalytic H₂ production and purification by CO preferential oxidation^{3,4} will be presented as successful case history.

References

- M. Melchionna and P. Fornasiero, The role of ceria-based nanostructured materials in energy applications. *Mater. Today*, 17, 2014, 349-357.
- E. Moretti, L. Storaro, A. Talon, P. Riello, A. Infantes-Molina, E. Rodríguez-Castellón. 3-D flower like Ce-Zr-Cu mixed oxide systems in the CO preferential oxidation (CO-PROX): Effect of catalyst composition. *Appl. Catal. B*, 168-169, 2015, 385-395.
- E. Rodríguez-Aguado, A. Infantes-Molina, A. Talon, L. Storaro, L. Leon-Reina, E. Rodríguez-Castellón, E. Moretti. Au nanoparticles supported on nanorod-like TiO₂ as catalysts in the CO-PROX reaction under dark and light irradiation: Effect of acidic and alkaline synthesis conditions. *Int. J. Hydrog. Energy*, 44, 2019, 923-936.
- A. Infantes-Molina, A. Villanova, A. Talon, Aldo, M.G. Kohan, A. Gradone, R. Mazzaro, V. Morandi, A. Vomiero, E. Moretti. Au-Decorated Ce-Ti Mixed Oxides for Efficient CO Preferential Photooxidation. *ACS Applied Materials & Interfaces*, 12, 2020, 38019-38030

Investigations on Spatial Self-Phase Modulation of Fullerenes in Solution

Friday, 26th March - 15:20: Oral Session 2-1 (Room 1) - Abstract ID: 50

Ms. Stefanie Dengler¹, Dr. Bernd Eberle¹

1. Fraunhofer IOSB, Institute of Optonics, System Technologies and Image Exploitation, Gutleuthausstr. 1, 76275 Ettlingen, Germany

Introduction

Several nonlinear effects can occur, when an intense electromagnetic wave travels through a medium. They manifest themselves through field dependent variations of different optical constants, e.g. thermal or intrinsic induced refractive index changes, which can lead to spatial self-phase modulation (SSPM). SSPM refers to a phenomenon where concentric circular diffraction rings appear in the far field.

In this work, we report on SSPM in C_{60} and C_{70} solutions and on an example for a laser protection device based on SSPM materials.

Methods

To measure the SSPM effect, a 532 nm cw laser beam was focused into a corresponding sample. A screen was placed behind the sample and the diffraction pattern images were recorded using a high-speed camera.

Fig. 1: Experimental setup to measure the far field diffraction ring pattern.

To determine whether SSPM is a thermal effect or is caused by intrinsic $\chi^{(3)}$ changes of the samples, measurements in two different solvents (1,2-dichlorobenzene and toluene) and different sample temperatures were performed.

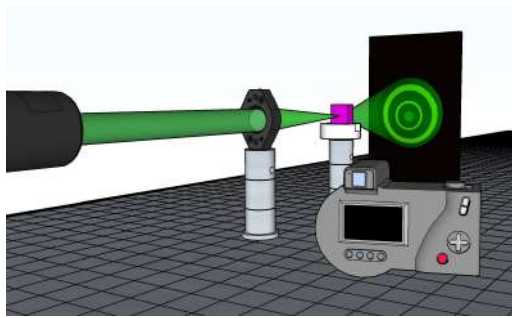
Results and Discussion

The dynamic process of SSPM in solutions can be divided into two parts. First, the spot begins to expand and a series of expanding concentric rings appear, starting from the centre. Second, the upper part of the symmetric rings distorts until a stable “collapsed” pattern is reached (see Fig. 2).

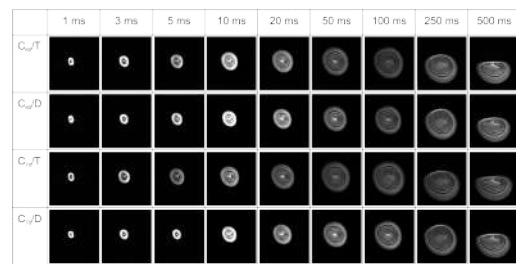
We found a solvent as well as a temperature dependent pattern behaviour, indicating a thermal SSPM effect. The ring formation can be explained as follows: Initially, a considerable amount of laser energy is absorbed by the fullerenes. Next, the thermal energy is transferred to the solvent which leads to an axially symmetric temperature gradient and thus to a spatial density profile. Additionally, we showed that the deformation process is attributed to laser induced thermal convection.

Fig. 2: Self-diffraction pattern of C_{60} and C_{70} in 1,2-dichlorobenzene (D) and toluene (T) at 105 mW input power. Using such SSPM materials we realized a laser protection device, depicted in Fig. 3. In the low power regime, the beam can pass the device undisturbed. Beyond the onset of the SSPM material a considerable amount of the laser beam is blocked by the aperture and leads to optical limiting.

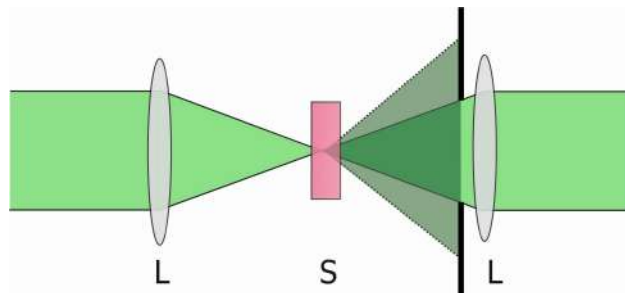
Fig. 3. Laser protection device (L: lens, S: sample)



Exp setup.png



Sspm fullerene.png



Laser protection device.png

Sensitized photoluminescence of rare earth-based semiconducting nanocrystals

Friday, 26th March - 15:35: Oral Session 2-1 (Room 1) - Abstract ID: 104

Dr. Guillaume Gouget¹, Dr. Morgane Pellerin², Dr. Rabih Al Rahal Al Orabi², Dr. Lauriane Pautrot-D'Alençon², Dr. Thierry Le Mercier², Prof. Christopher B. Murray³

1. University of Pennsylvania, 2. Solvay, 3. University of Penn

Nanocrystals (NCs) with luminescent rare earth (RE) ions are attractive for their potential applications in several fields such as bio-imaging, light-emitting displays, anti-counterfeiting technologies, telecommunication, lasing, and high-energy photon detection. The narrow absorption cross-section of RE ions is a major drawback for their photoluminescence (PL) efficiency. Semiconducting NCs as RE hosts are attracting for broadband sensitization of RE PL in the visible range, with tunable absorption range depending on the size and shape of the NCs in the quantum-confined regime.

RE chalcogenides would be ideal host nanostructures, with high insertion rates of RE emitters and bandgap energies between 1.6 and 2.9 eV in the sulfides of the lanthanide series. Bulk RE sulfides are diverse by means of composition, with RE +2 and/or +3 valences and S -2 and/or -1 valences stabilized among various structures. However, europium monosulfide is the only representative stabilized as colloidal dispersions of NCs to date. New synthetic routes to RE chalcogenides NCs with controlled compositions, sizes and shapes are necessary to develop technologies based on photoluminescent RE ions sensitized by semiconducting NCs.

We present an original synthesis of colloidal RE sulfide NCs, based on the reaction of RE iodides and elemental sulfur or (bis-trimethylsilyl)sulfide ((TMS)₂S) in oleylamine. Mono-, sesqui- and disulfide NCs are isolated, as demonstrated with EuS, La₂S₃ and LaS₂ (Figure 1). Phase speciation at the nanoscale between γ-La₂S₃ and LaS₂ relies on the choice of sulfur source. LaS₂ nanoellipsoids and nanoplates with thickness down to 2.8 nm are obtained. Size- and shape-dependent light absorption is characterized for EuS, La₂S₃ and LaS₂. We observe that Er³⁺ PL at 663 nm is excited in 10 % Er-doped La₂S₃ NCs via absorption of La₂S₃ semiconducting host from 390 to 450 nm (Figure 2).

These results should attract interest for applications relying on sensitized RE PL and motivate future works to stabilize diversified compositions and morphologies of RE chalcogenides as colloidal NCs.

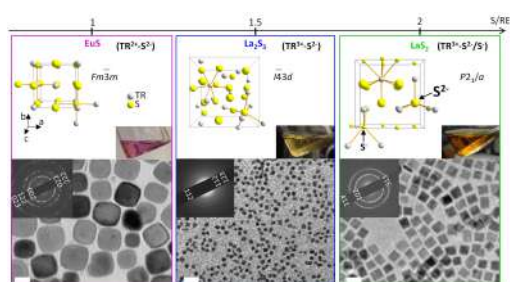


Figure 1. Mono-, sesqui- and disulfides stabilized from rare-earth iodide precursors. Scale bar: 20 nm.

Fig1 re-sulfide ncs.png

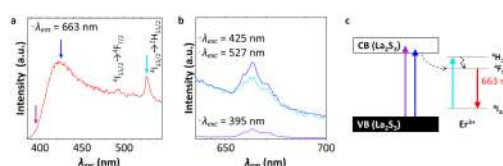


Figure 2. Photoluminescence of Er³⁺ ions sensitized by La₂S₃ host nanostructure. a) Excitation spectrum and b) emission spectra of La₂S₃:Er³⁺ (10 %). c) Energy diagram with (left) La₂S₃ valence band (VB) and conduction band (CB) and (right) simplified Er³⁺ energy level diagram.

Fig2 sensitized-pl la2s3-er.png

TOWARDS MULTIFUNCTIONAL VO₂ MEMRISTORS FOR ULTRAFAST TUNABLE NANO-OPTOELECTRONICS

Friday, 26th March - 15:50: Oral Session 2-1 (Room 1) - Abstract ID: 77

Prof. Malik Maaza¹

1. UNISA & NRF

Optoelectronic Ultrafast Tunability in VO₂ Based Mott/Peierls Nanostructures

•Within the smart MIT materials family, there is a significant population of Vanadium oxides among which Vanadium Dioxide (VO₂) is of a specific interest from technological viewpoint. Because its reversible Semiconductor-Metallic phase transition is close to room temperature (68°C) and its ultrafast time scale wise (120fs), it is gaining interest within the nanocommunity. In its nanoscaled configuration, this smart oxide is multi-functional. This contribution reports on VO₂ nanostructures as a tunable ultrafast nanoplasmonic & ultrafast optical limiter as well as an effective femtosecond optoelectronic gating.

Heterogeneous catalysts at atomic scale: from growth mechanisms to properties

Friday, 26th March - 14:50: Oral Session 2-2 (Room 2) - Abstract ID: 166

Dr. Maria Chiara Spadaro¹

1. Catalan Institute of Nanoscience and Nanotechnology (ICN2)

Heterogeneous and electrochemical catalysis is a diverse area of research that finds applications in clean energy technology and the reduction of environmental pollution.

Colloidal synthesis method is the most widely used for this purpose thanks to its high control over the produced catalyst in terms of size-shape-composition, even at large scale production. Cluster beam deposition (CBD) is a solvent-free technique that offers high degree of flexibility on cluster's size and composition and results one of the most promising techniques in this scenario also being solvent-free and environmentally friendly. The latest main limitation is the overall scale of production, which has been recently addressed.

To correctly address structure-activity relationship, cluster analysis must be complemented with novel and advanced characterization techniques at the single particle level, such as transmission electron microscopy (TEM). By acquiring high resolution (HR) TEM and scanning (S) TEM images it is possible to determine clusters' structure, exposed planes or edges/steps; as well as their chemical composition by acquiring EELS or EDX maps in STEM mode.

In this invited talk diverse research findings will be presented, giving a deeper insight into the investigation of the synthesis process. The nanostructures here presented find application in diverse chemical reactions depending on their composition, structure and defect density distribution. Finally, direct activity-structure dependence is investigated with atomic resolved electron microscopy characterisation.

Acknowledgment

MCS receives funding from the European Union's Horizon 2020 research and innovation programme under the Marie Skłodowska-Curie grant agreement No 754510 (PROBIST). ICN2 acknowledge funding from Generalitat de Catalunya 2017 SGR 327 and the Spanish MINECO project ENE2017-85087-C3. ICN2 is supported by the Severo Ochoa program from Spanish MINECO (Grant No. SEV-2017-0706) and is funded by the CERCA Programme-Generalitat de Catalunya.

Zeolitic-Imidazolate Framework-8 Nanoparticles as mediators to control the selectivity in the oxidative ring-opening reaction of dimethylfuran

Friday, 26th March - 15:20: Oral Session 2-2 (Room 2) - Abstract ID: 89

Dr. Carolina Carrillo Carrion¹

1. Department of Organic Chemistry, University of Córdoba

Introduction

The conversion of renewable biomass resources to synthetically valuable chemicals is a hot topic of current research, but remains a formidable challenge with regards to product selectivity, particularly in oxidative ring-opening reactions of furans. This is mainly due to the high degree of functionality and fairly reactive nature of the furan ring. For industrial processes, there is a significant incentive to optimise product selectivity, since even a small increase in selectivity can bring significant economic benefits. In this regard, the development of new approaches (even uncatalysed) to control product selectivity, not relying on the catalyst itself but on the use of a mediator, could be promising.

Methods

In this work, we address the selectivity issue with a simple and efficient uncatalysed approach by using zeolitic-imidazolate framework-8 nanoparticles (ZIF-8 NPs) as selectivity mediators on the base of their unique ordered structure. As reaction of interest, we selected the oxidative ring-opening of 2,5-dimethylfuran (DMF) to 3-hexene-2,5-dione (target product) using hydrogen peroxide as oxidant and under mild conditions (Scheme 1). This reaction illustrates a promising route for the preparation of valuable enediones from biomass-derived furan compounds in a controlled and cost-effective manner.

INSERT IMAGE UPLOADED

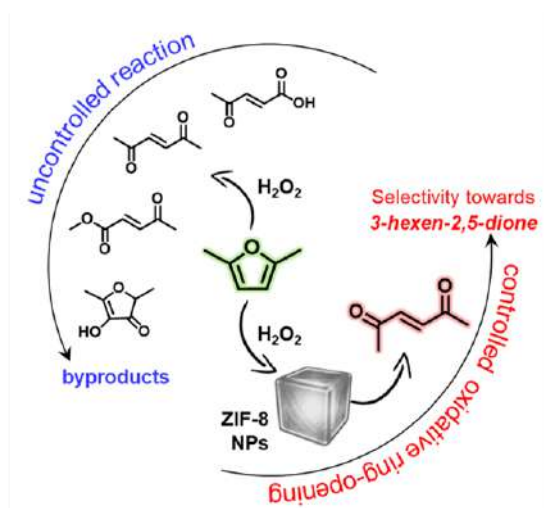
Scheme 1. Schematic illustration of the use of ZIF-8 NPs, having a well-defined porous structure, as a mediator for the selective ring-opening transformation of DMF to 3-hexene-2,5-dione.

Results

A quantitative conversion of DMF with 85% of selectivity to the target 3-hexene-2,5-dione (in comparison to 27% selectivity in the blank reaction) was achieved in the presence of ZIF-8 NPs, and importantly, under mild conditions (60 °C, and methanol as solvent). The influence of the particle size of the ZIF-8 (nanosized versus micro-sized) was also studied to clarify the ZIF-8 performance. We confirmed that the ordered structure of nanosized ZIF-8 particles as well as the larger surface area of ZIF-8 nanoparticles (in comparison to ZIF-8 microparticles) is the key to controlling the product selectivity of the oxidative ring-opening reaction. Furthermore, we performed computational studies based on chemisorption models of ZIF-8 to propose a plausibly explanation of the observed selectivity.

Discussion

This work may pave the way towards the development of alternative, sustainable and cost-effective strategies (i.e., without involving complex and noble metal-containing catalysts) to improve the product selectivity in biomass conversion with a view to green and sustainable developments in the chemical industry.



Scheme 1.png

Silver and molybdenum disulfide photocatalysts for the production of hydrogen and degradation of ciprofloxacin

Friday, 26th March - 15:35: Oral Session 2-2 (Room 2) - Abstract ID: 97

***Mr. Gerardo Claudio*¹, *Dr. Abniel Machin*², *Dr. Loraine Soto-Vázquez*³, *Ms. Carla Colón-Cruz*¹, *Mr. Carlos A. Valentin*¹, *Mr. Kenneth Fontánez*⁴, *Dr. Florian I. Petrescu*⁵, *Dr. Edgard Resto*³, *Dr. Carmen Morant*⁶, *Dr. Francisco Márquez*¹**

1. Nanomaterials Research Group, School of Natural Sciences and Technology, Universidad Ana G. Méndez-Gurabo Campus, Gurabo 00778, Puerto Rico, 2. Arecibo Observatory, Universidad Ana G. Méndez-Cupey Campus, San Juan 00926, Puerto Rico, 3. Materials Characterization Center, Molecular Sciences Research Center, University of Puerto Rico, San Juan 00926, Puerto Rico,

4. Department of Chemistry, University of Puerto Rico-Río Piedras, San Juan 00925, Puerto Rico, 5. IFToMM-ARoTMM, Bucharest Polytechnic University, 060042 Bucharest, Romania, 6. Department of Applied Physics, Autonomous University of Madrid and Instituto de Ciencia de Materiales Nicolas Cabrera, 28049 Madrid, Spain

Different silver-based catalysts were synthesized containing different amounts of molybdenum disulfide (MoS₂; 5, 10, and wt.%) and characterized by FE-SEM, HRTEM, BET, XRD, Raman, XPS, and UV-vis. The photocatalytic activity of the composites was studied by the production of hydrogen via water splitting under UV-vis light and the degradation of the antibiotic ciprofloxacin. The maximum hydrogen production of all the silver-based catalysts was obtained with MoS₂ loading of 20 wt.% under irradiation at 400 nm. 5%Ag@TiO₂ NWs-20%MoS₂ was the catalyst with the highest hydrogen production (1,792 $\mu\text{mol/hg}$), being ca. 24 times greater than the amount obtained with the pristine TiO₂ NWs catalyst. The enhancement of the catalytic activity is attributed to a synergism between the silver nanoparticles incorporated, the molybdenum disulfide, and the high surface area of the composites. In the case of the degradation of ciprofloxacin, all the silver-based catalysts degraded more than 70% of the antibiotic in 60 minutes. The catalyst that exhibited the best result was 5%Ag@TiO₂-P25-5%MoS₂, with 90.72% of degradation. The control experiments and stability tests showed that photocatalysis was the route of degradation and the selected silver-based catalysts were stable after seven cycles, with less than 3% loss of efficiency per cycle. These results suggest that the catalysts could be employed in additional cycles without the need to re-synthesize again, thus reducing remediation costs.

The surface chemistry of colloidal nanocrystals; empowered by NMR

Friday, 26th March - 14:50: Oral Session 2-3 (Room 3) - Abstract ID: 167

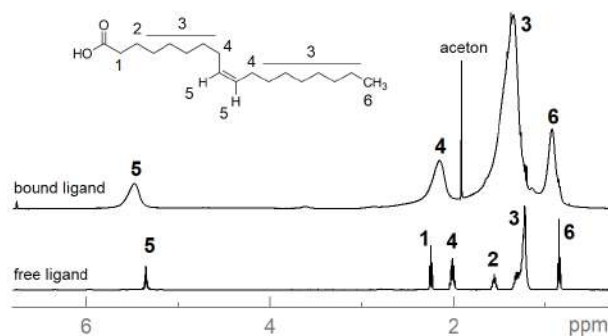
Prof. Jonathan De Roo¹

¹. University of Basel

Colloidal nanocrystals are hybrid objects in which the properties of core and surface both determine the characteristics of the entire nanocrystal (Figure 1). The surface is often capped by (in)organic ligands which determine colloidal stability and the physical and chemical properties. As a result, nanocrystal surface chemistry, i.e., the understanding of and control over the ligand shell, has become one of the central themes in nanocrystal research.

Here, we study the organic ligands through solution NMR spectroscopy. First, the various NMR tools which provide information specific to nanocrystal surfaces are introduced. We will discuss the origin of the NMR line broadening of nanocrystal-bound ligands (Figure 1). Next we go over several general issues with solvents that are commonly used in nanocrystal synthesis at high temperatures (> 240 °C). In particular, 1-octadecene (ODE) and trioctylphosphine oxide (TOPO) are popular solvents but they tend to polymerize or decompose, respectively. The formed impurities are hard to remove from the nanocrystal product. I will show how surface chemistry can be used to enable nanoribbon memristors and photon upconversion. This truly means we have access to a surface chemistry on-demand.

As such, we establish surface chemistry as a key enabler in a variety of applications and NMR as the method of choice for characterizing the surface. This is a versatile field, with fundamental chemistry and spectroscopy leading to exiting innovations in physics and engineering and finally solving real-life problems.



Nmr.png

Estimating the effect of semiconductor quantum dot surface charge on their interaction with proteins

Friday, 26th March - 15:20: Oral Session 2-3 (Room 3) - Abstract ID: 226

Mrs. Tatiana Tsoy¹, Prof. Alexander Karaulov², Prof. Igor Nabiev³, Dr. Alyona Sukhanova⁴

1. 1 Laboratory of Nano-Bioengineering, National Research Nuclear University MEPhI (Moscow Engineering Physics Institute), 115409 Moscow, Russian Federation, **2.** 2 Sechenov First Moscow State Medical University (Sechenov University), 119146 Moscow, Russian Federation, **3.** 1 Laboratory of Nano-Bioengineering, National Research Nuclear University MEPhI (Moscow Engineering Physics Institute), 115409 Moscow; **3.** Laboratoire de Recherche en Nanosciences, LRN-EA4682, Université de Reims Champagne-Ardenne, 51100 Reims, France, **4.** 3 Laboratoire de Recherche en Nanosciences, LRN-EA4682, Université de Reims Champagne-Ardenne, 51100 Reims, France

Introduction:

Quantum dots (QDs) are semiconductor nanocrystals with unique fluorescence characteristics. They can be widely used for bioimaging and detection in nano-bioanalytical systems [1]. Their interactions with human body components may affect both the body components and the QD properties. The biodistribution of QDs may be changed upon their interaction with blood proteins, with a dynamic protein layer (so-called protein corona) formed on the QD surface [2]. The goal of our study is to develop the protocol for studying QD interaction with human serum and analyzing the protein corona components.

Methods:

We used the standard protocol of solubilization of CdSe/ZnS core/shell QDs with a fluorescence maximum at 593 nm that we developed earlier [3]. After solubilization, the QD surface was modified with polyethylene glycol (PEG) derivatives. Combining PEG derivatives with different end groups (–OH, –COOH, and –NH₂), we obtained QDs with different surface charges: low positive (30% PEG-NH₂ and 70% PEG-OH), low negative (100% PEG-OH), and high negative (30% PEG-COOH and 70% PEG-OH). We characterized the solubilized QDs by measuring their hydrodynamic size, zeta-potential, and optical properties. The QDs were incubated with human blood serum samples from healthy donors for 24 h at 37°C. After incubation, the samples were precipitated by centrifugation at 20,000 g for 6 h, and protein patterns were analyzed using 1D PAGE under denaturing conditions and MALDI-TOF mass spectrometry (MS) or MS combined with liquid chromatography. Albumin and IgG depletion prepacked *SpinTrap*[™] columns were used to facilitate the detection of less abundant QD-interacting proteins.

Results:

The experimental conditions for estimating the effect of the QD surface charge on the protein corona composition have been selected. We have shown that the pattern of QD-interacting serum proteins strongly depends on the QD surface properties. These patterns can be differentially analyzed using SDS-PAGE, with individual proteins in the complexes identified by MS.

Discussion:

The approach developed can be used for the separation and differential analysis of the serum proteins interacting with nanoparticles (NPs) as dependent on the NP surface charge. Because the protein profile should reflect the effects of NPs on the components of the human body, these data are crucial for the risk assessment of nanomaterials.

[1] Bilan, R. et al., *ChemBioChem* (2016) 17, 2103–2114.

[2] Shemetov, A. et al., *ACS Nano* (2012) 6, 4585–4602.

[3] Brazhnik, K. et al., *Nanomedicine: NBM* (2015) 11(5), 1065–1075.

Full ground states of dipolar particles controlled from external fields

Friday, 26th March - 15:35: Oral Session 2-3 (Room 3) - Abstract ID: 102

Mr. Ebenezer KEMGANG ¹

1. UNIVERSITE DE LORRAINE - Laboratoire de Physique et Chimie Théoriques

During the last decades, several experiment and theoretical works allowed to understand how the crystallization and phase transitions of a set of dipolar particles may be assisted by: External field, specific molecules or even by the confinement effects. However, in the presence of both gravity and external magnetic field notably, the ground state predictions of many bodies of such the particles becomes a very complex task. In this work, the overall ground state structures of a collection of N magnetic hard spheres, subjected to both gravity and external homogeneous magnetic field is predicted theoretically, using an efficient minimization algorithm called differential evolution, and analytical calculations. We find a graceful expression of transition gravity strength and plot it as a function of total number of spheres. In the regime of strong magnetic field, at weak gravity, a single standing chain emerges as ground state. Upon increasing gravity, at prescribed N , the standing chain splits into many chains separated infinitely far apart when the total number of hard spheres is not too large, or into a standing ribbon whose structure is made up of two touching parallel and shifted chains for large total number of particles. Specifically for two hard spheres, we establish the full ground state phase diagram as a function of gravity and magnetic field strengths. Three dimeric states emerge: A lying state, an inclined state and a standing state. We find that the orientation angles of the dimer axis and the dipole moment in the newly discovered inclined phase are related by a strikingly simple Snell-Descartes-like law. We argue that our findings can be experimentally verified in colloidal and granular systems.

Coated superparamagnetic iron oxide nanoparticles: synthesis and characterization

Friday, 26th March - 15:50: Oral Session 2-3 (Room 3) - Abstract ID: 81

Dr. Solenne Fleutot¹, Dr. Pierre Venturini¹, Mr. Thomas Girardet¹, Dr. Franck Cleymand¹

1. IJL - UMR CNRS 7198, Université de Lorraine, Nancy, France

Coated superparamagnetic iron oxide nanoparticles (NPs) can be used for several applications (environmental, biomedical applications ...) [1]. In this context, numerous synthesis and functionalization methods have been reported [2] to control composition, size, and surface state of NPs and capped NPs to perform and control their magnetic properties [3].

In this study, capped NPs (NPs@Cit) have been synthesized in a controlled range size of 5-15 nm by a method derived from the co-precipitation synthesis [4] to which we add an “in-situ” functionalization of the nanoparticles by citrate ions (Cit). The influence of citrate addition during the synthesis on each physicochemical parameter of the nanoparticles was studied. A comparison with the standard synthesis results will be presented. Indeed, if this method provides nanoparticles dispersed in aqueous medium, essential point for biomedical applications, it usually leads to samples tending to aggregate. The nanoparticles aggregation should be avoided by the electrostatic repulsions caused by citrates bounded to the NPs surfaces. In addition, free hydroxyl and carboxylate functional groups of the citrate can be used as anchor functional groups for further functionalization. A special attention has been given to the reproducibility of samples and to their colloidal stability over time in aqueous suspension.

Beside the influence of the in situ functionalization, several synthesis parameters such as the ratio ligand (citrate) / precursor (iron species) and the citrate addition time compared to the nanoparticles precipitation have been studied especially for their effects on NPs' size, composition, colloidal stability and magnetic properties. The influence of these parameters was considered in relation to the nucleation and growth of nanoparticles. To evaluate the influence of monitored parameters on the size, composition and colloidal stability, a physicochemical and magnetic characterization was conducted systematically by classical methods: Transmission Electron Microscopy (TEM), X-Ray diffraction (XRD) and Dynamic Light Scattering (DLS). Magnetic measurements were performed using a SQUID VSM. Iron oxidation degree was determined by Mössbauer spectroscopy and X-ray photoelectron spectroscopy (XPS). XPS was allowed to characterize the nature of the interactions between iron oxide core and citrate shell.

[1] M. Colombo, S. Carregal-Romero, M. F. Casula, *Chem. Soc. Rev.* **41**, 4306-4334 (2012)

[2] A-H. Lu, E. L. Salabas, F. Schütz, *Angewandte Chemie.* **46**, 1222-1244 (2007)

[3] A. K. Gupta, S. Wells, *IEEE Trans. Nanobio.* **3**, 66-73 (2004)

[4] A. Bee, R. Massart, S. Neveu, *J. Magn. Magn. Mater.* **149**, 6 (1995)

TBD

Friday, 26th March - 16:25: Plenary Session (Room 1) - Abstract ID: 316

Ms. Aleksandra Radenovic¹

1. EPFL

TBD

Scanning transmission electron microscopy at high spatial and energy resolution

Friday, 26th March - 17:10: Plenary Session (Room 1) - Abstract ID: 105

Prof. Quentin Ramasse¹

1. SuperSTEM Laboratory & University of Leeds

The functional properties of materials are increasingly controlled and tuned through structural or chemical architectures whose engineering takes place at the nano or even atomic level. This enables emergent properties relying on the interplay between charge, spin or local atomic-scale chemistry. A particularly powerful means of characterization of these physico-chemical effects lies within a combination of high-resolution scanning transmission electron microscopy and energy-loss spectroscopy (STEM-EELS). Recent instrumentation advances have pushed the energy resolution of these instruments below 10meV while maintaining atomic-sized probes, thus truly realizing the promise of placing a ‘synchrotron in a microscope’ [1].

As a result, it is now possible to fingerprint the functional chemistry of materials as diverse as organic grains in chondrites or metal organic framework glass blends at the nano-scale while simultaneously correlating it with their vibrational response in the sub 100meV energy range. This enables a direct comparison with bulk optical characterization at unprecedented length scales [2]. Further methodological developments have demonstrated the ability to balance momentum and spatial resolution to either determine the electronic band structure of materials in momentum space from nanometre-sized volumes or carry out phonon spectroscopy at the atomic scale, culminating recently in the observation of a phonon signature localized at a single atom defect [3]. It is expected that building on these recent achievements, further improvements in energy resolution and the introduction of new direct/hybrid electron detectors will widen the range of chemistries that can be spectroscopically and spatially resolved, providing the ideal spectroscopic tool to understand the nanoscale organisation of organic and metal-organic bonding and complex interfacial structures in emerging hybrid composite materials.

References

- [1] Q.M. Ramasse, *Ultramicroscopy* **180**, 41-51 (2017).
- [2] C. Vollmer *et al.*, *Meteoritics & Planetary Science* **55**, 1293-1319 (2020); S.M. Collins *et al.*, *J. Am. Chem. Soc.* **140**, pp. 17862-17866 (2018); S.M. Collins *et al.*, *Nano Letters* **20**, 1272-1279 (2020).
- [3] F.S. Hage *et al.*, *Science Advances* **4**, eaar7495 (2018); F.S. Hage *et al.*, *Phys. Rev. Lett.* **122**, 016103 (2019); F.S. Hage *et al.*, *Science* **367** 1124 (2020).

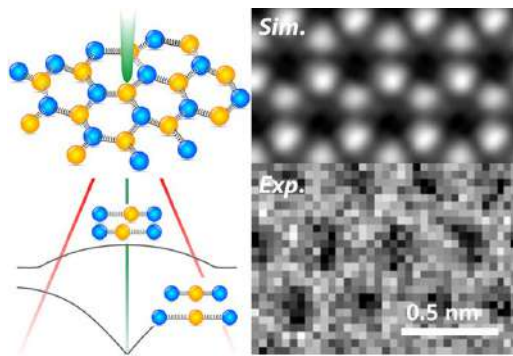


FIG. 1. Balancing spatial and momentum resolution by selecting optical parameters in vibrational STEM-EELS enables mapping phonon dispersion in momentum space (left) or their spatial localization at the atomic scale (right).

Figure1.jpg

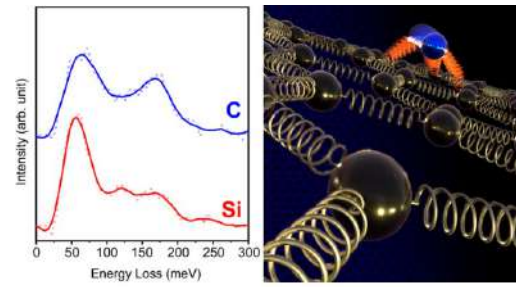


FIG. 2. Single atom vibrational spectroscopy in the STEM: the background subtracted spectrum from a single Si impurity in graphene exhibits a unique signature when compared to a neighbouring C atom. .

Figure2.jpg

Authors Index

AB. RAHIM, N.	40	Balalykin, N.	51
Abbarchi, M.	77, 196	Bandere, D.	35
Abuzar, M.	4	Barbu-Tudoran, L.	30
Acharya, A.	143	Bargan, A.	93
Afanas'ev, V.	141	Barge, A.	164
Afanasev, K.	135	Bayazit, M.	137
Afghah, F.	59	Bele, A.	93
Agonia, A.	152	Bellel, A.	145
Agostiano, A.	78, 119, 121, 156, 165	BEN Ali, A.	173
Ahmed, Z.	62	Benfenati, F.	86
Akaoglu, C.	59	BENMERKHI, A.	27
Akbulut, O.	59	Bentz, B.	22
Akhlaghi, O.	59	Bertran Serra, E.	89
AKHTAR, S.	149	Bessa, J.	8
Al Rahal Al Orabi, R.	200	Beznos, O.	155
Al-khabbaz, H.	149	Bhaskar, S.	28
ALAŞ, M.	15, 38	Bhat, V.	194
Alekseyev, A.	91	Bhattacharyya, K.	71
Alexandratou, E.	182	Boginskaya, I.	135
Alheshibri, A.	149	Bondarenko, V.	108
Ali-Boucetta, H.	62	Bonizzi, A.	60, 126
Allevi, R.	60, 126	Boscaro, V.	164
Alshaikh, I.	89	Boticas, I.	8
Alshehri, S.	193	Botnari, O.	171
Altürk, R.	14	Bouabdellaoui, M.	77
Amade Rovira, R.	89	bouabida, n.	6
Amal, R.	1	Bouherour, M.	145
AMINA, B.	24	Bounouioua, A.	27
Andújar, J.	89	Bozzini, S.	81
Angella, L.	85	Bramini, M.	86
Aouabdia, N.	145	Brangule, A.	35
Aprà, P.	136, 164	Brasili, E.	96
Arbiol, J.	41	Brescia, R.	78
Armirotti, A.	86	Brousse, T.	17, 52
Atiya, G.	111	Brugnetti, G.	95
Atta, S.	118	Bulaeva, N.	135
aylak, a.	70		
Azaïs, T.	98	Cabanas-Danes, J.	181
Azoulay, R.	111	Cabot, A.	41
		Cabrita, E.	183
Bafhaid, H.	62	Calin, M.	54
Bakardijeva, S.	55	Calò, A.	16, 26

Camargo, P.	123	Curri, M.	78, 119, 121, 165
Campello, M.	152	Cuzzocrea, S.	81
Carabelli, V.	136	Cölfen, H.	68
Carney, R.	125	Dardano, P.	131
Carrion, C.	203	Dascalu, M.	93
Carvalho, A.	157	DAvilla, G.	12
Casari, C.	10, 44	De Angelis, G.	96
Castagnola, V.	86	De Caro, L.	78
Castaldo, R.	119	De Leo, V.	156
Castellanos González, J.	139	De Luca, A.	129
Catalan, G.	2	De Martino, S.	131
Catucci, L.	156	De Roo, J.	206
Cazacu, M.	93	De Sio, L.	119
Cecchini, M.	85	de Souza Rodrigues, M.	12
Chatterjee, S.	43	De Stefano, L.	129, 131
CHEHADI, Z.	77	Del Grosso, A.	85
Cherraj, A.	169	Del Río Castillo, A.	139
Chesnokova, N.	155	Delle Cave, D.	129
Chezganov, D.	188	Dengler, S.	198
Chhowalla, M.	67	Depalo, N.	119, 121
Chianese, G.	129	Desiderio, G.	134, 138
Chitas, R.	64	Detsi, A.	150, 151, 176, 182
Chizallet, C.	114	Di Bartolomeo, A.	31
Chronopoulou, L.	96	Di Paola, R.	81
Chrysina, E.	82	Dibenedetto, C.	78
Chubenko, E.	108	Dick Thelander, K.	116
Ciriaco, F.	156	Distler, J.	81
Claude, J.	196	Doğan, G.	14
Claudio, G. (Nanomaterials Research Group, School of Natural Sciences and Technology, Universidad Ana G. Méndez-Gurabo Campus, Gurabo 00778, Puerto Rico)	161	Drinek, V.	55
Claudio, G. (Universidad Ana)	205	Dronov, A.	108
Cleymand, F.	169, 209	Dubkov, S.	25
Codullo, V.	81	Dudin, A.	50, 91
Colombo, M.	81	Dunin-Borkowski, R.	41
Colon-Cruz, C.	170	Durães, L.	157
Colón-Cruz, C.	161, 205	Eberle, B.	198
Comparelli, R.	156	Efimov, A.	101
Cordeiro, R.	157	Ellington, A.	152
Cordoba de Torresi, S.	12, 123	Elsayed, K.	149
Corsi, F.	60, 126	Emil, R.	191
COSTAGLIOLA DI POLIDORO, A.	103	Estevinho, B.	84
Cotto, M.	170	Evdokimov, V.	135
Cruz, C.	152, 183	Fabris, L.	118
Csapó, E.	80	Facibeni, A.	10, 44
Cunha, F.	8	Faella, E.	31
		Fajgar, R.	55
		Faneca, H.	157, 178

Fangueiro, R.	8	Grignani, E.	126
Fanizza, E.	78, 119, 121, 165	Grillo, A.	31
Farcau, C.	30	Gromov, D.	25, 91
Farinha, D.	178	Grosso, D.	77, 196
Favier, F.	17	Guglielmelli, A.	119
Fedorova, Y.	50	Guo, W.	53
Felemban, T.	149	Gupta, I.	46
Ferrara, C.	95	Gupta, N.	43
Fielden, J.	193	Gómez-Romero, P.	36
Flavia Nogueira, A.	113	Gür, E.	38
Fleutot, S.	169, 209	Haag, R.	117
Follink, B.	76, 163	hachemaoui, a.	6
Fonseca, D.	84	Halma, M.	181
Fonseca-Moutinho, J.	152	Hamdi, R.	149, 173
Fontáñez, K.	161, 205	Heggen, M.	41
Forestiere, C.	131	Herlem, G.	88
Fracchia, M.	95	Hodaei, A.	59
Frangipane, V.	81	Huber, T.	168, 171
fransaer, J.	53	Huran, J.	51
Freitas, C.	8	Ibáñez, M.	133
Funston, A.	76, 163	Ilickas, M.	110
Fusco, R.	81	Imbert, L.	183
G.Wildgoose, G.	193	Inamdar, S.	194
Gallardo, E.	152	Ingrosso, C.	78
Galliani, M.	85	Ioana-Raluca, S.	54
Gallicchio, M.	164	Ion, T.	191
Gandhi, S.	46	Jandova, V.	55
Gavrilin, I.	108	Jedraczka, A.	20
Gavrilov, S.	108	Joshi, M.	4
Gentile, G.	119	Juhász, Á.	80
GENÇ ALTÜRK, R.	15, 38, 70	Kalenichenko, D.	99
George, S.	65	Karacabey, P.	14
ghalem, S.	175	Karaulov, A.	101, 207
Ghigna, P.	95	Karayianni, M.	82
Ghosh Chaudhuri, M.	71	Katopodi, A.	150, 151, 176
Ghosh, A.	71	Kavetsou, E.	150, 151, 176, 182
Giancaspro, M.	121	KEMGANG, E.	208
Giannini, C.	78, 121	Khani, n.	59
Girardet, T.	169, 209	Kitsyuk, E.	50
Giubileo, F.	31	Kobzev, A.	51
Giustra, M.	81	Koc, B.	59
Gloter, A.	98	Kolczyk-Siedlecka, K.	20
Golukhova, E.	135	Konopko, L.	168, 171
Gomes, P.	84	Korostylev, E.	101
Goubard, N.	17	Kost, O.	135, 155
Gouget, G.	200		
Grevtsov, N.	108		

Kostejn, M.	55	Martínez Hernández, A.	139
Koster, H.	125	Mastrogiacomio, R.	119
Kováčová, E.	51	Masuda, A.	186
Kriukova, I.	75	Maurelli, A.	156
Krivenkov, V.	101	Mazzucchelli, S.	60, 126
Kryukova, O.	135	McKiernan, E.	106
Kuchеров, M.	174	Mehellou, Y.	62
Kui, Y.	11	Mejri, A.	88
Kumar Maiti, P.	71	Meloni, F.	81
KUMARI, S.	18	meriem, B.	24
Kupcik, J.	55	Merlano, A.	49
Kurochkin, I.	135	Mezzanotte, L.	103
Kurt, H.	137	Migawa, M.	178
Kutyla, D.	20	Milani, A.	10, 44
		Milliron, D.	66
L. Martins, M.	64, 84	Minervini, G.	165
Lasala, P.	119	Miranda, A.	183
Laurikenas, P.	110	Miranda, B.	131
Le Mercier, T.	200	Modaresialam, M. (IM2NP univeristy aix-marseille)	
Leal Seabra, C.	84		196
Lebedev, E.	25, 39, 91	Modaresialam, M. (Nova Team, Institut Matériaux	
Leiro, V.	84	Microélectronique et Nanosciences de	
Lewis, D.	105	Provence, (IM2NP) -UMR CNRS 7334,	
Li Bassi, A.	10, 44	Aix-Marseille Université, Faculté des	
Liang, Z.	41	sciences de Saint Jérôme, 13397 Marseille	
Liessi, N.	86	Cedex 20, France.)	77
Liz-Marzán, L.	123	mohamed, B.	27, 175
Llorca, J.	41	mohamedredha, l.	175
Lonardo, E.	129	Morant, C. (Department of Applied Physics,	
Lungu, I.	32	Autonomous University of Madrid and	
López-Gallego, F.	123	Instituto de Ciencia de Materiales Nicolas	
		Cabrera, 28049 Madrid, Spain)	161, 205
M.G, K.	194	Morant, C. (Universidad Autónoma de Madrid)	170
Maaza, M.	73, 167, 201	Morante, J.	41
Machin, A.	161, 170, 205	Morari, V.	191
Malavasi, L.	3	Morasso, C.	60, 126
Managò, S.	129	Moretta, R.	131
Mandlekar, N.	4	Moretti, E.	197
Maniecki, T.	25	Morosini, M.	81
Marabotti, P.	10, 44	Moura, A.	84
Maragliano, L.	86	Murray, C.	200
Marcantoni, A.	136	Mutlu, A.	38
Marchini Rodrigues Puerta da Silva, A.	12	Márquez, F.	161, 205
Mardosaite, R.	110		
Marquez, F.	170	Nabiev, I. (Laboratoire de Recherche en	
martinez, j.	57	Nanosciences, LRN-EA4682, Université de	
Martinez-de-Oliveira, J.	152	Reims Champagne-Ardenne, 51100	
Martí Gonzalez, J.	89	Reims, France,)	99, 101, 207

Nabiev, I. (LRN-EA4682, Université de Reims Champagne-Ardenne, Reims, France; LNBE, NRNU MEPhI, Moscow, Russian Federation; Sechenov University, Moscow, Russian Federation)	75	Picaud, F.	88
Nag, A.	74	Piccolo, F.	136, 164
Nakase, M.	186	Pispas, S.	82
Nassif, N.	98	Pitterou, I.	150, 151, 182
Nechaeva, N.	135	pokhriyal, a.	36
Negri, S.	126	Politano, G.	134, 138
Nifontova, G.	99, 101	Popov, I.	171
Nikolaeva, A.	168, 171	Popova, E.	155
Nimesh, S.	43	Portoghesi, F.	96
Noureddine, C.	24	Potlog, T.	32
Nozdrin, M.	51	Prosperi, D.	81, 126
Nunes, C.	64	Pugliese, O.	119
Nunes, J.	152	Pujari, V.	194
Nuraeva, A.	188	r, a.	179
Nuta, A.	54	Rached, A.	173
Olivero, P.	136	Racles, C.	93
Orehkova, A.	96	Radenovic, A.	210
P.K, H.	104	Raja Othman, R.	147
Palmeira-de-Oliveira, A.	152	Ramamurthy, S.	28
Palmeira-de-Oliveira, R.	152	Ramasse, Q.	211
Palocci, C.	96	Ramos, A.	98
pandolfi, I.	81	Račkauskas, S.	110
Panniello, A.	78, 165	Rea, I. (1) Institute of Applied Sciences and Intelligent Systems, National Research Council, Napoli, Italy.)	131
Panyosak, A.	184	Rea, I. (Institute of Applied Science and Intelligent System (ISASI), National Research Council of Naples, Via Pietro Castellino 111, 80131, Naples.)	129
Panzarea, F.	121	Redmond, G.	159
Parlanti, G.	85	Redoane, B.	24
Parreira, P.	64, 84	Resto, E.	161, 205
Pascual, E.	89	Ribeiro de Barros, H.	123
Pashnina, E.	188	riccardi, p.	34, 48, 190
Pasqua, G.	96	Ritter, C.	95
Pasquarelli, A.	136	Rizzi, F.	119
Patil, M.	194	Rizzuto, M.	126
Paulo, A.	152	Robu, S.	32
Pautrot-D'Alençon, L.	200	Roffo, F.	154
Peggiani, S.	10, 44	Rojalin, T.	125
Pelella, A.	31	Rosado, T.	152
Pellerin, M.	200	Ruffo, R.	95
Pereverzeva, S.	91	Russo, V.	10, 44
Peterman, E.	181	Ryan, K.	118
Petrescu, F.	161, 205	Ryazanov, R.	25, 39, 91
Petridou, G.	150	Ryzhikov, I.	135
Petrovicova, B.	95		

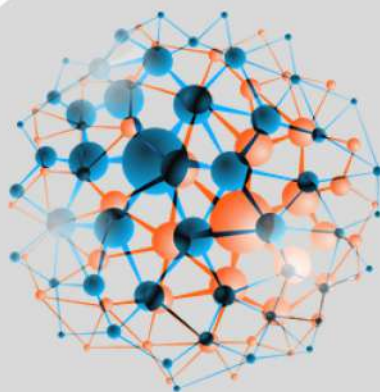
Sacco, M.	164	Sottani, C.	126
Safari, K.	176	Spadaro, L.	95
Salazar, Á.	49	Spadaro, M.	202
Salgado, G.	183	Spanou, A.	176
Salvati, A.	128	Spanou, R.	150
Samokhvalov, P.	75	Stamatiou, I.	182
Santangelo, S.	95	Stiubianu, G.	93
Santi, M.	85	Stratmann, S.	181
Santos, T.	183	Striccoli, M.	78, 119, 121, 165
Sapra, S.	46	Sukhanova, A.	99, 101, 207
Sarmiento, A.	178	Sulciute, A.	110
Sasinková, V.	51	Sumeya, B.	24
Scavo, M.	119	Sysa, A.	39
Schmitzer, S.	121	T.S, T.	194
Seabra, C.	64	Takeshita, K.	186
SEENI MOHAMED, M.	40	Tang, P.	41
Segal Peretz, T.	111	Teixeira, C.	84
Selmane, M.	98	Tikhomirova, V.	135, 155
Selyakov, D.	141	Tiuleanu, P.	32
Serafini, P.	10	Tiwari, R. (Department of Textile and Fibre Engineering, Indian Institute of Technology Delhi, Hauz Khas, New Delhi 110016, India)	4
Seres, L.	80	Tomagra, G.	136
Sevieri, M.	60, 126	Tommasi, R.	78
Sharma, S.	143	Tonazzini, I.	85
Shirkov, G.	51	Torabfam, M.	137
Shomrat, N.	111	Torino, E.	63, 103, 154
Shur, V.	188	Tosa, N.	30
Sibillano, T.	121	Touraya, B.	175
Signore, G.	85	Tovani, C.	98
Silva, F.	126	Tramontano, C.	129
Silva, P.	8	Triolo, C.	95
Simone, P.	95	Trivella P. da Silva, R.	12
Simonetti, G.	96	truffi, m.	60, 126
Singhal, M.	43	Tsoulos, T.	118
Sitia, L. (Dipartimento di Scienze Biomediche e Cliniche “L. Sacco”, università di Milano)	60	Tsoy, T.	207
Sitia, L. (Nanomedicine Laboratory Department of Biomedical and Clinical Sciences “L. Sacco” University of Milan)	126	Tugui, C.	93
Skadiņš, I.	35	Urban, F.	31
Skibińska, K.	20	Ursu, C.	93
Skrypnik, A.	51	Valentin, C.	161, 205
Smeraldo, A.	63	van Oijen, A.	181
Sorescu, A.	54	Varzi, V.	136, 164
sorokina, I.	25, 39	Veaceslav, U.	191
Sorrentino, L.	126	Velasco Santos, C.	139
Soto-Vázquez, L.	161, 205	Vena, C.	134, 138

Venturini, P.	209	Yalçın, M.	15
Versace, C.	134, 138	Yang, D.	41
Vischio, F.	121	Yüce, M.	137
Wang, L.	69	Zabinski, P.	20
Watanabe, S.	186	Zafer, C.	38
Weisbord, I.	111	Zaim, A.	147
Wuite, G.	181	Zarubin, S.	101
Xie, S.	53	Zehe, C.	159
Xu, L.	181	Zhang, X.	53
		Zhou, Y.	41
Yadav, A.	76, 163	Zvaigzne, M.	101
Yadav, P.	43		
yahiaoui, a.	6	Özdemir, S.	15

ANNIC 2021

APPLIED NANOTECHNOLOGY AND NANOSCIENCE
INTERNATIONAL CONFERENCE

THANK YOU !



24, 25, 26 MARCH 2021

ONLINE